

Soil Microbial Community Responses to Changing Environments

BY

MICHAEL P. RICKETTS

B.S., University of Illinois Urbana Champaign, 1998

THESIS

Submitted as partial fulfillment of the requirements
for the degree of Doctor of Philosophy in Biological Sciences
in the Graduate College of the
University of Illinois at Chicago, 2019

Chicago, Illinois

Defense Committee:

Dr. Miquel Gonzalez-Meler, Chair and Advisor
Dr. Rachel Poretsky
Dr. Mary Ashley
Dr. D'Arcy Meyer Dombard, Earth and Environmental Sciences
Dr. Sarah O'Brien, Research and Development Services

*For my mother.
She would've freaked!*

ACKNOWLEDGEMENTS

I would first like to thank my academic advisor, Miquel Gonzalez-Meler, who believed in me when I needed someone to, and others would not; who saw great potential in me and nurtured my curiosity; and who, above all else, cared for and befriended me.

Also, I would like to thank my committee members for the invaluable guidance and support they have provided over the years. In particular, Mary Ashley, who advised an ambitious middle-aged clinical laboratory technician on how to get into a graduate program in the environmental biological sciences, Sarah O'Brien, whose career I am mirroring and who has always been a source of advice and friendship over food and beers, D'Arcy Meyer Dombard, whose mentorship, laboratory facilities, and Midwestern friendly demeanor were integral to the completion of this work, and Rachel Poretsky, whose expertise in microbial ecology and bioinformatics allowed me to have a shoulder to cry on.

This work would not have been possible without financial support from the United States (U.S.) Department of Energy (DOE) Terrestrial Ecosystem Science Program (DE-SC 0006607) and U.S. Forest Service grant (15-JV-11242302-038) awarded to Miquel Gonzalez-Meler, the National Science Foundation (NSF) - Long Term Ecological Research maintenance funding to Jeffrey M. Welker (9412782, 0632184, 0612534, 0856728), the U.S. DOE, Office of Science, Office of Biological and Environmental Research contract (DE-AC02-06CH11357), the NSF (DGE-0549245), "Landscape Ecological and Anthropogenic Processes" awarded to Charles E. Flower, and multiple internal University of Illinois at Chicago (UIC) awards, including the Elmer Hadley Graduate Research Award, the W.C. and May Preble Deiss Award for Graduate Research, and the Bodmer International Travel Award.

I would like to thank members of my lab group at UIC (past and present), Elena Blanc-Betes,

Jessica Rucks, Douglas Lynch, Charles Flower, Michelle Frack, Frank Anderson, Mila Kellen Marshall, Jenny Dalton, Nicholas Glass, Stephanie Kadej, and Theresa Ewa, as well as my graduate student friends and colleagues, Sandra Troxell-Smith, Alexandra Silva, Matthew McCary, and Margaret Malone. The assistance provided in the laboratory and the field, the ideas shared drawing on the whiteboard, and the friendships that grew from our time together will always be treasured.

Of course, I must thank my friends and family for all of their support and encouragement. To my bandmates, thank you for understanding that I can't do everything at the same time, and that sometimes priorities change, but that doesn't mean that I don't still love you. To my father, Stephen Ricketts, thank you for always being so supportive both financially and emotionally, for encouraging me to follow my dreams and push through when times are hard, and for your unwavering love. And a special thank you to my older brother, Matthew Ricketts, whom I have always looked up to and admired. Not a single day of my life has passed when I could not lean on you, and you have inspired me in music, in literature, and in science, more than you will ever know.

The love of my life, Anne K. Sigmond, deserves a standing ovation. Her patience and support have been unparalleled. When I have had stress or been overwhelmed, she has calmed me. When I became frustrated or angry, she made me laugh. When I needed time to work, she gave it to me. And when I was tired, she would hold me. She has been my rock and I thank her from the bottom of my heart.

Lastly, I would like to thank my mother, Carol K. Ricketts. There is no one in existence who would have wanted to see this more. It was she who instilled in me a love and curiosity for nature and its beauty. It was she who taught me that there is nobility and honor in sacrifice if it is

something you believe in and care about. It was she who showed me that while life is fleeting, love is eternal. I could never thank you enough. I wish I could have shared this with you, Mom...

CONTRIBUTION OF AUTHORS

Chapter 1 is a personal statement about my graduate school experience that includes some general background material pertinent to the dissertation topic. I am the sole author of this chapter

Chapter 2 is a published manuscript.

Ricketts, M. P., C. E. Flower, K. S. Knight, and M. A. Gonzalez-Meler. 2018. Evidence of ash tree (*Fraxinus* spp.) specific associations with soil bacterial community structure and functional capacity. *Forests* 9:1–16.

I was the primary author performed all data analyses and bioinformatics. Charles E. Flower conceived and designed sample collection and performed the field work. Kathleen S. Knight provided the plot network and contributed materials. Miquel A. Gonzalez-Meler contributed reagents/materials/analysis tools, provided feedback on experimental design, and edited the manuscript.

Chapter 3 is an unpublished collaboration with personnel at Argonne National Laboratory. I was the primary author and performed all statistical analysis. Roser Matamala and Julie Jastrow conceived, designed, and performed sample collection and experiments. Dion Antonopoulos and Jason Koval performed all sequencing related work and bioinformatics, and wrote portions of the Methods section.

Chapter 4 is a published manuscript.

Ricketts, M. P., R. S. Poretsky, J. M. Welker, and M. Gonzalez-Meler. 2016. Soil bacterial community and functional shifts in response to altered snowpack in moist acidic tundra of Northern Alaska. *Soil* 2:459–474.

I was the primary author and performed all sample collections, laboratory work, bioinformatics, and statistical analysis. Miquel A. Gonzalez-Meler and Jeffrey M. Welker designed the experiment. Rachel S. Poretsky provided insight and expertise into the bioinformatics and data analyses. All co-authors contributed to providing edits to the manuscript.

Chapter 5 is an unpublished follow-up to Chapter 4 using the same samples but a different method. I was the primary author and performed all sample collections, laboratory work, bioinformatics, and statistical analysis. Miquel A. Gonzalez-Meler and Jeffrey M. Welker designed the experiment. Miquel A. Gonzalez-Meler provided comments and edits on figures and text.

TABLE OF CONTENTS

1	PERSONAL STATEMENT	1
1.1	In the beginning... Motivation.....	1
1.2	Being small in a large world	2
1.3	The soil environment	3
1.4	Modern tools and technology – The age of genomics	4
1.5	References.....	6
2	EVIDENCE OF ASH TREE (FRAXINUS SPP.) SPECIFIC ASSOCIATIONS WITH SOIL BACTERIAL COMMUNITY STRUCTURE AND FUNCTIONAL CAPACITY	8
2.1	Introduction.....	8
2.2	Materials and Methods.....	11
2.2.1	Site description.....	11
2.2.2	Soil collection and characterization	13
2.2.3	DNA extraction, sequencing, quality control and bioinformatics	14
2.2.4	Statistical analyses	15
2.3	Results.....	17
2.3.1	Environmental and site differences.....	17
2.3.2	Bacterial community differences	19
2.3.3	Bacterial functional differences	22
2.4	Discussion	26
2.5	Conclusions.....	32
2.6	Acknowledgments.....	33
2.7	References.....	34
3	CARBON MINERALIZATION SUSCEPTIBILITY IN ARCTIC TUNDRA SOILS: HOW ORGANIC MATTER CHEMISTRY AND TEMPERATURE RELATE TO BACTERIAL COMMUNITY STRUCTURE AND SOIL RESPIRATION.....	39
3.1	Introduction.....	39
3.2	Materials and methods	42
3.2.1	Study sites	42
3.2.2	Soil incubations and temperature sensitivity	44
3.2.3	Soil analysis	45
3.2.4	DNA extraction and high-throughput 16S rRNA sequencing	46
3.2.5	Statistical analysis.....	48
3.3	Results.....	49
3.3.1	Incubation effects on soil bacterial abundance and CMP	49
3.3.2	Predictive RDA analyses of bacterial community structure	53
3.3.3	Correlation analysis	56
3.4	Discussion	59
3.4.1	Bacterial abundance responses to warming	60
3.4.2	Drivers/predictors of bacterial community structure	62
3.4.3	Relationships between soil chemistry, CMP, and bacterial abundance.....	64
3.5	Conclusions.....	65
3.6	Acknowledgements.....	66

3.7	References.....	67
4	SOIL BACTERIAL COMMUNITY AND FUNCTIONAL SHIFTS IN RESPONSE TO ALTERED SNOW PACK IN MOIST ACIDIC TUNDRA OF NORTHERN ALASKA.....	73
4.1	Introduction.....	73
4.2	Methods.....	76
4.2.1	Site description and sample collection.....	76
4.2.2	DNA extraction, sequencing, and analysis	79
4.2.3	Statistical analyses	81
4.3	Results.....	82
4.3.1	Environmental changes.....	82
4.3.2	Bacterial community shifts	86
4.3.3	PICRUSt functional analysis	89
4.4	Discussion.....	92
4.4.1	Bacterial community shifts	93
4.4.2	Functional shifts.....	97
4.4.3	Ecosystem response to snow accumulation	100
4.5	Conclusions.....	101
4.6	Additional Information	102
4.6.1	Data and code availability.....	102
4.6.2	Author contributions	102
4.6.3	Acknowledgements.....	102
4.7	References.....	104
5	SHOTGUN METAGENOMIC ANALYSIS OF MICROBIAL SOIL ORGANIC MATTER DECOMPOSITION AND NUTRIENT CYCLING IN AN ARCTIC SNOWFENCE EXPERIMENT	114
5.1	Introduction.....	114
5.2	Methods.....	118
5.2.1	Site description and sample collection.....	118
5.2.2	Shotgun sequencing and analysis.....	119
5.2.3	Functional gene analysis	119
5.2.4	Statistical analyses	120
5.3	Results.....	122
5.3.1	Treatment effects on soil environment	122
5.3.2	Microbial taxonomic abundance analysis.....	123
5.3.3	Drivers of microbial functional capacity	126
5.3.4	Microbial functional gene abundance analysis	129
5.4	Discussion.....	133
5.4.1	Microbial taxonomic responses	134
5.4.2	Microbial genetic functional responses	136
5.5	Conclusions.....	142
5.6	Acknowledgements.....	143
5.7	References.....	144
6	BROADER IMPACTS	149
7	APPENDICES	151

7.1	Supplementary materials – Chapter 2	151
7.2	Supplementary materials – Chapter 3	157
7.3	Supplementary materials – Chapter 4	159
7.4	Supplementary materials – Chapter 5	176
8	VITA.....	206

LIST OF FIGURES

Figure 1.1. Conceptual diagram representing the relationships, interactions, and feedbacks that occur between soil microorganisms and both biotic and abiotic environmental factors. Solid lines indicate direct effects while dotted lines indicate indirect effects.	5
Figure 2.1. Map of study sites within Delaware county, Ohio.	11
Figure 2.2. Non-metric multidimensional scaling (NMDS) plot where each point represents the bacterial/archaeal community structure of a sample (stress=0.080, Shepard plot non-metric $R^2=0.992$). Color indicates ash v. non-ash plots and shape indicates forest site. Ellipses represent 95% confidence intervals of centroids for ash and non-ash plots. Bacterial/archaeal community structures differed significantly between ash and non-ash plots (adonis $p=0.002$).	20
Figure 2.3. Boxplot comparing the average Hellinger transformed abundances of the 10 most abundant bacterial/archaeal phyla between ash (blue) and non-ash (orange) plots. Mann-Whitney U -test significance is denoted by asterisks, where $*=p<0.05$, $**=p<0.01$, and $***=p<0.001$	21
Figure 2.4. Linear relationships between canopy tree health (mean AC) of ash plots only ($n=11$) and Hellinger transformed abundances of the 10 most abundant bacterial phyla.	22
Figure 2.5. Functional gene abundance comparisons between ash and non-ash plots at KEGG levels 2 (a) and 3 (b). Extended bar graphs show differences in the mean proportions of functional genes required for biogeochemical cycling ordered by decreasing effect size. Error bars represent 95% Welch’s inverted confidence intervals. Welch’s two-tailed t-test was used with Benjamini-Hochberg FDR procedure to obtain corrected q -values. All statistics and graphics were produced using STAMP software.	24
Figure 2.6. Pearson’s correlation matrix comparing the ten most abundant bacterial phyla to level 3 KEGG functional categories, ordered as in Figure 2.4. Circle color indicates either a positive (blue) or negative (red) correlation, and circle size and shading are proportional to correlation coefficients regardless of statistical significance. Bonferroni adjusted significance ($p<0.05$) is indicated by white asterisks.	25
Figure 2.7. Theoretical diagram representing possible successional trajectories of bacterial communities over time in forests suffering ash decline as a result of EAB infestation, where in Scenario 1 the communities stay the same, in Scenario 2 they become more similar to communities in non-ash plots, and in Scenario 3 they develop a community structure different than in either ash or non-ash plots. NMDS ordination space represents hypothetical differences in bacterial community structure based on Figure 2.2.	31
Figure 3.1. Log ₂ -fold change (log ₂ FC) response of bacterial class abundances to incubations where positive values indicate increased abundance over 60 days, and negative values indicate decreased abundance over 60 days. All results shown are significant ($p<1e^{-5}$) with false discovery rates (FDR) $<1e^{-5}$ and log ₂ FC values >1 or <-1 . Bacterial phyla are ordered from top to bottom with the most abundant phyla at the top. Panels are separated by incubation temperature, color indicates the soil layer, and the shape indicates the site.	51
Figure 3.2. Relative abundances of bacterial classes which showed significant differential abundances between initial un-incubated samples and incubated samples (see Figure 1). Results	

are separated by site, soil layer, and incubation temperature. Bacterial classes are grouped by phylum where base colors indicate the phylum and classes are separated by tint..... 52

Figure 3.3. Distance-based redundancy analysis ordinations of bacterial community structure separated by site (colors) and soil layer (shapes), and constrained by descriptive variables (A), FTIR spectral peak absorbance values assigned to soil chemical properties (B), and ratios of FTIR peaks absorbance values (C). Arrows indicate strength of correlations between bacterial community structure and explanatory variables. 55

Figure 3.4. Venn diagram illustrating variance partitioning from the three different redundancy analysis models explaining bacterial community structure. 56

Figure 3.5. Correlation matrices of bacterial classes (ordered from left to right by decreasing abundance) selected from differential analysis (Fig. 1) with most important soil chemical variables identified from redundancy analysis and Mantel tests, and carbon mineralization potential (CMP). Colors indicate strength and direction of correlation (r_P), where red=positive correlations and blue=negative correlations. Squares containing “x” indicate a significant correlation ($p_B < 0.05$). 58

Figure 4.1. Modified from Walker et al., 1999. Schematic of snow accumulation depth at moist acidic tundra site from snow fence manipulation. Three soil cores were obtained from each treatment zone (labeled Deep, Intermediate, and Low) and a Control zone located >30 m outside the effect of the snowfence. 77

Figure 4.2. Non-metric multidimensional scaling (NMDS) plot using Bray-Curtis dissimilarity matrices (Stress=0.090, Shepard plot non-metric $R^2=0.992$). Each point represents the bacterial community structure within one of the 41 total samples used for DNA extraction from all soil depths (Organic, Transition, and Mineral). Colours indicate %C ranging from 1.4% (light blue) to 48.6% (dark blue), bubble size indicates %N ranging from 0.09% (small) to 1.95% (large), and shapes indicate snow accumulation treatments (Control, Deep, Int., Low). Ellipse centroids represent treatment group means while the shape is defined by the covariance within each group. 83

Figure 4.3. Averaged relative abundance of the six most abundant bacterial phylum relative to the control, separated by snow accumulation treatment, and in order of greatest abundance (top to bottom). Error bars represent standard error (standard error of controls ranged from 12.929 in Chloroflexi to 0.026 in Verrucomicrobia). Significance determined by Kruskal-Wallis tests is indicated by asterisks ($*=p < 0.1$, $**=p < 0.05$), while post-hoc Nemenyi test results are indicated by “a, b, ab”, except where significant differences were to the control. 87

Figure 4.4. Averaged relative abundance of genes for enzyme functional groups relative to the control and separated by snow accumulation treatment. Functional groups involved in soil organic matter decomposition are ordered from recalcitrant to labile substrates (top to bottom). Error bars represent standard error (standard error of controls ranged from 1.220 in the lignin group to 0.008 in the superoxides group). Significance determined by Kruskal-Wallis tests is indicated by asterisks ($*=p < 0.1$, $**=p < 0.05$), while post-hoc Nemenyi test results are indicated by “a, b, ab”, except where significant differences were to the control. 90

Figure 5.1. Relative abundances across treatments of bacteria and fungi at the kingdom (A) and phylum levels (B and C). Statistical significance ($p < 0.1$) of relative abundance differences between treatment groups as ascertained by Kruskal-Wallis is represented by “*”. Nemenyi

posthoc testing was performed on bacterial:fungal relative abundance ratios in A), while in B) and C) the relative abundances of individual phyla were used. Significant differences found in posthoc tests are represented by “a” and “b”..... 124

Figure 5.2. Non-metric multidimensional scaling (NMDS) ordinations showing differences in community structure at the OTU level for both bacteria (A; stress=0.041) and fungi (B; stress=0.039). R^2 and p -values are the results of adonis (PERMANOVA) tests evaluating the effects of the treatment on community structure. 126

Figure 5.3. Constrained ordinations from canonical correspondence analysis (CCA) of overall microbial community genetic functional capacity Each point represents the functional gene matrix from a single sample as assigned by SEED subsystems at the “function” level. Distances between sample points indicate differences in the overall functional capacity of the communities. Ordinations are constrained by microbial taxonomy (A) and soil environmental characteristics (B). Arrow length and direction indicate corollary power and influence on functional gene matrix structure..... 128

Figure 5.4. Heatmap and Kruskal-Wallis analysis of gene groups organized by association with various carbohydrate polymers found in organic matter, catabolic vs. anabolic processes, and methane/CO₂, N, and P metabolism. Columns in heatmap represent the four snow depth treatment zones. Black boxes indicate the maximum average relative abundance while white boxes indicate minimum average relative abundance ($n=3$). Maximum and minimum average values are shown in columns left of the heatmap. Asterisks (“*”) indicate Nemenyi posthoc differences with $p<0.01$ 131

Supplementary Figures

Supplementary Figure S2.1. Boxplot comparing the average Hellinger transformed abundances of the 20 most abundant bacterial/archaeal classes between ash (blue) and non-ash (orange) plots. Mann-Whitney U -test significance is denoted by asterisks, where $*=p<0.05$. .. 155

Supplementary Figure S2.2. Boxplot comparing the average Hellinger transformed abundances of the 30 most abundant bacterial/archaeal orders between ash (blue) and non-ash (orange) plots. Mann-Whitney U -test significance is denoted by asterisks, where $*=p<0.05$. .. 156

Supplementary Figure S3.1. Example of Fourier transformed mid infrared (FTIR) spectra identifying peaks associated with soil chemical properties. 157

Supplementary Figure S4.1. Linear fit regression of Acidobacteria relative abundance with respect to soil C:N, %C, %N, and pH across all snow treatment sites and all soil depths ($n=41$). Shaded areas indicate 95% confidence intervals. 161

Supplementary Figure S4.2. Linear fit regression of Proteobacteria relative abundance with respect to soil C:N, %C, %N, and pH across all snow treatment sites and all soil depths ($n=41$). Shaded areas indicate 95% confidence intervals. 161

Supplementary Figure S4.3. Linear fit regression of Verrucomicrobia relative abundance with respect to soil C:N, %C, %N, and pH across all snow treatment sites and all soil depths ($n=41$). Shaded areas indicate 95% confidence intervals. 162

Supplementary Figure S4.4. Linear fit regression of Actinobacteria relative abundance with respect to soil C:N, %C, %N, and pH across all snow treatment sites and all soil depths ($n=41$).

Shaded areas indicate 95% confidence intervals.	162
Supplementary Figure S4.5. Linear fit regression of Bacteroidetes relative abundance with respect to soil C:N, %C, %N, and pH across all snow treatment sites and all soil depths ($n=41$). Shaded areas indicate 95% confidence intervals.	163
Supplementary Figure S4.6. Linear fit regression of Chloroflexi relative abundance with respect to soil C:N, %C, %N, and pH across all snow treatment sites and all soil depths ($n=41$). Shaded areas indicate 95% confidence intervals.	163
Supplementary Figure S4.7. Linear fit regression of estimated gene copy number of genes required for arabinoside degradation with respect to soil C:N, %C, %N, and pH across all snow treatment sites and all soil depths ($n=41$). Shaded areas indicate 95% confidence intervals.	164
Supplementary Figure S4.8. Linear fit regression of estimated gene copy number of genes required for cellulose degradation with respect to soil C:N, %C, %N, and pH across all snow treatment sites and all soil depths ($n=41$). Shaded areas indicate 95% confidence intervals.	164
Supplementary Figure S4.9. Linear fit regression of estimated gene copy number of genes required for chitin degradation with respect to soil C:N, %C, %N, and pH across all snow treatment sites and all soil depths ($n=41$). Shaded areas indicate 95% confidence intervals.	165
Supplementary Figure S4.10. Linear fit regression of estimated gene copy number of genes required for lignin degradation with respect to soil C:N, %C, %N, and pH across all snow treatment sites and all soil depths ($n=41$). Shaded areas indicate 95% confidence intervals.	165
Supplementary Figure S4.11. Linear fit regression of estimated gene copy number of genes required for N mobilization with respect to soil C:N, %C, %N, and pH across all snow treatment sites and all soil depths ($n=41$). Shaded areas indicate 95% confidence intervals.	166
Supplementary Figure S4.12. Linear fit regression of estimated gene copy number of genes required for Pectin degradation with respect to soil C:N, %C, %N, and pH across all snow treatment sites and all soil depths ($n=41$). Shaded areas indicate 95% confidence intervals.	166
Supplementary Figure S4.13. Linear fit regression of estimated gene copy number of genes required for P mobilization with respect to soil C:N, %C, %N, and pH across all snow treatment sites and all soil depths ($n=41$). Shaded areas indicate 95% confidence intervals.	167
Supplementary Figure S4.14. Linear fit regression of estimated gene copy number of genes required for superoxide regulation with respect to soil C:N, %C, %N, and pH across all snow treatment sites and all soil depths ($n=41$). Shaded areas indicate 95% confidence intervals.	167
Supplementary Figure S4.15. Linear fit regression of estimated gene copy number of genes required for superoxide regulation with respect to soil C:N, %C, %N, and pH across all snow treatment sites and all soil depths ($n=41$). Shaded areas indicate 95% confidence intervals.	168
Supplementary Figure S4.16. Heatmap of raw gene abundance (# of OTU's) for all detected bacterial Phyla. Columns represent snow accumulation treatment groups, where the control = "CTL", 100% more snow accumulation="DEEP", 50% more snow="INT", and 25% less snow than control="LOW".	171
Supplementary Figure S4.17. Heatmap of raw gene abundance (# of OTU's) for all detected bacterial Classes. Columns represent snow accumulation treatment groups, where the control = "CTL", 100% more snow accumulation="DEEP", 50% more snow="INT", and 25% less snow	

than control="LOW".	172
Supplementary Figure S4.18. Heatmap of raw gene abundance (# of OTU's) for all detected bacterial Orders. Columns represent snow accumulation treatment groups, where the control ="CTL", 100% more snow accumulation="DEEP", 50% more snow="INT", and 25% less snow than control="LOW".	173
Supplementary Figure S4.19. Heatmap of raw gene abundance (# of OTU's) for all detected bacterial Families. Columns represent snow accumulation treatment groups, where the control ="CTL", 100% more snow accumulation="DEEP", 50% more snow="INT", and 25% less snow than control="LOW".	174
Supplementary Figure S4.20. Heatmap of raw gene abundance (# of OTU's) for all detected bacterial OTU's. Columns represent snow accumulation treatment groups, where the control ="CTL", 100% more snow accumulation="DEEP", 50% more snow="INT", and 25% less snow than control="LOW".	175

LIST OF TABLES

Table 2.1. Summary of site characteristics.	12
Table 2.2. Summary of statistical results. Adonis tests were used to analyze differences in overall bacterial community structure and overall soil chemical characteristics between categorical variables (a). Continuous variables were analyzed individually (b) for differences between ash and non-ash plots (Mann-Whitney <i>U</i> test), differences in forest sites (Kruskal-Wallis), and for correlations between overall bacterial community structure and individual variables (Mantel test). Text in bold and italics represents a significant result ($p < 0.05$).	18
Table 3.1. Average \pm standard error of soil carbon characteristics ($n=30$), carbon mineralization potential (CMP) calculated from the incubation experiment ($n=5$), and calculated temperature sensitivity (Q_{10}) over 60-day incubations ($n=5$). *=samples removed as outliers.....	43
Table 3.2. Statistical results of Mantel tests and distance-based redundancy analyses (dbRDA) evaluating the effects of soil chemical and site properties on bacterial community structure. All results are statistically significant ($p < 0.05$). Asterisks (*) indicate p -values less than 0.001.....	54
Table 4.1. Abiotic characteristics of soil from snow accumulation treatments (Low= $\sim 25\%$ less snow pack than the Control, Int.= $\sim 50\%$ more snow pack than the Control, Deep= $\sim 100\%$ more snow pack than the Control). Values are means \pm standard errors. Soil chemical properties were obtained from samples used for DNA extraction, while temperature and thaw depth were measured <i>in situ</i> ($n=12$). Organic and mineral samples were analyzed separately using the Nemenyi post hoc test. Results are indicated by _{a,b,c} only where $p < 0.05$	85
Table 4.2. Statistical analysis of beta diversity using adonis and Mantel tests. Bray Curtis distance matrices of bacterial communities for each sample were compared between soil layers (Organic, Transition, Mineral) and snow accumulation treatments (Control, Deep, Int., Low), and to soil chemical properties. Sample sizes were $n=15$ for “Organic”, $n=13$ for “Mineral”, and $n=41$ for “All layers”. Significance is indicated by asterisks (*= $p < 0.05$, **= $p < 0.01$, ***= $p < 0.001$)......	89
Table 5.1. Abiotic characteristics of soil from snow accumulation treatments. Soil chemical properties were obtained from samples used for DNA extraction ($n=3$), while temperature and thaw depth were measured <i>in situ</i> ($n=12$). Values are means \pm standard errors. Nemenyi posthoc results are indicated by _{a,b,c} only where $p < 0.05$	122
Table 5.2. Adonis (PERMANOVA) statistics for the effects of snow accumulation treatment, and soil chemical and physical properties on bacterial, fungal, and overall microbial (bacterial + fungal) community structure.....	125
Table 5.3. Statistics from constrained correspondence analysis (CCA), adonis (PERMANOVA), and Mantel tests examining the effects of microbial taxonomic relative abundances on overall microbial community functional capacity. †=variables removed from the full model due to collinearity determined by variance inflation factors (VIF).	127
Table 5.4. Statistics from constrained correspondence analysis (CCA), adonis (PERMANOVA), and Mantel tests examining the effects of the soil environment on overall microbial community functional capacity. Blank cells indicate that test assumptions did not pass. †=variables not	

included in the full model due to collinearity determined by variance inflation factors (VIF).. 129

Supplementary Tables

- Supplementary Table S2.1.** Summary statistics of re-analyzed data using only sites that have ash canopy condition (AC) values less than or equal to 3, resulting in 2 sites (BHN and KRS), consisting of 6 ash plots (meanAC=2.42±0.30) and 4 non-ash plots. Adonis tests were used to analyze differences in overall bacterial community structure and overall soil chemical characteristics between categorical variables (a). Continuous variables were analyzed individually (b) for differences between ash and non-ash plots, and differences between sites using Mann-Whitney *U* tests, and for correlations between overall bacterial community structure and individual variables using Mantel tests. Text in bold and italics represents a significant result ($p<0.05$)..... 151
- Supplementary Table S2.2.** Means and standard errors of all measured variables separated by forest site. Alpha diversity was calculated using the Shannon diversity index (H). Kruskal Wallis test significance ($p<0.05$) is indicated by “*”. Nemenyi post hoc test significant differences ($p<0.05$) are indicated by superscripts “a” and “b”. 153
- Supplementary Table S2.3.** Plot level characteristics of soil pH, tree community health (AC), total basal area (BA), percent dominance of tree genera by BA, and alpha-diversity as calculated by the Shannon diversity index..... 154
- Supplementary Table S3.1.** List of wavelength peak numbers associated with soil chemical properties. Adapted from Matamala et al. 2019. For complete list of references a-z, see Matamala et al. 2019..... 158
- Supplementary Table S4.1.** List of targeted KEGG ortholog enzymes used in the PICRUSt analyses. For more information see materials and methods in main text. 159
- Supplementary Table S4.2.** Effects of soil depth characteristics (Organic, Transition, Mineral) on soil chemistry, bacterial phylum relative abundance, and relative abundance of genes organized by functional groups, as determined by the Kruskal-Wallis test. Degrees of freedom=2 for all analyses. *= $p<0.05$, **= $p<0.01$, ***= $p<0.001$ 169
- Supplementary Table S4.3.** Statistical analyses of alpha diversity using non-parametric two-sample t-tests with 999 Monte Carlo permutations. Pairwise comparisons of Shannon diversity metrics from each sample were made between each soil layer (Organic, Transition, Mineral) and each snow accumulation treatment (Control, Deep, Intermediate, Low). *= $p<0.05$, **= $p<0.01$, ***= $p<0.001$ 170
- Supplementary Table S5.1.** Manually curated list of functions, as assigned by the KEGG orthologous classification system, organized by the roles they perform in the metabolism of specific carbohydrate groups related to organic matter, methane/CO₂ metabolism, nitrogen metabolism, and phosphorus metabolism. Columns 1-4 represent the KEGG classification tiers. “EC#” represents the enzyme commission number, “CAZy” represents the classifications from the Carbohydrate Active Enzymes database, and “Role” represents the role these functions were assigned to. See Figure 5.4. 176
- Supplementary Table S5.2.** Kruskal-Wallis and posthoc Nemenyi test results comparing the relative abundances of functional genes between snow fence treatment zones (Ctl, Deep, Int, Low). Genes are grouped into functional categories based on the SEED Subsystems

classification system. Posthoc Nemenyi test results are only shown for functional groups with Kruskal-Wallis p -values <0.15 and are displayed as the treatment zone with the highest abundance, followed by the treatment zone with the lowest abundance, followed by the p -value (e.g. “highest-lowest=0.10”). 202

LIST OF ABBREVIATIONS

AC	Ash-tree canopy Condition
AIC	Akaike Information Criterion
BA	Basal Area
C	Carbon
CAZy	Carbohydrate Active enZymes database
CCA	Constrained (Canonical) Correspondence Analysis
CMP	Carbon Mineralization Potential
dbRDA	distance-based Redundancy Analysis
DOC	Dissolved Organic Carbon
DNA	DeoxyRibonucleic Acid
EA	Elemental Analyzer
EAB	Emerald Ash Borer
EC	Enzyme Commission
FDR	False Discovery Rate
FTIR	Fourier Transformed InfraRed
GHG	Green House Gas
GH	Glycoside Hydrolase
GT	GlycosylTransferases
KEGG	Kyoto Encyclopedia of Genes and Genomes
KO	KEGG Orthology
MG-RAST	MetaGenomic Rapid Annotations using Subsystems Technology
MIR	Mid InfraRed

N	Nitrogen
OTU	Operational Taxonomic Unit
NMDS	Non-metric MultiDimensional Scaling
NPP	Net Primary Productivity
NEE	Net Ecosystem Exchange
OM	Organic Matter
P	Phosphorus
PCR	Polymerase Chain Reaction
RDA	Redundancy Analysis
rRNA	ribosomal RiboNucleic Acid
S	Sulfur
SE	Standard Error
SOC	Soil Organic Carbon
SOM	Soil Organic Matter
TC	Total Carbon
TCA	TriCarboxylic Acid
TN	Total Nitrogen
TOC	Total Organic Carbon
VIF	Variance Inflation Factors

SUMMARY

Soil microbial ecology is a rapidly evolving field of science dedicated to understanding how soil microorganisms interact with each other and their environment. The term “soil microorganisms” refers to bacteria, archaea, fungi, and viruses that live within the soil environment. They are an essential component to Earth’s ecosphere through the roles they play in biogeochemical cycling, decomposition processes, and nutrient regulation, all of which affect ecosystem scale productivity and global climate patterns. The ability of soil microbial communities to perform these functions is determined in part by the genetic capacity of the community to produce enzymes and other proteins required for biochemical transformations, and the rate at which these functions occur may be influenced by the abundance of microorganisms and their associated genetic capacities, as well as biotic and abiotic environmental factors that influence community structure and affect enzyme kinetics. This dissertation explores the relationships between soil microbial community structure, the genetic functional capacity of the community to decompose soil organic matter (SOM) and cycle nutrients, and variations in the biotic and abiotic environment.

Plant-microbe interactions have been an active area of research for decades, and while symbiotic relationships have been well established between plants and soil microbes, much less is known about taxa-specific associations or the mechanisms behind the establishment and maintenance of microbial community symbionts. Chapter 2 examines the relationships between soil bacterial communities and ash trees in temperate deciduous forest ecosystem impacted by the effects of emerald ash borer (EAB), an invasive beetle introduced from Asia that kills >99% of ash trees. The goal of this study was threefold; 1) to determine if ash trees associate with a unique assemblage of bacteria, 2) to predict potential functional shifts within the belowground

community and subsequent consequences for ecosystem dynamics in response to the loss of ash trees from the system, and 3) to explore relationships between bacterial relative abundances, the functional roles they facilitate, and tree community composition. In comparing plots that contained ash trees to those that did not, our results showed distinct differences in soil microbial community structure, primarily driven by differences in the Acidobacteria phylum. Greater estimated gene abundances for genes related to carbohydrate metabolism, sulfur cycling, and phosphorus cycling in plots without ash trees suggests that belowground functional capacity may also be affected by the presence (or loss) of ash trees. However, co-occurring influential factors such as soil pH or corollary relationships with other tree species could not be ruled out as underlying driving forces of bacterial community structure, thus making it difficult to predict the effects of the rapid removal of ash trees from this ecosystem due to emerald ash borer infestation. To resolve these issues and gain a more thorough understanding of how vegetation shifts might affect belowground dynamics requires a more detailed examination that separates and clarifies the relationships between soil chemistry and microbial community structure.

Compared to the rapid removal of a dominant tree species from a forest due pest infestation, vegetation shifts in the Arctic occur at a much slower pace, transitioning from tussock grass species to shrub or sedges species over decadal time scales. Due to major differences in climate and geology, Arctic soils have many unique characteristics that differentiate them from temperate forest soils. Seasonal freeze-thaw cycles repeatedly churn and mix the soil layers (*i.e.* cryoturbation) resulting in highly unaggregated soil structure with very high particulate organic matter content. Additionally, these soils contain nutrient-rich carbon (C) substrates that have been buried and frozen for long periods of time, potentially millennia, which has limited microbial decomposition of these substrates. As global temperatures rise, thawing soils may

alleviate this temperature limitation, resulting in increased rates of decomposition, microbial metabolism, and C mineralization, releasing greenhouse gases into the atmosphere, and further accelerating climate change. Chapter 3 examines how variations in temperature (via soil incubations) and soil chemistry (via site and soil layer differences) affect soil bacterial community structure, specifically identifying which bacterial taxa are most differentially affected by thawing soils from different soil layers and analyzing the relationships between these specific taxa and influential soil chemical factors characterized by Fourier transformed infrared (FTIR) spectroscopy. The results show that the greatest bacterial abundance responses to increased temperatures occur in permafrost soils and primarily occur in four taxonomic classes, Alpha-, Beta-, and Gammaproteobacteria, and Sphingobacteriia from the phylum Bacteroidetes. The relative abundances of these bacterial classes were also positively correlated with C mineralization, suggesting they may be major contributors to SOM decomposition in thawing permafrost soils. In addition, analysis of FTIR spectra showed absorbance peaks associated with silicates, and peak ratios associated with amides:aliphatics (a proxy for SOM degradation state), had the greatest influence in driving bacterial community structure. Altogether, these results provide insights into how FTIR spectral analysis may be used to predict bacterial community structure, and how Arctic bacterial communities respond to warming in the context of a controlled incubation laboratory experiment.

In chapter 4, I examine bacterial community responses to experimental soil warming within the context of their natural environment. Climate change predictions for Arctic regions include increased temperature and precipitation (*i.e.* more snow), resulting in increased winter soil insulation, increased soil temperature and moisture, and shifting plant community composition. Using an 18-year snow fence study site designed to mimic anticipated increases in precipitation

and temperature in the Arctic, I collected soil cores from three pre-established treatment zones representing varying degrees of snow accumulation, where Deep snow is approximately 100%, and Intermediate snow is approximately 50%, of increased snowpack relative to the control, and Low snow approximately 25% decreased snowpack relative to the control. We performed 16S rRNA amplicon sequencing to reveal phylogenetic community differences between samples and determine how soil bacterial communities might respond (structurally and functionally) to changes in winter precipitation and soil chemistry. We analyzed relative abundance changes of the six most abundant phyla (ranging from 82-96% of total detected phyla per sample) and found four (Acidobacteria, Actinobacteria, Verrucomicrobia, and Chloroflexi) responded to deepened snow. All six phyla correlated with at least one of the soil chemical properties (%C, %N, C:N, pH); however, a single predictor was not identified, suggesting that each bacterial phylum responds differently to soil characteristics. Overall, bacterial community structure (beta diversity) was found to be associated with the snow accumulation treatment and all soil chemical properties. Bacterial functional potential was inferred using ancestral state reconstruction (PICRUST) to approximate functional gene abundance, revealing a decreased abundance of genes required for SOM decomposition in the organic layers of the deep snow accumulation zones. These results suggest that predicted climate change scenarios may result in altered soil bacterial community structure and function, and indicate a reduction in decomposition potential, alleviated temperature limitations on extracellular enzymatic efficiency, or both. To more accurately determine the genetic functional responses of the soil microbial community to this long-term snow depth manipulation, further sequencing would be necessary.

Finally, in chapter 5 I use shotgun sequencing on the same metagenomic samples obtained in chapter 4 to further characterize the soil microbial community's functional responses to altered

snow accumulation, focusing on the community's genetic capacity to produce enzymes required for SOM decomposition and nutrient cycling, which will ultimately influence the fate of C stored in this ecosystem. In addition to more reliable functional information, shotgun sequencing also provides information on fungal community dynamics in relation to bacteria. We found that soil microbial communities under deeper snowpack have higher bacteria:fungi relative abundance ratios, decreased relative abundance of genes encoding enzymes for the breakdown of hemicellulose, chitin, and starch, and increased relative abundance of genes required for nitrogen fixation, ammonification, and nitrate reduction, but only past a snow-depth threshold 50-100% greater than the control. Additionally, genetic evidence suggested a phosphorus substrate preference shift from insoluble to soluble organic forms with increasing snow pack. These results substantiate the results from chapter 4 and suggest predicted increased snowfall and soil temperatures in the Arctic may 1) increase soil nutrient availability, potentially facilitating plant community shifts, and 2) decrease fungal abundance leading to reduced SOM decomposition potential and the possible re-accrual of soil C in this ecosystem over time.

*Some days are different.
One could almost believe that one day is just like another.
But some days have something a little more.
Nothing much.
Just a small thing.
Tiny.
Most of the time we don't notice these things,
Because little things are not made to be noticed.
They are there to be discovered.
When we take the time to look for them...
the small things appear.
Here or there.
Tiny.
But suddenly so present...
they seem enormous.
The small things are treasures.
True treasures.
There are no greater treasures than the little things.
One is enough to enrich the moment.
Just one is enough to change the world.*

Selection from "Little Bird" by Germano Zullo

1 PERSONAL STATEMENT

1.1 In the beginning... Motivation

Upon entering graduate school, I had only a vague idea of the direction my research would take. I did not have a M.S. degree project that I might continue or that might lead me into more focused areas of interest. I was not “continuing” my education so much as going back to it. Having graduated with a B.S. degree in cell and structural biology over decade earlier, my path back to graduate school was a winding one. I had chosen an atypical career path after graduation, deciding that instead of focusing on a career in clinical laboratory work, I would focus on being a musician in a touring rock band. And although unstable, this period of my life was integral in developing a conception and philosophy of existence and mankind’s role in it, by broadening my horizons, opening my eyes to the larger world, and allowing me to immerse myself in nonfiction books, the most influential of which include Hawking 1988, Sheldrake 1990, Wilson 1992, 1998, Chapin et al. 2002. Years of touring resulted in endless hours in the van on the way to the next show, providing ample time for reading and reflection, as an ever changing and often beautiful landscape passed by. It was during this time that a passion for environmental science and conservation began to emerge, spurred by the realization that non-human life on Earth was under one of the greatest threats it has faced in millennia, the ever-growing human population. With previous experience in microbiology working in hospital laboratories and a deep seeded interest in agriculture having grown up in a farming family, my curiosities were driven naturally towards the field of soil microbial ecology, one of the fastest growing fields of science with enormous potential for discovery and application. And thus, my graduate journey into soil science, microbial genomics, and ecosystem dynamics had begun.

1.2 Being small in a large world

My first few years in graduate school were exploratory. I tried and failed many times to set up laboratory experiments based on my developing ideas, which at the time were very scattered. However, each failure led to a new idea, typically inspired from reading the literature. Reading was essential to my development during this stage. Review articles helped to provide context into the current state of the field, revealing unanswered questions, identifying useful laboratory and field techniques, and providing literature for further reading. I began to realize the degree of complexity inherent in soil ecosystems and to understand the challenges associated not only with identifying and characterizing soil microbial communities, but also with determining how they might affect global processes, and in turn, be affected by them.

Soil microbes primarily affect larger scale properties through their metabolic activity, biogeochemical cycling, and decomposition processes, which regulate nutrient turnover affecting plant community diversity and productivity (Van Der Heijden et al. 2008), and release a variety of gases into the atmosphere, including a number of greenhouse gases such as N₂O, CO₂, and CH₄ (Oertel et al. 2016). Because of the extraordinarily vast number of microbes in the environment, these processes easily scale up to global level importance. Some estimates predict the total number of prokaryotic cells on Earth to be $4-6 \times 10^{30}$, equaling 350–550 Pg of C, with 2.6×10^{29} of those inhabiting soils (Whitman et al. 1998). However, bacterial abundances can vary greatly between geographic regions, habitats, and ecosystem types due to differences in climate, topography, or other environmental factors, and this can affect the amount of influence microorganisms may have in any particular system. In the following years, the more I learned about microbial controls over ecosystem dynamics, as well as environmental influences over soil microbial community structure, the more focused my interests became. This idea of something

so small having such a large impact is a dichotomy that continues to fascinate me, and linking these spatial scales became a primary motivator in my research moving forward.

1.3 The soil environment

The soil environment is unique in its complexity. There are many soil types, made up of varying materials, structures, chemistries, and other characteristics unique to each ecosystem and changing with soil depth. The soil matrix is made up of minerals, organic matter, water, and pore space, and its structure, which is partially determined by soil aggregate formation, is often changing as physical and biological processes occur (Bronick and Lal 2005). Soil microorganisms live within this soil matrix, typically in the pore spaces, in water films, or attached to the surfaces of organo-mineral complexes in biofilms (Young and Crawford 2004, Flemming and Wingender 2010). In addition, soil microbes have evolved alongside a myriad of other organisms, including micro- and macrofauna and rooting plant species, and therefore many have become obligate symbionts, requiring a consortium of other microorganisms, or perhaps a host symbiont such as a plant or an animal, to perform necessary life functions (Zilber-Rosenberg and Rosenberg 2008, Lambers et al. 2009). This makes soil microorganisms very difficult to culture, isolate and characterize *in vitro* using standard microbiological techniques. Prior to genomic sequencing technology, it is estimated that only 0.1 to 1% of soil microbes were known (Torsvik et al. 2002, Rappé and Giovannoni 2003), however current estimates now predict global microbial diversity to exceed 1 trillion species (Locey and Lennon 2016). Therefore, it soon became obvious that to address my emerging questions related to how soil microbial communities respond to changing environments would require the use of modern genomic techniques in concert with experimental field manipulations or opportunistic natural

disturbances, and soil chemical/physical characterization.

1.4 Modern tools and technology – The age of genomics

After determining the types of data I would need to explore soil microbial communities in their natural environments, I began searching for opportunities and funding to initiate my projects. While high-throughput sequencing methods have become more affordable, it can still be relatively expensive. Fortunately, I was able to become involved in previously established projects/experiments that fit well with my research questions and was able to secure funding for genomic sequencing of soil microbial communities which would provide me with an enormous wealth of taxonomic and functional data. As opposed to older microbiology methods which must remove the organism from its natural environment for characterization, the sequencing approach instead allows the direct extraction of genomic materials from a minimally disturbed environment, essentially providing researchers with a snapshot of the microbial community and its genetic functional capacity.

However, it is important to recognize the many caveats that exist when using these methods, some of which stem from technical variation and uncertainty associated with sample collection, nucleic acid extraction, PCR amplification, and sequencing bias, but others that are inherent to microbial ecology, such as varying gene copy numbers between different microorganisms. These caveats, which also inevitably result in proportional data, can make it difficult to draw biologically meaningful or accurate conclusions and has spurred the development of entirely new areas of research in bioinformatics and statistical analysis. Thus, in order for me to understand and correctly interpret my results, I had to gain a basic understanding of these methods. Learning various computer languages (*i.e.* unix/linux, python, R) to work with large genomic files and

data sets, while simultaneously learning how and when to use constantly evolving statistical analyses, was one of the most challenging periods of my graduate school experience. However, it was necessary in order to identify patterns within such large data sets linking soil microbial abundances to both biotic and abiotic environmental factors, which act on each other both directly and indirectly. These relationships, interactions, and feedbacks are at the heart the challenges we face as microbial ecologists and is what makes the study of soil microbial dynamics so complex. And this led me to the development of a conceptual framework from which I could more holistically interpret my results (Figure 1.1). Using this context as a guide enabled me to more fully understand what could be happening in any given ecosystem, and how and why soil microbial communities respond the way they do to changing environments. The following chapters provide examples of this and have launched me into a brave new world of emerging questions and bright horizons. Enjoy the ride!

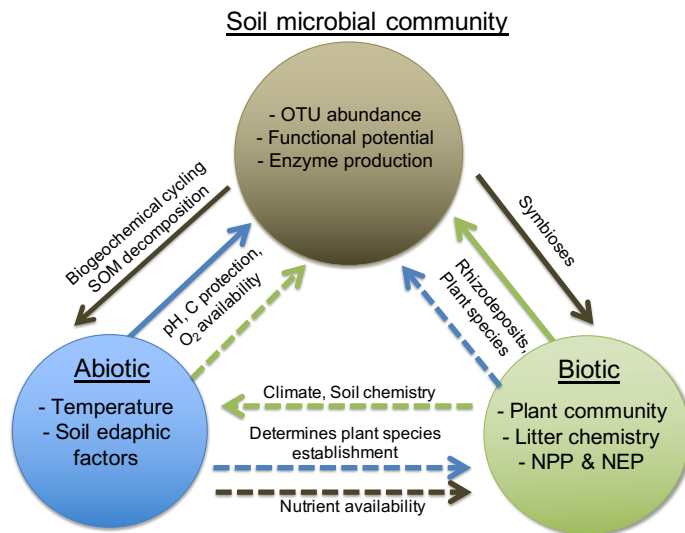


Figure 1.1. Conceptual diagram representing the relationships, interactions, and feedbacks that occur between soil microorganisms and both biotic and abiotic environmental factors. Solid lines indicate direct effects while dotted lines indicate indirect effects.

1.5 References

- Bronick, C. J., and R. Lal. 2005. Soil structure and management: A review. *Geoderma* 124:3–22.
- Chapin, F. S. I., P. A. Matson, and H. A. Mooney. 2002. *Principles of Terrestrial Ecosystem Ecology*. 1st edition. Springer-Verlag, New York, NY.
- Flemming, H. C., and J. Wingender. 2010. The biofilm matrix. *Nature Reviews Microbiology* 8:623–633.
- Hawking, S. W. 1988. *A Brief History of Time: From the Big Bang to Black Holes*. 1st edition. Bantam Books, New York, NY.
- Van Der Heijden, M. G. A., R. D. Bardgett, and N. M. Van Straalen. 2008. The unseen majority: Soil microbes as drivers of plant diversity and productivity in terrestrial ecosystems. *Ecology Letters* 11:296–310.
- Lambers, H., C. Mougél, B. Jaillard, and P. Hinsinger. 2009. Plant-microbe-soil interactions in the rhizosphere: an evolutionary perspective. *Plant and Soil* 321:83–115.
- Locey, K. J., and J. T. Lennon. 2016. Scaling laws predict global microbial diversity. *Proceedings of the National Academy of Sciences*:1–6.
- Oertel, C., J. Matschullat, K. Zurba, F. Zimmermann, and S. Erasmi. 2016. Greenhouse gas emissions from soils—A review. *Chemie der Erde - Geochemistry* 76:327–352.
- Rappé, M. S., and S. J. Giovannoni. 2003. The uncultured microbial majority. *Annual Reviews in Microbiology* 57:369–394.
- Sheldrake, R. 1990. *The Rebirth of Nature*. 1st edition. Rider.
- Torsvik, V., L. Øvreås, and L. Ovreas. 2002. Microbial diversity and function in soil: from genes to ecosystems. *Current opinion in microbiology* 5:240–5.
- Whitman, W. B., D. C. Coleman, and W. J. Wiebe. 1998. Prokaryotes: The unseen majority. *Proceedings of the National Academy of Sciences* 95:6578–6583.
- Wilson, E. O. 1992. *The Diversity of Life*. 10th edition. The Belknap Press of Harvard University Press, Cambridge, Massachusetts.
- Wilson, E. O. 1998. *Consilience: The Unity of Knowledge*. 1st edition. Alfred A. Knopf, Inc, New York, NY.
- Young, I. M., and J. W. Crawford. 2004. Interactions and self-organization in the soil-microbe complex. *Science* 304:1634–1637.

Zilber-Rosenberg, I., and E. Rosenberg. 2008. Role of microorganisms in the evolution of animals and plants: The hologenome theory of evolution. *FEMS Microbiology Reviews* 32:723–735.

2 EVIDENCE OF ASH TREE (*FRAXINUS SPP.*) SPECIFIC ASSOCIATIONS WITH SOIL BACTERIAL COMMUNITY STRUCTURE AND FUNCTIONAL CAPACITY

This chapter is a reprint (with minimal reformatting) of an original article published by MDPI journals in the journal *Forests*. It has been licensed under an open access Creative Commons CC BY 4.0 license, where the authors retain the copyright. There is no need for reproduction permissions from the publisher.

Ricketts, M. P., C. E. Flower, K. S. Knight, and M. A. Gonzalez-Meler. 2018. Evidence of ash tree (*Fraxinus spp.*) specific associations with soil bacterial community structure and functional capacity. *Forests* 9:1–16.

2.1 Introduction

Anthropogenic disturbances to Earth's ecosystems have the potential to alter the abundances and distributions of organisms worldwide, (Parmesan and Yohe 2003; Settele et al. 2014) and therefore the structure and function of their environments (Cramer et al. 2001; Drewniak and Gonzalez-Meler 2017; Gonzalez-Meler, Rucks, and Aubanell 2014; McNickle et al. 2016). Such disturbances include warming air temperatures, changing precipitation patterns, severe weather events, atmospheric nutrient deposition, or the introduction of invasive species. In temperate forest ecosystems of eastern North America, ash trees (*Fraxinus spp.*) have suffered significant declines over the past two decades due to the infestation of the invasive emerald ash borer (EAB; *Agrilus planipennis*), a wood boring beetle introduced from Asia (Cappaert et al. 2005; Wang et al. 2010). The EAB selectively deposits eggs on the bark of ash trees where hatched larvae burrow into cambial tissue to feed, creating serpentine galleries and severing the distribution of water and nutrients between the roots and shoots (Flower et al. 2018). This results in ~99% ash tree mortality within two to five years after infestation (McCullough and Katovich 2004; Knight, Robert, and Rebeck 2008) and complete mortality within a stand in roughly five to seven years. (Costilow, Knight, and Flower 2017). Ash trees are widely distributed throughout North America

and are a major component of forest and urban tree communities, representing roughly 2.5% of the aboveground biomass stocks in the US and storing ~0.303 Pg of carbon (C) (Birdsey 1992; Birdsey and Heath 1995; Goodale et al. 2002; Flower, Knight, and Gonzalez-Meler 2013). The widespread decline of ash has multiple cascading effects on ecosystem productivity, structure, and function, as the transformation from live standing biomass to fallen trees (Higham et al. 2017), plant litter, and soil organic matter (SOM) unfolds. Specifically, rapidly reduced water flux and plant respiration, coupled with large inputs of coarse woody debris and altered tree community composition, may significantly alter ecosystem hydrology, C and nutrient dynamics, forest tree community succession, edaphic factors, and belowground microbial community structure and function (Lovett et al. 2006; Telander et al. 2015; Flower and Gonzalez-Meler 2015; Flower et al. 2018).

Soil microorganisms play a key role in the decomposition of SOM and regulation of nutrient availability to plants (Hopkins et al. 2013; Cheng et al. 2014), both of which have important implications for ecosystem biogeochemical cycling and net primary productivity (NPP) (Van Der Heijden, Bardgett, and Van Straalen 2008). Microbial functional responses to disturbances or environmental shifts, such as EAB-induced ash decline, are dependent on the microbial community's resilience to change and the degree of functional redundancy within the community (Allison and Martiny 2008). While functional redundancies often exist between microbial taxa, large shifts in microbial community structure may result in the altered functional capacity of the community to access and degrade SOM or perform nutrient transformations and mobilization (Ricketts et al. 2016; Bailey et al. 2013; Schimel and Schaeffer 2012; Allison and Martiny 2008). Thus, identifying factors that influence microbial community structure is important to understanding potential changes in the functions of decomposers. A variety of edaphic factors

are thought to influence soil microorganisms, including pH, C-availability, moisture, O₂ availability, and bulk density (Fierer 2017). In particular, soil pH has been shown to be one of the governing forces driving soil microbial community structure (Fierer and Jackson 2006; Lauber et al. 2009; Cho, Kim, and Lee 2016). Aboveground vegetation may also influence belowground microbial community structure, with specific plant species associating with (and even recruiting) unique microbial assemblages (Schlatter et al. 2015; Bakker, Bradeen, and Kinkel 2013; Prescott and Grayston 2013). These above-belowground associations are most often studied at the community or ecosystem level (*e.g.* forest *vs.* grassland, deciduous *vs.* coniferous forests), while soil microbial associations with individual plant species or genera remain poorly understood.

This study aimed to examine soil microbial community associations with ash trees to better understand belowground consequences of EAB disturbance. Microbial functional potentials were estimated with respect to nutrient and C-cycling processes that, in turn, may affect forest recovery trajectories. If soil microbes exhibit a different community structure under stands with ash trees when compared to stands without ash trees, this would suggest a strong, genera specific relationship between the presence of, decline of, or mortality of ash trees and soil microbial communities. If instead belowground microbial communities are similar across the heterogeneous forest landscape, this would indicate a whole forest, community level influence governed by varying degrees of environmental, physical, and edaphic factors. To address these competing hypotheses, we used 16S rRNA metagenomic sequencing methods, which specifically target bacterial and archaeal organisms, to analyze archived soil DNA samples collected from paired ash and non-ash forest plots in 2011 during the early stages of EAB infestation. If differences were observed in the soil bacterial community structure between ash and non-ash

plots, then we expected the functional potential to cycle C and nutrients to reflect the specific differences in the bacterial community. This work provides a unique snapshot of soil bacterial communities, their functional potentials, and their associations with dominant tree genera, during the early stages of EAB disturbance in an ash-dominated forest near the core area of infestation.

2.2 Materials and Methods

2.2.1 Site description

In 2011, four forest sites, Bohannon Nature Preserve (BHN), Kraus Nature Preserve (KRS), Seymour Woods State Nature Preserve (SYM), and Stratford Ecological Center (STR), were selected within Delaware County, Ohio (Figure 2.1 and Table 2.1). These sites are secondary successional forests largely dominated by ash (*Fraxinus americana* L., *F. pennsylvanica* Marshall and *F. quadrangulata*). Other canopy tree genera include maple (*Acer saccharinum*, *A. saccharum*, *A. rubrum*), oak (*Quercus palustris*, *Q. rubra*, *Q. alba*.), beech (*Fagus grandifolia*), shagbark hickory (*Carya ovata*), cottonwood (*Populus deltoids*), elm (*Ulmus americana*, *U. rubrum*), black cherry (*Prunus serotina*), black walnut (*Juglans nigra*), and willow (*Salix* spp.).

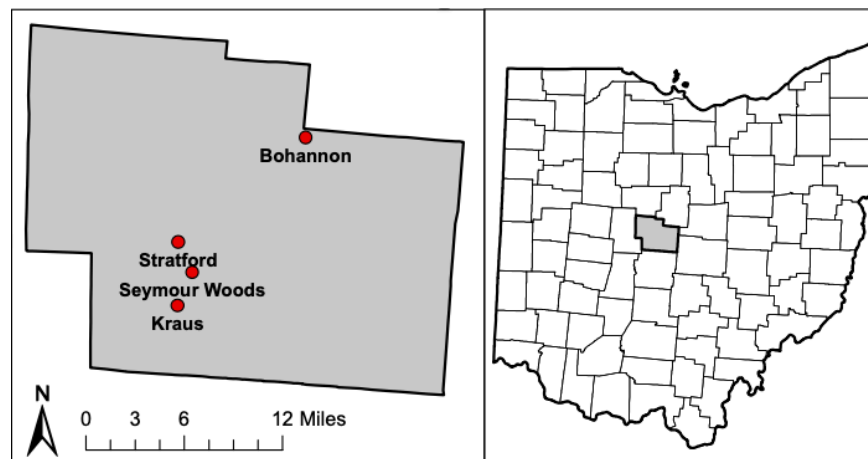


Figure 2.1. Map of study sites within Delaware county, Ohio.

Table 2.1. Summary of site characteristics.

Forest	Soil Type ¹	Number of plots (Ash / Non-ash)	Basal area (m ² /ha)	Relative BA of ash trees (%)
Bohannon Woods (BHN)	Cardington silt loam	3 /2	37.7±2.5	49.3±5.7
Kraus Woods (KRS)	Glynwood silt loam	3 /2	34.7±3.0	63.2±4.4
Seymour (SYM)	Blount silt loam	2 /2	26.0±3.0	46.5±6.0
Stratford (STR)	Glynwood silt loam	3 /3	33.9±5.0	35.5±13.0

¹ Primary soil type ascertained from NRCS web soil survey

In each site, we randomly established two or three “ash” plots (11.28 m radius), which contained ash trees as a major component of the canopy ($48.8 \pm 4.8\%$ (mean \pm S.E.) of total basal area), and two or three “non-ash” plots, which did not contain ash trees as a major component of the understory or canopy (defined as $<5\%$ of total basal area; see Table 2.1 and Supplementary Table S2.3 for details). Ash and non-ash plots were located between 50–100 m away from one another and were selected to represent similar topography, soil type, and moisture regimes. Within each plot, trees >10 cm in diameter at breast height were identified and measured and the total basal area (BA) per hectare (m²/ha), number of stems per hectare (#/ha), and relative tree dominance (%) by BA were calculated (Table 2.1 and Supplementary Table S2.3).

By 2011, EAB had reached forests of central Ohio and ash trees had begun to exhibit visual symptoms of infestation at our sites. While this may not be ideal for establishing baseline associations with healthy ash trees, we were able to collect samples in the early stages of EAB infestation before complete ash mortality occurred, which is rapidly becoming more difficult to find in high-density ash tree forests. To quantify the health of trees within the plots, we used ash

tree canopy condition (AC), a metric for tracking the health of ash trees exposed to EAB, which is correlated to EAB densities and tree physiology (Flower et al. 2013; Smith 2006). This assessment is a non-linear five-point categorical scale which assigns healthy trees a value of 1 and standing dead trees a value of 5. At the plot-level, ash canopy health was calculated as the mean AC of all ash trees within a plot. To account for the potential effects associated with ash trees in later states of decline, we performed a separate analysis which removed all sites that contained any plots with mean AC scores >3, resulting in two sites consisting of six ash (AC=2.42 ± 0.30) and four non-ash plots (Supplementary Table S2.1).

2.2.2 Soil collection and characterization

To characterize potential associations between ash trees and soil bacterial communities, we randomly selected 30 locations in each plot and extracted 0–10 cm soil cores with a 1.9 cm diameter soil probe (Oakfield Model L tube sampler soil probe), which was cleaned and sterilized with 100% ethanol between plots. Soils were sampled in late July during the peak period of NPP. Roots were removed and soil samples from each plot were homogenized on site, placed in a cooler with dry ice, and stored at –80 °C until DNA extraction. Soil subsamples were analyzed for pH and a variety of solubilized soil minerals (Ca, K, Mg, P, Al, B, Cu, Fe, Mn, Na, S, and Zn) by the University of Maine Soils Lab using a modified Morgan nutrient extraction procedure and a TJA Model 975 AtomComp ICP-AES. Soil C and nitrogen (N) concentrations (%) were measured at the University of Illinois at Chicago (UIC) Stable Isotope lab using a Costech (Valencia, CA, USA) elemental analyzer (EA). Prior to analysis, samples were dried until no mass lost in a 60 °C oven, pulverized using a ball mill, and ~5mg of sample was placed into a tin capsule.

2.2.3 DNA extraction, sequencing, quality control and bioinformatics

DNA was extracted from ~0.25g of each soil sample using MoBio's PowerSoil[®]-htp 96 Well Soil DNA Isolation Kit as per the manufacturer's protocol. The V4 region of the 16S SSU rRNA gene was amplified using PCR primers 515F/806R following protocols outlined by the Earth Microbiome Project (Gilbert, Jansson, and Knight 2014). Final amplicon DNA concentrations were quantified using the PicoGreen[®] dsDNA Assay Kit and amplicons were sequenced using an Illumina MiSeq instrument (2 × 150 bp paired-end). All sequences have been deposited in the NCBI Sequence Read Archive under SRA study #SRP136455. Initial sequence data quality filtering, paired-end assembly, demultiplexing, closed reference operational taxonomic unit (OTU) picking, and phylogenetic assignments were performed using the QIIME software package version 1.9.1 (<http://qiime.org/>) (Caporaso, Kuczynski, and Stombaugh 2010). OTU abundance data was normalized to account for estimated 16S rRNA gene copy number within each OTU assignment using the python script *normalize_by_copy_number.py* from the PICRUST software package (Langille et al. 2013). OTU picking identified 9387 OTU's, with an average of 2283 ± 146 OTU's per sample. In total, there were 39 phyla identified, the 10 most abundant of which encompassed 98% of all bacteria/archaea. Sequences were rarefied at 5900 sequences per sample for diversity analysis. More detailed methods can be found in Ricketts *et al.*, 2016 (Ricketts et al. 2016).

The genetic functional potential of bacterial/archaeal communities was determined by estimating gene abundance using the PICRUST software package version 1.1.0 (<http://picrust.github.io/picrust/>) (Langille et al. 2013). Genetic pathways necessary for biogeochemical metabolisms were selected based on the KEGG ortholog hierarchical system, which is a knowledge database dedicated to linking genomic information to cellular and

metabolic functional pathways (Kanehisa and Goto 2000). This framework allows individual gene abundance data to be collated into broader functional groups, providing a more practical basis for functional gene analysis. We focused our analysis specifically on the energy metabolism and carbohydrate metabolism level 2 KEGG groups. Within these groups, all level 3 KEGG metabolic pathways, organized at a finer functional scale, were also analyzed.

2.2.4 *Statistical analyses*

Bacterial community differences were explored by examining Hellinger transformed abundance data in two ways. First, the bacterial abundance differences of the 10 most abundant phyla (98.1% of total bacteria), the 20 most abundant classes (93.8% of total bacteria), and the 30 most abundant orders (90.9% of total bacteria), were analyzed between ash and non-ash plots using Mann–Whitney U tests and between sites using Kruskal-Wallis and posthoc Nemenyi tests, both with a significance threshold of $p < 0.05$, using the R statistical program (R Core Team 2013). Second, overall bacterial community structure differences between ash and non-ash plots and between sites, were analyzed by comparing Bray-Curtis dissimilarity matrices of Hellinger transformed bacterial abundances using adonis tests (similar to PERMANOVA) in R with 99,999 permutations. Assumptions of the adonis test were verified using the *betadisper* function in the R package *vegan* (Oksanen et al. 2017), which tests the multivariate homogeneity of group dispersions (variances). A non-metric multidimensional scaling (NMDS) plot (stress=0.080, Shepard plot non-metric $R^2=0.994$) was created using the R package *phyloseq* (McMurdie and Holmes 2013) and the same Bray–Curtis dissimilarity matrices to visualize differences in bacterial community structure between ash and non-ash plots and sites.

All other variables, including AC, BA, stem density, relative tree dominance, bacterial and

tree alpha-diversities (Shannon diversity index), and soil factors, were analyzed for differences between ash and non-ash plots using Mann-Whitney U tests ($p < 0.05$) and for differences between sites using Kruskal-Wallis with the posthoc Nemenyi tests ($p < 0.05$). Euclidean distance matrices constructed from each variable using the *dist* function in the R package *vegan* (Oksanen et al. 2017) were compared to the soil bacterial community Bray-Curtis distance matrix (described above) using Mantel tests ($p < 0.05$) to determine how strongly each variable correlated with (or influenced) bacterial community structure. In addition, the overall soil environment was analyzed by combining all soil variables into a single Euclidian dissimilarity matrix, which was tested for ash vs. non-ash differences and site differences using adonis tests and effects on bacterial community structure using a Mantel test. To better understand the effects of EAB-induced tree stress on bacterial community structure within ash plots, linear relationships between mean AC and the ten most abundant bacterial phyla were analyzed and a Mantel test for mean AC (as described above) was performed using only ash plots.

Ash vs. non-ash differences in PICRUSt estimated functional gene abundances for the selected KEGG ortholog groups were tested in STAMP (Parks et al. 2014) using Welch's two-tailed t -test. To assess the significance and adjust for potential false discoveries, we utilized the Benjamini-Hochberg procedure where original p -values were ranked in order of significance, multiplied by the number of comparisons (Lvl 2 $n=64$, Lvl 3 $n=328$), and divided by their respective rank numbers to obtain a corrected p -value (q -value). The significance threshold used was $q < 0.05$. In addition, Pearson's correlations were used to determine relationships between Hellinger transformed bacterial phyla abundance and level 3 KEGG ortholog functional group gene abundance. To account for potential false discoveries here, we used the more conservative Bonferroni adjustment, where original p -values are simply multiplied by the number of

comparisons ($n=240$) and assigned a threshold of $p<0.05$. It is important to remember that relationships between bacterial abundance and gene abundance are predetermined by algorithms used by the PICRUSt software, as all estimated gene abundance information is directly derived from bacterial abundance data in combination with genomic databases. However, it does provide information on inherent functional relationships within each bacterial phylum and reveals potential differences in function as a result of abundance differences in individual bacterial taxonomic groups.

2.3 **Results**

2.3.1 *Environmental and site differences*

The overall soil environment was similar between ash and non-ash plots (adonis $H=0.098$, $p=0.065$), but differed across sites (adonis $H=0.301$, $p=0.003$). Specifically, only two of the 16 soil variables, Cu ($W=12.5$, $p=0.006$) and Fe ($W=18$, $p=0.016$), differed between ash and non-ash plots (Table 2.2), where Cu and Fe were both greater in non-ash plots. Between sites, the %C ($H=11.51$, $p=0.009$), %N ($H=12.96$, $p=0.005$), C:N ($H=10.15$, $p=0.017$), P ($H=12.35$, $p=0.006$), Al ($H=9.71$, $p=0.021$), and Zn ($H=9.79$, $p=0.020$) were different (Table 2.2). Posthoc tests revealed both %C and %N to be significantly lower at SYM compared to the other sites, while C:N remained constant across sites, with the exception of being significantly lower at BHN. Similarly, soil P, Al, and Zn were lower at SYM (Supplementary Table S2.2).

Analysis of non-soil variables revealed ash tree health (mean AC) to be variable between sites ($H=9.24$, $p=0.026$; Table 2.2). Total BA (m^2/ha) did not differ between ash and non-ash plots or between sites, although it was somewhat lower at SYM where the stem density ($\#/ha$) was highest ($H=8.78$, $p=0.032$) due to a large number of small trees (Supplementary Table S2.2).

and Supplementary Table S2.3). Of the five most abundant tree genera, only oak species relative dominance differed between ash and non-ash plots ($p=0.003$) and only beech tree relative dominance differed between sites ($p=0.007$; Table 2.2). Oak trees had a higher relative dominance in non-ash plots vs. ash plots and beech trees were more dominant in KRS than any of the other sites. Tree community alpha-diversity was not different between plots ($W=60.5$,

Table 2.2. Summary of statistical results. Adonis tests were used to analyze differences in overall bacterial community structure and overall soil chemical characteristics between categorical variables (a). Continuous variables were analyzed individually (b) for differences between ash and non-ash plots (Mann-Whitney U test), differences in forest sites (Kruskal-Wallis), and for correlations between overall bacterial community structure and individual variables (Mantel test). Text in bold and italics represents a significant result ($p<0.05$).

(a)	Adonis test					
	Bacterial community		Soil environment			
Categorical variables	R^2	p -value	R^2	p -value		
Ash v. Non-ash	0.334	0.002	0.098	0.066		
Forest site	0.140	0.502	0.301	0.003		
(b)	Mann-Whitney U test (Ash v. Non-ash)		Kruskal-Wallis test (Forest site; $df=3$)		Mantel test (Bacterial community)	
Continuous variables	W	p -value	H	p -value	r -statistic	p -value
Mean AC (ash only)	-	-	9.24	0.026	-0.060	0.620
Mean Stems (#/ha)	75.5	0.051	8.78	0.032	-0.127	0.870
Mean BA (m ² /ha)	69	0.152	5.23	0.156	0.060	0.261
Soil pH	73	0.080	3.88	0.275	0.289	0.006
%C	49.5	1.000	11.51	0.009	-0.173	0.981
%N	58	0.541	12.96	0.005	-0.175	0.986
C:N	34.5	0.270	10.15	0.017	-0.134	0.911
Ca	69	0.152	4.53	0.210	0.304	0.007
K	42	0.603	3.71	0.295	-0.030	0.594
Mg	67	0.201	4.81	0.186	0.274	0.011
P	49	1.000	12.35	0.006	-0.088	0.846
Al	29	0.131	9.71	0.021	0.177	0.045
B	40	0.494	3.64	0.303	-0.075	0.708
Cu	12.5	0.006	0.32	0.957	0.047	0.304
Fe	18	0.016	1.49	0.685	0.273	0.010

Mn	48	0.941	2.11	0.550	-0.143	0.921
Na	56	0.656	6.37	0.095	0.002	0.439
S	24	0.056	0.88	0.831	-0.143	0.924
Zn	40	0.503	9.79	0.020	0.083	0.241

$p=0.425$) or sites ($H=5.67$, $p=0.129$) and did not correlate with the soil bacterial community (mantel r -statistic $=-0.048$, $p=0.631$; Table 2.2 and Supplementary Table S2.2).

2.3.2 Bacterial community differences

Soil bacterial community structure (*i.e.* beta-diversity) differed between ash and non-ash plots (adonis $R^2=0.334$, $p=0.002$), but not between sites (adonis $R^2=0.140$, $p=0.501$; Figure 2.2 and Table 2.2). Ash tree relative dominance was the only tree genera to show a significant correlation with bacterial community structure (mantel r -statistic $=0.264$, $p=0.007$). Although the overall soil environment did not show a strong relationship with bacterial community structure (mantel r -statistic $=0.053$, $p=0.305$), certain individual soil variables did, including soil pH (mantel r -statistic $=0.289$, $p=0.006$), Ca (mantel r -statistic $=0.304$, $p=0.007$), Mg (mantel r -statistic $=0.274$, $p=0.011$), and Al (mantel r -statistic $=0.177$, $p=0.045$; Table 2.2). It should be noted that Mg, Ca, and Al are all highly correlated with soil pH (>0.79 , $p<0.001$).

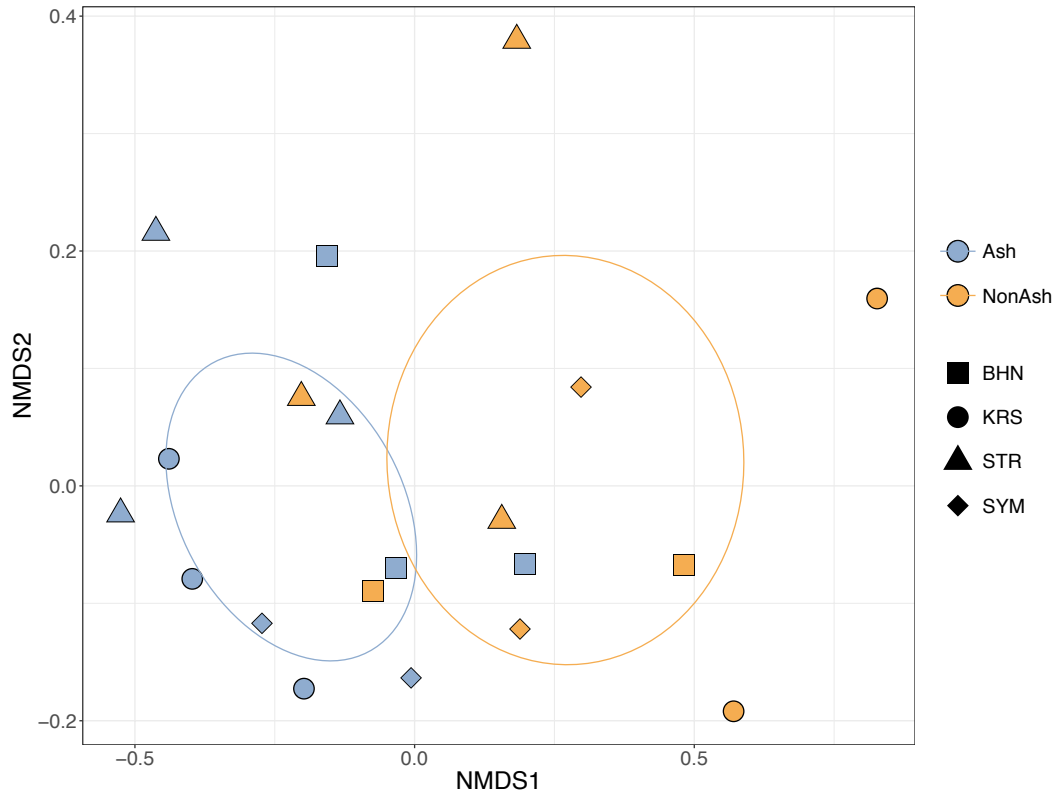


Figure 2.2. Non-metric multidimensional scaling (NMDS) plot where each point represents the bacterial/archaeal community structure of a sample (stress=0.080, Shepard plot non-metric $R^2=0.992$). Color indicates ash v. non-ash plots and shape indicates forest site. Ellipses represent 95% confidence intervals of centroids for ash and non-ash plots. Bacterial/archaeal community structures differed significantly between ash and non-ash plots (adonis $p=0.002$).

We also found significant differences between ash and non-ash plots in the relative abundances of seven out of 10 of the most abundant bacterial phyla (Figure 2.3); however, between forest sites, there were no abundance differences in any of the phyla. Likewise, EAB-induced tree stress (*i.e.* mean AC) did not affect bacterial abundances (Figure 2.4). All phyla were less abundant in non-ash plots, except Acidobacteria and Elusimicrobia, which were more abundant in non-ash plots ($p=0.004$ and $p=0.261$ respectively). At finer taxonomic levels, these differences were not as noticeable, with only two out of 20 of the most abundant classes and two out of 30 of the most abundant orders showing significant differences between ash and non-ash

plots (Supplementary Figure S2.1 and Supplementary Figure S2.2). Interestingly, all four of these differences were in the Actinobacteria phylum, which were more abundant in the ash plots. Soil bacterial alpha-diversity did not vary between ash and non-ash plots ($W=54$, $p=0.766$) or between sites ($H=4.07$, $p=0.254$) and showed no relationship with bacterial community structure (mantel r -statistic=0.264, $p=0.007$; Table 2.2 and Supplementary Figure S2.2).

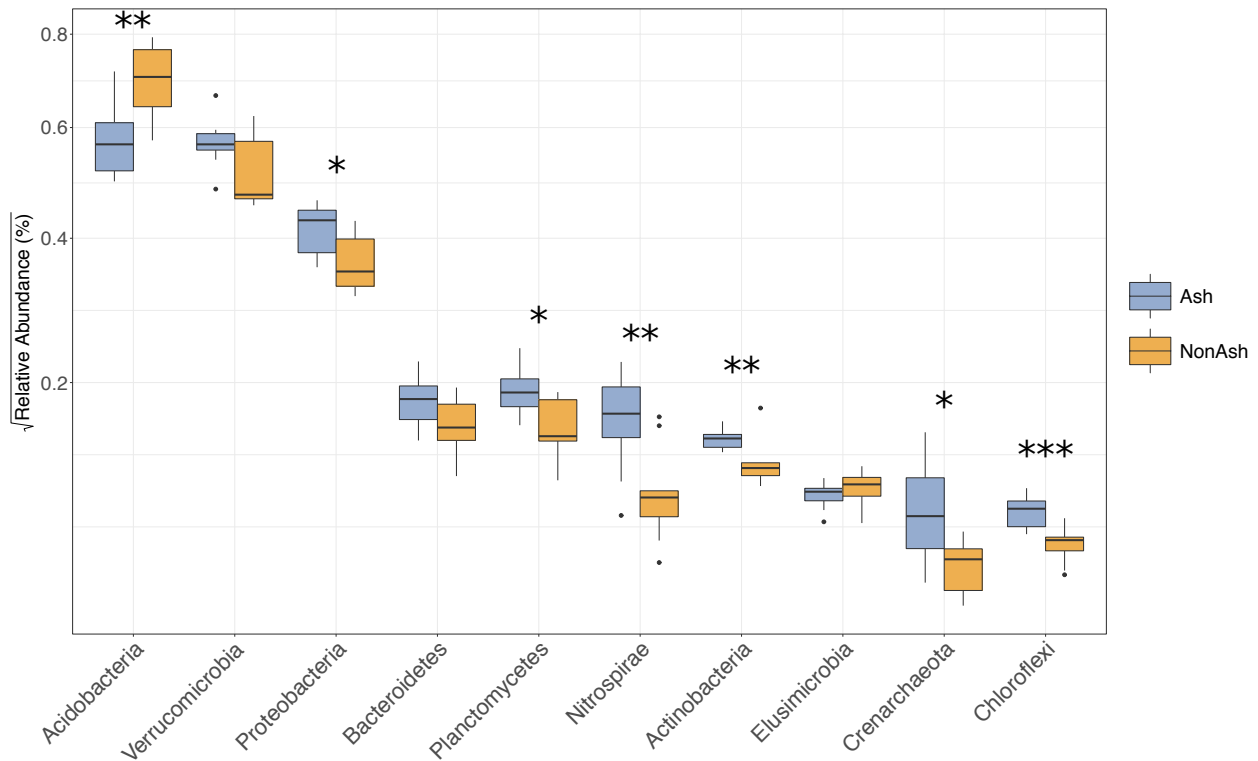


Figure 2.3. Boxplot comparing the average Hellinger transformed abundances of the 10 most abundant bacterial/archaeal phyla between ash (blue) and non-ash (orange) plots. Mann-Whitney U -test significance is denoted by asterisks, where $*=p<0.05$, $**=p<0.01$, and $***=p<0.001$.

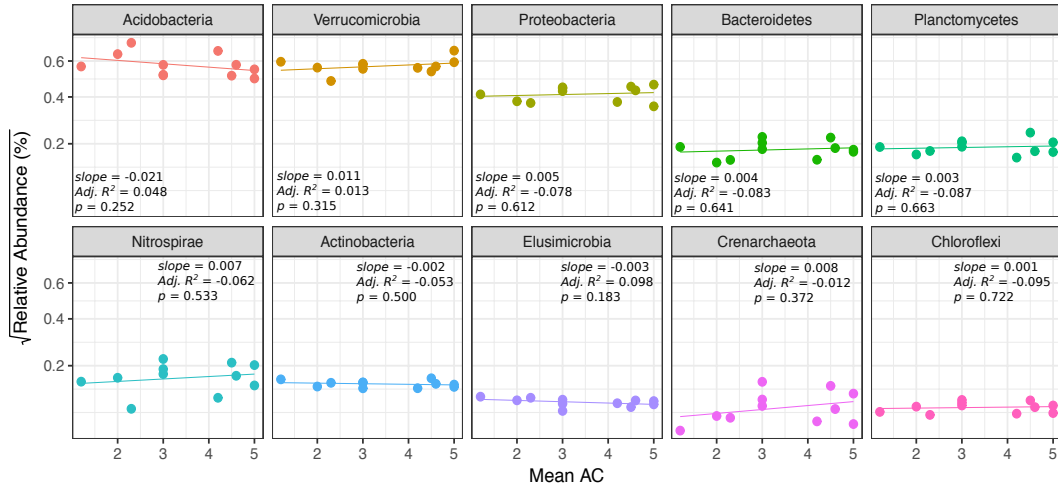


Figure 2.4. Linear relationships between canopy tree health (mean AC) of ash plots only ($n=11$) and Hellinger transformed abundances of the 10 most abundant bacterial phyla.

2.3.3 Bacterial functional differences

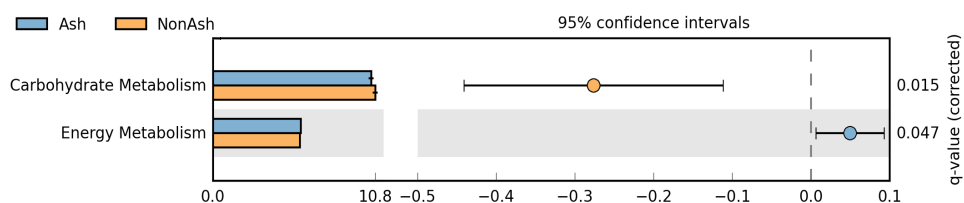
Bacterial community differences between ash and non-ash plots resulted in estimated functional potential differences. At KEGG level 2 (see methods), differences in PICRUSt-estimated functional gene abundances were found in both energy metabolism (ash>non-ash; $d=1.13$, $q=0.047$) and carbohydrate metabolism (non-ash>ash; $d=-1.68$, $q=0.015$; Figure 2.5). At KEGG level 3 within the energy metabolic pathways, three of the nine ortholog groups (carbon fixation pathways in prokaryotes, $d=1.82$, $q=0.060$; methane metabolism, $d=1.80$, $q=0.048$; and carbon fixation in photosynthetic organisms, $d=1.56$, $q=0.018$) were significantly more abundant in ash plots than non-ash. In contrast, four of the nine groups (sulfur metabolism, $d=-1.66$, $q=0.018$; photosynthesis, $d=-1.37$, $q=0.029$; oxidative phosphorylation, $d=-1.37$, $q=0.029$; and photosynthesis proteins, $d=-1.27$, $q=0.042$) were more abundant in non-ash plots (Figure 2.5b). Nitrogen metabolism capacity was not different in ash vs. non-ash plots.

Within the KEGG carbohydrate metabolic pathways, seven out of 15 ortholog groups were

significantly more abundant in non-ash plots (Figure 2.5b). These include pentose and glucuronate interconversions ($d=-1.74$, $q=0.037$), galactose metabolism ($d=-1.71$, $q=0.023$), ascorbate and aldarate metabolism ($d=-1.68$, $q=0.020$), starch and sucrose metabolism ($d=-1.70$, $q=0.018$), inositol phosphate metabolism ($d=-1.67$, $p=0.018$), amino sugar and nucleotide sugar metabolism ($d=-1.65$, $q=0.018$), and the pentose phosphate pathway ($d=-1.36$, $q=0.023$).

However, four out of the 15 groups were significantly more abundant in ash plots, including the tricarboxylic acid (TCA) cycle (a.k.a. Krebs cycle; $d=1.74$, $q=0.027$), pyruvate metabolism ($d=1.66$, $q=0.018$), butanoate metabolism ($d=1.61$, $q=0.018$), and glycolysis/gluconeogenesis ($d=1.38$, $q=0.025$).

a) KEGG Level 2



b) KEGG Level 3

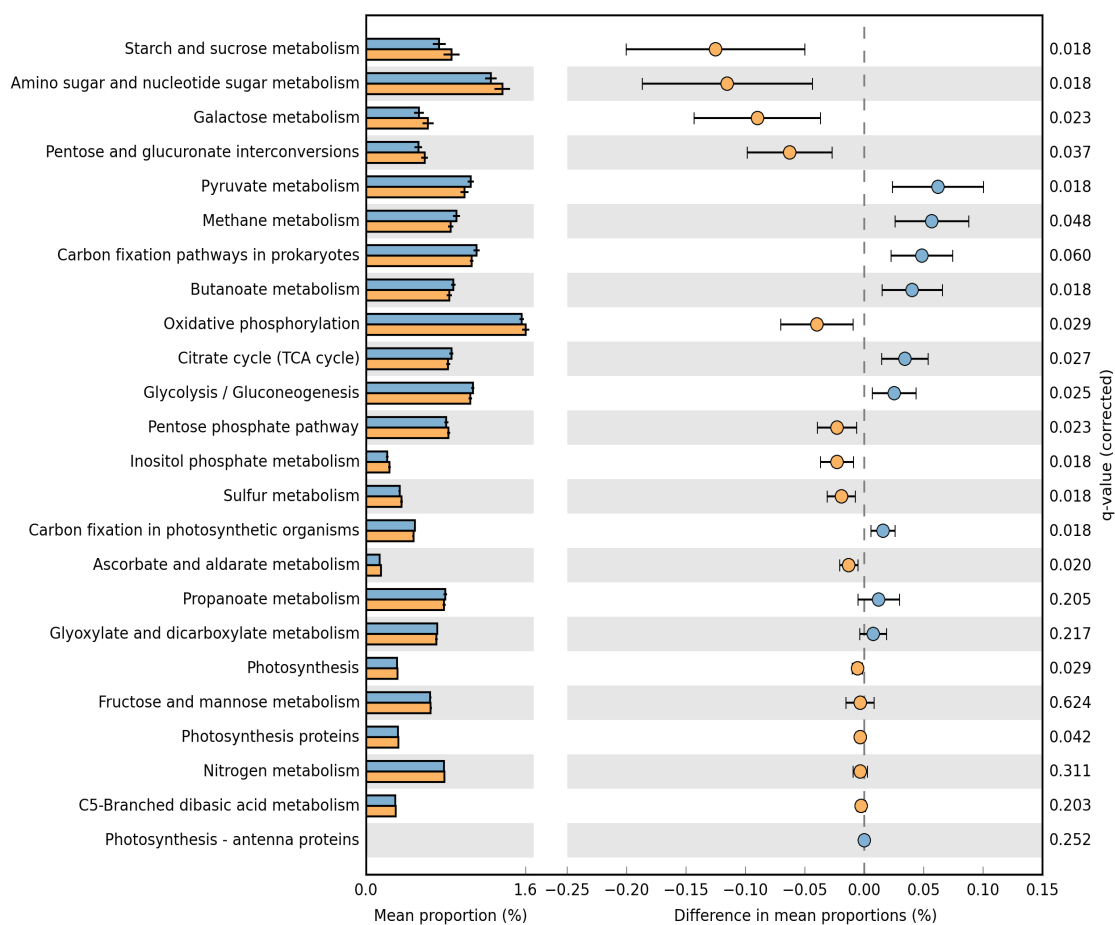


Figure 2.5. Functional gene abundance comparisons between ash and non-ash plots at KEGG levels 2 (a) and 3 (b). Extended bar graphs show differences in the mean proportions of functional genes required for biogeochemical cycling ordered by decreasing effect size. Error bars represent 95% Welch's inverted confidence intervals. Welch's two-tailed t-test was used with Benjamini-Hochberg FDR procedure to obtain corrected q -values. All statistics and graphics were produced using STAMP software.

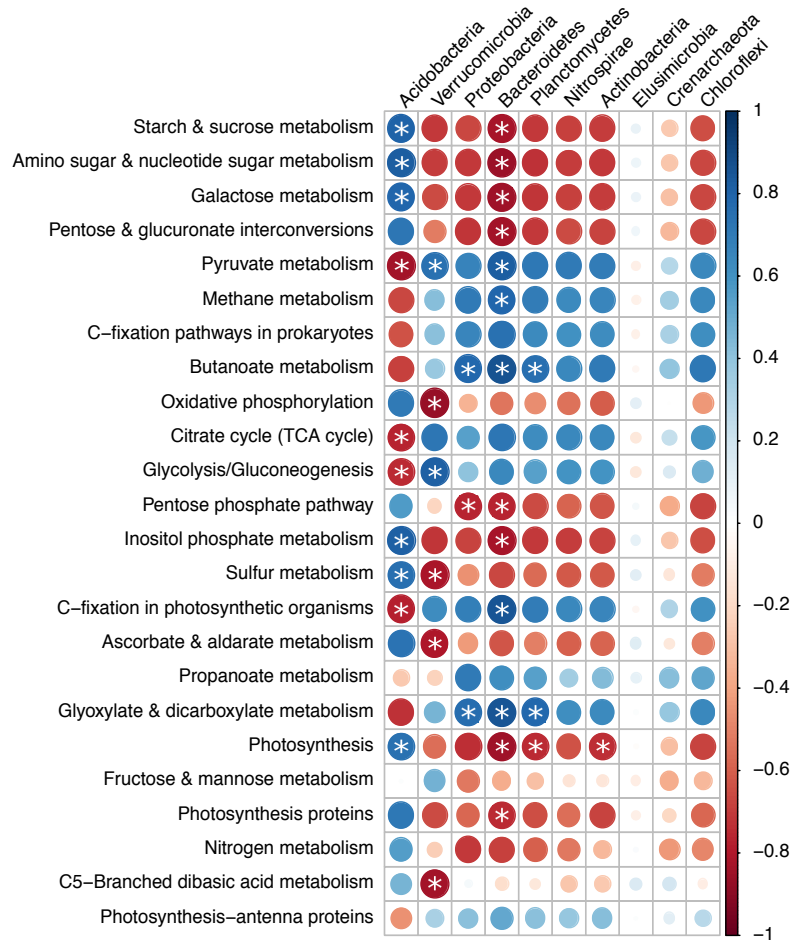


Figure 2.6. Pearson’s correlation matrix comparing the ten most abundant bacterial phyla to level 3 KEGG functional categories, ordered as in Figure 2.4. Circle color indicates either a positive (blue) or negative (red) correlation, and circle size and shading are proportional to correlation coefficients regardless of statistical significance. Bonferroni adjusted significance ($p < 0.05$) is indicated by white asterisks.

General patterns in the correlation relationships between bacterial phyla and functional roles reveal that Acidobacteria specializes in unique functional roles compared to other phyla (Figure 2.6). Acidobacteria, the most abundant phylum and with large differences between ash and non-ash plots, was positively correlated with many of the KEGG level 3 functional groups, including those that were significantly higher in non-ash plots (Figure 2.5). Specifically, Acidobacteria relative abundance correlated with starch and sucrose metabolism ($r=0.810$, $p=0.004$), amino

sugar and nucleotide sugar metabolism ($r=0.821$, $p=0.002$), galactose metabolism ($r=0.799$, $p=0.006$), inositol phosphate metabolism ($r=0.817$, $p=0.003$), and sulfur (S) metabolism ($r=0.755$, $p=0.029$). Although Bacteroidetes was not one of the seven phyla which differed between ash and non-ash plots, it did have the most corollary relationships with the KEGG functional groups we analyzed (13 out of 24 with $r>0.750$ and $p<0.05$).

2.4 **Discussion**

Here, we present evidence that plots containing ash trees at varying stages of EAB-induced decline have different belowground bacterial and functional characteristics than non-ash plots, in spite of having similar soil environmental factors (Table 2.1 and Table 2.2). These soil bacterial community differences between ash and non-ash plots (Figure 2.2), which were largely driven by Acidobacteria relative abundance (Figure 2.3), suggest that in temperate forest ecosystems, ash trees may exhibit a genera specific relationship with soil microorganisms and contribute to shaping soil bacterial community assemblages, which may influence specific functional capacities. The estimated functional data suggest that soil communities in ash plots may have different functional capabilities from those in non-ash plots with respect to C and P metabolism, but not with N metabolism (Figure 2.5). Based on these results and because of the inherent linkage between above- and belowground communities, the loss of ash trees to EAB infestation will likely drive changes in soil microbial communities that lead to altered C and nutrient cycling in this forest ecosystem beyond the expected increase in litter inputs. These fundamental biogeochemical and successional shifts may make this ecosystem susceptible to invasive plant species or pathogenic microorganisms (Hobbs and Huenneke 1992).

Although the direct effects of tree decline on the belowground community were not explicitly

evaluated in this study, the degree of EAB disturbance severity, as indicated by AC, did not affect the overall soil bacterial community structure (Mantel test—Table 2.2) or the individual abundances of major bacterial phyla within the ash stands (Figure 2.4). Likewise, the removal of sites with severely affected ash trees from the analysis ($AC > 3$) did not alter the results (Supplementary Table S2.1). This indicates that ash associated bacterial communities may persist throughout EAB infestation and the eventual ash tree mortality. Changes in the microbial community may be expected some years after ash mortality is completed, depending on the species that occupy the newly available niche. The ash legacy ecosystem effects on soil properties deserve further investigation.

Other studies have reported that dominant tree genera may contribute to shaping soil microbial communities (Kaiser et al. 2010; Urbanová, Šnajdr, and Baldrian 2015; Lejon et al. 2005), but to our knowledge, few studies have investigated soil microbial community associations with ash trees specifically. The mechanisms by which trees exert influence on soil communities are generally attributed to direct and persistent inputs to the soil environment, likely from the chemical nature of litter deposition and root exudates. However, while there were obvious differences in bacterial community structure between ash and non-ash plots in our study (Figure 2.2 and Figure 2.3), determining causation can be challenging. A variety of biotic and abiotic factors may contribute to shaping the soil microbiome at a given site. For example, the presence/absence of other non-ash tree species within the plots may confound the interpretation of results. Oak tree relative dominance was low in the plots with ash trees and was higher in plots without ash trees (Table 2.2 and Supplementary Table S2.3). These results may indicate that the bacterial community differences we see between ash and non-ash plots could also be due to oak tree influence. However, results from the Mantel test analysis suggest that oak tree

dominance did not have an effect on bacterial community structure ($p=0.338$), while ash tree dominance did ($p=0.007$), providing a stronger case for soil bacterial association with ash trees specifically. Likewise, bacterial community structure has been shown to be highly influenced by soil pH (Fierer and Jackson 2006; Lauber et al. 2009; Cho, Kim, and Lee 2016), which along with other correlated soil variables (Mg, Al, and Ca), is supported by our data (Table 2.2). The most abundant phylum in these sites was Acidobacteria, which are known to prefer acidic environments (Ward et al. 2009). This phylum had a 1.5-fold greater relative abundance in non-ash plots when compared to ash plots (Figure 2.3) and may very well be driving the overall soil bacterial community structure differences at these sites. While soil pH was only marginally statistically different between ash and non-ash plots ($W=73$, $p=0.080$), it was more acidic in non-ash plots where Acidobacteria were more abundant. So, while ash trees are tolerant of a wide range of soil pH values, including very acidic ones (Burns and Honkala 1990), it is possible that soil pH may be contributing to both bacterial and tree community structure.

Besides being the most abundant phyla in these soils and a major driver of bacterial community structure, Acidobacteria exhibit a number of interesting patterns. Overall, our data reveal opposite trends in Acidobacteria relative abundance (ash vs. non-ash) and functional correlations when compared to eight of the nine remaining most abundant bacterial phyla (Figure 2.3 and Figure 2.6). Acidobacteria were found to be more abundant in non-ash plots, while the other eight phyla were more abundant in ash plots (Figure 2.3). This pattern also holds true for correlations made with functional gene abundances, where a positive correlation with Acidobacteria often occurred alongside a negative correlation with the other phyla and vice versa (Figure 2.6). Our data suggests that Acidobacteria correlate positively with the breakdown of complex sugars leading to glycolysis (*i.e.* starch, sucrose, galactose and amino sugar

metabolisms), while other phyla, such as Proteobacteria, Verrucomicrobia, and Bacteroidetes, correlate positively with enzymes tied more closely to the TCA cycle (*i.e.* glycolysis/gluconeogenesis and pyruvate, glycoxylate, dicarboxylate, and butanoate metabolisms). Even though the relative abundances of some major phyla (*e.g.* Verrucomicrobia and Bacteroidetes) did not differ greatly between ash and non-ash plots (Figure 2.3) and were highly correlated with the above-mentioned functions (Figure 2.6), the ash vs. non-ash differences in these same functional groups were still significant (Figure 2.5). This suggests that the combined directional relationships of non-Acidobacteria phyla with these functions may also contribute to ash vs. non-ash functional differences; however, Acidobacteria remain the most likely driver of relative abundance and functional differences. Acidobacteria are typically aerobic heterotrophs capable of utilizing a range of C sources from simple sugars to hemicellulose, cellulose, and chitin. Although this group is able to reduce nitrate and nitrite (Ward et al. 2009; Kielak et al. 2016), it is incapable of N₂ fixation or nitrification and overall N metabolism was not affected by Acidobacteria abundance differences in this study, indicating some degree of functional redundancy within the bacterial community for N cycling. However, inositol phosphate and sulfur metabolic capacities, which are indicative of organic phosphorus (P) and sulfur cycling capacities, respectively, are both positively correlated with Acidobacteria and are greater in non-ash forest plots when compared to ash plots (Figure 2.5). Phosphatases are enzymes which extract P from organic sources and their activity varies according to climate variables, soil C and N, and organic-P (as opposed to available-P measured in this study) (Margalef et al. 2017). As climate, soil C, and soil N did not vary between ash and non-ash plots, organic-P appears to be a proportionally larger source of microbial P in non-ash forest stands. Because a substantial amount of organic-P is thought to be in microbial biomass (Turner et al.

2013), this enhanced capacity to access organic-P in non-ash plots may indicate a relative difference in P availability between ash and non-ash plots via solubilisation, mobilization, and/or microbial turnover (Richardson and Simpson 2011). Based on our results, if future soil bacterial communities in ash forests become more similar to those in non-ash plots in the wake of EAB infestation, then these differences in P metabolism may be an indicator of future soil transformations. It also highlights the potential role of Acidobacteria in the biogeochemical cycling of nutrients in this forest system. Therefore, future abundance shifts in this phylum due to ash tree decline as a result of EAB could result in alterations of both soil C and nutrient dynamics that will go beyond the addition of dead ash woody litter, which is currently the subject of ongoing investigations.

While our results suggest that ash trees may contribute to shaping soil bacterial community structure and the loss of ash due to EAB infestation may lead to belowground alterations, this may not hold true for all tree species and/or may not affect the bacterial community over time. Ecosystem responses of soil microbes to disturbance remain poorly understood and above-belowground associations may vary across the plant kingdom. For example, Ferrenberg *et al.*, (2014) found that soil bacterial communities remained stable over a five year chronosequence following coniferous tree mortality due to bark beetle in the Rocky Mountains. Ecological resilience in the belowground environment, where the slow turnover of the plant-derived soil C may have a long legacy of the vegetation history of the site, may retain structural and functional attributes long after the removal of trees from the system. Therefore, collecting data on specific above- belowground relationships, as done here, is imperative to understanding if and how communities may respond to the loss of a given species or genera.

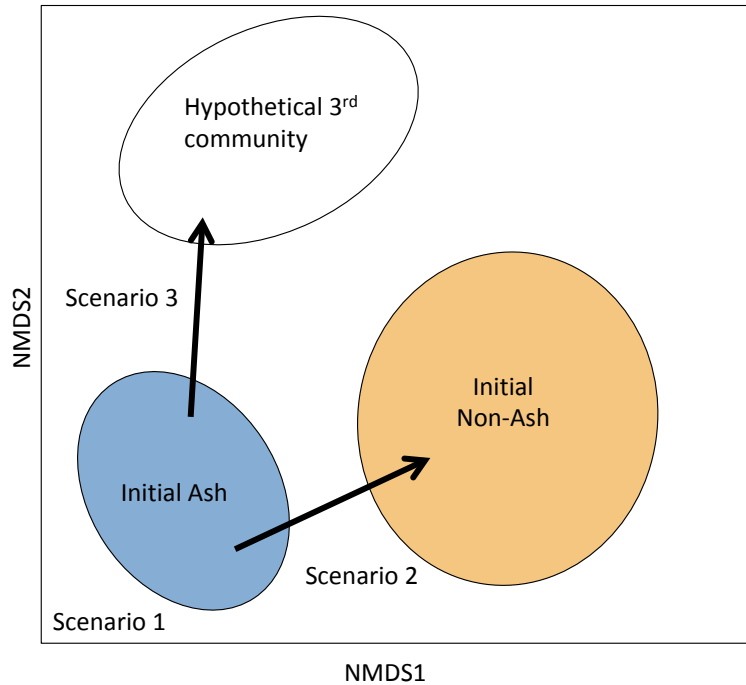


Figure 2.7. Theoretical diagram representing possible successional trajectories of bacterial communities over time in forests suffering ash decline as a result of EAB infestation, where in Scenario 1 the communities stay the same, in Scenario 2 they become more similar to communities in non-ash plots, and in Scenario 3 they develop a community structure different than in either ash or non-ash plots. NMDS ordination space represents hypothetical differences in bacterial community structure based on Figure 2.2.

Research is underway to track the successional trajectory of bacterial communities over time in the wake of ash decline. If soil bacterial communities are resilient to disturbance, driven by edaphic factors that have long-term legacy effects and are not directly influenced by live ash trees, then the loss of ash trees in temperate forests may not affect bacterial community structure (Figure 2.7; Scenario 1). However, if instead ash trees form unique assemblages with their belowground bacterial community and the ecological memory of the soil environment is short-lived, then the loss of ash trees will likely cause major shifts in microbial community structure and, in consequence, ecosystem function. The successional trajectory of these communities could either become more similar to those in non-ash plots (Figure 2.7; Scenario 2), or progress into an

unknown community structure potentially driven by incoming replacement plant species (Figure 2.7; Scenario 3). The resilience of belowground communities and the functions they perform after disturbance will ultimately govern the future states of overall ecosystem biogeochemical cycling and aboveground community structure.

2.5 Conclusions

Using archived DNA samples extracted from forest soils which were collected in the early stages of EAB infestation, we compared the bacterial community structures of plots containing ash trees to those that did not contain ash trees and found that they were different. This indicates that either ash trees directly or indirectly associate with, or influence, belowground microbial organisms. However, co-occurring factors such as soil pH, correlations with other tree species, or the active decline of ash tree health cannot be fully ruled out as contributing driving forces of bacterial community structure. Estimated functional gene abundances within the soil community were also different between ash and non-ash plots as a result of phylogenetic community differences. Specifically, greater relative abundances of Acidobacteria in non-ash plots may drive increases in sugar metabolisms which lead to glycolysis, but decrease functional pathways more tightly linked to the TCA cycle, likely altering C dynamics. Although N cycling was not affected by these bacterial abundance differences, both P and S metabolic potential was elevated in non-ash plots. While we are unable to determine how the loss of ash trees due to EAB will affect belowground community structure and function over time, we provide a foundational framework to predict future successional trajectories and establish a context within which to generate new hypotheses.

2.6 Acknowledgments

This research was supported by the National Science Foundation DGE-0549245, “Landscape Ecological and Anthropogenic Processes” (C.E.F.), the UIC Hadley grant (M.P.R.), the US Forest Service grant 15-JV-11242302-038 (M.A.G-M.), and the Stable Isotope Lab at UIC. Open access publishing fees were supported by the Research Open Access Publishing (ROAAP) Fund of UIC. The authors thank D. Johnston for assistance in the conception and sample collection phase of this research, as well as K. Costilow for assistance with sample collection. We would also like to thank J. Dalton, C. Whelan, E. Dias de Oliveira, and S. O’Brien for comments and advice.

2.7 References

- Allison, S. S. D., and J. B. H. Martiny. 2008. Resistance, resilience, and redundancy in microbial communities. *Proceedings of the National Academy of Sciences of the United States of America* 105:11512–11519.
- Bailey, V. L., S. J. Fansler, J. C. Stegen, and L. A. McCue. 2013. Linking microbial community structure to β -glucosidic function in soil aggregates. *The ISME journal* 7:2044–2053.
- Bakker, M. G., J. M. Bradeen, and L. L. Kinkel. 2013. Effects of plant host species and plant community richness on streptomycete community structure. *FEMS Microbiology Ecology* 83:596–606.
- Birdsey, R. A. 1992. Carbon storage and accumulation in United States forest ecosystems. Gen. Tech. Rep. WO-59. United States Department of Agriculture, Forest Service, Washington, DC.
- Birdsey, R. A., and L. S. Heath. 1995. Carbon Changes in U.S. Forests. Pages 56–70 in L. A. Joyce, editor. *Productivity of America's Forests and Climate Change*. Gen. Tech. Rep. RM-GTR-271. United States Department of Agriculture, Forest Service, Rocky Mountain Forest and Experiment Station, Fort Collins, CO.
- Burns, R. M., and B. H. Honkala. 1990. Fraxinus. Pages 333–357 *Silvics of North America: Volume 2, Hardwoods*. Agriculture Handbook 654. United States Department of Agriculture, Forest Service, Washington, DC.
- Caporaso, J., J. Kuczynski, and J. Stombaugh. 2010. QIIME allows analysis of high-throughput community sequencing data. *Nature* ... 7:335–336.
- Cappaert, D., D. G. McCullough, T. M. Poland, and N. W. Siegert. 2005. Emerald Ash Borer in North America: A Research and Regulatory Challenge. *American Entomologist* 51:152–165.
- Cheng, W., W. J. Parton, M. A. Gonzalez-Meler, R. Phillips, S. Asao, G. G. McNickle, E. Brzostek, and J. D. Jastrow. 2014. Synthesis and modeling perspectives of rhizosphere priming. *New Phytologist* 201:31–44.
- Cho, S.-J., M.-H. Kim, and Y.-O. Lee. 2016. Effect of pH on soil bacterial diversity. *Journal of Ecology and Environment* 40:10.
- Costilow, K. C., K. S. Knight, and C. E. Flower. 2017. Disturbance severity and canopy position control the radial growth response of maple trees (*Acer* spp.) in forests of northwest Ohio impacted by emerald ash borer (*Agrilus planipennis*). *Annals of Forest Science* 74.
- Cramer, W., A. Bondeau, F. I. Woodward, I. C. Prentice, R. A. Betts, V. Brovkin, P. M. Cox, V.

- Fisher, J. A. Foley, A. D. Friend, C. Kucharik, M. R. Lomas, N. Ramankutty, S. Sitch, B. Smith, A. White, and C. Young-Molling. 2001. Global response of terrestrial ecosystem structure and function to CO₂ and climate change: Results from six dynamic global vegetation models. *Global Change Biology* 7:357–373.
- Drewniak, B., and M. A. Gonzalez-Meler. 2017. Earth system model needs for including the interactive representation of nitrogen deposition and drought effects on forested ecosystems. *Forests* 8:1–22.
- Ferrenberg, S., J. E. Knelman, J. M. Jones, S. C. Beals, W. D. Bowman, and D. R. Nemergut. 2014. Soil bacterial community structure remains stable over a 5-year chronosequence of insect-induced tree mortality. *Frontiers in Microbiology* 5:1–11.
- Fierer, N. 2017. Embracing the unknown: disentangling the complexities of the soil microbiome. *Nature Reviews Microbiology* 15:579–590.
- Fierer, N., and R. B. Jackson. 2006. The diversity and biogeography of soil bacterial communities. *Proceedings of the National Academy of Sciences of the United States of America* 103:626–31.
- Flower, C. E., and M. A. Gonzalez-Meler. 2015. Responses of Temperate Forest Productivity to Insect and Pathogen Disturbances. *Annual Review of Plant Biology* 66:547–569.
- Flower, C. E., K. S. Knight, and M. A. Gonzalez-Meler. 2013a. Impacts of the emerald ash borer (*Agrilus planipennis* Fairmaire) induced ash (*Fraxinus* spp.) mortality on forest carbon cycling and successional dynamics in the eastern United States. *Biological Invasions* 15:931–944.
- Flower, C. E., K. S. Knight, J. Rebeck, and M. a. Gonzalez-Meler. 2013b. The relationship between the emerald ash borer (*Agrilus planipennis*) and ash (*Fraxinus* spp.) tree decline: Using visual canopy condition assessments and leaf isotope measurements to assess pest damage. *Forest Ecology and Management* 303:143–147.
- Flower, C. E., D. J. Lynch, K. S. Knight, and M. A. Gonzalez-Meler. 2018. Biotic and abiotic drivers of sap flux in mature green ash trees (*Fraxinus pennsylvanica*) experiencing varying levels of emerald ash borer (*Agrilus planipennis*) infestation.
- Gilbert, J. A., J. K. Jansson, and R. Knight. 2014. The Earth Microbiome project: successes and aspirations. *BMC Biology* 12:69.
- Gonzalez-Meler, M. A., J. S. Rucks, and G. Aubanell. 2014. Mechanistic insights on the responses of plant and ecosystem gas exchange to global environmental change: Lessons from Biosphere 2. *Plant Science* 226:14–21.
- Goodale, C. L., M. J. Apps, R. A. Birdsey, C. B. Field, L. S. Heath, R. A. Houghton, J. C. Jenkins, G. H. Kohlmaier, S. Liu, G. Nabuurs, S. Nilsson, and A. Z. Shvidenko. 2002.

- Forest Carbon Sinks in the Northern Hemisphere. *Ecological applications* 12:891–899.
- Van Der Heijden, M. G. A., R. D. Bardgett, and N. M. Van Straalen. 2008. The unseen majority: Soil microbes as drivers of plant diversity and productivity in terrestrial ecosystems. *Ecology Letters* 11:296–310.
- Higham, M., B. M. Hoven, D. L. Gorchov, and K. S. Knight. 2017. Patterns of Coarse Woody Debris in Hardwood Forests across a Chronosequence of Ash Mortality Due to the Emerald Ash Borer (*Agrilus planipennis*). *Natural Areas Journal* 37:406–411.
- Hobbs, R. J., and L. F. Huenneke. 1992. Disturbance , Diversity , and Invasion : Implications for Conservation. *Conservation Biology* 6:324–337.
- Hopkins, F., M. A. Gonzalez-meler, C. E. Flower, D. J. Lynch, C. Czimczik, J. Tang, and J.-A. Subke. 2013. Ecosystem-level controls on root-rhizosphere respiration. *The New phytologist* 199:339–351.
- Kaiser, C., M. Koranda, B. Kitzler, L. Fuchslueger, J. Schneckner, P. Schweiger, F. Rasche, S. Zechmeister-Boltenstern, A. Sessitsch, and A. Richter. 2010. Belowground carbon allocation by trees drives seasonal patterns of extracellular enzyme activities by altering microbial community composition in a beech forest soil. *New Phytologist* 187:843–858.
- Kanehisa, M., and S. Goto. 2000. KEGG: kyoto encyclopedia of genes and genomes. *Nucleic acids research* 28:27–30.
- Kielak, A. M., C. C. Barreto, G. A. Kowalchuk, J. A. van Veen, and E. E. Kuramae. 2016. The ecology of Acidobacteria: Moving beyond genes and genomes. *Frontiers in Microbiology* 7:1–16.
- Knight, K., P. Robert, and J. Rebbeck. 2008. How fast will trees die? A transition matrix model of ash decline in forest stands infested by emerald ash borer. Emerald ash borer research and development meeting; 2007 October 23-24; Pittsburgh, PA. FHTET 2008-07. Morgantown, WV: U.S. Department of Agriculture, Forest Service, Forest Health Technology Enterprise Team:28–29.
- Langille, M. G. I., J. Zaneveld, J. G. Caporaso, D. McDonald, D. Knights, J. A. Reyes, J. C. Clemente, D. E. Burkepille, R. L. Vega Thurber, R. Knight, R. G. Beiko, and C. Huttenhower. 2013. Predictive functional profiling of microbial communities using 16S rRNA marker gene sequences. *Nature biotechnology* 31:814–821.
- Lauber, C. L., M. Hamady, R. Knight, and N. Fierer. 2009. Pyrosequencing-based assessment of soil pH as a predictor of soil bacterial community structure at the continental scale. *Applied and environmental microbiology* 75:5111–20.
- Lejon, D. P. H., R. Chaussod, J. Ranger, and L. Ranjard. 2005. Microbial Community Structure and Density Under Different Tree Species in an Acid Forest Soil (Morvan, France).

Microbial Ecology 50:614–625.

Lovett, G. M., C. D. Canham, M. A. Arthur, K. C. Weathers, and R. D. Fitzhugh. 2006. Forest ecosystem responses to exotic pests and pathogens in eastern North America. *Bioscience* 56:395–405.

Margalef, O., J. Sardans, M. Fernández-Martínez, R. Molowny-Horas, I. A. Janssens, P. Ciais, D. Goll, A. Richter, M. Obersteiner, D. Asensio, and J. Peñuelas. 2017. Global patterns of phosphatase activity in natural soils. *Scientific Reports* 7:1–13.

McCullough, D. G., and S. A. Katovich. 2004. Emerald ash borer. *Pest alert*:4–5.

McMurdie, P. J., and S. Holmes. 2013. Phyloseq: An R Package for Reproducible Interactive Analysis and Graphics of Microbiome Census Data. *PLoS ONE* 8.

McNickle, G. G., M. A. Gonzalez-Meler, D. J. Lynch, J. L. Baltzer, and J. S. Brown. 2016. The world's biomes and primary production as a triple tragedy of the commons foraging game played among plants. *Proceedings of the Royal Society B: Biological Sciences* 283:20161993.

Oksanen, J., F. G. Blanchet, M. Friendly, R. Kindt, P. Legendre, D. Mcglinn, P. R. Minchin, R. B. O'Hara, G. L. Simpson, P. Solymos, M. H. H. Stevens, E. Szoecs, and H. Wagner. 2017. *vegan: Community Ecology Package*.

Parks, D. H., G. W. Tyson, P. Hugenholtz, and R. G. Beiko. 2014. STAMP: Statistical analysis of taxonomic and functional profiles. *Bioinformatics* 30:3123–3124.

Parmesan, C., and G. Yohe. 2003. A globally coherent fingerprint of climate change impacts across natural systems. *Nature* 421:37–42.

Prescott, C. E., and S. J. Grayston. 2013. Tree species influence on microbial communities in litter and soil: Current knowledge and research needs. *Forest Ecology and Management* 309:19–27.

R Core Team. 2013. *R: A language and environment for statistical computing*. Vienna, Austria.

Richardson, A. E., and R. J. Simpson. 2011. Soil Microorganisms Mediating Phosphorus Availability Update on Microbial Phosphorus. *Plant Physiology* 156:989–996.

Ricketts, M. P., R. S. Poretsky, J. M. Welker, and M. Gonzalez-Meler. 2016. Soil bacterial community and functional shifts in response to altered snowpack in moist acidic tundra of Northern Alaska. *Soil* 2:459–474.

Schimel, J. P., and S. M. Schaeffer. 2012. Microbial control over carbon cycling in soil. *Frontiers in microbiology* 3:1–11.

- Schlatter, D. C., M. G. Bakker, J. M. Bradeen, and L. L. Kinkel. 2015. Plant community richness and microbial interactions structure bacterial communities in soil. *Ecology* 96:134–142.
- Settele, J., R. J. Scholes, R. A. Betts, S. Bunn, P. Leadley, D. Nepstad, J. T. Overpeck, and M. A. Tobaoda. 2014. Chapter 4 - Terrestrial and inland water systems. Pages 271–359 in C. B. Field, V. R. Barros, D. J. Dokken, K. J. Mach, M. D. Mastrandrea, T. E. Bilir, M. Chatterjee, K. L. Ebi, Y. O. Estrada, R. C. Genova, B. Girma, E. S. Kissel, A. N. Levy, S. MacCracken, P. R. Mastrandrea, and L. L. White, editors. *Climate Change 2014: Impacts, Adaptation, and Vulnerability. Part A: Global and Sectoral Aspects. Contribution of Working Group II to the Fifth Assessment Report of the Intergovernmental Panel on Climate Change*. Cambridge University Press, Cambridge, United Kingdom and New York, NY, USA.
- Smith, A. 2006. Effects of community structure on forest susceptibility and response to the emerald ash borer invasion of the Huron River watershed in southeast Michigan. Ohio State University.
- Telander, A. C., R. A. Slesak, A. W. D’Amato, B. J. Palik, K. N. Brooks, and C. F. Lenhart. 2015. Sap flow of black ash in wetland forests of northern Minnesota, USA: Hydrologic implications of tree mortality due to emerald ash borer. *Agricultural and Forest Meteorology* 206:4–11.
- Turner, B. L., H. Lambers, L. M. Condrón, M. D. Cramer, J. R. Leake, A. E. Richardson, and S. E. Smith. 2013. Soil microbial biomass and the fate of phosphorus during long-term ecosystem development. *Plant and Soil* 367:225–234.
- Urbanová, M., J. Šnajdr, and P. Baldrian. 2015. Composition of fungal and bacterial communities in forest litter and soil is largely determined by dominant trees. *Soil Biology and Biochemistry* 84:53–64.
- Wang, X.-Y., Z.-Q. Yang, J. R. Gould, Y.-N. Zhang, G.-J. Liu, and E. Liu. 2010. The Biology and Ecology of the Emerald Ash Borer, *Agrilus planipennis*, in China. *Journal of Insect Science* 10:1–23.
- Ward, N. L., J. F. Challacombe, P. H. Janssen, B. Henrissat, P. M. Coutinho, M. Wu, G. Xie, D. H. Haft, M. Sait, J. Badger, R. D. Barabote, B. Bradley, T. S. Brettin, L. M. Brinkac, D. Bruce, T. Creasy, S. C. Daugherty, T. M. Davidsen, R. T. Deboy, J. C. Detter, R. J. Dodson, A. S. Durkin, A. Ganapathy, M. Gwinn-giglio, C. S. Han, H. Khouri, H. Kiss, S. P. Kothari, R. Madupu, K. E. Nelson, W. C. Nelson, I. Paulsen, K. Penn, Q. Ren, M. J. Rosovitz, J. D. Selengut, S. Shrivastava, S. A. Sullivan, R. Tapia, L. S. Thompson, K. L. Watkins, Q. Yang, C. Yu, N. Zafar, L. Zhou, and C. R. Kuske. 2009. Three Genomes from the Phylum Acidobacteria Provide Insight into the Lifestyles of These Microorganisms in Soils. *Applied and environmental microbiology* 75:2046–2056.

3 CARBON MINERALIZATION SUSCEPTIBILITY IN ARCTIC TUNDRA SOILS: HOW ORGANIC MATTER CHEMISTRY AND TEMPERATURE RELATE TO BACTERIAL COMMUNITY STRUCTURE AND SOIL RESPIRATION

3.1 Introduction

Climate is linked to a complex set of physical, chemical and biological components that drive global biogeochemical cycles and are being impacted by rapidly changing environments worldwide. The carbon (C) cycle in particular has received much attention because two major greenhouse gases (GHG), CO₂ and CH₄, are integral parts of the radiative force of Earth's atmosphere. Trace gas abundance in the atmosphere is a function of biological and anthropogenic emissions and uptake by ecosystems in the biosphere, and so in turn is directly affected by biogeochemical cycling. In particular, changes occurring in Arctic ecosystems have relatively greater potential to alter global C-cycling dynamics, primarily through two feedback mechanisms: 1) ice-albedo feedbacks, which change surface reflectance and thus energy absorption, are predicted to amplify warming in the polar regions causing Arctic temperatures to increase 1.5 to 4.5 times that of the global mean (Holland and Bitz 2003, Anisimov et al. 2007); 2) soil respiration feedbacks, which produce CO₂ and CH₄, are expected to increase in response to warming soil temperatures, further contributing to GHG buildup in the atmosphere (Davidson and Janssens 2006, Schuur et al. 2015). The soil respiration feedback is also augmented by accelerating permafrost thaw as microbial decomposers gain access to large stores of soil organic carbon (SOC) that have been frozen for millennia (Ping et al. 2008, Schuur et al. 2013). The soil respiration feedback is important because Arctic permafrost contains 1,330–1,580 Pg of C (1 Pg=1 billion tons), approximately 50% of the global SOC pool (Hugelius et al. 2014, Schuur et al. 2015, Strauss et al. 2017). The mineralization of even a small fraction of this old, frozen C could cause cascading climate feedbacks, as mentioned above. However, the amount of C that

could potentially be mineralized from a soil over a given time period (*i.e.* C-mineralization potential=CMP) varies depending on a number of environmental parameters and soil characteristics, including SOC accessibility, its chemical composition, and the O₂ availability modified by soil moisture (Dungait et al. 2012, Ping et al. 2015).

Microbial accessibility to SOC is determined by a variety of different mechanisms. For example, SOC accessibility may be limited by 1) soil aggregation properties, where the binding of soil particles to each other serve to physically protect SOC within the aggregates from microbial decomposition; and/or by 2) the adsorption of SOM with organomineral complexes, providing physical protection of SOC from extracellular enzyme activity (Six et al. 2002). Arctic soils are unique in that they typically have very little to no aggregation, partially due to constant and repetitive mixing via the freeze-thaw cycles of cryoturbation (Ping et al. 1998). Instead, SOC in Arctic soils is protected via a third mechanism, temperature, where subzero temperatures inhibit microbial access to (and mineralization of) SOC stored in permafrost. Predicted soil warming in the Arctic can alleviate the temperature limitation of microbial decomposition of existing SOC. As such, it is paramount to elucidate the temperature sensitivity associated with soil respiration (Q_{10}) to characterize the CMP of Arctic soils (Mikan et al. 2002, Wallenstein et al. 2009). It is well established that increased temperatures yield increased soil respiration (Hopkins et al. 2013), however accurate estimates of Q_{10} for Arctic soils is elusive due to the inherent difficulty of collecting samples from deep layers and the degree of variation in C substrate availability and quality due to soil mixing via cryoturbation.

With increasing soil temperatures, the CMP of thawed Arctic soils may be determined by a combination of microbial community functional capacity and soil chemical composition. Soil

microorganisms mediate the process of C-mineralization via a variety of metabolic pathways that are dependent not only on local environmental conditions, but also community composition (Ricketts et al. 2016). While Arctic soil microbes in general are adapted to surviving in cold environments, active communities in permafrost layers consist of organisms specialized at thriving in sub-zero temperatures known as psychrophiles (Morita 1975, Tribelli and López 2018). These microbes likely subsist on dissolved nutrient and carbon sources which seep into permafrost layers through cracks (Michaelson 2003). In contrast, non-psychrophilic (but cold tolerant) microorganisms lying dormant in permafrost which are able to maximize production once temperature limitations to SOC accessibility are alleviated (see above), will rapidly outcompete psychrophilic organisms. Therefore, microbial community composition in Arctic soils is likely to shift as old SOC becomes available for decomposition (Monteux et al. 2018). However, the degree to which these communities may utilize these new resources depends on degradation state, or chemical availability, of the substrate. Fourier-transformed infrared (FTIR) spectroscopy is a well-established method which can describe in detail the chemical composition of SOM, and has been established as a reliable predictor of SOM decomposability/stability and CMP in a number of studies (Artz et al. 2008, Calderón et al. 2011, 2013, Matamala et al. 2019). Individual spectral peaks are associated with a wide variety of soil chemical characteristics, and the ratios between certain peaks have been shown to represent the decomposition state of OM (Haberhauer et al. 1998, Artz et al. 2006). These studies highlight the importance of soil chemistry in determining SOM quality, and demonstrate the utility of FTIR spectroscopy in the study of soil C dynamics.

This research explores how Arctic soil microbial communities respond to increasing temperatures and thawing permafrost predicted under future climate change scenarios. The

objectives of this study were to 1) identify specific soil bacterial taxa whose abundances are affected by increased temperatures in active and permafrost soil layers, 2) determine how differing soil chemistries between sites and soil layers affect overall bacterial community structure, and 3) examine how bacterial taxa abundance relates to soil chemistry and carbon mineralization potential. Soil samples were collected from across the northern slope of Alaska, and soil DNA was extracted from samples after a 60-day period at five different incubation temperatures, as well as from the initial un-incubated samples. 16S rRNA amplicon sequencing was performed to determine bacterial community composition, and soil chemistry of each sample was determined by FTIR spectral analysis. Due to increased metabolic rates and nutrient rich substrate availability in warmed/incubated soils (particularly in permafrost) compared to un-incubated soils, we hypothesize that the relative abundance of non-psychrophilic, generalist bacterial taxa will increase in both active layer and permafrost samples in response to increased temperatures, while the relative abundances of psychrophilic, specialist bacteria will decrease. We also hypothesize that soil chemical attributes representative of organic matter quality will have the greatest influence in shaping overall bacterial community structure, and correlate positively with taxa that increased in response to the incubation experiment. Likewise, the taxa which showed the largest positive abundance responses to increased temperatures should also correlate positively with CMP.

3.2 Materials and methods

3.2.1 Study sites

For this study, soil was collected from four tundra sites across Northern Alaska. One site was located in the Arctic coastal plain near Prudhoe Bay (CL), while the other three were in the

Arctic foothills region; two from Sagwon Hills (SU and SL) and one from Happy Valley (HU). The sites were described in detail in Matamala et al. (2019). Briefly, the foothills sites (SU, SL, and HU) were located on moist acidic tundra while the coastal plain site (CL) was on wet non-acidic tundra. Two sites (CL and SL) represent lowland areas where the soils are poorly drained and had developed from alluvium parent material, while the other two sites (HU and SU) were located in upland areas in soils developed from loess and loess/moraine parent materials with normal tundra drainage (Table 3.1). Soils were sampled horizontally from a 1m³ pit. At each site, blocks of soil samples were collected from the active organic layers, active mineral layers, and upper permafrost layers. Samples were frozen on site for transportation and kept frozen until processing for incubations, chemical analysis, and DNA extractions.

Table 3.1. Average \pm standard error of soil carbon characteristics ($n=30$), carbon mineralization potential (CMP) calculated from the incubation experiment ($n=5$), and calculated temperature sensitivity (Q_{10}) over 60-day incubations ($n=5$). *=samples removed as outliers.

Site	Land cover type [†]		Soil type [‡]					
Coastal Plain lowland (CL)	Wet non-acidic tundra		Ruptic-Histic Aquiturbel					
	TOC (mg C/g _{soil})	C:N	CMP (mg CO ₂ -C/g soil-C) at individual incubation temperatures					Q ₁₀
			-1°C	1°C	4°C	8°C	16°C	
Organic	60.0 \pm 1.8	17.1 \pm 0.3	3.3 \pm 0.4	7.8 \pm 1.4	7.7 \pm 0.9	9.4 \pm 0.9	20.7 \pm 2.2	2.15
Mineral	12.2 \pm 0.6	17.3 \pm 0.2	4.6 \pm 0.3	9.0 \pm 1.6	8.9 \pm 0.8	9.7 \pm 0.9	13.9 \pm 1.7	1.56
Permafrost	100.9 \pm 4.5	14.4 \pm 0.1	2.5 \pm 0.3	4.5 \pm 0.6	4.2 \pm 0.1	5.3 \pm 0.5	7.6 \pm 0.3	1.64
Sagwon Hills lowland (SL)	Moist acidic tundra		Glacic Histoturbel					
Organic	484.0 \pm 2.3	16.9 \pm 0.2	0.8 \pm 0.1	1.9 \pm 0.1	3.0 \pm 0.3	5.4 \pm 0.9	8.0 \pm 0.6*	2.41
Mineral	37.7 \pm 0.6	20.9 \pm 0.3	1.3 \pm 0.1	1.5 \pm 0.1	1.8 \pm 0.1	2.3 \pm 0.2	3.7 \pm 0.5	1.86
Permafrost	198.2 \pm 11.9	19.4 \pm 0.2	1.9 \pm 0.2	4.8 \pm 0.5	4.7 \pm 0.6	6.7 \pm 1.4	10.3 \pm 0.7	1.97

Sagwon Hills upland (SU)		Moist acidic tundra			Ruptic-Histic Aquiturbel			
Organic	242.5±20.9	38.8±1.3	5.1±0.5	10.7±0.9	9.7±0.7	13.2±1.4	14.6±0.4*	2.69
Mineral	47.6±1.4	16.4±0.2	1.3±0.2	2.0±0.2	2.2±0.1	3.3±0.5	4.4±0.7	1.78
Permafrost	88.5±6.3	17.8±0.3	1.0±0.3	2.8±0.9	2.5±0.9	4.8±0.7	6.9±0.6	2.13

Happy Valley upland (HU)		Moist acidic tundra			Ruptic Histoturbel			
Organic	416.4±7.8	19.6±0.2	1.4±0.1	4.2±0.3	4.5±0.7	7.1±0.8	11.0±1.6	2.18
Mineral	36.3±1.2	19.3±0.2	1.6±0.1	2.8±0.3	2.4±0.1	4.7±0.6	6.0±0.9	1.89
Permafrost	93.0±9.1	15.7±0.2	4.0±0.6	7.7±0.6	8.4±1.2	9.5±1.6	18.6±1.6	2.06

† (Walker et al. 2004), ‡(Michaelson et al. 2013).

3.2.2 Soil incubations and temperature sensitivity

Frozen soil subsamples, obtained by chipping away chunks from the frozen blocks, were used to determine chemical composition (Table 3.1), and for aerobic soil incubation as described in Matamala et al. (2019). Briefly, approximately 3-4 cm³ of soil from each soil layer of each site were incubated in plastic cylinders in closed 250 ml glass jars. The jar lids were equipped with quick connect fittings that allowed for air sampling of the jar. Soils were incubated at five temperatures, -1, 1, 4, 8, and 16°C, in an ethylene glycol bath that maintained the temperature at ±0.2 °C from target. Soil incubations at -1°C were newly added for this study. We incubated a total of 300 soil samples (5 temperatures × 4 sites × 3 horizons × 5 samples). Soils were incubated for 60 days and CO₂ production was measured about four times a day using an automated soil respirometer equipped with a CO₂ non-dispersive infrared detector (Micro-Oxymax, Columbus Instruments). Total C mineralized per sample was estimated by fitting the CO₂ production data obtained during the 60-day incubation period to a two pool model using SigmaPlot 13.0 Curve Fit Wizard. The CO₂ produced during the first 10-24 hours of incubation

were removed before curve fitting to remove thawing effects.

For this study, we calculated Q_{10} for all soil layers and sites by the “same time method” using all incubation temperatures, including -1, 1, 4, 8, and 16°C. To calculate Q_{10} , we fitted the accumulated amount of CO₂ released during the 60-day incubation to an exponential function:

$$C_{cum} = a e^{\beta T} \quad (1)$$

Where “ C_{cum} ” is the cumulative amount of CO₂-C released during the 60-day incubation on a per dry soil C basis, “ a ” is the scaling parameter, “ β ” is the soil temperature sensitivity parameter, and “ T ” is temperature. Q_{10} was then calculated using the following equation:

$$Q_{10} = e^{10\beta} \quad (2)$$

3.2.3 Soil analysis

A C:N elemental analyzer (Elementar VarioMax Cube) was used to determine total nitrogen (TN) and total carbon (TC) by combustion at 900°C, and total organic carbon (TOC) at 650°C, for both incubated and un-incubated soil samples. A FTIR spectrometer (PerkinElmer Spectrum 100 Series) was used to determine the chemical composition of SOM from the MIR (mid infrared) spectra of un-incubated and incubated soil subsamples. The FTIR spectra of incubated soils at 1, 4, 8 and 16°C for site and layer, and replicated 5 times (240 soils), was used in Matamala et al. (2019) to investigate the predictive capabilities of the FTIR spectra for determining the short-term carbon mineralization potential of tundra soils. In this study we used those 240 soil samples and added 120 more samples to the dataset (total $n=360$). Of those 120 samples, 60 were incubated at -1°C (4 sites × 3 layers × 5 replicates) and 60 were un-incubated soils (4 sites × 3 layers × 5 replicates). Five subsamples per soil were scanned against a KBr

background and an average spectrum was obtained. Each spectrum was collected at 1 cm^{-1} resolution over the range of $4000\text{-}450\text{ cm}^{-1}$. Baseline correction was done to all samples before averages were taken using a two-point band correction at 4000 and 2400 cm^{-1} . Absorbance values from spectral bands were selected for analysis based on associations with soil chemical or mineralogical characteristics (Supplementary Figure S3.1), as previously determined by Matamala et al. (2019) and listed in Supplementary Table S3.1. Ratios of spectral band absorbance values were selected based on evidence suggesting associations with OM decomposition state referenced in Matamala et al. (2017).

3.2.4 DNA extraction and high-throughput 16S rRNA sequencing

Frozen non-incubated and freeze-dried incubated soil subsamples from each temperature were used for determining the microbial community structure. For each site, triplicate subsamples were taken from seven replicate samples of non-incubated organic layer soil ($n=84$), three replicate samples of non-incubated mineral and permafrost layer soils ($n=72$), and five replicate samples of incubated soils from all temperatures and layers ($n=60$ for each temperature and layer), for an ideal total of 1,056 subsamples. However, due to low DNA extraction yields, 24 subsamples were removed prior to sequencing. DNA was extracted using the PowerSoil[®] -htp 96 Well Soil DNA Isolation Kit (4×96 well plate option, MO BIO Laboratories Inc., Carlsbad, CA, USA) following the manufacturer's instructions and eluted in a final volume of $100\mu\text{L}$ per sample. Approximately $0.1\text{-}0.25\text{ g}$ of freeze-dried soil were loaded into each well of the extraction plate. The protocol detailed by MoBio was then followed resulting in $100\text{ }\mu\text{L}$ of eluted DNA. The concentration of extracted DNA was quantified using the Quant-iT PicoGreen dsDNA assay (Invitrogen, Inc., Carlsbad, CA, USA), and ranged from 15 to $40\text{ ng}/\mu\text{L}$. Targeted amplicon sequencing of the 16S rRNA encoding genes from each sample was conducted as

described previously in Flynn et al. (2017).

Polymerase chain reaction (PCR) amplification was carried out using a 5 PRIME MasterMix (Gaithersburg, MD, USA). We used primer set 515F-806R targeting the V4 variable region of the 16S rRNA genes of bacteria and archaea (Bates et al. 2011, Caporaso et al. 2011). Samples were barcoded for downstream multiplexing (Caporaso et al. 2012) and pooled products from the samples were quantified using the PicoGreen assay. DNA concentrations were standardized by dilution to 2 ng μL^{-1} and primer dimers were eliminated using the UltraClean PCR Clean-Up Kit (MoBio Laboratories, Inc., USA). Paired-end amplicon sequencing (2 \times 151 bp) was performed on an Illumina MiSeq Sequencer (Illumina, San Diego, CA, USA) running v3 chemistry at the Environmental Sample Preparation and Sequencing Facility at Argonne National Laboratory following protocols detailed in Caporaso et al. (2012). Forward and reverse reads were merged by using the PEAR (pair-end read merger) software (Zhang et al. 2014). Another 42 subsamples were filtered out due low quality sequences using the default settings in QIIME (v1.9.1; `split_libraries_fastq.py`; Phred<3, consecutive low quality base calls<3, % consecutive high quality base calls per read>75%, barcode errors<1.5; Caporaso et al. 2010), resulting in a total of 990 remaining samples. De novo clustering of operational taxonomic units (OTU) at the 97% similarity level was performed using QIIME's `pick_de_novo_otus.py` command, singletons were discarded, and subsequent tables and summaries were generated. Alignment was performed using PyNAST and the Greengenes 13_8 reference database to assign taxonomy to representative sequences from each OTU cluster (Caporaso et al. 2010, McDonald et al. 2012). The resulting OTU's were used to determine: 1) what organisms were present in a given sample, and 2) how abundant that organism was within the overall community. Taxa not present more than once in at least 20% of the samples were filtered to remove OTUs with potentially small

means and misrepresented large coefficients of variance.

3.2.5 *Statistical analysis*

All statistical analyses were performed using R software. Differential expression analysis using the edgeR package (Robinson et al. 2009, McCarthy et al. 2012) was performed to examine changes in bacterial abundance over the 60-day incubation period. Samples were grouped by site, soil layer, and incubation temperature. OTU's were merged at the class taxonomic level and filtered to include only the 25 most abundant classes, which constitute 95% of all OTU's. Pairwise comparisons were made between abundances of bacteria from the unincubated samples and abundances of bacteria after 60 days at each of the 5 temperatures. The edgeR package uses negative binomial model-based normalization of the read counts to adjust for differences in library size (i.e. total # of reads per sample), and account for technical variation. The Cox-Reid profile-adjusted likelihood (CR) method was used to estimate dispersions and fit generalized linear models (GLM). Quasi-likelihood F-tests were used to determine differential abundances of bacterial classes. Results were filtered to only include differences with p -values and false discovery rates (FDR) $< 1e^{-5}$, and \log_2 fold change > 1 or < -1 .

To determine relationships between FTIR spectra and bacterial community structure, we performed distance-based redundancy analyses (dbRDA) with Hellinger transformed bacterial community matrices as the response variables, and either a combination of non-FTIR factors (including categorical descriptors), individual absorbance peaks (representing specific soil chemical characteristics), or ratios of absorbance peaks (representing soil decomposition state) as explanatory variables (Non-FTIR model, FTIR peaks model, FTIR ratios model, respectively). Samples from the organic and mineral horizons were reclassified as “active layer” to focus on

major differences observed in the permafrost layer. Models were analyzed for multicollinearity using variance inflation factors (VIF) and optimized by selectively removing variables until all VIF values were less than 25. Individual factors were also analyzed separately using dbRDA and Mantel tests to determine their degree of explanatory power (% variance explained) and correlation with bacterial community structure (Mantel r-statistic correlation coefficient= r_M).

The top seven soil chemical factors which best explained bacterial community structure were selected based on dbRDA and Mantel tests (>6.5% variation explained and $r_M > 0.1$). Pearson's correlation coefficients (r_P) with Bonferroni adjusted p -values (p_B ; # of comparisons=184) were calculated between these seven factors, as well as CMP, and all bacterial classes which showed significant abundance responses to the incubations.

3.3 Results

3.3.1 Incubation effects on soil bacterial abundance and CMP

Bacterial abundance differences between un-incubated and 60-day incubated soil samples were seen in 23 of the 25 most abundant bacterial classes ($p < 1e^{-5}$ and FDR $< 1e^{-5}$). The majority of significant differences occurred at positive incubation temperatures and were most pronounced in permafrost samples (Figure 3.1). The largest differences were seen in Alphaproteobacteria, Betaproteobacteria, Gammaproteobacteria, and Bacteroidetes (Sphingobacteriia), which consistently showed \log_2 fold changes > 5 over 60 days at all positive incubation temperatures. Negative responses tended to be more diverse with fairly consistent responses in Verrucomicrobia (Pedosphaerae), Deltaproteobacteria, Chloroflexi (Anaerolineae and Ellin6529), Caldiserica (WCHB1-03), Bacteroidetes (Bacteroidia), and Actinobacteria (Thermoleophilia) which showed \log_2 fold < -2 over 60 days at most positive incubation

temperatures. Only 4 of the top 25 classes showed significant abundance shifts at -1°C.

Bacterial relative abundance patterns at the class level varied by site, however certain general patterns were observed between soil layers and incubation temperatures (Figure 3.2). With the exception of the SU site, Verrucomicrobia and Acidobacteria were more prevalent in the active layer (organic and mineral) than in permafrost samples, while Actinobacteria were more prevalent in the permafrost than in the active layer. Proteobacteria were abundant in every sample, but showed the greatest abundances in incubated permafrost samples, particularly from the SL and HU sites. Caldiserica [WCHB1-03] was found to be extraordinarily abundant in the un-incubated initial permafrost samples from site SL but decreased in abundance in response to incubations (Figure 3.2).

The carbon mineralization potential (CMP; mg CO₂-C g⁻¹ soil over 60-days) significantly varied both by site (Kruskal-Wallis $H=41.24$, $p<0.001$) and soil layer (Kruskal-Wallis $H=24.15$, $p<0.001$). The highest CMP was observed in the organic layers of the CP and SH sites, and in the permafrost layers of the HV site. Site CP also exhibited the highest CMP of all sites in the mineral soil layer (Table 3.1).

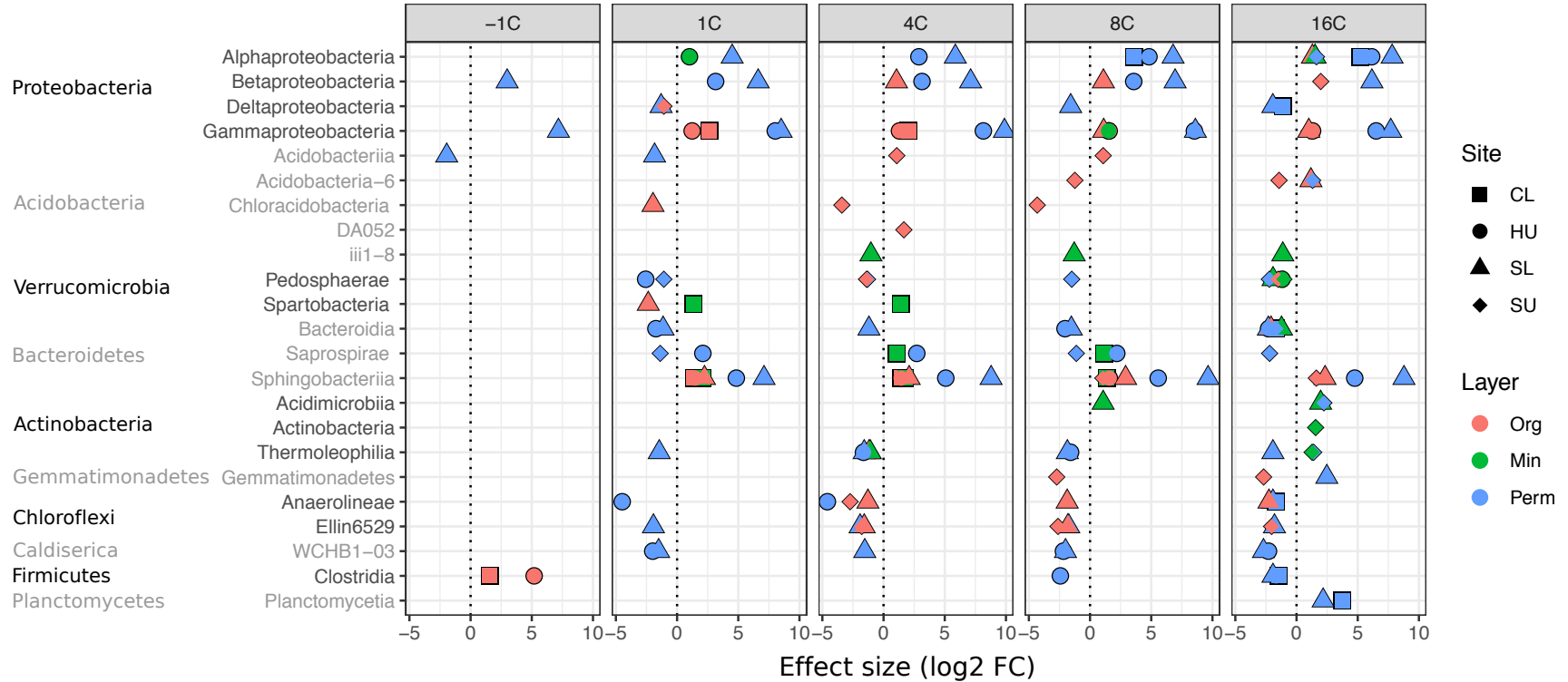


Figure 3.1. Log₂-fold change (log₂ FC) response of bacterial class abundances to incubations where positive values indicate increased abundance over 60 days, and negative values indicate decreased abundance over 60 days. All results shown are significant ($p < 1e^{-5}$) with false discovery rates (FDR) $< 1e^{-5}$ and log₂FC values > 1 or < -1 . Bacterial phyla are ordered from top to bottom with the most abundant phyla at the top. Panels are separated by incubation temperature, color indicates the soil layer, and the shape indicates the site.

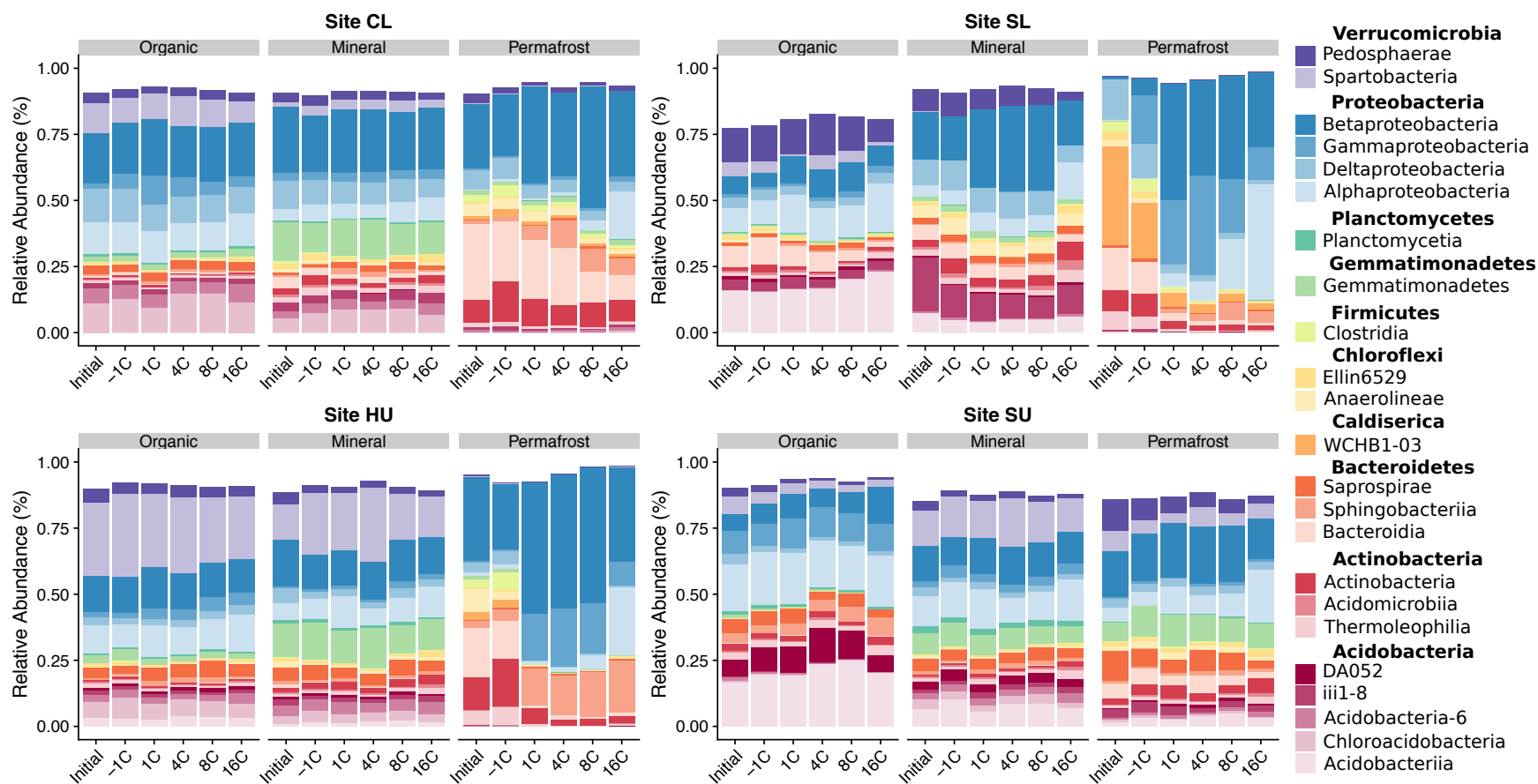


Figure 3.2. Relative abundances of bacterial classes which showed significant differential abundances between initial un-incubated samples and incubated samples (see Figure 1). Results are separated by site, soil layer, and incubation temperature. Bacterial classes are grouped by phylum where base colors indicate the phylum and classes are separated by tint.

3.3.2 Predictive RDA analyses of bacterial community structure

Site and soil layer were the simplest and most powerful predictors of bacterial community structure, explaining 31% and 20% of variation respectively, followed by acidic vs. non-acidic tundra type, which explained 13% of variation (Figure 3.3 and Table 3.2). The incubation temperature explained only 3% of variation and was the least reliable predictor of bacterial community structure (Table 3.2). While the additive model using these categorical variables performed the best (64% variation explained), the models using FTIR spectral data also performed well at predicting bacterial community structure, with the FTIR peaks model explaining 46% of variation and the FTIR ratios model explaining 30% of the variation (Table 3.2, Figure 3.3, and Figure 3.4). The degree of variation explained overlapped between models, especially between the categorical model and the FTIR peaks model (31%; Figure 3.4). The most important individual variables from the FTIR data include the amides/aliphatics (1656/2924) peaks ratio ($r_M=0.193$, RDA=11.03%), the silicates peak ($r_M=0.129$, RDA=10.97%), the aliphatics/carbohydrates (2924/1060) peaks ratio ($r_M=0.180$, RDA=6.59%), and the lignin/carbohydrates (1521/1060) peaks ratio ($r_M=0.131$, RDA=7.70%). Forward selection of variables based on Akaike information criterion did not result in more parsimonious models.

Table 3.2. Statistical results of Mantel tests and distance-based redundancy analyses (dbRDA) evaluating the effects of soil chemical and site properties on bacterial community structure. All results are statistically significant ($p < 0.05$). Asterisks (*) indicate p -values less than 0.001.

Explanatory models	Mantel r -statistic	dbRDA % variation explained
Descriptive model	-	65.08 *
<i>Individual variables</i>		
Site	-	31.82 *
Soil layer	-	20.40 *
Acidic vs Non Acidic	-	13.53 *
Incubation Temperature	-	3.24 *
C:N	0.248 *	10.81 *
TOC	0.122 *	7.78 *
FTIR peaks model	-	46.70 *
<i>Individual peaks (cm^{-1})</i>		
Clays (3694)	0.043	5.15 *
Phenolic OH (3394)	0.060	5.56 *
Aliphatics (2924)	0.104 *	6.81 *
Inorganic C (2516)	0.037	5.33 *
Silicates (1788)	0.129 *	11.11 *
Amides (1656)	0.033	2.88 *
Carboxylics (1423)	0.112 *	5.23 *
Carbohydrates (1060)	0.094 *	7.54 *
FTIR ratios model	-	30.12 *
<i>Individual ratios</i>		
Amides/Aliphatics (1656 / 2924)	0.193 *	11.17 *
Amides/Carboxylics (1656 / 1423)	0.052	3.40 *
Aliphatics/Carbohydrates (2924 / 1060)	0.180 *	6.67 *
Lignins/Carbohydrates (1521 / 1060)	0.131 *	7.80 *

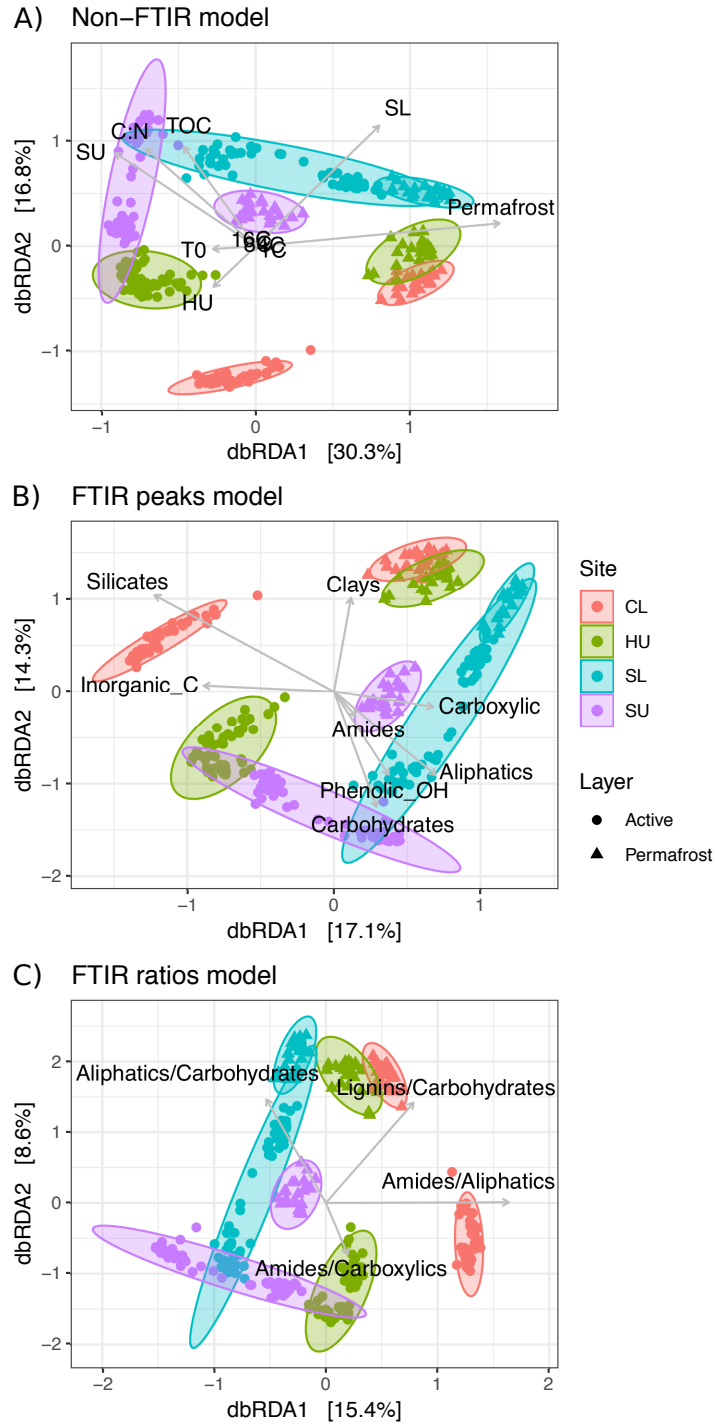


Figure 3.3. Distance-based redundancy analysis ordinations of bacterial community structure separated by site (colors) and soil layer (shapes), and constrained by descriptive variables (A), FTIR spectral peak absorbance values assigned to soil chemical properties (B), and ratios of FTIR peaks absorbance values (C). Arrows indicate strength of correlations between bacterial community structure and explanatory variables.

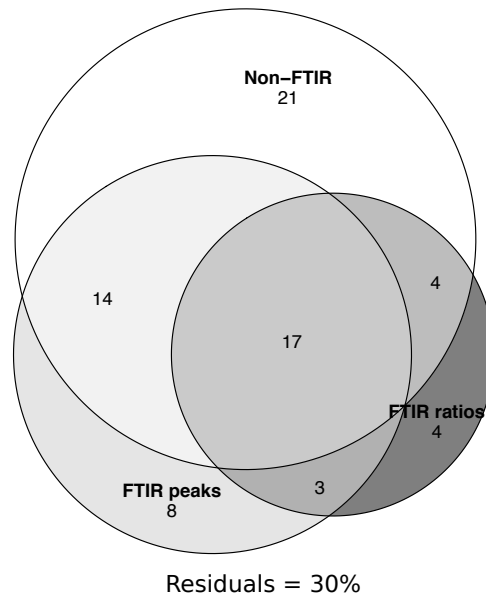


Figure 3.4. Venn diagram illustrating variance partitioning from the three different redundancy analysis models explaining bacterial community structure.

3.3.3 Correlation analysis

Nearly all bacterial phyla (except Alphaproteobacteria, Acidobacteria [DA052], and Bacteroidetes [Bacteroidia]) showed abundance correlations ($r_P > 0.30$ and $p_B < 0.05$) with at least two soil chemical characteristics in the active soil layer samples, however there were almost no significant correlations in the permafrost layer samples (Figure 3.5). The number and strength of correlations varied by site with the strongest and highest number of correlations occurring in the active layers of the SU, SL, and CL sites. The active layer of the SU site contained 24 strong correlations ($r_P < -0.70$ or > 0.70 and $p < 1e^{-10}$) where Gemmatimonadetes, Acidobacteria [iii1-8 and Acidobacteria-6], Chloroflexi [Anaerolineae], and Firmicutes [Clostridia] were all correlated negatively with both C:N and the aliphatics peak, while positively correlated with the amides/aliphatics ratio and the lignin/carbohydrates ratio. Additionally, the amides/aliphatics ratio was positively correlated with Verrucomicrobia [Spartobacteria] and Chloroacidobacteria,

and C:N was correlated negatively with Chloroacidobacteria. The active layer of the SL site contained 11 strong correlations ($r_P < -0.70$ or > 0.70 and $p < 1e^{-10}$) where TOC correlated negatively with Chloroflexi [Anaerolineae], and the aliphatics peak correlated negatively with Gemmatimonadetes, Acidobacteria-6, and Chloroflexi [Anaerolineae] while the lignins/carbohydrates ratio correlated positively with these same three bacterial classes as well as Bacteroidetes [Saprospirae]. Plancomycetia correlated negatively with the lignins/carbohydrates ratio and the silicates peak, while Chloroflexi [Anaerolineae] correlated positively with the amides/aliphatics ratio. The active layer of the CL site contained 6 strong correlations ($r_P < -0.70$ or > 0.70 and $p < 1e^{-10}$) where TOC correlated negatively with Acidobacteria [Acidobacteriia and iii1-8], Chloroflexi [Ellin6529], Actinobacteria [Thermoleophilia], and Gemmatimonadetes, and the aliphatics peak correlated negatively with Chloroflexi [Ellin6529].

Other general patterns were observed but were not consistent across sites or soil layers. For instance, the aliphatics/carbohydrates peak ratio showed very little correlation with bacterial phyla except in the active layer of site CL where it was negatively correlated with many phyla. Also, Acidobacteriia and Gammaproteobacteria appear to have opposite relationships with most soil chemical characteristics compared to the other bacterial classes, but only in the active layers of the HU, SL, and SU sites (Figure 3.5).

CMP correlated negatively with most bacterial classes, except for Alphaproteobacteria, which in permafrost samples correlated positively with CMP in all sites and had a maximum correlation of $r_P = 0.81$ ($p_B < 0.001$) in the SL site. Gammaproteobacteria (primarily in active layer samples), Bacteroidetes [Sphingobacteriia], and Planctomycetia also occasionally correlated positively with CMP, but varied by site and soil layer (Figure 3.5).

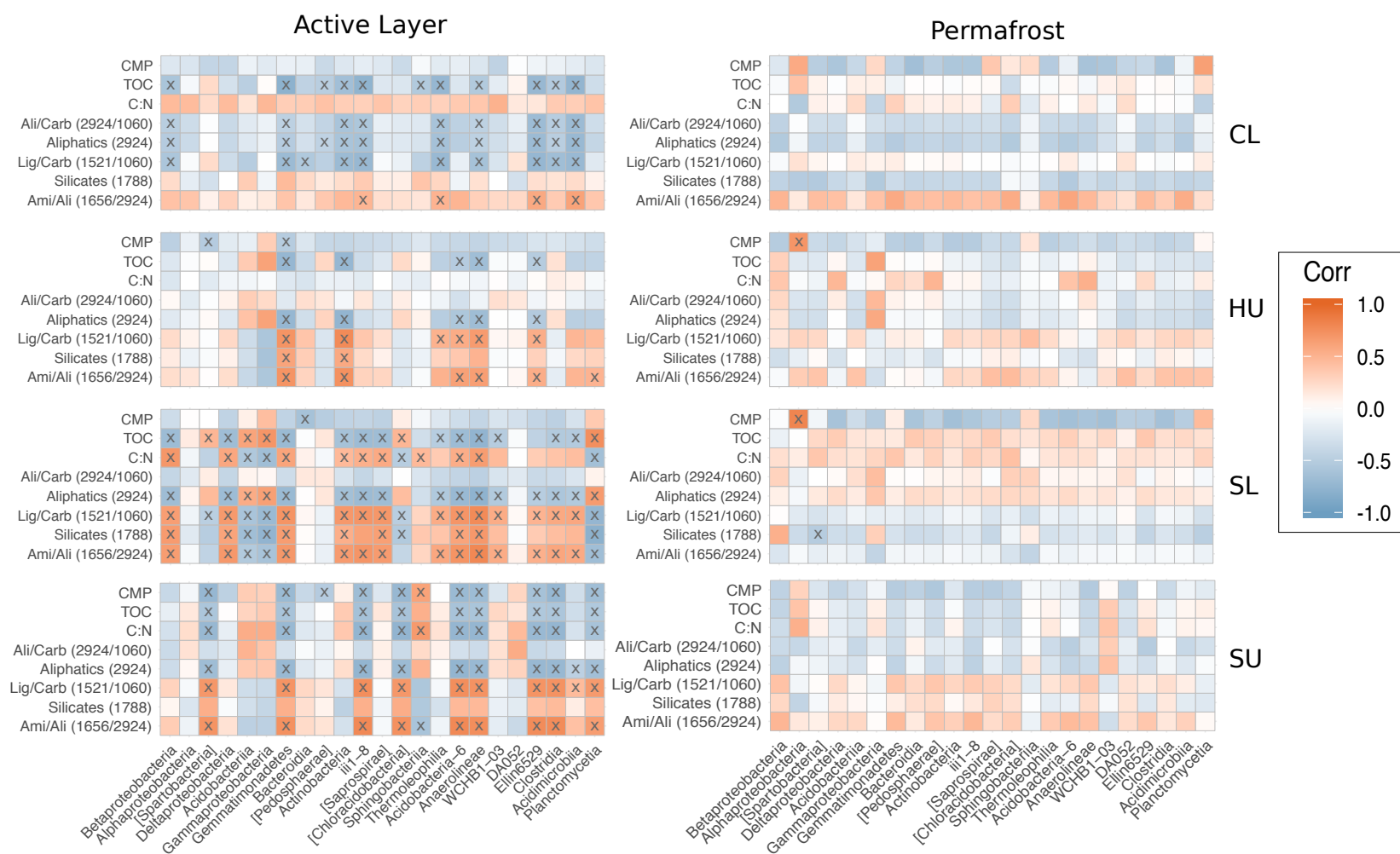


Figure 3.5. Correlation matrices of bacterial classes (ordered from left to right by decreasing abundance) selected from differential analysis (Fig. 1) with most important soil chemical variables identified from redundancy analysis and Mantel tests, and carbon mineralization potential (CMP). Colors indicate strength and direction of correlation (r_P), where red=positive correlations and blue=negative correlations. Squares containing “x” indicate a significant correlation ($p_B < 0.05$).

3.4 Discussion

This study identified soil bacterial taxa which respond to warming soil temperatures and thawing permafrost in soils from Northern Alaska, and examined how soil chemistry relates to bacterial abundance while evaluating the efficacy of using FTIR spectral data to predict soil bacterial community structure. We compared the abundances of bacterial taxa from un-incubated soil samples to those that had been incubated for 60 days at five different temperatures and found the largest abundance differences occurred in permafrost layer samples incubated at temperatures above freezing, with four classes of bacteria becoming differentially more abundant in incubated samples (Figure 3.1 and Figure 3.2). Comparison of dbRDA models revealed that site and soil layer most effectively explain the variation in bacterial community structure (Figure 3.3 and Table 3.2), and also encompass much of the variation explained by FTIR spectral data (Figure 3.4). However, within the soil chemical variables we measured, the amides/aliphatics FTIR ratio, the silicates FTIR peak, and C:N most effectively explained bacterial community variance, suggesting that these soil characteristics, or the soil attributes they represent (*i.e.* OM quality, mineral content, decomposability), may be good predictors of bacterial community structure. Further correlation analysis between bacterial abundance and these soil chemical variables revealed many strong relationships in active layer samples, but relatively few in permafrost samples, and identified how individual bacterial classes respond to influential soil chemical characteristics (Figure 3.5). Overall, this research reveals which bacteria opportunistically take advantage of thawing SOM, elucidates the relationships between soil bacteria and the soil chemical environment, and provides a basis for understanding bacterial community dynamics in a changing ecosystem.

3.4.1 *Bacterial abundance responses to warming*

Soil bacterial communities are governed by their environment. While soil chemistry is primarily determined by site specific factors (*e.g.* parent material, climate, topography, plant community), inherent microscale variations within the soil matrix dictate resource availability and redox potential for a bacterial community and are relatively stable over short time periods. Broader environmental factors such as moisture/O₂-availability and temperature, however, can change rapidly and are in constant flux, particularly in the active soil layer (organic + mineral layers). In comparison, permafrost soils innately remain frozen, limiting microbial access to water and organic matter. Microbial communities that are active in permafrost must survive on limited dissolved organic carbon (DOC) and nutrients seeping in through water films (Michaelson 2003), are adapted to thrive in very low temperatures, and generally have lower metabolic rates than microorganisms in the active layer (Rivkina et al. 2000, Price and Sowers 2004, Mackelprang et al. 2017). Our results indicate that while the abundances of certain bacteria in the active soil layer do change in response to temperature manipulations, the most pronounced abundance differences between un-incubated and incubated samples occurred in permafrost samples (Figure 3.1), demonstrating the transformation of an psychrophilic community adapted to subzero temperatures, to a more generalist, copiotrophic community able to take advantage of newly available thawed organic matter and water. This fundamental difference can be seen by comparing the bacterial community structures of permafrost samples to active layer samples, and is also shown to be a primary explanatory variable and driver of bacterial community structure (Figure 3.3A and Table 3.2). Additionally, specific examples can be seen in the most responsive bacteria to positive incubations temperatures, including Alphaproteobacteria, Betaproteobacteria, Gammaproteobacteria, and Bacteroidetes [Sphingobacteriia] (Figure 3.1), which have been

classified as copiotrophic organisms before. Both Betaproteobacteria and Bacteroidetes abundances in particular have been associated with higher levels of available soil C (Fierer et al. 2007). Additionally, Bacteroidetes has been associated with decomposition-related genes encoding enzymes such as mannase and chitinase (Yergeau et al. 2009), and has been found in upper permafrost layers exhibiting increased β -glucosidase and phosphatase activity (Coolen et al. 2011), both of which indicate an environment rich in organic-C sources. In contrast, the abundances of Verrucomicrobia and Acidobacteria from our samples generally decreased in response to warming and were relatively less abundant in the active layer vs. the permafrost samples (Figure 3.1 and Figure 3.2). This opposing patterns between these bacterial phyla are commonly observed in copiotrophic vs oligotrophic environments (*e.g.* rhizosphere vs. bulk soil), suggesting in our study the transformation of a psychrophilic, C and nutrient limited bacterial community to a more generalized, competitive, copiotrophic community.

Bacterial community phylogeny has been characterized before in permafrost soils before (Yergeau et al. 2010, Hultman et al. 2015, Müller et al. 2018), however bacterial community response to thaw is relatively understudied (Mackelprang et al. 2011, Monteux et al. 2018). Actinobacteria, specifically of the suborder Micrococccineae (which contains the family Intrasporangiaceae and the genus *Arthrobacter*, mentioned in Müller et al. 2018 and Johnson et al. 2007 respectively), has commonly been found in permafrost samples (Hansen et al. 2007, Johnson et al. 2007, Yergeau et al. 2010, Müller et al. 2018) and has responded positively to warming in previous experiments (Mackelprang et al. 2011). Our results showed increased abundance in the classes Actinobacteria and Acidomicrobia at higher incubation temperatures, but not in Actinobacteria [Thermoleophilia], a thermophilic class of bacteria which decreased in samples incubated in temperatures above freezing relative to un-incubated samples in the SL and

HU sites (Figure 3.1). A similar pattern was also seen in another thermophile, the *Caldiserica* (Figure 3.1 and Figure 3.2), also observed by Monteux et al. (2018), leading us to wonder how thermophilic organisms typically found in very hot environments ended up in permafrost soils. We speculate they are relics from geothermal or volcanic activity of the distant past at sites SL and HU (Boyd and Boyd 1971, Mironov et al. 2013), and once exposed after thaw, quickly get outcompeted.

3.4.2 Drivers/predictors of bacterial community structure

As bacterial communities respond to thawing soils in the Arctic, it is important to consider the effects of soil chemistry on influencing community structure. Soil chemistry is notoriously heterogeneous, and highly variable between soil layers and location. Additionally, many soil chemical factors, such as pH, and C and N concentrations, have been shown to be influential drivers of community structure (Lauber et al. 2009, Kaiser et al. 2016). Here we used a variety of samples from different soil layers and from four sites across the Alaskan tundra to explore the relationships between soil bacterial abundance and a variety of soil chemical indicators, including FTIR spectral peaks associated with specific soil chemical characteristics, FTIR band ratios associated with SOM decomposability/stability, and a suite of categorical descriptors and commonly used indicators. Our analysis shows that certain individual FTIR spectra are more important predictors of bacterial community structure than others, specifically the amides/aliphatics peak ratio and the silicates peak (Table 3.2). As a measure of SOM decomposability, the amides/aliphatics peak ratio likely differentiates community structure based on the abundance of specialist psychrophilic vs. generalist copiotrophic bacteria. While silicates have not specifically been linked to influencing bacterial community structure to our knowledge, the idea of soil mineralogical influence on soil bacteria is not new (Uroz et al. 2009, 2015), and

could explain the degree of explanatory power associated with silicates in our samples. However, neither of these FTIR soil chemical variables perform better than more common categorical descriptors or field measurements (*e.g.* soil pH, C:N, moisture, texture). Most of the bacterial community variation explained by FTIR measurements could be explained more easily by site location and soil layer, in effect capturing the differences between soil chemistry at different sites and between different soil layers (Figure 3.3).

Although the additive models from our study using FTIR spectral data were generally not useful in predicting soil bacterial community structure, the potential for soil spectral analysis in bacterial community profiling remains promising. There is already much research linking infrared spectral data to a variety of soil properties from different size fractions, soil layers, and regions (Reeves 2010, Calderón et al. 2011, 2013, Peltre et al. 2014, Matamala et al. 2017), many of which are either regulated by, or influence microbial community structure. Additionally, FTIR spectral analysis has been shown to reliably predict the degradation state and/or stability of the OM in the Arctic soils used in our data set (Matamala et al. 2019). However, to our knowledge, few studies have explored the use of FTIR spectra in predicting soil bacterial community structure, but in those that have, FTIR spectra drastically improved the explanatory power of the models (Yang et al. 2019). In our study, while the use of dbRDA provides a powerful tool for determining the driving factors behind bacterial community structure, it does not allow for the collinearity of factors, forcing selection of individual, unrelated peaks as explanatory variables (Micheal H. Graham 2003). If instead, the complete spectral band could be utilized to “fingerprint” the soil chemical profile, this would provide a much more powerful predictive tool. With analytical tools constantly improving and a developing interest in the use of machine learning models, we aim to focus future research on selection, validation, and

verification of appropriate analysis techniques, such as partial least squared regression analysis, for the extrapolation of microbial community and functional data from IR spectral analyses of soils.

3.4.3 Relationships between soil chemistry, CMP, and bacterial abundance

As with predictive analysis, research using correlations to directly link bacterial abundance of specific taxa to FTIR spectral peak absorbance is limited. One study (Davinic et al. 2012) established distinguishable associations of bacterial phyla to FTIR spectral bands among different soil aggregate size-fractions, and found correlation patterns to be driven more by SOM chemistry than C content, lower abundance bacteria to have stronger relationships to soil chemistry than the dominant bacteria, and opposing correlation patterns between bacterial phyla to change depending on the size-fraction. The data from our study shows similar opposing correlation patterns between different bacteria and soil chemical characteristics, but was not consistent between site and soil layer (Figure 3.5). Although soil aggregate size-fractions are not applicable to our study due to the nature of Arctic soils, the soil chemical differences associated with site and soil layer may be enough to drive changes in correlation patterns. The most noticeable pattern emerging from our correlation analysis was the larger number and greater strength of bacterial correlations to soil chemistry in the active layers compared to the permafrost layers (Figure 3.5). This may indicate fundamentally tighter associations in the active layer where microbial communities that excel at mining OM are already established, versus those in permafrost layers that may still be adjusting to newly available substrates.

While the link between FTIR derived soil chemistry and CMP of the soils from this study have been well established and described in Matamala et al. (2019), the bacterial abundance

relationships to CMP analyzed in this study were less clear. Other studies have shown microbial community structure (as well as DOC chemistry) in thawed permafrost soils to be a good predictor of CO₂ production (Ernakovich et al., 2017). Thus, bacterial abundance should correlate with CMP. In our study, the majority of bacterial class abundances were negatively correlated to CMP, with the notable exception of Alphaproteobacteria (and somewhat Bacteroidetes [Sphingobacteriia] and Planctomycetia) from permafrost samples (Figure 5), indicating these bacteria to be the major players in the mineralization of C from thawing permafrost environments. In addition, the Q₁₀ calculated from CMP were generally lowest in mineral layer soils, highest in organic layer samples, and somewhere in-between in permafrost samples (Table 3.1). This is reflective of the C-availability in the various soil layers upon thaw, where the organic layers have the most recently deposited C substrate from plants, followed by a substantial amount of older C substrates which have been frozen in permafrost.

3.5 Conclusions

We incubated 360 soil samples, representing both the permafrost and active layers and collected from across the Alaskan Northern Slope, to determine how soil bacterial communities respond to increased temperatures within the context of their soil chemical microenvironment, and examine corollary patterns and relationships between bacterial abundance, C mineralization potential, and soil chemistry by FTIR spectral analysis. We found Alphaproteobacteria, Betaproteobacteria, Gammaproteobacteria, and Bacteroidetes [Sphingobacteriia] abundances greatly increased after 60-day aerobic incubations at positive temperatures, indicating the majority of C mineralized during this period was due the growth of these organisms. FTIR spectral peaks associated with silicates and peak ratios associated with OM degradation state (*i.e.*

amides/aliphatics ratio) were the most influential soil chemical factors driving bacterial community structure. Correlations between bacterial class abundances and important soil chemical factors, including C mineralization, were generally stronger in active layer samples when compared to permafrost samples, likely due to greater community stability in the active layer. Carbon mineralization potential in permafrost was most strongly correlated with Alphaproteobacteria (and somewhat with Bacteroidetes [Sphingobacteriia]) abundance, further supporting the importance of these organisms in mineralization of organic C from recently thawed permafrost. Overall, these results support and further characterize soil bacterial community shifts that may occur as a frozen environment with limited access to C sources, such as is found in undisturbed permafrost, transitions to a more copiotrophic, C-rich environment, such as is predicted in thawing permafrost due to climate change.

3.6 Acknowledgements

Funding for this research was provided by the United States Department of Energy, Office of Science, Office of Biological and Environmental Research under contract DE-AC02-06CH11357. We would also like to thank Scott M. Hoffman for technical support.

3.7 References

- Anisimov, O., D. Vaughan, T. Callaghan, C. Furgal, H. Marchant, T. Prowse, H. Vilhjalmsson, and J. Walsh. 2007. Impacts, adaptation and vulnerability. Contribution of working group II to the fourth assessment report of the Intergovernmental Panel on Climate Change,. *Climate change*:653–685.
- Artz, R. R. E., S. J. Chapman, and C. D. Campbell. 2006. Substrate utilisation profiles of microbial communities in peat are depth dependent and correlate with whole soil FTIR profiles. *Soil Biology and Biochemistry* 38:2958–2962.
- Artz, R. R. E., S. J. Chapman, A. H. Jean Robertson, J. M. Potts, F. Laggoun-Défarge, S. Gogo, L. Comont, J. R. Disnar, and A. J. Francez. 2008. FTIR spectroscopy can be used as a screening tool for organic matter quality in regenerating cutover peatlands. *Soil Biology and Biochemistry* 40:515–527.
- Bates, S. T., D. Berg-Lyons, J. G. Caporaso, W. A. Walters, R. Knight, and N. Fierer. 2011. Examining the global distribution of dominant archaeal populations in soil. *ISME Journal* 5:908–917.
- Boyd, W. L., and J. W. Boyd. 1971. Distribution of Thermophilic Bacteria in Arctic and Subarctic Habitats. *Oikos* 22:37–42.
- Calderón, F., M. Haddix, R. T. Conant, K. Magrini-Bair, and E. Paul. 2013. Diffuse-Reflectance Fourier-Transform Mid-Infrared Spectroscopy as a Method of Characterizing Changes in Soil Organic Matter. *Soil Sci. Soc. Am. J.* 77:1591–1600.
- Calderón, F. J., J. B. Reeves, H. P. Collins, and E. A. Paul. 2011. Chemical Differences in Soil Organic Matter Fractions Determined by Diffuse-Reflectance Mid-Infrared Spectroscopy. *Soil Science Society of America Journal* 75:568.
- Caporaso, J. G., C. L. Lauber, W. A. Walters, D. Berg-Lyons, C. A. Lozupone, P. J. Turnbaugh, N. Fierer, and R. Knight. 2011. Global patterns of 16S rRNA diversity at a depth of millions of sequences per sample. *Proceedings of the National Academy of Sciences* 108:4516–4522.
- Caporaso, J. G., C. L. Lauber, W. a Walters, D. Berg-Lyons, J. Huntley, N. Fierer, S. M. Owens, J. Betley, L. Fraser, M. Bauer, N. Gormley, J. a Gilbert, G. Smith, and R. Knight. 2012. Ultra-high-throughput microbial community analysis on the Illumina HiSeq and MiSeq platforms. *The ISME journal* 6:1621–4.
- Caporaso, J., J. Kuczynski, and J. Stombaugh. 2010. QIIME allows analysis of high-throughput community sequencing data. *Nature methods* 7:335–336.
- Coolen, M. J. L., J. van de Giessen, E. Y. Zhu, and C. Wuchter. 2011. Bioavailability of soil

- organic matter and microbial community dynamics upon permafrost thaw. *Environmental Microbiology* 13:2299–2314.
- Davidson, E. a, and I. a Janssens. 2006. Temperature sensitivity of soil carbon decomposition and feedbacks to climate change. *Nature* 440:165–73.
- Davinic, M., L. M. Fultz, V. Acosta-Martinez, F. J. Calderón, S. B. Cox, S. E. Dowd, V. G. Allen, J. C. Zak, and J. Moore-Kucera. 2012. Pyrosequencing and mid-infrared spectroscopy reveal distinct aggregate stratification of soil bacterial communities and organic matter composition. *Soil Biology and Biochemistry* 46:63–72.
- Dungait, J. A. J., D. W. Hopkins, A. S. Gregory, and A. P. Whitmore. 2012. Soil organic matter turnover is governed by accessibility not recalcitrance. *Global Change Biology* 18:1781–1796.
- Ernakovich, J. G., L. M. Lynch, P. E. Brewer, F. J. Calderon, and M. D. Wallenstein. 2017. Redox and temperature-sensitive changes in microbial communities and soil chemistry dictate greenhouse gas loss from thawed permafrost. *Biogeochemistry* 134:183–200.
- Fierer, N., M. a. Bradford, and R. B. Jackson. 2007. Toward an ecological classification of soil bacteria. *Ecology* 88:1354–1364.
- Flynn, T. M., J. C. Koval, S. M. Greenwald, S. M. Owens, K. M. Kemner, and D. A. Antonopoulos. 2017. Parallelized, Aerobic, Single Carbon-Source Enrichments from Different Natural Environments Contain Divergent Microbial Communities. *Frontiers in Microbiology* 8:1–14.
- Haberhauer, G., B. Rafferty, F. Strebl, and M. H. Gerzabek. 1998. Comparison of the composition of forest soil litter derived from three different sites at various decompositional stages using FTIR spectroscopy. *Geoderma* 83:331–342.
- Hansen, A. A., R. A. Herbert, K. Mikkelsen, L. L. Jensen, T. Kristoffersen, J. M. Tiedje, B. A. Lomstein, and K. W. Finster. 2007. Viability, diversity and composition of the bacterial community in a high Arctic permafrost soil from Spitsbergen, Northern Norway. *Environmental Microbiology* 9:2870–2884.
- Holland, M. M., and C. M. Bitz. 2003. Polar amplification of climate change in coupled models. *Climate Dynamics* 21:221–232.
- Hopkins, F., M. A. Gonzalez-meler, C. E. Flower, D. J. Lynch, C. Czimczik, J. Tang, and J.-A. Subke. 2013. Ecosystem-level controls on root-rhizosphere respiration. *The New phytologist* 199:339–351.
- Hugelius, G., J. Strauss, S. Zubrzycki, J. W. Harden, E. A. G. Schuur, C. L. Ping, L. Schirmer, G. Grosse, G. J. Michaelson, C. D. Koven, J. A. O'Donnell, B. Elberling, U. Mishra, P. Camill, Z. Yu, J. Palmtag, and P. Kuhry. 2014. Estimated stocks of circumpolar

permafrost carbon with quantified uncertainty ranges and identified data gaps. *Biogeosciences* 11:6573–6593.

- Hultman, J., M. P. Waldrop, R. Mackelprang, M. M. David, J. McFarland, S. J. Blazewicz, J. Harden, M. R. Turetsky, a. D. McGuire, M. B. Shah, N. C. VerBerkmoes, L. H. Lee, K. Mavrommatis, J. K. Jansson, H. H. J, W. MP, M. R, D. MM, M. J, B. SJ, H. H. J, T. MR, M. AD, S. MB, V. NC, L. LH, M. K, and J. JK. 2015. Multi-omics of permafrost, active layer and thermokarst bog soil microbiomes. *Nature*.
- Johnson, S. S., M. B. Hebsgaard, T. R. Christensen, M. Mastepanov, R. Nielsen, K. Munch, T. Brand, M. T. P. Gilbert, M. T. Zuber, M. Bunce, R. Ronn, D. Gilichinsky, D. Froese, and E. Willerslev. 2007. Ancient bacteria show evidence of DNA repair. *Proceedings of the National Academy of Sciences* 104:14401–14405.
- Kaiser, K., B. Wemheuer, V. Korolkow, F. Wemheuer, H. Nacke, I. Schöning, M. Schrumpf, and R. Daniel. 2016. Driving forces of soil bacterial community structure, diversity, and function in temperate grasslands and forests. *Scientific Reports* 6:1–12.
- Lauber, C. L., M. Hamady, R. Knight, and N. Fierer. 2009. Pyrosequencing-based assessment of soil pH as a predictor of soil bacterial community structure at the continental scale. *Applied and Environmental Microbiology* 75:5111–5120.
- Mackelprang, R., A. Burkert, M. Haw, T. Mahendrarajah, C. H. Conaway, T. A. Douglas, and M. P. Waldrop. 2017. Microbial survival strategies in ancient permafrost: insights from metagenomics. *The ISME Journal*:1–14.
- Mackelprang, R., M. P. M. Waldrop, K. M. DeAngelis, M. M. David, K. L. Chavarria, S. J. Blazewicz, E. M. Rubin, and J. K. Jansson. 2011. Metagenomic analysis of a permafrost microbial community reveals a rapid response to thaw. *Nature* 480:368–71.
- Matamala, R., F. J. Calderón, J. D. Jastrow, Z. Fan, S. M. Hofmann, G. J. Michaelson, U. Mishra, and C. L. Ping. 2017. Influence of site and soil properties on the DRIFT spectra of northern cold-region soils. *Geoderma* 305:80–91.
- Matamala, R., J. D. Jastrow, F. J. Calderón, C. Liang, Z. Fan, G. J. Michaelson, and C. L. Ping. 2019. Predicting the decomposability of arctic tundra soil organic matter with mid infrared spectroscopy. *Soil Biology and Biochemistry* 129:1–12.
- McCarthy, D. J., Y. Chen, and G. K. Smyth. 2012. Differential expression analysis of multifactor RNA-Seq experiments with respect to biological variation. *Nucleic Acids Research* 40:4288–4297.
- McDonald, D., M. N. Price, J. Goodrich, E. P. Nawrocki, T. Z. Desantis, A. Probst, G. L. Andersen, R. Knight, and P. Hugenholtz. 2012. An improved Greengenes taxonomy with explicit ranks for ecological and evolutionary analyses of bacteria and archaea. *ISME Journal* 6:610–618.

- Michaelson, G. J. 2003. Soil organic carbon and CO₂ respiration at subzero temperature in soils of Arctic Alaska. *Journal of Geophysical Research* 108:8164.
- Michaelson, G. J., C.-L. Ping, and M. Clark. 2013. Soil Pedon Carbon and Nitrogen Data for Alaska: An Analysis and Update. *Open Journal of Soil Science* 03:132–142.
- Micheal H. Graham. 2003. Confronting Multicollinearity in Ecological Multiple Regression. *Ecology* 84:2809–2815.
- Mikan, C. J., J. P. Schimel, and A. P. Doyle. 2002. Temperature controls of microbial respiration in arctic tundra soils above and below freezing. *Soil Biology and Biochemistry* 34:1785–1795.
- Mironov, V. A., V. A. Shcherbakova, E. M. Rivkina, and D. A. Gilichinsky. 2013. Thermophilic bacteria of the genus *Geobacillus* from permafrost volcanic sedimentary rocks. *Microbiology* 82:389–392.
- Monteux, S., J. T. Weedon, G. Blume-Werry, K. Gavazov, V. E. J. Jassey, M. Johansson, F. Keuper, C. Olid, and E. Dorrepaal. 2018. Long-term in situ permafrost thaw effects on bacterial communities and potential aerobic respiration. *ISME Journal*:1–13.
- Morita, R. Y. 1975. Psychrophilic Bacteria. *Bacteriological Reviews* 39:144–167.
- Müller, O., T. Bang-Andreasen, R. A. White, B. Elberling, N. Taş, T. Kneafsey, J. K. Jansson, and L. Øvreås. 2018. Disentangling the complexity of permafrost soil by using high resolution profiling of microbial community composition, key functions and respiration rates. *Environmental Microbiology* 00.
- Peltre, C., S. Bruun, C. Du, I. K. Thomsen, and L. S. Jensen. 2014. Assessing soil constituents and labile soil organic carbon by mid-infrared photoacoustic spectroscopy. *Soil Biology and Biochemistry* 77:41–50.
- Ping, C. L., J. G. Bockheim, J. M. Kimble, G. J. Michaelson, and D. A. Walker. 1998. Characteristics of cryogenic soils along a latitudinal transect in arctic Alaska. *Journal of Geophysical Research* 103:28,917-28,928.
- Ping, C. L., J. D. Jastrow, M. T. Jorgenson, G. J. Michaelson, and Y. L. Shur. 2015. Permafrost soils and carbon cycling. *Soil* 1:147–171.
- Ping, C. L., G. J. Michaelson, M. T. Jorgenson, J. M. Kimble, H. Epstein, V. E. Romanovsky, and D. a. Walker. 2008. High stocks of soil organic carbon in the North American Arctic region. *Nature Geoscience* 1:615–619.
- Price, P. B., and T. Sowers. 2004. Temperature dependence of metabolic rates for microbial growth, maintenance, and survival. *Proceedings of the National Academy of Sciences* 101:4631–4636.

- Reeves, J. B. 2010. Near- versus mid-infrared diffuse reflectance spectroscopy for soil analysis emphasizing carbon and laboratory versus on-site analysis: Where are we and what needs to be done? *Geoderma* 158:3–14.
- Ricketts, M. P., R. S. Poretsky, J. M. Welker, and M. A. Gonzalez-Meler. 2016. Soil bacterial community and functional shifts in response to altered snowpack in moist acidic tundra of Northern Alaska. *SOIL* 2:459–474.
- Rivkina, E. M., E. I. Friedmann, C. P. McKay, and D. A. Gilichinsky. 2000. Metabolic activity of Permafrost Bacteria below the freezing point. *Applied and Environmental Microbiology* 66:3230–3233.
- Robinson, M. D., D. J. McCarthy, and G. K. Smyth. 2009. edgeR: A Bioconductor package for differential expression analysis of digital gene expression data. *Bioinformatics* 26:139–140.
- Schuur, E. A. G., B. W. Abbott, W. B. Bowden, V. Brovkin, P. Camill, J. G. Canadell, J. P. Chanton, F. S. Chapin, T. R. Christensen, P. Ciais, B. T. Crosby, C. I. Czimczik, G. Grosse, J. Harden, D. J. Hayes, G. Hugelius, J. D. Jastrow, J. B. Jones, T. Kleinen, C. D. Koven, G. Krinner, P. Kuhry, D. M. Lawrence, a. D. McGuire, S. M. Natali, J. A. O'Donnell, C. L. Ping, W. J. Riley, A. Rinke, V. E. Romanovsky, a. B. K. Sannel, C. Schädel, K. Schaefer, J. Sky, Z. M. Subin, C. Tarnocai, M. R. Turetsky, M. P. Waldrop, K. M. Walter Anthony, K. P. Wickland, C. J. Wilson, and S. A. Zimov. 2013. Expert assessment of vulnerability of permafrost carbon to climate change. *Climatic Change* 119:359–374.
- Schuur, E. a. G., a. D. McGuire, C. Schädel, G. Grosse, J. W. Harden, D. J. Hayes, G. Hugelius, C. D. Koven, P. Kuhry, D. M. Lawrence, S. M. Natali, D. Olefeldt, V. E. Romanovsky, K. Schaefer, M. R. Turetsky, C. C. Treat, and J. E. Vonk. 2015. Climate change and the permafrost carbon feedback. *Nature* 520:171–179.
- Six, J., R. T. Conant, E. a Paul, and K. Paustian. 2002. Stabilization mechanisms of soil organic matter: Implications for C-saturatin of soils. *Plant and Soil* 241:155–176.
- Strauss, J., L. Schirrmeister, G. Grosse, D. Fortier, G. Hugelius, C. Knoblauch, V. Romanovsky, C. Schädel, T. Schneider von Deimling, E. A. G. Schuur, D. Shmelev, M. Ulrich, and A. Veremeeva. 2017. Deep Yedoma permafrost: A synthesis of depositional characteristics and carbon vulnerability. *Earth-Science Reviews* 172:75–86.
- Tribelli, P., and N. López. 2018. Reporting Key Features in Cold-Adapted Bacteria. *Life* 8:8.
- Uroz, S., C. Calvaruso, M. P. Turpault, and P. Frey-Klett. 2009. Mineral weathering by bacteria: ecology, actors and mechanisms. *Trends in Microbiology* 17:378–387.
- Uroz, S., L. C. Kelly, M. P. Turpault, C. Lepleux, and P. Frey-Klett. 2015. The Mineralosphere Concept: Mineralogical Control of the Distribution and Function of Mineral-associated Bacterial Communities. *Trends in Microbiology* 23:751–762.

- Walker, D. A., H. E. Epstein, W. A. Gould, A. M. Kelley, A. N. Kade, J. A. Knudson, W. B. Krantz, G. Michaelson, R. A. Peterson, C. L. Ping, M. K. Reynolds, V. E. Romanovsky, and Y. Shur. 2004. Frost-boil ecosystems: Complex interactions between landforms, soil, vegetation and climate. *Permafrost and Periglacial Processes* 15:171–188.
- Wallenstein, M. D., S. K. McMahon, and J. P. Schimel. 2009. Seasonal variation in enzyme activities and temperature sensitivities in Arctic tundra soils. *Global Change Biology* 15:1631–1639.
- Yang, Y., R. A. Viscarra Rossel, S. Li, A. Bissett, J. Lee, Z. Shi, T. Behrens, and L. Court. 2019. Soil bacterial abundance and diversity better explained and predicted with spectro-transfer functions. *Soil Biology and Biochemistry* 129:29–38.
- Yergeau, E., H. Hogues, L. G. Whyte, and C. W. Greer. 2010. The functional potential of high Arctic permafrost revealed by metagenomic sequencing, qPCR and microarray analyses. *The ISME journal* 4:1206–14.
- Yergeau, E., S. A. Schoondermark-Stolk, E. L. Brodie, S. Déjean, T. Z. DeSantis, O. Gonçalves, Y. M. Piceno, G. L. Andersen, and G. A. Kowalchuk. 2009. Environmental microarray analyses of Antarctic soil microbial communities. *ISME Journal* 3:340–351.
- Zhang, J., K. Kobert, T. Flouri, and A. Stamatakis. 2014. PEAR: A fast and accurate Illumina Paired-End reAd mergeR. *Bioinformatics* 30:614–620.

4 SOIL BACTERIAL COMMUNITY AND FUNCTIONAL SHIFTS IN RESPONSE TO ALTERED SNOW PACK IN MOIST ACIDIC TUNDRA OF NORTHERN ALASKA

This chapter is a reprint (with minimal reformatting) of an original article published by Copernicus Publications in the journal SOIL. It has been licensed under an open access Creative Commons Attribution 3.0 License, where the authors retain the copyright. There is no need for reproduction permissions from the publishers.

Ricketts, M. P., R. S. Poretsky, J. M. Welker, and M. Gonzalez-Meler. 2016. Soil bacterial community and functional shifts in response to altered snowpack in moist acidic tundra of Northern Alaska. *Soil* 2:459–474.

4.1 Introduction

Broad and rapid environmental changes are driving both above- and belowground community shifts in the Arctic (Elmendorf et al., 2012a, 2012b; Tape et al., 2006, 2012; Wallenstein et al., 2007). It is well established that soil microbial communities may alter their composition in response to changing environmental factors such as nutrient availability, moisture, pH, temperature, and aboveground vegetation shifts (Lauber et al., 2009; Morgado et al., 2015; Semenova et al., 2015), and ecological and climate induced changes to Arctic soil microbial community structure and function have important effects on ecosystem carbon (C) cycling and nutrient availability for plant growth (Deslippe et al., 2012; Graham et al., 2012; Waldrop et al., 2010; Zak and Kling, 2006). Because many of these environmental features are rapidly changing in Arctic tussock tundra ecosystems (Anisimov et al., 2007; Liston and Hiemstra, 2011), and because of the large amounts of C stored in Arctic soils (Hugelius et al., 2013; Ping et al., 2008; Schuur et al., 2009; Tarnocai et al., 2009), it is imperative to examine microbial responses in this system.

Soil microorganisms play a key role in the decomposition of soil organic matter (SOM) on a

global scale, releasing nutrients into the soil and stored C into the atmosphere in the forms of CO₂ and CH₄, two major greenhouse gases that contribute to global warming (Anisimov et al., 2007). Decomposition of SOM by soil microorganisms amounts to at least half of the 80-90 Gt C released each year by soil respiration, the second largest terrestrial flux after gross primary productivity (GPP; Davidson and Janssens, 2006; Hopkins et al., 2013; Raich et al., 2002). Because global soils contain about 2,000 Gt of C, ~1,500 Gt of which is in the form of SOM (Batjes, 1996; IPCC, 2000), large scale changes in the rate of microbial decomposition will have an impact on the rate at which CO₂ accumulates in the atmosphere (Schimel and Schaeffer, 2012).

The decomposition rate of SOM, resulting in heterotrophic respiration from soils (R_h), has been shown to be sensitive to temperature and moisture (Davidson and Janssens, 2006; Frey et al., 2013; Hopkins et al., 2012, 2013; Xia et al., 2014). As the Arctic climate warms, increasing R_h may be capable of producing a positive feedback on the climate system as C stored in soils over millennia is released back to the atmosphere (Czimczik and Welker, 2010; Jonasson et al., 1999; Lupascu et al., 2014b; Mack et al., 2004; Nowinski et al., 2010; Shaver and Chapin, 1980, 1986).

Northern latitude permafrost soils may house over 50% of the world's soil organic C (SOC; the C component of SOM), approximately twice the amount of C present in the atmosphere (Hugelius et al., 2013; Ping et al., 2008; Schuur et al., 2009; Tarnocai et al., 2009). In addition, Arctic ecosystems are more susceptible to the effects of climate change, warming at approximately twice the rate as temperate zones and exhibiting increased winter precipitation patterns (Anisimov et al., 2007; Liston and Hiemstra, 2011). Deeper snow has a suite of

cascading consequences in tundra ecosystems as snow acts to insulate soil from extreme winter air temperatures resulting in soil temperatures under deeper snow pack up to 10°C warmer than soils under ambient snow depths (Schimel et al., 2004). Altered soil conditions under deeper snow may thus lead to increased SOM decomposition, causing changes in SOC stocks while also releasing nutrients for plant and microbial growth (Anisimov et al., 2007; Leffler and Welker, 2013; Rogers et al., 2011; Welker et al., 2005). The predicted increase in soil temperature as a result of deeper winter snow accumulation should enhance the rate of SOM decomposition by: 1) a direct temperature effect on enzyme kinetics, and 2) by increasing substrate availability to decomposers as the active layer deepens and permafrost thaws (Lützow and Kögel-Knabner, 2009; Nowinski et al., 2010; Schuur et al., 2008). Therefore, warming and deeper snow in the Arctic are likely to expose C stored over millennia to decomposers, resulting in a major source of C to the atmosphere.

However, ecosystem C loss may be offset by increased soil moisture, causing hypoxic conditions and limiting R_h (Blanc-Betes et al. 2016). Also, microbial mineralization of plant nutrients, such as nitrogen (N) and phosphorus (P), from SOM decomposition are likely to contribute to increased net primary productivity (NPP; Hinzman et al., 2005; Natali et al., 2012; Pattison and Welker, 2014) and cause shifts in vegetation from herbaceous species (Cottongrass tussock- *Eriophorum vaginatum*) towards woody species (Arctic shrubs – *Betula nana* and *Salix pulchra*) that may produce a larger amount of plant litter compounds that are more resistant to decomposition (Bret-Harte et al., 2001; Pearson et al., 2013; Sturm et al., 2005; Wahren, 2005). The balance between these processes will determine the extent to which Arctic tundra ecosystems feedback on the global climate, making the fate of this stored C unclear (Sistla et al., 2013).

This study examined changes in soil bacterial community composition due to increased winter snow accumulation and subsequent altered biotic and abiotic factors using a long-term snow fence manipulation experiment that mimics changes in winter precipitation by creating a gradient of snow depths from much deeper than ambient to shallower than ambient levels (Jones et al., 1998; Pattison and Welker, 2014; Welker et al., 2000). We postulated that increased soil thermal insulation from deeper winter snow accumulation would elicit bacterial community response via: 1) altered soil physical characteristics such as soil temperature, moisture, or O₂ availability, and 2) altered soil chemistry produced by increased microbial mineralization of SOM resulting in increased nutrient availability and changes in plant species composition and litter. Here we evaluated phylum level shifts in bacterial community phylogeny using 16S rRNA gene analysis and predicted bacterial functions using the program PICRUSt (Langille et al., 2013) to test whether increased snow accumulation and associated changes in soil conditions (warmer temperatures, altered plant inputs, and increased hypoxia) would cause shifts in bacterial community structure and functional potential that reflect increased SOM decomposition and nutrient mineralization.

4.2 Methods

4.2.1 Site description and sample collection

The study utilized a long-term snow depth manipulation experiment site (Jones et al., 1998; Walker et al., 1999) established in 1994 in a moist acidic tundra ecosystem located near Toolik Lake Field Station, Alaska (68°37'N, 149°32'W). It consists of a strategically placed snow fence designed to simulate the increased precipitation patterns and continuous snow-cover episodes predicted under global warming scenarios, resulting in a gradient of increasing snow

accumulation (and thus increasing soil thermal insulation, soil temperatures, and active layer thaw depth/permafrost thaw) with proximity to the fence. While snowfall varied from year to

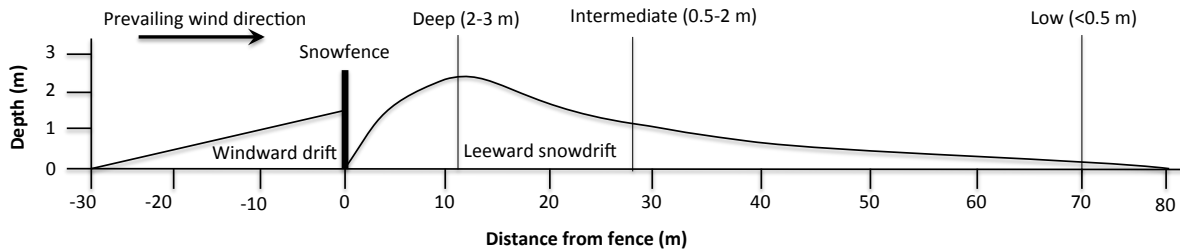


Figure 4.1. Modified from Walker et al., 1999. Schematic of snow accumulation depth at moist acidic tundra site from snow fence manipulation. Three soil cores were obtained from each treatment zone (labeled Deep, Intermediate, and Low) and a Control zone located >30 m outside the effect of the snowfence.

year, the wind drift from the fence provided consistent relative snow accumulation at similar distances from the fence every winter (Fahnestock et al., 2000; Welker et al., 2005). The soil is classified as Typic Aquiturbel, exhibiting characteristics of cryoturbation and poor drainage (Ping et al., 1998; Soil Survey, 2015). Four experimental zones were identified according to their snow accumulation regime: Control (“Control”, taken >30 m outside the effects of the snowfence), deep snow (“Deep” ~100% increase in snow pack relative to the control), intermediate snow (“Int.”, ~50% increase in snow pack relative to the control), and low snow (“Low”, ~25% decrease in snow pack relative to the control; Figure 4.1). The Deep snow zone is unique in that it is waterlogged during thaw periods, and dominated not by Cottongrass tussock or woody shrub species (e.g. *Eriophorum vaginatum*, *Betula nana*, or *Salix pulchra*), but by a sedge species, *Carex bigelowii*. However, the vegetative history of this plot includes a transition from tussock cottongrass to woody shrub species, and finally to wet sedge species (Arft et al., 1999; Walker and Wahren, 2006).

Three replicate soil cores were taken approximately 15-20 m apart from each experimental snow zone (totalling 12 soil cores) in August of 2012 and analyzed separately. All soil coring equipment was cleaned and sterilized in the field between each sample using water and 100% ethanol. The top 10-16 cm representing the organic layers was taken first using a sharpened steel pipe (5.5 cm diameter X 20 cm length) and serrated knife to cut through surface vegetation and to minimize soil compaction. A slide hammer with 5.1 cm x 30.5 cm split soil core sampler (AMS Inc., ID, USA) was used to obtain the remainder of the active layer down to permafrost (~35–65 cm soil depth), including mineral soil layers. The soil cores were stored in sterile Whirlpak® bags, immediately frozen on site, and shipped to the Stable Isotope Laboratory at the University of Illinois at Chicago where they were sectioned horizontally into 2 cm depth segments using a sterilized ice-core cutter, providing a 2 cm resolution soil depth profile for each core. A portion of each segment was ground into a fine powder using a Spexmill mixer/mill 8000 (SPEX SamplePrep, NJ, USA) and analyzed for C and N concentration and stable isotopes using a Costech (Valencia, CA, USA) elemental analyzer (EA) in line with a Finnigan Deltaplus XL IRMS (isotope ratio mass spectrometer; Bremen, Germany). Soil pH was measured from portions of the same segments by creating a soil slurry mixture (2 ml H₂O : 1 g soil) and using an Accumet Basic AB15 pH meter with a calomel reference pH electrode (Thermo Fisher Scientific Inc., MA, USA). In addition, at the time of collection, soil temperature, soil moisture, and active layer thaw depth were measured and recorded at four points around each soil core hole (n=12 per treatment) to characterize the soil environment. Soil temperatures (°C) were measured using a 12 cm Taylor TruTemp Digital Instant Read Probe Thermometer (Taylor Precision Products, Inc., NM, USA), surface (top 12 cm) volumetric water content (%) was measured using a HydroSense Soil Water Content Measurement System (Campbell Scientific Inc., UT, USA), and active layer

thaw depths (cm) were measured by inserting a meter stick attached to a metal rod into the ground until it hit ice.

4.2.2 DNA extraction, sequencing, and analysis

Samples from organic and mineral layers of each soil core, as well as the transition between the two, were selected for DNA extraction initially based on visual examination of each individual core section and further classified by %C in saturated soils as per the Soil Survey Division Staff, (1993; Organic $\geq 12\%$ SOC, Mineral: $< 12\%$ SOC). Organic samples were collected just below where plant tissue transitioned into dark brown/black soil (mean soil depth \pm standard error [S.E.] = 5.6 ± 1.3 cm; Control $n=4$, Deep $n=4$, Int. $n=3$, Low $n=4$), transitional samples were taken from the visual border between organic and mineral layers based on change in soil colour (mean soil depth \pm S.E. = 14.8 ± 1.8 cm; Control $n=3$, Deep $n=3$, Int. $n=4$, Low $n=3$), and mineral samples were collected 10 cm below this transition (mean soil depth \pm S.E. = 25.1 ± 1.7 cm; Control $n=3$, Deep $n=4$, Int. $n=3$, Low $n=3$), totaling 41 samples. To maintain consistency, only these samples were used to analyze %C, %N, and pH relationships. Samples were sent to Argonne National Laboratory for DNA extraction, amplification, and sequencing as per standards used by the Earth Microbiome Project (Gilbert et al., 2014). DNA extractions were performed using MoBio's PowerSoil®-htp 96 Well Soil DNA Isolation Kit as per protocol, the V4 region of the 16S rRNA gene was amplified using PCR primers 515F/806R (Caporaso et al., 2012), DNA quantification was performed using PicoGreen, and 2×150 bp paired-end sequencing was performed using an Illumina MiSeq instrument.

Samples were barcoded prior to sequencing for downstream sample identification and paired-end assembly, demultiplexing, quality filtering, operational taxonomic unit (OTU) picking, and

preliminary diversity analyses were performed using the QIIME software package version 1.8.0 (Caporaso et al. 2010). Forward and reverse reads were assembled using fastq-join (Aronesty, 2011) with 15bp overlap at 15% maximum difference. Quality filtering included removal of reads that didn't have at least 75% consecutive high quality (phred>q20) base calls and truncation of reads with more than three consecutive low quality (phred<q20) base calls. This resulted in an assembled-read median sequence length of 253 bp.

To reveal phylogenetic abundance and relationships, sequence reads were assigned taxonomic identities using closed reference OTU picking that clusters and matches each read to a reference database. Any read that did not match a sequence in the reference database was discarded. All default QIIME parameters were used (reference database=Greengenes (13_8), OTU picking method=uclust, and sequence similarity threshold=97%). Because many organisms are known to possess multiple copies of the 16S rRNA gene in their genome, the abundance assignments were corrected based on known copy numbers using PICRUSt's *normalize_by_copy_number.py* script. The relative abundances of the six most abundant phyla, comprising 82% - 96% of total detected phyla per sample, were analyzed for treatment effects, and alpha and beta diversities were examined using the Shannon diversity index to estimate within sample diversity, and Bray-Curtis dissimilarity matrices to determine community structure differences.

The genetic functional potential of bacterial communities was determined using the software package PICRUSt version 1.0.0 (Langille et al., 2013) which predicts functional gene copy numbers in a community based on 16S rRNA sequencing results. Recent advances in sequencing technologies and bioinformatics has greatly enhanced our current knowledge of the genetic

potential of soil microorganisms, allowing us to determine what genes a group of organisms is likely to possess based on ancestral state reconstruction of metagenome assemblies from current genomic databases (Langille et al., 2013; Martiny et al., 2013). PICRUSt utilizes this knowledge, revealing functional potential, in the form of gene abundance, associated with phylogenetic community structure. For this study, we targeted Kyoto Encyclopedia of Gene and Genomes (KEGG) ortholog assignments for enzymatic genes commonly associated with SOM decomposition, nutrient (nitrogen and phosphate) mobilization, and environmental stress responses (Sinsabaugh et al., 2008; Waldrop et al., 2010; full list in Supplementary Table S4.1). These genes were then grouped according to functional role, resulting in the following nine gene groups: 1) lignin degradation, 2) chitin degradation, 3) cellulose degradation, 4) pectin degradation, 5) xylan degradation, 6) arabinoside degradation, 7) nitrogen mobilization, 8) phosphate mobilization, and 9) superoxide dismutation.

4.2.3 *Statistical analyses*

Differences between soil layers (Organic, Transition, Mineral) and snow accumulation treatments (Control, Deep, Int., Low), including abiotic measurements and relative abundance of bacterial 16S rRNA and functional genes, were determined using the Kruskal-Wallis test in the R statistical software package with a significance threshold of $p < 0.05$. Due to significant differences between soil layers (Supplementary Table), each layer was analyzed separately. Only organic and mineral layers are reported. All abiotic factors, phyla relative abundances and relative abundances of functional genes were analyzed individually to elucidate the treatment effects for each group, and pairwise comparisons were made to determine significant differences between treatments using the Nemenyi post hoc test. In addition, linear regressions were performed to determine relationships between soil chemical properties (%C, %N, C:N, and pH)

and bacterial abundance at the phylum level, as well as the gene abundances of SOM degrading enzymes (Supplementary Figure S4.1-S4.15). To ensure accurate comparisons, soil chemical properties were measured from the same samples that DNA was extracted from. Only R^2 values >0.30 are discussed.

Bacterial diversity statistics were calculated using QIIME (Caporaso et al. 2010), specifically the *compare_alpha_diversity.py*, *compare_categories.py*, and *compare_distance_matrices.py* scripts. Pairwise comparisons of the Shannon alpha diversity metrics from soil layer and each treatment group were made using non-parametric two-sample t-tests with 999 Monte Carlo permutations. Beta diversity was analyzed by comparing Bray-Curtis dissimilarity matrices of bacterial abundance data from each sample to soil chemical properties, and between soil layers and snow accumulation treatments using adonis tests with 999 permutations. Organic and mineral layers were also analyzed separately when comparing snow accumulation treatments and soil chemical properties. Analyses of soil chemical properties were further substantiated by Mantel tests, again using 999 permutations. This data was visualized by creating a non-metric multidimensional scaling (NMDS) plot (Stress=0.090, Shepard plot non-metric $R^2=0.992$) in the R package phyloseq (McMurdie and Holmes, 2013) using the same Bray-Curtis dissimilarity matrices (Figure 4.2).

4.3 Results

4.3.1 *Environmental changes*

Significant differences in soil temperature ($n=12$, $H=33.29$, $df=3$, $p<0.001$), active layer thaw depth ($n=12$, $H=21.35$, $df=3$, $p<0.001$), and organic layers %C ($n=4$, $H=9.74$, $df=3$, $p=0.021$) were associated with the four different snow zones. Post hoc tests revealed higher temperatures

in the Deep snow zone relative to the Control ($p=0.009$), the Int. ($p=0.001$), and the Low snow zone ($p<0.001$; Table 4.1). Active layer depth data revealed similar results, increasing in the Deep snow accumulation zone and decreasing as snow pack was experimentally reduced. Only in the Deep zone was the active layer thaw depth significantly ($p=0.020$) deeper than the Control zone. However, along the snow accumulation gradient, thaw depth significantly increased from Low to Deep plots (Low/Int. - $p=0.021$, Low/Deep - $p<0.001$; Table 4.1). Soil moisture was not

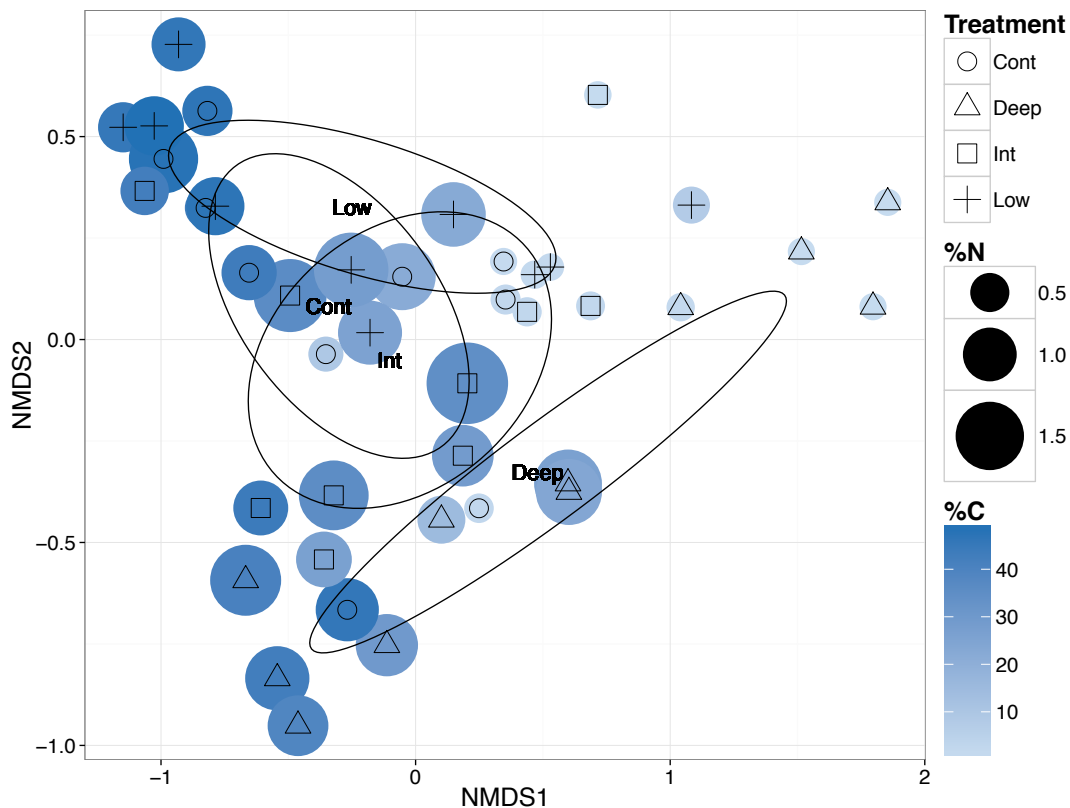


Figure 4.2. Non-metric multidimensional scaling (NMDS) plot using Bray-Curtis dissimilarity matrices (Stress=0.090, Shepard plot non-metric $R^2=0.992$). Each point represents the bacterial community structure within one of the 41 total samples used for DNA extraction from all soil depths (Organic, Transition, and Mineral). Colours indicate %C ranging from 1.4% (light blue) to 48.6% (dark blue), bubble size indicates %N ranging from 0.09% (small) to 1.95% (large), and shapes indicate snow accumulation treatments (Control, Deep, Int., Low). Ellipse centroids represent treatment group means while the shape is defined by the covariance within each group.

correlated with snow accumulation, possibly the result of surface hydrology at the site, which was largely saturated throughout the growing season. In the organic soil layers, the %C concentration of soil declined with increased snow accumulation (Low/Deep - $p=0.03$), while the %N concentration only slightly increased (Low/Deep - $p=0.32$). This resulted in a decreasing trend in C:N ratios across snow accumulation treatment zones and relative to the control (Control/Deep - $p=0.14$; Table 4.1). Soil pH tended to increase (became more neutral) with increased snow accumulation (Low/Deep - $p=0.06$). The changes in the mineral soil layers were less pronounced than in the organic layers. C:N ratios again showed a decreasing trend as snow accumulation increased, while soil pH increased in the Deep zone but did not show a trend along the treatment gradient (Table 4.1).

Table 4.1. Abiotic characteristics of soil from snow accumulation treatments (Low= \sim 25% less snow pack than the Control, Int.= \sim 50% more snow pack than the Control, Deep= \sim 100% more snow pack than the Control). Values are means \pm standard errors. Soil chemical properties were obtained from samples used for DNA extraction, while temperature and thaw depth were measured *in situ* ($n=12$). Organic and mineral samples were analyzed separately using the Nemenyi post hoc test. Results are indicated by _{a,b,c} only where $p<0.05$.

Treatment	Soil Layers	Sample Depths (cm)	%C	%N	C:N	pH	Temp @ 12 cm (°C)	Thaw Depth (cm)
Control	Organic (n=4)	6.75 \pm 3.12	45.21 \pm 1.09 _{ab}	1.01 \pm 0.20	50.04 \pm 9.44	4.59 \pm 0.09	4.32 \pm 0.27 _b	59.17 \pm 1.23 _{bc}
	Mineral (n=3)	26.00 \pm 5.51	2.57 \pm 0.39	0.15 \pm 0.03	17.67 \pm 1.34	5.15 \pm 0.05 _{ab}		
Low	Organic (n=4)	5.50 \pm 1.89	46.63 \pm 0.73 _a	1.06 \pm 0.07	44.59 \pm 2.54	4.44 \pm 0.08	2.92 \pm 0.24 _b	50.92 \pm 3.20 _c
	Mineral (n=3)	27.00 \pm 1.15	4.18 \pm 1.92	0.22 \pm 0.11	19.42 \pm 0.65	5.16 \pm 0.20 _{ab}		
Int.	Organic (n=3)	3.67 \pm 0.67	40.59 \pm 2.43 _{ab}	1.17 \pm 0.25	38.38 \pm 8.85	4.69 \pm 0.41	4.08 \pm 0.25 _b	61.88 \pm 1.19 _{ab}
	Mineral (n=3)	23.67 \pm 2.03	2.58 \pm 0.49	0.14 \pm 0.02	18.58 \pm 1.45	5.01 \pm 0.04 _a		
Deep	Organic (n=4)	6.00 \pm 3.70	36.51 \pm 4.27 _b	1.40 \pm 0.07	26.27 \pm 3.41	5.61 \pm 0.21	6.49 \pm 0.20 _a	65.42 \pm 1.49 _a
	Mineral (n=4)	24.00 \pm 4.42	1.65 \pm 0.19	0.10 \pm 0.01	16.41 \pm 0.56	5.83 \pm 0.17 _b		

4.3.2 Bacterial community shifts

Some bacteria exhibited shifting trends in response to snow depth, both across treatments and relative to the control, while other community shifts were either not significant or did not appear to be the result of the snow depth treatments (Figure 4.3 and Supplementary Figure S4.16-S4.20). Noticeable trends at the phylum level included a 1.6-fold increased abundance in Verrucomicrobia ($p=0.068$), a 2.1-fold increase in Actinobacteria ($p=0.083$), and a 329.0-fold increase in Chloroflexi ($p=0.010$) in the organic layers from the Low to Deep snow zones. Acidobacteria showed decreased abundance in all treatments relative to the Control, with the Deep zone exhibiting the largest difference with a 1.98-fold decrease ($p=0.055$; Figure 4.3). In the mineral layers, significant increases in the phylum Chloroflexi (7.18-fold increase; $p=0.011$) occurred from the Control to Deep zones, while significant decreases (2.84-fold decrease; $p=0.019$) were observed from Control to Deep zones in the phylum Verrucomicrobia (Figure 4.3).

Bacterial abundance in each phylum correlated with at least one of the soil chemical properties we measured (%C, %N, C:N, or pH). The best overall predictor was %C, correlating with four out of the six phyla. It showed negative relationships with Actinobacteria ($R^2=0.38$, $p<0.001$; Supplementary Figure S4.4) and Chloroflexi ($R^2=0.34$, $p<0.001$; Supplementary Figure S4.6), and positive relationships with Bacteroidetes ($R^2=0.33$, $p<0.001$; Supplementary Figure S4.5) and Proteobacteria ($R^2=0.32$, $p<0.001$; Supplementary Figure S4.2). Actinobacteria was also negatively correlated with %N ($R^2=0.34$, $p<0.001$; Supplementary Figure S4.4), and Chloroflexi, positively with soil pH ($R^2=0.34$, $p<0.001$; Supplementary Figure S4.6). The best and only predictor for Acidobacteria abundance was soil pH, which correlated negatively

($R^2=0.46$, $p<0.001$; Supplementary Figure S4.1). Verrucomicrobia abundance correlated positively with %N ($R^2=0.36$, $p<0.001$; Supplementary Figure S4.3).

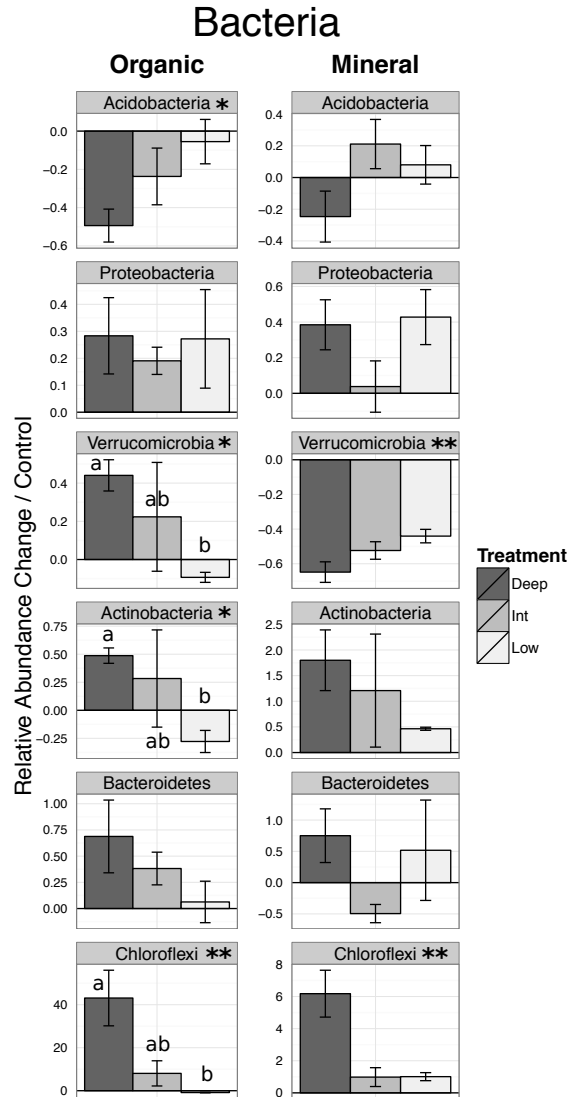


Figure 4.3. Averaged relative abundance of the six most abundant bacterial phylum relative to the control, separated by snow accumulation treatment, and in order of greatest abundance (top to bottom). Error bars represent standard error (standard error of controls ranged from 12.929 in Chloroflexi to 0.026 in Verrucomicrobia). Significance determined by Kruskal-Wallis tests is indicated by asterisks ($*=p<0.1$, $**=p<0.05$), while post-hoc Nemenyi test results are indicated by “a, b, ab”, except where significant differences were to the control.

Soil depth significantly affected bacterial relative abundance in all phyla except for Acidobacteria (Supplementary Table S4.2). The organic layers were more abundant in Proteobacteria (1.59-fold difference; $p < 0.001$), Verrucomicrobia (1.48-fold difference; $p < 0.001$), and Bacteroidetes (2.27-fold difference; $p = 0.001$). Phyla that were more abundant in the mineral layers were Actinobacteria (4.48-fold difference; $p < 0.001$) and Chloroflexi (14.21-fold difference; $p < 0.001$).

Alpha diversity, measured using the Shannon index, was found to differ between soil layers (organic / mineral – $p = 0.003$), but not between snow accumulation treatments (Supplementary Table S4.3). However, beta diversity of bacterial communities visualized by a NMDS plot of Bray-Curtis dissimilarity indices constructed from community matrices (Stress=0.090, Shepard plot non-metric $R^2 = 0.992$; Figure 4.2) revealed significant differences in community structure between all samples (organic, transition, and mineral) associated with winter snow pack (adonis $R^2 = 0.13$, $p = 0.017$), %C (adonis $R^2 = 0.24$, $p < 0.001$; Mantel r statistic=0.63, $p < 0.001$), %N (adonis $R^2 = 0.14$, $p < 0.001$; Mantel r statistic=0.34, $p < 0.001$), C:N (adonis $R^2 = 0.19$, $p < 0.001$; Mantel r statistic=0.42, $p < 0.001$), and pH (adonis $R^2 = 0.15$, $p < 0.001$; Mantel r statistic=0.49, $p < 0.001$). In addition, analysis of each soil layer separately showed that soil chemical properties and snow accumulation treatment affected bacterial community structure more in the organic layers than in the mineral layers, and that in the organic layer, the snow pack treatment ($p < 0.001$), %C ($p = 0.004$), and pH ($p < 0.001$) are the main drivers of community shifts (Table 4.2).

Table 4.2. Statistical analysis of beta diversity using adonis and Mantel tests. Bray Curtis distance matrices of bacterial communities for each sample were compared between soil layers (Organic, Transition, Mineral) and snow accumulation treatments (Control, Deep, Int., Low), and to soil chemical properties. Sample sizes were $n=15$ for “Organic”, $n=13$ for “Mineral”, and $n=41$ for “All layers”. Significance is indicated by asterisks ($=p<0.05$, $**=p<0.01$, $***=p<0.001$).

	Samples	Adonis			Mantel test	
		R^2	df	p -value	r statistic	p -value
Soil layers	All	0.320	2	<0.001***	n/a	n/a
	All	0.126	3	0.017*	n/a	n/a
Snow pack	Organic only	0.421	3	<0.001***	n/a	n/a
	Mineral only	0.485	3	0.003**	n/a	n/a
%C	All	0.239	1	<0.001***	0.633	<0.001***
	Organic only	0.212	1	0.004**	0.490	0.008**
	Mineral only	0.055	1	0.720	0.047	0.791
%N	All	0.141	1	<0.001***	0.341	<0.001***
	Organic only	0.111	1	0.131	-0.0245	0.883
	Mineral only	0.051	1	0.788	0.032	0.844
C:N	All	0.191	1	<0.001***	0.415	<0.001***
	Organic only	0.165	1	0.022*	0.180	0.269
	Mineral only	0.108	1	0.195	-0.063	0.629
pH	All	0.147	1	<0.001***	0.490	<0.001***
	Organic only	0.368	1	<0.001***	0.709	<0.001***
	Mineral only	0.297	1	0.004**	0.526	<0.001***

4.3.3 PICRUS*t* functional analysis

Of the functional gene groups examined, the most significant treatment effects occurred in the organic soil layers. A 1.27-fold decrease in the abundance of genes involved in cellulose degradation ($p=0.018$) and a 1.56-fold decrease in the abundance of genes involved in chitin degradation ($p=0.029$) was observed in the Deep zone relative to the Control (Figure 4.4).

Enzymes

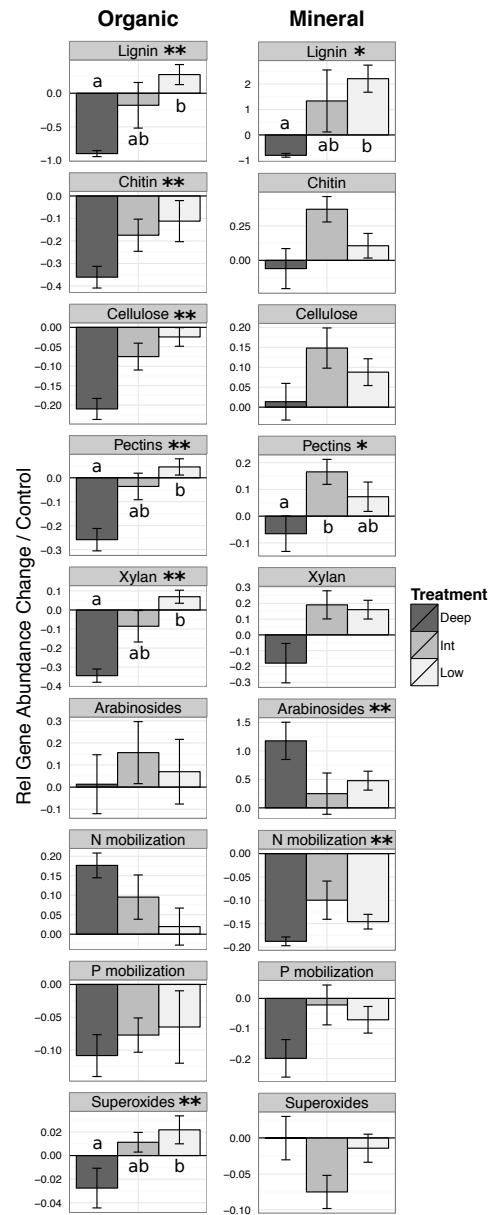


Figure 4.4. Averaged relative abundance of genes for enzyme functional groups relative to the control and separated by snow accumulation treatment. Functional groups involved in soil organic matter decomposition are ordered from recalcitrant to labile substrates (top to bottom). Error bars represent standard error (standard error of controls ranged from 1.220 in the lignin group to 0.008 in the superoxides group). Significance determined by Kruskal-Wallis tests is indicated by asterisks ($*=p<0.1$, $**=p<0.05$), while post-hoc Nemenyi test results are indicated by “a, b, ab”, except where significant differences were to the control.

Also, across treatments from Low to Deep, lignin degrading gene abundance decreased 12.29-fold ($p=0.023$), pectin degrading gene abundance decreased 1.41-fold ($p=0.018$), and xylan degrading gene abundance decreased 1.63-fold ($p=0.014$; Figure 4.4). A similar trend was observed in enzymes responsible for the regulation of oxygen radicals with a 1.05-fold decrease in the Deep zone compared to the Low ($p=0.083$). Shifts along the snow accumulation gradient were also observed in gene groups involved in nutrient mobilization with a 1.18-fold increase in genes necessary for N mobilization ($p=0.14$), and a 1.12-fold decrease in genes necessary for phosphate mobilization ($p=0.39$) in the Deep zone relative to the Control.

Trends in the mineral layers were less clear. Significant shifts included a 2.18-fold increase in genes encoding for enzymes involved in arabinoside degradation ($p=0.049$) and a 1.23-fold decrease in enzymes involved in N mobilization ($p=0.019$) in the Deep zone relative to the Control (Figure 4.4). Genes for lignin-degrading enzymes again showed decreasing abundance along the treatment gradient from Low to Deep (16.23-fold decrease; $p=0.051$). However, relative to the Control, lignin-degrading genes in both Int. and Low zones exhibited much greater abundances than they did in the organic layers (Figure 4.4).

All soil chemical properties were found to be poor predictors of gene abundance, with the exception of genes associated with lignin degradation. Both %C and C:N showed positive relationships ($R^2=0.32$, $p<0.001$ and $R^2=0.54$, $p<0.001$, respectively; Supplementary Figure S4.10), and soil pH showed a negative relationship ($R^2=0.41$, $p<0.001$; Supplementary Figure S4.10).

While the analysis did reveal significant changes in enzyme gene abundance across the snow

zones, many of the KEGG ortholog groups of enzymes targeted in this study were either not found in any of the samples or were found in very low quantities, including phenol oxidases, peroxidases, and laccases (Supplementary Table S4.1).

4.4 Discussion

This study documents changes in soil bacterial community structure in the active layer of moist acidic tundra in response to long-term (18 year) experimental changes in winter precipitation. We examined how changes in bacterial community functional potential as a result of climate forcing factors might affect SOM degradation and alter the C balance of this Arctic tundra ecosystem. Low temperatures in Arctic ecosystems limit soil C availability and decomposability (Conant et al., 2011; Davidson and Janssens, 2006). However, global warming-induced permafrost thaw may partially alleviate this temperature limitation, potentially releasing large amounts of C into the atmosphere via SOM decomposition and further increasing the rate of global warming (Lupascu et al., 2013, 2014a; Lützow and Kögel-Knabner, 2009; Schuur et al., 2008).

After 18 years of experimental winter snow addition, bacterial community structure and functional potential in Arctic moist acidic tundra changed under deeper winter snow accumulation. Our results indicate that increased snow pack reduced the abundance of genes associated with SOM decomposition in the organic soil layers, suggesting a reduced SOM decomposition potential. Possible explanations for this functional shift may include: 1) altered bacterial C substrate preferences towards more labile sources under lowered O₂ availability that would result in a decreased abundance of genes associated with SOM decomposition, and 2) a

reduced amount of enzymatic machinery (and fewer gene copies; Rocca et al., 2014) necessary to accomplish similar metabolic results, as increased soil temperatures under snow accumulation may alleviate kinetic limitations of enzyme functioning (German et al., 2012; Sinsabaugh et al., 2008).

4.4.1 *Bacterial community shifts*

Our results indicate that altered snow accumulation has a significant effect on soil bacterial community structure in Arctic moist acidic tussock tundra ecosystems. While large differences in relative abundances were found between soil layers (Supplementary Table S4.2), the most notable effects of snow accumulation occurred in the organic layers. For instance, we observed shifts in the relative abundance in many of the most abundant phyla including Verrucomicrobia, Acidobacteria, and Actinobacteria, particularly in the Deep snow zone (Figure 4.3). Shifts in Verrucomicrobia were primarily driven by increases in the order Chthoniobacterales in the Deep snow zones relative to the Low snow zones. This order contains facultative aerobic heterotrophs able to utilize saccharide components of plant biomass, but unable to use amino acids or organic acids other than pyruvate (Sangwan et al., 2004). Shifts in Actinobacteria were dominated by the order Actinomycetales, gram-positive facultative bacteria that have been linked to the stimulation of ectomycorrhizal growth which degrade recalcitrant C (Goodfellow and Williams, 1983; Maier et al., 2004; Pridham and Gottlieb, 1948). While not as abundant, the phylum Chloroflexi also responded to snow pack treatments, increasing in abundance from Low to Deep snow zones (Figure 4.3). Shifts in Chloroflexi were the result of increasing abundance of the class Anaerolineae in the Deep zone. Anaerolineae include green non-sulfur bacteria able to thrive in anaerobic environments and have previously been found in similar cold, water-saturated

soils (Costello and Schmidt, 2006). These results appear consistent with the increased soil moisture and decreased partial pressure of O₂ documented under increased snow pack at the study site (Blanc-Betes et al., 2016).

These shifts in bacterial phyla indicate that even at the coarsest level of phylogeny and a high degree of variance between samples, deeper snow in winter and associated changes in soil conditions may be driving changes in the belowground community. Bacterial community shifts may be resulting in potentially altered substrate use preference by decomposers, and different genetic functional activity. This is supported by other studies from Arctic soil and permafrost ecosystems that provide evidence of altered microbial community composition and rapid functional response to temperature manipulations, thawing soils, or fertilization treatments (Deslippe et al., 2012; Koyama et al., 2014; Mackelprang et al., 2011). For example, Actinobacteria abundance was found to increase in response to both increased temperature (Deslippe et al., 2012) and in freshly thawed permafrost soils (Mackelprang et al., 2011), similar to the response we observed in the Deep zone (Figure 4.3). Mackelprang et al. (2011) also reported varying shifts in a wide array of functional genes in response to permafrost thaw. In addition, Koyama et al. (2014) documented a decrease in the oligotrophic Acidobacteria phylum in response to fertilizer soil inputs which they attributed to be a direct result of competition with copiotrophic α -, β -, and γ - Proteobacteria which increased in abundance with fertilizer treatment. While oligotrophic organisms such as Acidobacteria are adapted to survive in low nutrient environments, they are often outcompeted in more fertile soils by generalist copiotrophs (such as Proteobacteria) who are better equipped to harvest available nutrients. Our results did not show a clear pattern for Proteobacteria, but they do show that Acidobacteria abundance shifts associate

negatively with Proteobacteria shifts in the Deep zone where C:N soil values are lowest (most fertile; Table 4.1 and Figure 4.3).

Correlations between soil chemical characteristics (%C, %N, C:N, and pH) and bacterial phylum abundance partially support findings reported in Fierer et al. (2007). They identified C mineralization rates (a proxy for C availability) to be the best predictor of bacterial abundance in the dominant phyla, including positive relationships with Bacteroidetes and β -Proteobacteria, and a negative relationship with Acidobacteria (Fierer et al., 2007). We acknowledge that C mineralization and availability differ from %C in that regardless of carbon concentration, physical and chemical factors in the Arctic such as temperature limitations, and high tannin concentrations may limit C mineralization (Davidson and Janssens, 2006; Schimel et al., 1996). Physical protection of SOM by soil aggregates and associations with organo-minerals, also known to limit C mineralization, does not play as large of a role in Arctic soils compared to other soil types (Höfle et al., 2013; Ping et al., 2015). Regardless of these difference in C measurement, our study did find weak positive relationships between %C and Proteobacteria (Supplementary Figure S4.2) as well as Bacteroidetes (Supplementary Figure S4.5), similar to Fierer et al., 2007. Interestingly, although N can be a limiting factor for microbial growth, %N only correlated to two phyla: positively with Verrucomicrobia (Supplementary Figure S4.3) and negatively with Actinobacteria (Supplementary Figure S4.4). While identifying individual abiotic factors that may predict bacterial abundance at the phylum level is informative, it is important to recognize that often a variety of interacting factors determine microbial community composition, and effects at the phylum scale may be too coarse for adequate interpretation. Our results suggest that while C:N (a proxy for SOM quality) is a poor indicator of individual

bacterial phylum abundance, %C and %N (and in some cases soil pH) alone may be more relevant in these acidic tundra soils. More detailed studies that address the relationships between soil chemical/abiotic characteristics and microbial community composition at finer phylogenetic scales are needed to adequately identify dependable predictors.

While the alpha diversity of soil bacterial communities via the Shannon index did differ between soil layer, it did not differ between snow pack treatment zones. Also, it does not elucidate community structural or functional differences between samples, and it fails to distinguish shifts in genetic potential among treatments. In contrast, beta diversity analyses better revealed soil bacterial community responses to snow accumulation. Bacterial community structure significantly shifted between snow pack treatment zones at all soil depths / layers (Table 4.2). The NMDS plot (Figure 4.2) shows bacterial community structures to be associated with the snow accumulation treatment as soil chemical properties changed (%C, %N, C:N, and pH), indicating that bacterial β -diversity may respond to indirect changes in soil chemistry in response to winter snow accumulation. The initial effects of increased snow pack result in altered physical factors (greater active layer thaw depth and increased soil temperatures and moisture; Blanc-Betes et al., 2016) which may lead to increased SOM availability and faster enzyme activities with the potential to enhance SOM decomposition. Higher SOM mineralization may promote the documented shifts in aboveground plant communities and increased NPP (Natali et al., 2012; Sturm et al., 2005, Anderson-Smith 2013), and vegetation shifts to more shrubby species may alter the chemistry and quality of new litter inputs, ultimately affecting decomposer communities. Moreover, soil moisture and compaction can reduce O₂ diffusion into the soil, inhibiting aerobic SOM decomposition (Blanc-Betes et al., 2016; O'Brien et al., 2010), and

altering bacterial community composition by selecting for microorganisms that utilize simple C substrates, leaving behind complex organic compounds and plant polymers. In addition, tannins produced by expanding woody shrubs may act to inhibit microbial activity (Schimel et al., 1996), further slowing decomposition. This is supported by the lower relative abundance of genes required for SOM decomposition in the Deep snow accumulation zone where we observed the most significant shifts in bacterial community composition (Figure 4.3 and Figure 4.4). The balance between these two competing processes, and the functional shifts associated with them, will ultimately influence the C balance of the system.

4.4.2 *Functional shifts*

To examine the influence of shifting bacterial abundances on soil community functioning and the C balance of Arctic ecosystems, we focused on the genetic potential of the bacterial community to produce enzymes required for the degradation of various forms of SOM. We did this by using PICRUSt software to estimate functional gene abundance via ancestral state reconstruction (Langille et al., 2013). While this method does not provide direct measurements of gene abundance (*e.g.* does not account for horizontal gene transfer or unknown functional / taxonomic linkages that may exist in the sampled tundra soils), it does offer valuable insights into the functional capacities of bacterial communities using 16S rRNA data (Langille et al., 2013). Furthermore, gene abundance in itself is not a direct measurement of gene expression or enzyme activity (Wood et al., 2015). However it does provide a measure of genetic potential and may be positively correlated to enzyme activity and gene expression (Morris et al., 2014; Neufeld et al., 2001; Rocca et al., 2014). To accurately measure enzymatic functional potential or gene expression would require a targeted metagenomic and metatranscriptomic approach.

Many bacterial genes encoding for enzymes associated with the degradation of lignin and other complex plant compounds (such as peroxidases, phenol oxidases, and laccases) were not detected in this study. This suggests that bacterial communities preferentially degrade microbial biomass and polysaccharide polymers, and that the decomposition of more recalcitrant forms of C in Arctic soils is performed by other microorganisms such as fungi. Fungi typically play a key role in the degradation of recalcitrant organic matter by specializing in the production of oxidative enzymes (Deslippe et al., 2012; Morgado et al., 2015). The absence of bacterial genes that encode for peroxidases, phenol oxidases, and laccases, could also be due to the presence of tannins in the soil, which are common in the Alaskan floodplain and are produced by encroaching shrub species (DeMarco et al., 2014; Schimel et al., 1996). Tannic compounds have been shown to inhibit microbial activity and decrease decomposition by binding to vital enzymes (Schimel et al., 1996). If production of phenol oxidases and peroxidases yield little to no benefit for bacteria in this ecosystem due to competition with fungi and interference from tannins and other phenolic compounds, genes encoding for these enzymes may be reduced (Rocca et al., 2014).

The PICRUSt predicted copies of genes for enzymes responsible for SOM decomposition, while generally more abundant in the organic layers (Supplementary Table S4.2), were less abundant in the organic layers of the Deep snow zone than in the Control and Low snow accumulation zones (Figure 4.4). The genes most affected encode enzymes required for the breakdown of plant derived litter, such as cellulose, xylan, or pectin, all major constituents of plant cell walls. Xylans in particular are common in woody plant tissues (Timell, 1967). The observed decrease of these genes in Deep snow pack suggests bacterial preference of readily

available substrates, such as microbial biomass or root exudates (Sullivan and Welker, 2005; Sullivan et al., 2007, 2008). Production of these substrates may have been stimulated by increased soil temperatures and NPP predicted under a climate change scenario, and require less energetic investment in exo-enzyme production (Schimel, 2003). The production of enzymes for the degradation of complex polysaccharides is energetically demanding. Therefore, in an energy and nutrient limited ecosystem such as the Arctic tundra (Hobbie et al., 2002; Jonasson et al., 1999; Mack et al., 2004; Shaver and Chapin, 1980, 1986; Sistla et al., 2012), more labile substrates are likely preferable, which may lead to accumulation of SOM, and thus SOC (Lupascu et al., 2013, 2014a).

Our results indicating reduced decomposition potential under deeper snow pack is consistent with other long-term warming and snowfence studies from Arctic tundra ecosystems that report zero net C loss (or even C gain) during the growing season (Natali et al., 2012, 2014; Sistla et al., 2013). We speculate that initial soil conditions likely favour decomposer activity and decomposition rates increase in response to increased temperatures, resulting in C loss. Over time changing soil conditions (*e.g.* increased moisture, decreased O₂ availability, changes in chemistry of litter inputs) may select for microorganisms that use anaerobic metabolic pathways such as methanogenesis (Blanc-Betes et al. 2016). These hypoxic soil conditions would limit aerobic decomposition. As bacterial communities increase the abundance of genes encoding for enzymes involved in N mobilization, newly available N would enhance microbial biomass production, plant NPP, leaf litter N content, and induce plant community shifts (Pattison and Welker, 2014; Schimel, 2003; Welker et al., 2005). A decrease in SOM decomposition is possibly supported by data from this study, which shows a decreased abundance of genes

involved in SOM decomposition in conjunction with trends suggesting increased abundance of N mobilization genes in the organic layers as snow pack increases (Figure 4.4).

Increased temperature may provide an alternate explanation to the decreased PICRUSt predicted abundance of genes associated with SOM decomposition in the organic layers of the Deep snow accumulation zone (Figure 4.4). Enzyme activity is partially regulated by the rate of gene expression as well as by post-transcriptional regulating factors, which include environmental factors (Gross et al., 1989). Michaelis-Menten enzyme kinetics are sensitive to temperature (German et al., 2012), increasing the maximum rate of enzyme activity (V_{\max}) by increasing the catalytic constant of the reaction (Razavi et al., 2015). Increased V_{\max} may represent an excess potential enzyme activity for the given substrate or growth conditions, resulting in a down regulation of genes required for the enzyme (*e.g.* Gonzalez-Meler et al., 1999, 2001), because fewer enzymes are needed to achieve similar V_{\max} at higher temperatures. Therefore, increases in soil temperature under deeper snow may partially explain the decrease in PICRUSt predicted abundance of genes required for SOM decomposition (Table 4.1 and Figure 4.4).

4.4.3 *Ecosystem response to snow accumulation*

Whether bacterial communities are responding to changing plant inputs and corresponding altered SOM quality (decreased C:N; Table 4.1) or whether they are directly altering SOM chemistry through selective decomposition remains unclear. From the results of our study, it is clear that increased snow accumulation may lead to changes in both bacterial community composition and SOM chemistry in the organic soil layers (Table 4.1 and Figure 4.3). Unlike other ecosystems where plants are the first responders to abiotic climate change factors, in the

Arctic, microbes are likely the first responders to changes in temperature by initially increasing nutrient mineralization. These released nutrients facilitate plant community shifts and increase ecosystem NPP (Chapin III et al., 1995). Over time, the combination of increased snow accumulation and soil compaction may lead to hypoxic/anaerobic soil conditions (*e.g.* Blanc-Betes et al., 2016) and further vegetative shifts to wet-sedge (*Carex*) species, limiting SOM decomposition. This in combination with a recent history of more recalcitrant plant litter inputs could result in re-accrual of SOC (*e.g.* Sistla et al., 2012), ultimately mitigating the positive feedback loop hypothesized in current literature (Davidson and Janssens, 2006; Natali et al., 2014; Schuur et al., 2009; Sturm et al., 2005).

4.5 Conclusions

The results presented here support the hypothesis that bacterial community structure and function shift as a result of consistently deepened snowpack. Increases in soil hypoxia under deepened snow may have resulted in an increased abundance of anaerobic or facultative bacteria, slowing decomposition. Decreases in PICRUSt predicted gene copies suggest that SOM decomposition may be slowed under accumulated snow, and bacterial community substrate preference may shift to more labile compounds. Concentrations of C and N, as opposed to C:N, better explained bacterial community responses to snow pack treatments. Together these results strongly suggest that soil decomposers of moist acidic tundra are key in determining the direction and magnitude of permafrost C feedbacks on the climate system.

4.6 Additional Information

4.6.1 *Data and code availability*

All data used in this report are publically accessible through two separate data repositories. The 16S rRNA gene sequences derived from Illumina Mi-Seq sequencing have been deposited in the NCBI Sequence Read Archive (SRA) under accession number SRP068302. All computer script text files used in QIIME and R packages, as well as BIOM and Excel files, are available via the NSF Arctic Data Center, doi:10.18739/A2DP96.

4.6.2 *Author contributions*

M. P. Ricketts, J. M. Welker, and M. A. Gonzalez-Meler designed the experiment. R. S. Poretsky provided expertise and insight into the bioinformatics and data analyses. M. P. Ricketts performed all sample collections, lab work, and data analyses. M. P. Ricketts prepared the manuscript with contributions from all co-authors.

4.6.3 *Acknowledgements*

This research was supported by funding from the Department of Energy, Terrestrial Ecosystem Science Program to M. A. Gonzalez-Meler (DE-SC 0006607). J. M. Welker initiated and maintained the snow fence experiment with NSF funds beginning in 1994 (9412782, 0632184, 0612534, 0856728). Michael Ricketts received additional support from the Elmer Hadley Graduate Research Award, the W.C. and May Preble Deiss Award for Graduate Research, and the Bodmer International Travel Award. We would like to thank members of the Stable Isotope lab at the University of Illinois at Chicago (UIC), particularly Jessica Rucks and Gerard Aubanell for assistance with field work/sample collection and processing. We thank

Elena Blanc-Betes, Douglas Johnston, Dr. Douglas Lynch, and Dr. Charlie Flower for advice on experimental design, analyses, and comments on the manuscript. We would also like to thank Dr. D'Arcy Meyer Dombard (Earth and Environmental Sciences department, UIC) for use of her lab and soil expertise, and Imrose Kauser (Microbial Ecology lab, UIC) for help with the bioinformatics. Finally, we thank Olivia L Miller (Purdue University), Niccole Van Hoey (University of Alaska, Anchorage), all of the staff at Toolik Field Station, and field and lab UIC undergraduate assistants: Ben Thurnhoffer, Andres Davila, and Briana Certa.

4.7 References

- Anderson-Smith, M.: Remotely-sensed spectral data linked to increasing shrub abundance and greater growing season carbon uptake in Alaskan Arctic tundra (Master's Thesis), Retrieved from <http://search.proquest.com/docview/1426631801>, (UMI 1542572), 2013.
- Anisimov, O., Vaughan, D., Callaghan, T., Furgal, C., Marchant, H., Prowse, T., Vilhjalmsson, H., and Walsh, J.: Polar regions (Arctic and Antarctic), in: *Climate Change 2007: Impacts, adaptation and vulnerability. Contribution of working group II to the fourth assessment report of the Intergovernmental Panel on Climate Change*, Parry, M. L., Canziani, O. F., Palutikof, J. P., van der Linden, P. J., and Hanson, C. E., (Eds.), Cambridge University Press, Cambridge, 653–685, 2007.
- Arft, A., Walker, M., Gurevitch, J., Alatalo, J. M., Bret-Harte, M., Dale, M., Diemer, M., Gugerli, F., Henry, G. H. R., Jones, M. H., Hollister, R. D., Jonsdottir, I. S., Laine, K., Levesque, E., Marion, G. M., Molau, U., Molgaard, P., Nordenhall, U., Raszhivin, V., Robinson, C. H., Starr, G., Stenstrom, A., Stenstrom, M., Totland, O., Turner, P. L., Walker, L. J., Webber, P. J., Welker, J. M., and Wookey, P. A.: Responses of tundra plants to experimental warming: meta-analysis of the international tundra experiment, *Ecol. Monogr.*, 69, 491–511, 1999.
- Batjes, N.: Total carbon and nitrogen in soils of the world, *Eur. J. Soil Sci.*, 47, 151–163, 1996.
- Blanc-Betes, E., Welker, J. M., Sturchio, N. C., Chanton, J. P., and Gonzalez-Meler, M. A.: Winter precipitation and snow accumulation drive the methane sink or source strength of Arctic tussock tundra, *Glob. Chang. Biol.*, Accepted Author Manuscript. doi:10.1111/gcb.13242, 2016.
- Bret-Harte, M. S., Shaver, G. R., Zoerner, J. P., Johnstone, J. F., Wagner, J. L., Chavez, A. S., Gunkelman IV, R. F., Lippert, S. C., and Laundre, J. A.: Developmental plasticity allows *Betula nana* to dominate tundra subjected to an altered environment, *Ecology*, 82, 18–32, 2001.
- Caporaso, J. G., Kuczynski, J., Stombaugh, J., Bittinger, K., Bushman, F. D., Costello, E. K., Fierer, N., Gonzalez, A., Goodrich, J. K., Gordon, J. I., Huttley, G. A., Kelley, S. T., Knights, D., Koenig, J. E., Ley, R. E., Lozupone, C. A., McDonald, D., Muegge, B. D., Pirrung, M., Reeder, J., Sevinsky, J. R., Turnbaugh, P. J., Walters, W. A., Widmann, J., Yatsunencko, T., Zaneveld, J., and Knight, R.: QIIME allows analysis of high-throughput community sequencing data, *Nature Methods*, 7, 335–336, doi:10.1038/nmeth.f.303, 2010.
- Caporaso, J. G., Lauber, C. L., Walters, W. A., Berg-Lyons, D., Huntley, J., Fierer, N., Owens, S. M., Betley, J., Fraser, L., Bauer, M., Gormley, N., Gilbert, J. A., Smith, G., and Knight, R.: Ultra-high-throughput microbial community analysis on the Illumina HiSeq and MiSeq platforms, *ISME*, 6, 1621–1624, doi:10.1038/ismej.2012.8, 2012.

- Chapin III, F. S., Shaver, G. R., Giblin, A. E., Nadelhoffer, K. J., and Laundre, J. A.: Responses of Arctic tundra to experimental and observed changes in climate, *Ecology*, 76, 694–711, doi:10.2307/1939337, 1995.
- Conant, R. T., Ryan, M. G., Ågren, G. I., Birge, H. E., Davidson, E. A., Eliasson, P. E., Evans, S. E., Frey, S. D., Giardina, C. P., Hopkins, F. M., Hyvönen, R., Kirschbaum, M. U. F., Lavallee, J. M., Leifeld, J., Parton, W. J., Steinweg, J. M., Wallenstein, M. D., Wetterstedt, J. Å. M., and Bradford, M. A.: Temperature and soil organic matter decomposition rates - synthesis of current knowledge and a way forward, *Glob. Chang. Biol.*, 17, 3392–3404, doi:10.1111/j.1365-2486.2011.02496.x, 2011.
- Costello, E. K. and Schmidt, S. K.: Microbial diversity in alpine tundra wet meadow soil: novel Chloroflexi from a cold, water-saturated environment, *Environ. Microbiol.*, 8, 1471–1486, doi:10.1111/j.1462-2920.2006.01041.x, 2006.
- Czimczik, C. I. and Welker, J. M.: Radiocarbon content of CO₂ respired from high Arctic tundra in Northwest Greenland, *Arct. Antarct. Alp. Res.*, 42, 342–350, doi:10.1657/1938-4246-42.3.342, 2010.
- Davidson, E. A. and Janssens, I. A.: Temperature sensitivity of soil carbon decomposition and feedbacks to climate change, *Nature*, 440, 165–173, doi:10.1038/nature04514, 2006.
- DeMarco, J., Mack, M., and Bret-Harte, M.: Effects of arctic shrub expansion on biophysical versus biogeochemical drivers of litter decomposition, *Ecology*, 95, 1861–1875, 2014.
- Deslippe, J. R., Hartmann, M., Simard, S. W., and Mohn, W. W.: Long-term warming alters the composition of Arctic soil microbial communities, *FEMS Microbiol. Ecol.*, 82, 303–315, doi:10.1111/j.1574-6941.2012.01350.x, 2012.
- Elmendorf, S. C., Henry, G. H. R., Hollister, R. D., Björk, R. G., Bjorkman, A. D., Callaghan, T. V., Collier, L. S., Cooper, E. J., Cornelissen, J. H. C., Day, T. A., Fosaa, A. M., Gould, W. A., Grétarsdóttir, J., Harte, J., Hermanutz, L., Hik, D. S., Hofgaard, A., Jarrad, F., Jónsdóttir, I. S., Keuper, F., Klanderud, K., Klein, J. A., Koh, S., Kudo, G., Lang, S. I., Loewen, V., May, J. L., Mercado, J., Michelsen, A., Molau, U., Myers-Smith, I. H., Oberbauer, S. F., Pieper, S., Post, E., Rixen, C., Robinson, C. H., Schmidt, N. M., Shaver, G. R., Stenström, A., Tolvanen, A., Totland, Ø., Troxler, T., Wahren, C. H., Webber, P. J., Welker, J. M., and Wookey, P. A.: Global assessment of experimental climate warming on tundra vegetation: Heterogeneity over space and time, *Ecol. Lett.*, 15, 164–175, doi:10.1111/j.1461-0248.2011.01716.x, 2012a.
- Elmendorf, S. C., Henry, G. H. R., Hollister, R. D., Björk, R. G., Boulanger-Lapointe, N., Cooper, E. J., Cornelissen, J. H. C., Day, T. A., Dorrepaal, E., Elumeeva, T. G., Gill, M., Gould, W. A., Harte, J., Hik, D. S., Hofgaard, A., Johnson, D. R., Johnstone, J. F., Jónsdóttir, I. S., Jorgenson, J. C., Klanderud, K., Klein, J. A., Koh, S., Kudo, G., Lara, M., Lévesque, E., Magnússon, B., May, J. L., Mercado-Dí'az, J. A., Michelsen, A., Molau, U., Myers-Smith, I.

- H., Oberbauer, S. F., Onipchenko, V. G., Rixen, C., Martin Schmidt, N., Shaver, G. R., Spasojevic, M. J., Þórhallsdóttir, Þ. E., Tolvanen, A., Troxler, T., Tweedie, C. E., Villareal, S., Wahren, C-H., Walker, X., Webber, P. J., Welker, J. M., and Wipf, S.: Plot-scale evidence of tundra vegetation change and links to recent summer warming, *Nat. Clim. Chang.*, 2, 453–457, doi:10.1038/nclimate1465, 2012b.
- Fahnestock, J. T., Povirk, K. A., and Welker, J. M.: Abiotic and biotic effects of increased litter accumulation in arctic tundra. *Ecography*, 23, 623–631, doi:10.1034/j.16000587.2000.230513.x, 2000.
- Fierer, N., Bradford, M. A., and Jackson, R. B.: Toward an ecological classification of soil bacteria, *Ecology*, 88, 1354–1364, doi:10.1890/05-1839, 2007.
- Frey, S. D., Lee, J., Melillo, J. M., and Six, J.: The temperature response of soil microbial efficiency and its feedback to climate, *Nat. Clim. Chang.*, 3, 395–398, doi:10.1038/nclimate1796, 2013.
- German, D. P., Marcelo, K. R. B., Stone, M. M., and Allison, S. D.: The Michaelis-Menten kinetics of soil extracellular enzymes in response to temperature: a cross-latitudinal study, *Glob. Chang. Biol.*, 18, 1468–1479, doi:10.1111/j.1365-2486.2011.02615.x, 2012.
- Gilbert, J. A., Jansson, J. K., and Knight, R.: The Earth Microbiome project: successes and aspirations, *BMC Biol.*, 12, 69, doi:10.1186/s12915-014-0069-1, 2014.
- González-Meler, M. A., Ribas-Carbo, M., Giles, L., and Siedow, J. N.: The effect of growth and measurement temperature on the activity of the alternative respiratory pathway, *Plant Physiol.*, 120, 765–772, doi:10.1104/pp.120.3.765, 1999.
- González-Meler, M. A., Giles, L., Thomas, R. B., and Siedow, J. N.: Metabolic regulation of leaf respiration and alternative pathway activity in response to phosphate supply, *Plant Cell Environ.*, 24, 205–215, doi:10.1046/j.1365-3040.2001.00674.x, 2001.
- Goodfellow, M. and Williams, S. T.: Ecology of actinomycetes., *Annu. Rev. Microbiol.*, 37, 189–216, doi:10.1146/annurev.mi.37.100183.001201, 1983.
- Graham, D. E., Wallenstein, M. D., Vishnivetskaya, T. A., Waldrop, M. P., Phelps, T. J., Pfiffner, S. M., Onstott, T. C., Whyte, L. G., Rivkina, E. M., Gilichinsky, D. A., Elias, D. A., Mackelprang, R., VerBerkmoes, N. C., Hettich, R. L., Wagner, D., Wulfschleger, S. D., and Jansson, J. K.: Microbes in thawing permafrost: the unknown variable in the climate change equation., *ISME J.*, 6, 709–712, doi:10.1038/ismej.2011.163, 2012.
- Gross, R., Arico, B., and Rappuoli, R.: Families of bacterial signal-transducing proteins, *Mol. Microbiol.*, 3, 1661–1667, doi:10.1111/j.1365-2958.1989.tb00152.x, 1989.
- Hinzman, L. D., Bettez, N. D., Bolton, W. R., Chapin, F. S., Dyurgerov, M. B., Fastie, C. L.,

- Griffith, B., Hollister, R. D., Hope, A., Huntington, H. P., Jensen, A. M., Jia, G. J., Jorgenson, T., Kane, D. L., Klein, D. R., Kofinas, G., Lynch, A. H., Lloyd, A. H., McGuire, A. D., Nelson, F. E., Oechel, W. C., Osterkamp, T. E., Racine, C. H., Romanovsky, V. E., Stone, R. S., Stow, D. A., Sturm, M., Tweedie, C. E., Vourlitis, G. L., Walker, M. D., Walker, D. A., Webber, P. J., Welker, J. M., Winker, K. S., and Yoshikawa, K.: Evidence and implications of recent climate change in Northern Alaska and other Arctic regions, *Clim. Change*, 72, 251–298, doi:10.1007/s10584-005-5352-2, 2005.
- Hobbie, S. E., Nadelhoffer, K. J., and Högberg, P.: A synthesis: The role of nutrients as constraints on carbon balances in boreal and arctic regions, *Plant Soil*, 242, 163-170, doi:10.1023/A:1019670731128, 2002.
- Höfle, S., Rethemeyer, J., Mueller, C. W., and John, S.: Organic matter composition and stabilization in a polygonal tundra soil of the Lena Delta, *Biogeosciences*, 10, 3145-3158, doi:10.5194/bg-10-3145-2013, 2013.
- Hopkins, F., Gonzalez-Meler, M. A., Flower, C. E., Lynch, D. J., Czimczik, C., Tang, J., and Subke, J.-A.: Ecosystem-level controls on root-rhizosphere respiration, *New Phytol.*, 199, 339–351, 2013.
- Hopkins, F. M., Torn, M. S., and Trumbore, S. E.: Warming accelerates decomposition of decades-old carbon in forest soils, *P. Natl. Acad. Sci. U. S. A.*, 109, E1753–E1761, doi:10.1073/pnas.1120603109, 2012.
- Hugelius, G., Tarnocai, C., Broll, G., Canadell, J. G., Kuhry, P., and Swanson, D. K.: The Northern Circumpolar Soil Carbon Database: spatially distributed datasets of soil coverage and soil carbon storage in the northern permafrost regions, *Earth Syst. Sci. Data*, 5, 3–13, doi:10.5194/essd-5-3-2013, 2013.
- IPCC: IPCC special report on land use, land-use change, and forestry, Watson, R. T., Noble, I. R., Bolin, B., Ravindranath, N. H., Verardo, D. J., and Dokken, D.J., (Eds.), Cambridge University Press, Cambridge, 375, 2000.
- Jonasson, S., Michelsen, A., and Schmidt, I. K.: Coupling of nutrient cycling and carbon dynamics in the Arctic, integration of soil microbial and plant processes, *Appl. Soil Ecol.*, 11, 135-146, doi:10.1016/S0929-1393(98)00145-0, 1999.
- Jones, M. H., Fahnestock, J. T., Walker, D. A., Walker, M. D., and Welker, J. M.: Carbon dioxide fluxes in moist and dry Arctic tundra during the snow-free season : Responses to increases in summer temperature and winter snow accumulation, *Arctic, Antarct. Alp. Res.*, 30, 373–380, 1998.
- Koyama, A., Wallenstein, M. D., Simpson, R. T., and Moore, J. C.: Soil bacterial community composition altered by increased nutrient availability in Arctic tundra soils, *Front. Microbiol.*, 5, 1–16, doi:10.3389/fmicb.2014.00516, 2014.

- Langille, M. G. I., Zaneveld, J., Caporaso, J. G., McDonald, D., Knights, D., Reyes, J. A., Clemente, J. C., Burkepile, D. E., Vega Thurber, R. L., Knight, R., Beiko, R. G., and Huttenhower, C.: Predictive functional profiling of microbial communities using 16S rRNA marker gene sequences, *Nat. Biotechnol.*, 31, 814–821, doi:10.1038/nbt.2676, 2013.
- Lauber, C. L., Hamady, M., Knight, R., and Fierer, N.: Pyrosequencing-based assessment of soil pH as a predictor of soil bacterial community structure at the continental scale, 75, 5111–5120, doi:10.1128/AEM.00335-09, 2009.
- Leffler, A. J. and Welker, J. M.: Long-term increases in snow pack elevate leaf N and photosynthesis in *Salix arctica*: responses to a snow fence experiment in the High Arctic of NW Greenland, *Environ. Res. Lett.*, 8, 1-10, doi:10.1088/1748-9326/8/2/025023, 2013.
- Liston, G. E. and Hiemstra, C. A.: The Changing Cryosphere: Pan-Arctic Snow Trends (1979–2009), *J. Clim.*, 24, 5691–5712, doi:10.1175/JCLI-D-11-00081.1, 2011.
- Lupascu, M., Welker, J. M., and Czimczik, C. I.: Rates and radiocarbon content of summer ecosystem respiration to long-term deeper snow in the High Arctic of NW Greenland, *J. Geophys. Res. Biogeosciences*, 119, 1180–1194, doi:10.1002/2013JG002433, 2014a.
- Lupascu, M., Welker, J. M., Seibt, U., Maseyk, K., Xu, X., and Czimczik, C. I.: High Arctic wetting reduces permafrost carbon feedbacks to climate warming, *Nat. Clim. Chang.*, 4, 51–56, doi:10.1038/NCLIMATE2058, 2013.
- Lupascu, M., Welker, J. M., Seibt, U., Xu, X., Velicogna, I., Lindsey, D. S., and Czimczik, C. I.: The amount and timing of precipitation control the magnitude, seasonality and sources (^{14}C) of ecosystem respiration in a polar semi-desert, NW Greenland, *Biogeosciences Discuss.*, 11, 2457–2496, doi:10.5194/bgd-11-2457-2014, 2014b.
- Lützwow, M. and Kögel-Knabner, I.: Temperature sensitivity of soil organic matter decomposition—what do we know?, *Biol. Fert. Soils*, 46, 1–15, doi:10.1007/s00374-009-0413-8, 2009.
- Mack, M. C., Schuur, E. A. G., Bret-Harte, M. S., Shaver, G. R., and Chapin III, F. S.: Ecosystem carbon storage in arctic tundra reduced by long-term nutrient fertilization, *Nature*, 431, 440–443, doi:10.1038/nature02887, 2004.
- Mackelprang, R., Waldrop, M. P., DeAngelis, K. M., David, M. M., Chavarria, K. L., Blazewicz, S. J., Rubin, E.M., and Jansson, J. K.: Metagenomic analysis of a permafrost microbial community reveals a rapid response to thaw, *Nature*, 480, 368–371, doi:10.1038/nature10576, 2011.
- Maier, A., Riedlinger, J., Fiedler, H.-P., and Hampp, R.: Actinomycetales bacteria from a spruce stand: characterization and effects on growth of root symbiotic and plant parasitic soil fungi in dual culture, *Mycol. Prog.*, 3, 129–136, 2004.

- Martiny, A. C., Treseder, K., and Pusch, G.: Phylogenetic conservatism of functional traits in microorganisms, *ISME J.*, 7, 830–838, doi:10.1038/ismej.2012.160, 2013.
- McMurdie, P. J. and Holmes, S.: phyloseq: An R Package for Reproducible Interactive Analysis and Graphics of Microbiome Census Data. *PLoS ONE* 8(4): e61217, doi:10.1371/journal.pone.0061217, 2013.
- Morgado, L. N., Semenova, T. A., Welker, J. M., Walker, M. D., Smets, E., and Geml, J.: Summer temperature increase has distinct effects on the ectomycorrhizal fungal communities of moist tussock and dry tundra in Arctic Alaska., *Glob. Chang. Biol.*, 21, 959–72, doi:10.1111/gcb.12716, 2015.
- Morris, R., Schauer-Gimenez, A., Bhattad, U., Kearney, C., Struble, C. A., Zitomer, D., and Maki, J. S.: Methyl coenzyme M reductase (*mcrA*) gene abundance correlates with activity measurements of methanogenic H₂/CO₂-enriched anaerobic biomass, *Microb. Biotechnol.*, 7, 77–84, doi:10.1111/1751-7915.12094, 2014.
- Natali, S. M., Schuur, E. A. G., and Rubin, R. L.: Increased plant productivity in Alaskan tundra as a result of experimental warming of soil and permafrost, *J. Ecol.*, 100, 488–498, doi:10.1111/j.1365-2745.2011.01925.x, 2012.
- Natali, S., Schuur, E., Webb, E., Hicks Pries, C., and Crummer, K. G.: Permafrost degradation stimulates carbon loss from experimentally warmed tundra, *Ecology*, 95, 602–608, 2014.
- Neufeld, J. D., Driscoll, B. T., Knowles, R., and Archibald, F. S.: Quantifying functional gene populations: comparing gene abundance and corresponding enzymatic activity using denitrification and nitrogen fixation in pulp and paper mill effluent treatment systems, *Can. J. Microbiol.*, 47, 925–934, doi:10.1139/w01-092, 2001.
- Nowinski, N. S., Taneva, L., Trumbore, S. E., and Welker, J. M.: Decomposition of old organic matter as a result of deeper active layers in a snow depth manipulation experiment, *Oecologia*, 163, 785–792, doi:10.1007/s00442-009-1556-x, 2010.
- O'Brien, S. L., Jastrow, J. D., Grimley, D. A., and Gonzalez-Meler, M. A.: Moisture and vegetation controls on decadal-scale accrual of soil organic carbon and total nitrogen in restored grasslands, *Glob. Chang. Biol.*, 16, 2573–2588, doi:10.1111/j.1365-2486.2009.02114.x, 2010.
- Pattison, R. R. and Welker, J. M.: Differential ecophysiological response of deciduous shrubs and a graminoid to long-term experimental snow reductions and additions in moist acidic tundra, Northern Alaska, *Oecologia*, 174, 339–350, doi:10.1007/s00442-013-2777-6, 2014.
- Pearson, R. G., Phillips, S. J., Loranty, M. M., Beck, P. S. A., Damoulas, T., Knight, S. J., and Goetz, S. J.: Shifts in Arctic vegetation and associated feedbacks under climate change, *Nat. Clim. Chang.*, 3, 673–677, doi:10.1038/nclimate1858, 2013.

- Ping, C. L., Bockheim, J. G., Kimble, J. M., Michaelson, G. J., and Walker, D. A.: Characteristics of cryogenic soils along a latitudinal transect in arctic Alaska, *J. Geophys. Res.*, 103, 28,917-28,928, doi:10.1029/98JD02024, 1998.
- Ping, C. L., Jastrow, J. D., Jorgenson, M. T., Michaelson, G. J., and Shur, Y. L.: Permafrost soils and carbon cycling, *SOIL*, 1, 147-171, doi:10.5194/soil-1-147-2015, 2015.
- Ping, C. L., Michaelson, G. J., Jorgenson, M. T., Kimble, J. M., Epstein, H., Romanovsky, V. E., and Walker, D. A.: High stocks of soil organic carbon in the North American Arctic region, *Nat. Geosci.*, 1, 615–619, doi:10.1038/ngeo284, 2008.
- Pridham, T. G. and Gottlieb, D.: The utilization of carbon compounds by actinomycetales as an aid for species determination, *J. Bacteriol.*, 56, 107–114, 1948.
- Raich, J., Potter, C., and Bhagawati, D.: Interannual variability in global soil respiration, 1980–94, *Glob. Chang. Biol.*, 800–812, 2002.
- Razavi, B. S., Blagodatskaya, E., Kuzyakov, Y.: Nonlinear temperature sensitivity of enzyme kinetics explains canceling effect—a case study on loamy haplic Luvisol, *Front. Microbiol.*, 6, 1-13, doi:10.3389/fmicb.2015.01126, 2015.
- Rocca, J. D., Hall, E. K., Lennon, J. T., Evans, S. E., Waldrop, M. P., Cotner, J. B., Nemergut, D. R., Graham, E. B., and Wallenstein, M. D.: Relationships between protein-encoding gene abundance and corresponding process are commonly assumed yet rarely observed, *ISME J.*, 1–7, doi:10.1038/ismej.2014.252, 2014.
- Rogers, M. C., Sullivan, P. F., and Welker, J. M.: Exchange to increasing levels of winter snow depth in the high Arctic of Northwest Greenland, *Arctic, Antarct. Alp. Res.*, 43, 95–106, doi:10.1657/1938-4246-43.1.95, 2011.
- Sangwan, P., Chen, X., Hugenholtz, P., and Janssen, P. H.: *Chthoniobacter flavus* gen. nov., sp. nov., the First Pure-Culture Representative of Subdivision Two, *Spartobacteria* classis nov., of the Phylum Verrucomicrobia, *Appl. Environ. Microbiol.*, 70, 5875-5881, doi:10.1128/AEM.70.10.5875, 2004.
- Schimel, J.: The implications of exoenzyme activity on microbial carbon and nitrogen limitation in soil: a theoretical model, *Soil Biol. Biochem.*, 35, 549–563, doi:10.1016/S0038-0717(03)00015-4, 2003.
- Schimel, J. P., Bilbrough, C., and Welker, J. M.: Increased snow depth affects microbial activity and nitrogen mineralization in two Arctic tundra communities, *Soil Biol. Biochem.*, 36, 217–227, doi:10.1016/j.soilbio.2003.09.008, 2004.
- Schimel, J. P., Cleve, K. Van, Cates, R. G., Clausen, T. P., and Reichardt, P. B.: Effects of balsam poplar (*Populus balsamifera*) tannins and low molecular weight phenolics on

microbial activity in taiga floodplain soil: implications for changes in N cycling during succession, *Can. J. Bot.*, 74, 84–90, doi:10.1139/b96-012, 1996.

- Schimel, J. P. and Schaeffer, S. M.: Microbial control over carbon cycling in soil., *Front. Microbiol.*, 3, 1-11, doi:10.3389/fmicb.2012.00348, 2012.
- Schuur, E. A. G., Bockheim, J., Canadell, J. G., Euskirchen, E., Field, C. B., Goryachkin, S. V., Hagemann, S., Kuhry, P., Lafleur, P. M., Lee, H., Mazhitova, G., Nelson, F. E., Rinke, A., Romanovsky, V. E., Shiklomanov, N., Tarnocai, C., Venevsky, S., Vogel, J. G., and Zimov, S. A.: Vulnerability of permafrost carbon to climate change: Implications for the global carbon cycle, *Bioscience*, 58, 701-714, doi:10.1641/B580807, 2008.
- Schuur, E. A. G., Vogel, J. G., Crummer, K. G., Lee, H., Sickman, J. O., and Osterkamp, T. E.: The effect of permafrost thaw on old carbon release and net carbon exchange from tundra, *Nature*, 459, 556–559, doi:10.1038/nature08031, 2009.
- Semenova, T. A., Morgado, L. N., Welker, J. M., Walker, M. D., Smets, E., and Geml, J.: Long-term experimental warming alters community composition of ascomycetes in Alaskan moist and dry arctic tundra, *Mol. Ecol.*, 24, 424–437, doi:10.1111/mec.13045, 2015.
- Shaver, G. R. and Chapin III, F. S.: Response to fertilization by various plant growth forms in an Alaskan tundra: Nutrient accumulation and growth, *Ecology*, 61, 662-675, doi:10.2307/1937432, 1980.
- Shaver, G. R. and Chapin III, F. S.: Effect of fertilizer on production and biomass of the tussock tundra, Alaska, U.S.A., *Arct. Alp. Res.*, 18, 261-268, doi:10.2307/1550883, 1986.
- Sinsabaugh, R. L., Lauber, C. L., Weintraub, M. N., Ahmed, B., Allison, S. D., Crenshaw, C., Contosta, A. R., Cusack, D., Frey, S., Gallo, M. E., Gartner, T. B., Hobbie, S. E., Holland, K., Keeler, B. L., Powers, J. S., Stursova, M., Takacs-Vesbach, C., Waldrop, M. P., Wallenstein, M. D., Zak, D. R., and Zeglin, L. H.: Stoichiometry of soil enzyme activity at global scale, *Ecol. Lett.*, 11, 1252–1264, doi:10.1111/j.1461-0248.2008.01245.x, 2008.
- Sistla, S. A., Asao, S., and Schimel, J. P.: Detecting microbial N-limitation in tussock tundra soil: Implications for Arctic soil organic carbon cycling, *Soil Biol. Biochem.*, 55, 78-84, doi:10.1016/j.soilbio.2012.06.010, 2012.
- Sistla, S. A., Moore, J. C., Simpson, R. T., Gough, L., Shaver, G. R., and Schimel, J. P.: Long-term warming restructures Arctic tundra without changing net soil carbon storage, *Nature*, 497, 615–618, doi:10.1038/nature12129, 2013.
- Soil Survey Staff, Natural Resources Conservation Service, United States Department of Agriculture. Web Soil Survey. Available online at <http://websoilsurvey.nrcs.usda.gov/>. Accessed [11/17/2015].

Soil Survey Division Staff: Soil survey manual, Soil Conservation Service, U.S. Department of Agriculture Handbook, 18, 1993.

Sturm, M., Schimel, J., Michaelson, G., Welker, J. M., Oberbauer, S. F., Liston, G. E., Fahnestock, J., and Romanovsky, V. E.: Winter biological processes could help convert Arctic tundra to shrubland, *Bioscience*, 55, 17–26, doi:10.1641/0006-3568(2005)055[0017:WBPCHC]2.0.CO;2, 2005.

Sullivan, P. F., Arens, S. J. T., Chimner, R. A., and Welker, J. M.: Temperature and microtopography interact to control carbon cycling in a high Arctic fen, *Ecosystems*, 11, 61–76, doi: 10.1007/s10021-007-9107-y, 2008.

Sullivan, P. F., Sommerkorn, M., Rueth, H. M., Nadelhoffer, K. J., Shaver, G. R., and Welker, J. M.: Climate and species affect fine root production with long-term fertilization in acidic tussock tundra near Toolik Lake, Alaska, *Oecologia*, 153, 643–652, doi:10.1007/s00442-007-0753-8, 2007.

Sullivan, P. F. and Welker, J. M.: Warming chambers stimulate early season growth of an arctic sedge: Results of a minirhizotron field study, *Oecologia*, 142, 616–626, doi:10.1007/s00442-004-1764-3, 2005.

Tape, K. D., Hallinger, M., Welker, J. M., and Ruess, R. W.: Landscape heterogeneity of shrub expansion in Arctic Alaska, *Ecosystems*, 15, 711–724, doi:10.1007/s10021-012-9540-4, 2012.

Tape, K., Sturm, M., and Racine, C.: The evidence for shrub expansion in Northern Alaska and the Pan-Arctic, *Glob. Chang. Biol.*, 12, 686–702, doi:10.1111/j.1365-2486.2006.01128.x, 2006.

Tarnocai, C., Canadell, J. G., Schuur, E. A. G., Kuhry, P., Mazhitova, G., and Zimov, S.: Soil organic carbon pools in the northern circumpolar permafrost region, *Global Biogeochem. Cycles*, 23, 1–11, doi:10.1029/2008GB003327, 2009.

Timell, T. E.: Recent progress in the chemistry of wood hemicelluloses, *Wood Sci. Technol.*, 1, 45–70, doi:10.1007/BF00592255, 1967.

Wahren, C.: Vegetation responses in Alaskan arctic tundra after 8 years of a summer warming and winter snow manipulation experiment, *Glob. Chang. Biol.*, 11, 537–552, doi:10.1111/j.1365-2486.2005.00927.x, 2005.

Waldrop, M. P., Wickland, K. P., White, R., Berhe, A. A., Harden, J. W., and Romanovsky, V. E.: Molecular investigations into a globally important carbon pool: Permafrost-protected carbon in Alaskan soils, *Glob. Chang. Biol.*, 16, 2543–2554, doi:10.1111/j.1365-2486.2009.02141.x, 2010.

- Walker, M. and Wahren, C.: Plant community responses to experimental warming across the tundra biome, *P. Natl. Acad. Sci. U.S.A.*, 103, 1342–1346, doi:10.1073/pnas.0503198103, 2006.
- Walker, M., Walker, D., Welker, J., Arft, A., Bardsley, T., Brooks, P., Fahnestock, J. T., Jones, M., Losleben, M., Parsons, A., Seastedt, T., and Turner, P.: Long-term experimental manipulation of winter snow regime and summer temperature in arctic and alpine tundra, *Hydrol. Process.*, 13, 2315–2330, 1999.
- Wallenstein, M. D., McMahon, S., and Schimel, J.: Bacterial and fungal community structure in Arctic tundra tussock and shrub soils, *FEMS Microbiol. Ecol.*, 59, 428–435, doi:10.1111/j.1574-6941.2006.00260.x, 2007.
- Welker, J. M., Fahnestock, J. T., and Jones, M. H.: Annual CO₂ flux in dry and moist arctic tundra: Field responses to increases in summer temperatures and winter snow depth, *Clim. Change*, 44, 139–150, doi:10.1023/a:1005555012742, 2000.
- Welker, J. M., Fahnestock, J. T., Sullivan, P. F., and Chimner, R. A.: Leaf mineral nutrition of Arctic plants in response to warming and deeper snow in northern Alaska, *Oikos*, 109, 167–177, doi:10.1111/j.0030-1299.2005.13264.x, 2005.
- Wood, S. A., Almaraz, M., Bradford, M. A., McGuire, K. L., Naeem, S., Neill, C., Palm, C. A., Tully, K. L., and Zhou, J.: Farm management, not soil microbial diversity, controls nutrient loss from smallholder tropical agriculture, *Front. Microbiol.*, 6, 1–10, doi:10.3389/fmicb.2015.00090, 2015.
- Xia, J., Chen, J., Piao, S., Ciais, P., Luo, Y., and Wan, S.: Terrestrial carbon cycle affected by non-uniform climate warming, *Nat. Geosci.*, 7, 173–180, doi:10.1038/ngeo2093, 2014.
- Zak, D. R. and Kling, G. W.: Microbial community composition and function across an arctic tundra landscape., *Ecology*, 87, 1659–1670, 2006.

5 SHOTGUN METAGENOMIC ANALYSIS OF MICROBIAL SOIL ORGANIC MATTER DECOMPOSITION AND NUTRIENT CYCLING IN AN ARCTIC SNOWFENCE EXPERIMENT

5.1 Introduction

Soil microorganisms play an important role in influencing environmental conditions at both micro- and global scales but are also affected by a range of biotic and abiotic environmental factors. Biotic factors such as vegetation can directly influence soil microbial communities through root/rhizosphere interactions, providing readily available carbon (C) sources and potentially actively recruiting and maintaining specific microbial consortia through the exchange of specific molecules and signaling compounds (Paterson et al. 2007, Berendsen et al. 2012, Ricketts et al. 2018). Indirectly, plants may influence the soil microbial community through litter deposits, leading to altered soil organic matter (SOM) chemistry. Likewise, abiotic factors such as soil chemistry, temperature, O₂ availability, and C accessibility play a large role determining soil microbial community structure and function (Castro et al. 2010, Blanc-Betes et al. 2016, Ricketts et al. 2016). Untangling the relationships, interactions, and feedbacks between soil microbial communities and their environment is crucial to gain a holistic understanding of the dynamics in any ecosystem, but particularly in the Arctic where rapid and complex ecological changes are occurring.

Emerging sequencing technologies can advance our understanding of microbial diversity and function, and their impacts in regulating ecosystem processes in a changing Arctic. The Arctic is unique in that it houses large amounts of C stored frozen in the form of SOM. Sub-zero soil temperature limits soil microbial activity for much of the year in the active layer, and in the permafrost layers where soils have been frozen for more than two consecutive years (Ping et al.

2015). Permafrost soils alone contain approximately 50% of the world's soil organic carbon (SOC). There is growing concern that increasing global temperatures may lead to thawing soils and increase the microbial mineralization of these ancient C stores. Increased activity of decomposers can further accelerate global warming through the release of this SOC in the form of CO₂ and CH₄ into the atmosphere. Therefore, the response of soil microorganisms to forcing factors can have global effects. Additionally, increased nutrient availability, due to the thawing SOM and increased microbial mineralization, can increase the productivity and species composition of the Arctic plant communities, transitioning from tussock cottongrass species (*Eriophorum vaginatum*) to shrub species (*Betula nana* and/or *Salix pulchra*) or potentially sedge species (*Carex spp.*), depending on resulting soil moisture conditions. Therefore, soil microorganisms both as responders to forcing factors and regulators of SOM decomposition, play a large role in determining the future state of Arctic ecosystems and the global concentration of greenhouse gases.

Soil organic matter is comprised of a variety of organic compounds including oligosaccharides and complex carbohydrates (*e.g.* hexoses, disaccharides, cellulose, hemicellulose, pectin, starch), lignins, tannins, oils, fats, proteins, amides, organic acids, phenols, or alcohols, to name a few (Kögel-Knabner 2002). These compounds primarily come from the decaying necromass of plants and soil organisms (Paul 2016) and form the substrates of bacterial decomposers in the soil. Plant cell walls primarily contain a combination of cellulose, hemicellulose, and pectin polysaccharides, while fungal cell walls are known to uniquely contain a combination of chitin and glucan polymers (Bowman and Free 2006), and bacterial cell walls uniquely contain peptidoglycan polymers (up to 90% of the cell wall). To metabolize such a wide variety of chemical structures requires an equally wide variety of biochemical pathways

and specific enzyme families.

There are a number of databases and classification systems currently used to organize and link enzymes according to their genetic orthology (amino acid sequences), functional roles, or the chemical reactions they catalyse. These include the Enzyme Commission (EC) number classification system (NC-IUBMB and Webb 1992), the Kyoto Encyclopedia of Genes and Genomes (KEGG; Kanehisa and Goto 2000) orthology (KO) database, the SEED Subsystems database (Overbeek et al. 2005, 2014), and the Carbohydrate-Active Enzymes (CAZy) database (Lombard et al. 2014). The EC number classification system, first published in 1961, is organized based on the chemical reactions that are catalysed. While extremely useful, this system has its shortcoming, as many different enzymes may catalyse the same reaction. More recently, enzymes have classified by identifying the genes which encode them, organizing them according to homologous sequence similarity, and grouping them into tiered functional groups (*e.g.* KO and SEED Subsystems databases). The CAZy database focuses on enzymes specifically involved in the metabolism of carbohydrates. Specifically, its mission is to maintain an extensive and thorough catalogue which links sequence data to detailed information on the biochemical role of each gene, focusing on enzymes that “assemble, modify and breakdown oligo- and polysaccharides” (Lombard et al. 2014; <http://www.cazy.org>). In CAZy, enzymes are classified into sequenced-based families separated by biochemical function, including catabolic processes (glycoside hydrolases [GH], which catalyse the cleavage of the glycosidic bonds holding these polymers together), and anabolic processes (glycosyltransferases [GT], which catalyse glycoside synthesis). It should be noted that certain groups of polymers, such as hemicellulose and pectin, may use the same GTs, or complexes of GTs, for biosynthesis (Mohnen 2008, Harholt et al. 2010), and groups of polymers such as peptidoglycan and chitin may be broken down using the

same GHs, making functional classification of these group of enzymes very difficult.

Enzyme activities in soils are also affected by conditions determined by the soil physical, chemical, and biological environment such as the those affecting Arctic tundra soils (Gerday et al. 2000, German et al. 2012). Soil temperature and pH have direct effects on enzyme kinetics, where each enzyme has an optimum set of conditions. Likewise, the concentration of a given enzymes are determined by the rate at which they are produced by soil microbes, which is dependent on the composition and genetic capacity of the microbial community. In the Arctic, little is known about the genetic capacity of soil microorganisms to decompose SOM and catalyse nutrient transformations, and how changing environmental factors affect both enzyme kinetics and microbial community structure and function. Metagenomic shotgun sequencing within an *in situ* experimental context offers a holistic, community level snapshot of the genetic enzymatic potential of the soil microbial community, yielding both phylogenetic and functional information that can shed light on how soil microorganisms respond to the changing Arctic.

Here, we used shotgun metagenomic sequencing to evaluate changes in soil microbial community structure and genetic functional potential in response to a long-term snow depth manipulation experiment in Northern Alaska. The predicted changes in snow accumulation for Arctic tundra can alter soil physical factors (active layer depth, soil moisture, oxygen content), vegetation shifts (graminoids versus shrubs), and SOM chemistry over time. We focused on genes involved in SOM decomposition and nutrient cycling to determine how these processes might be affected by changes in winter precipitation climate conditions predicted for the tundra region. Based on previous findings that show altered soil chemistry, and shifts in soil bacterial community and associated estimates of gene abundance under deep snowpack (Ricketts et al.

2016), we hypothesize that genes required for OM decomposition will be less abundant in soils under deeper snowpack, but genes required for N metabolism will be more abundant.

5.2 Methods

5.2.1 Site description and sample collection

In early August of 2012, soil cores were collected from a long-term snow fence experiment site established in 1994 near Toolik Field Station, Alaska (Jones et al. 1998, Walker et al. 1999). The environment is classified as moist acidic tundra which is primarily dominated by cottongrass tussocks (*Eriophorum vaginatum*). Sphagnum mosses (*Sphagnum spp.*) covers inter-tussock areas along with a variety of other short-statured plant species, including Dwarf Birch (*Betula nana*), Diamond-leaf Willow (*Salix pulcha*), and wet sedge (*Carex spp.*). This experiment was designed to mimic the predicted increases in snow cover in the Arctic by producing a gradient of snow accumulation that decreases with increasing distance from the fence (Figure 4.1). Three treatment zones were established according to snow depth relative to a control zone (located >30m away from the effects of the snow fence); Deep (~100% increase), Intermediate (~50% increase), and Low (~25% decrease). Three soil cores were extracted from inter-tussock areas of each zone and subsamples were selected from each core for DNA extraction and sequencing. Detailed methods can be found in Ricketts et al. (2016), where 16S rRNA analysis of these samples can be found. For this study, DNA from 12 samples representing the organic horizon (mean soil depth \pm standard error [SE] = 5.6 ± 1.3 cm) of each treatment zone ($n=3$) were selected for further shotgun sequencing and analysis based on the community differences between treatments in the organic layer, observed in Ricketts et al. (2016).

5.2.2 *Shotgun sequencing and analysis*

All library preparation and sequencing was performed by the Genome Research Division of the Research Resources Center at the University of Illinois at Chicago. Each soil DNA sample (described above) was individually fragmented using a Covaris S2 acoustic shearing device (Covaris, Inc., Woburn, Massachusetts, USA), libraries were prepared using a Swift 2S library preparation kit (Swift Biosciences, Inc., Ann Arbor, MI, USA) resulting in average peak sizes ~500bp (range 454-536bp), final DNA fragment concentrations were quantified using an Invitrogen Qubit® 3.0 Fluorometer (Life Technologies, Inc., Carlsbad, CA, USA) and equally loaded across 4 lanes of an Illumina NextSeq instrument (Illumina, Inc., San Diego, CA, USA), and 2×151 paired-end sequencing was performed. Forward and reverse reads were not merged prior to analysis due to inadequate overlap between reads. All resulting files were concatenated by sample and uploaded to MG-RAST (Meyer et al. 2008) for analysis. Metagenomes were analyzed in MG-RAST for taxonomic gene abundance using the SILVA SSU database, and functional gene abundance using the SEED Subsystems and KEGG Ortholog databases. The annotation parameters used were e-value=5, %-identity=60, minimum alignment length=15 bp, and minimum abundance=1, using the representative hit method. To remove very low abundance, and potentially artificial or misclassified taxa, we filtered out OTU's that did not occur at least once in 20% of the samples. All OTU and gene counts were transformed into relative abundance (%) values.

5.2.3 *Functional gene analysis*

We performed two separate functional gene analyses; 1) using the pre-established functional classifications assigned by SEED Subsystems (Overbeek et al. 2005, 2014), and 2) using a

manually curated list of genes from KEGG ortholog assignments (Supplementary Table S5.1), selected and grouped according to the role they play in the microbial metabolism of carbohydrates, methane/CO₂, nitrogen (N), and phosphorus (P). For carbohydrate metabolism, we compared enzyme commission (EC) numbers, gene symbols, and gene names (given at the finest KEGG function level) within our dataset to the complete list of genes within the Carbohydrate-Active Enzymes (CAZy) database. The genes from our dataset that contained a match within CAZy were then grouped by the type of polymers their activity associates with (*i.e.* cellulose, hemicellulose, pectin, chitin, peptidoglycan, and starch), and whether they are involved in anabolic/biosynthetic (GTs) or catabolic/degradative processes (GHs). In two cases, multiple polymer groups were found to utilize the same enzymes and were thus grouped together (*i.e.* hemicellulose/pectin biosynthesis and peptidoglycan/chitin degradation). Genes that we were unable to definitively categorize, that did not have greater than 10 gene hits in at least one sample, or that were associated with eukaryotic organisms, were deleted. For the methane, N, and P metabolisms, we separated genes (again from the finest KEGG function level) according to their specific activity within their respective cycles, where methane metabolism (KEGG level 2) was split into methanogenesis and methanotrophy, N metabolism (KEGG level 2) was split into N-fixation, nitrification, nitrate reduction, denitrification, nitroalkane oxidase, and carbonic anhydrase, and P metabolism was split into inositol phosphate (a KEGG level 3 category), phosphomonoesters, phosphodiester, triphosphoric monoesters, and inorganic phosphate.

5.2.4 Statistical analyses

Kruskal-Wallis tests followed by Nemenyi posthoc tests were used to determine the effects of our treatment on soil properties (*i.e.* temperature, permafrost thaw depth, pH, %C, %N, C:N)

and the relative abundances of bacteria and fungi at the kingdom phylogenetic level (as well as the bacterial to fungal ratio), the eight most abundant bacterial phyla, the six most abundant fungal phyla, and functional gene groups at varying levels of the SEED Subsystems classification system as well as our manually curated list. Due to the limited number of replicates, and subsequent lack of statistical power in this experiment, we assigned a marginal significance threshold of $p < 0.1$ for all microbial abundance data tested using Kruskal-Wallis and Nemenyi tests.

To examine differences in overall soil microbial community structure (bacteria + fungi) between the snow fence treatment zones, we used non-metric multidimensional scaling (NMDS) plots in combination with adonis tests (similar to PERMANOVA) using the SILVA SSU assigned taxonomic relative abundance matrix at the OTU level. In addition, both bacterial and fungal communities were analyzed separately. We also used adonis tests to determine whether or not each measured soil property had an effect on microbial community structure.

Overall microbial functional capacity was evaluated using constrained (canonical) correspondence analysis (CCA). The SEED Subsystem functional gene abundance matrix (Hellinger transformed) at the “function” level was used as the response variable, and two models were evaluated to determine the degree of influence on microbial function. The “microbial taxonomy model” used the relative abundances of the 12 most abundant microbes as constraining factors, while the “soil environment model” used measured soil properties as constraining factors. Constraints were analyzed for collinearity using variance inflation factors (VIF) and removed from the full model if $VIF > 20$. Parsimonious model selection was performed using forward selection of factors based on Akaike information criterion (AIC). In addition, all

factors, including snow accumulation treatment, were analyzed separately as conditions to the models to determine the individual explanatory power of each factor. To further characterize the influence of the snow accumulation treatment, microbial taxa, and soil properties on microbial functional capacity, adonis and Mantel tests were performed for each explanatory factor.

5.3 Results

5.3.1 *Treatment effects on soil environment*

Greater snow accumulation in the Deep treatment zone over an 18 year time span resulted in increased soil temperatures ($n=12$, $H=33.29$, $df=3$, $p<0.001$) and greater active layer thaw depth ($n=12$, $H=21.35$, $df=3$, $p<0.001$) relative to the control, and lower soil C concentration ($n=3$, $H=7.67$, $df=3$, $p=0.053$), relative to the control (Table 5.1). Although not significant, soil N concentration, C:N, and soil pH did show trends with increasing snow depth, where soil N increased, C:N decreased, and soil pH increased (became less acidic).

Table 5.1. Abiotic characteristics of soil from snow accumulation treatments. Soil chemical properties were obtained from samples used for DNA extraction ($n=3$), while temperature and thaw depth were measured *in situ* ($n=12$). Values are means \pm standard errors. Nemenyi posthoc results are indicated by _{a,b,c} only where $p<0.05$.

Treatment	Sample Depths (cm)	%C	%N	C:N	pH	Temp @ 12 cm (°C)	Thaw Depth (cm)
Control	6.75 \pm 3.12	45.21 \pm 1.09 _{ab}	1.01 \pm 0.20	50.04 \pm 9.44	4.59 \pm 0.09	4.32 \pm 0.27 _b	59.17 \pm 1.23 _{bc}
Low	5.50 \pm 1.89	46.63 \pm 0.73 _a	1.06 \pm 0.07	44.59 \pm 2.54	4.44 \pm 0.08	2.92 \pm 0.24 _b	50.92 \pm 3.20 _c
Int.	3.67 \pm 0.67	40.59 \pm 2.43 _{ab}	1.17 \pm 0.25	38.38 \pm 8.85	4.69 \pm 0.41	4.08 \pm 0.25 _b	61.88 \pm 1.19 _{ab}
Deep	6.00 \pm 3.70	36.51 \pm 4.27 _b	1.40 \pm 0.07	26.27 \pm 3.41	5.61 \pm 0.21	6.49 \pm 0.20 _a	65.42 \pm 1.49 _a

5.3.2 Microbial taxonomic abundance analysis

The broadest and most notable phylogenetic treatment effect occurred at the kingdom taxonomic level, where the bacterial to fungal ratio increased as a result of snow accumulation ($H= 6.8974$, $df= 3$, $p= 0.075$). This is the result of a decrease in fungal abundance, as well as an increase in bacterial abundance, associated with snow depth (Figure 5.1A).

At the phylum taxonomic level, the relative abundance of unclassified bacteria across treatments ($29.35\% \pm 1.36$) was greater than any of the identified phyla, with Proteobacteria being the most abundant taxonomically classified phylum ($14.80\% \pm 0.61$). The unclassified bacteria also showed a treatment effect ($n=3$, $H=6.85$, $df=3$, $p=0.077$) with relative abundance being greater in the Deep zone relative to the Control ($p=0.061$). Of the taxonomically classified phyla, only 2 of the 9 most abundant bacterial phyla analyzed showed a treatment effect (Figure 5.1B), Actinobacteria ($n=3$, $H=6.90$, $df=3$, $p=0.075$) and Chloroflexi ($n=3$, $H=7.51$, $df=3$, $p=0.057$), where both phyla were greater in the Deep zone relative to the Low zone ($p=0.046$ and $p=0.061$, respectively).

Of the fungal phyla, Basidiomycota were the most abundant ($7.07\% \pm 1.53$), followed by Ascomycota ($5.90\% \pm 1.20$) and then the unclassified fungi ($1.17\% \pm 0.26$). While the effects of the snow-fence across treatment zones somewhat reduced the relative abundances of all three of these (Basidiomycota $n=3$, $H=6.59$, $df=3$, $p=0.086$; Ascomycota $n=3$, $H=7.05$, $df=3$, $p=0.070$; unclassified fungi $n=3$, $H=7.82$, $df=3$, $p=0.050$), the greatest differences occurred between the Deep zone and the Control zone (Basidiomycota $p=0.081$; Ascomycota $p=0.110$; unclassified fungi $p=0.046$).

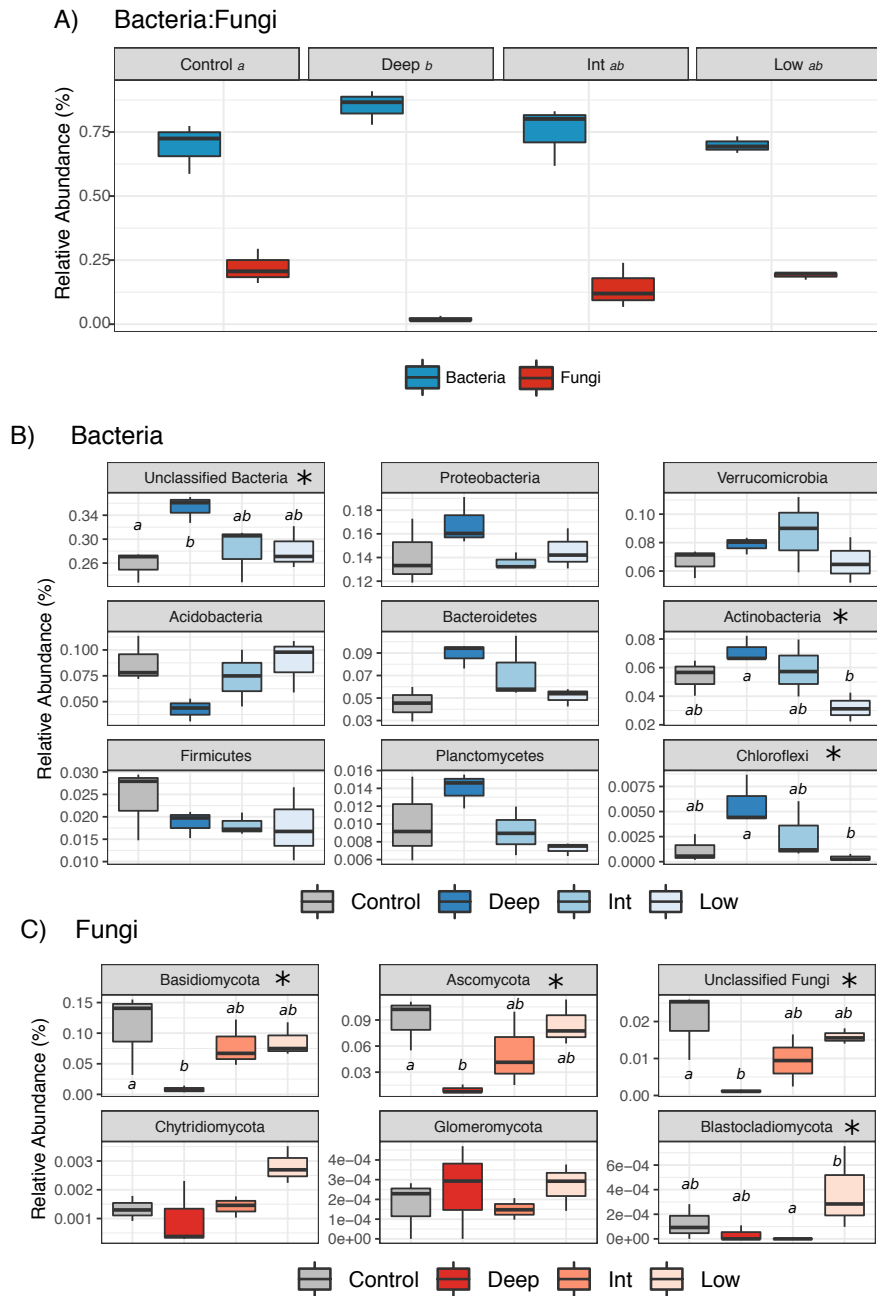


Figure 5.1. Relative abundances across treatments of bacteria and fungi at the kingdom (A) and phylum levels (B and C). Statistical significance ($p < 0.1$) of relative abundance differences between treatment groups as ascertained by Kruskal-Wallis is represented by “*”. Nemenyi posthoc testing was performed on bacterial:fungal relative abundance ratios in A), while in B) and C) the relative abundances of individual phyla were used. Significant differences found in posthoc tests are represented by “a” and “b”.

The overall microbial community structure was affected by the snow accumulation treatment (Table 5.2; $R^2=0.452$, $p=0.022$). Additionally, both bacterial and fungal communities, individually, were also affected by the snow accumulation treatment (Figure 5.2A and Table 5.2B; $R^2=0.449$, $p=0.036$ and $R^2=0.503$, $p=0.011$, respectively). However, it should be noted that soil pH had a greater influence on microbial community structure (overall, bacterial, and fungal) than any other factor, including our treatment (overall: $R^2=0.352$, $p=0.002$, bacterial: $R^2=0.379$, $p=0.002$, fungal: $R^2=0.332$, $p=0.002$). Soil temperature followed closely, primarily affecting fungal community structure ($R^2=0.254$, $p=0.008$) over bacteria ($R^2=0.183$, $p=0.063$). Soil %C, %N, and C:N did not have significant effects on soil microbial community structure (Table 5.2).

Table 5.2. Adonis (PERMANOVA) statistics for the effects of snow accumulation treatment, and soil chemical and physical properties on bacterial, fungal, and overall microbial (bacterial + fungal) community structure.

Explanatory variable	Overall microbial community		Bacterial community		Fungal community	
	R^2	p -value	R^2	p -value	R^2	p -value
Snow accumulation treatment	0.452	0.022*	0.449	0.036*	0.503	0.011*
Soil pH	0.352	0.002**	0.379	0.002**	0.332	0.002**
Temperature	0.198	0.037*	0.183	0.063	0.254	0.008**
%C	0.181	0.062	0.179	0.057	0.163	0.055
%N	0.093	0.342	0.090	0.352	0.117	0.199
C:N	0.156	0.091	0.152	0.122	0.178	0.063

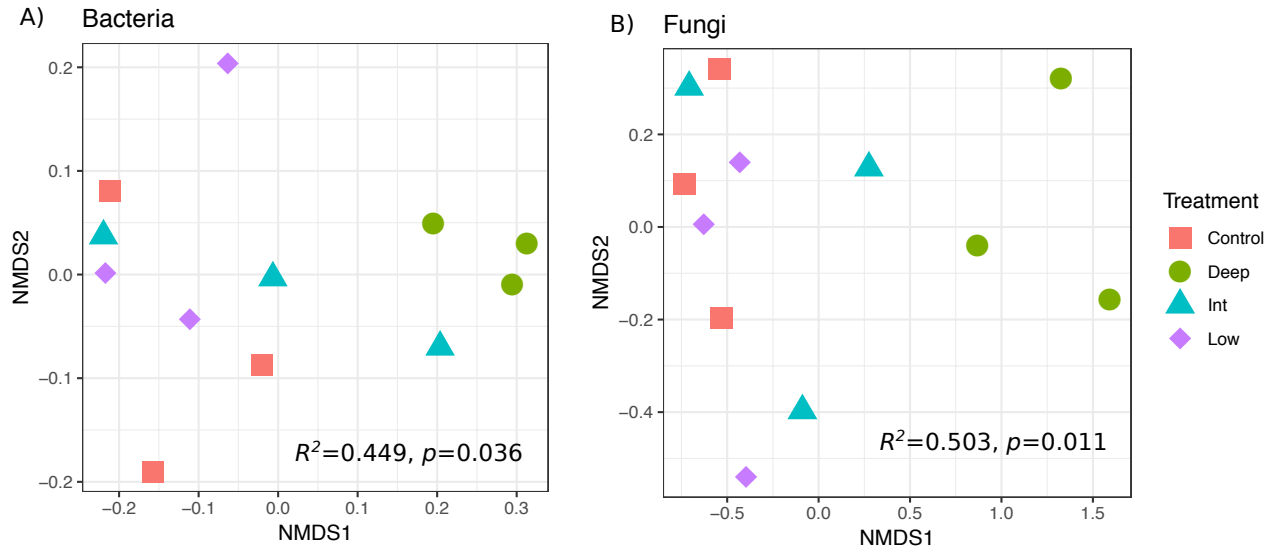


Figure 5.2. Non-metric multidimensional scaling (NMDS) ordinations showing differences in community structure at the OTU level for both bacteria (A; stress=0.041) and fungi (B; stress=0.039). R^2 and p -values are the results of adonis (PERMANOVA) tests evaluating the effects of the treatment on community structure.

5.3.3 Drivers of microbial functional capacity

Examination of factors which may contribute to shaping the overall genetic functional capacity of the soil microbial community showed a significant effect of the snow accumulation treatment and revealed a number of particularly influential microbial taxa and soil parameters (Figure 5.3). The snow accumulation treatment alone explained 40.1% of variation in genetic functional capacity (Figure 5.3 and Table 5.4; CCA Adj. $R^2=0.178, p=0.014, adonis R^2=0.508, p=0.011$). Of the two CCA models, the microbial taxonomy model performed better, explaining 87.8% of variation in genetic functional capacity (Figure 5.3A and Table 5.3; Adj. $R^2=0.324, p=0.013$), while the soil environment model predicted 51.2% of variation (Figure 5.3B and Table 5.4; Adj. $R^2=0.232, p=0.003$). The microbial taxonomy model originally consisted of 12 taxa, all but two (Firmicutes and Proteobacteria) of which showed significant effects on genetic

functional capacity when analyzed individually, with Ascomycota, Chloroflexi, and unclassified fungi showing the strongest effects (Table 5.3). After removal of collinear variables, the full microbial taxonomy model consisted of nine microbial taxa, and parsimonious model selection identified Ascomycota and Acidobacteria to be the best combination of predictors for genetic functional capacity (% variance explained=40.9%, Adj. R^2 =0.279, p <0.001). The soil environment model originally consisted of five measured soil variables, which when analyzed individually revealed soil pH to be the most influential driver of genetic functional capacity, followed by %C (Table 5.4). Soil temperature and %N did not have an effect. After the removal of C:N due to collinearity, parsimonious model selection of the four remaining variables identified soil pH and %C to be the best combination of predictors for genetic functional capacity (Figure 5.3B; % variance explained=38.9%, Adj. R^2 =0.253, p <0.001).

Table 5.3. Statistics from constrained correspondence analysis (CCA), adonis (PERMANOVA), and Mantel tests examining the effects of microbial taxonomic relative abundances on overall microbial community functional capacity. †=variables removed from the full model due to collinearity determined by variance inflation factors (VIF).

Microbial taxonomy	Constrained Correspondence Analysis (CCA)						
	Adonis		Mantel		CCA		
	R^2	p -value	r -statistic	p -value	% variance explained	Adj R^2	p -value
Full model ($n=9$)							
Parsimonious model (Ascomycota + Acidobacteria)							
Acidobacteria	0.294	0.008**	0.467	0.005**	18.8	0.108	0.018*
Firmicutes	0.134	0.165	0.233	0.081	10.3	0.013	0.252

Actinobacteria	0.377	9e-4***	0.631	<0.001***	25.0	0.176	<0.001***
Planctomycetes †	0.226	0.032*	0.400	0.006**	18.6	0.106	0.018*
Chloroflexi	0.427	1e-4***	0.710	<0.001***	28.8	0.217	<0.001***
Bacteroidetes †	0.379	3e-4***	0.538	<0.001***	24.1	0.165	0.002**
Verrucomicrobia	0.247	0.015*	0.306	0.038*	17.7	0.093	0.036*
Proteobacteria	0.089	0.393	0.032	0.366	9.1	0.002	0.388
Unclassified bacteria	0.324	0.003**	0.414	0.007**	23.4	0.158	0.004**
Basidiomycota	0.219	0.038*	0.396	0.008**	17.0	0.086	0.036*
Ascomycota	0.457	1e-4***	0.740	<0.001***	30.6	0.237	<0.001***
Unclassified fungi †	0.422	1e-4***	0.706	<0.001***	27.9	0.207	<0.001***

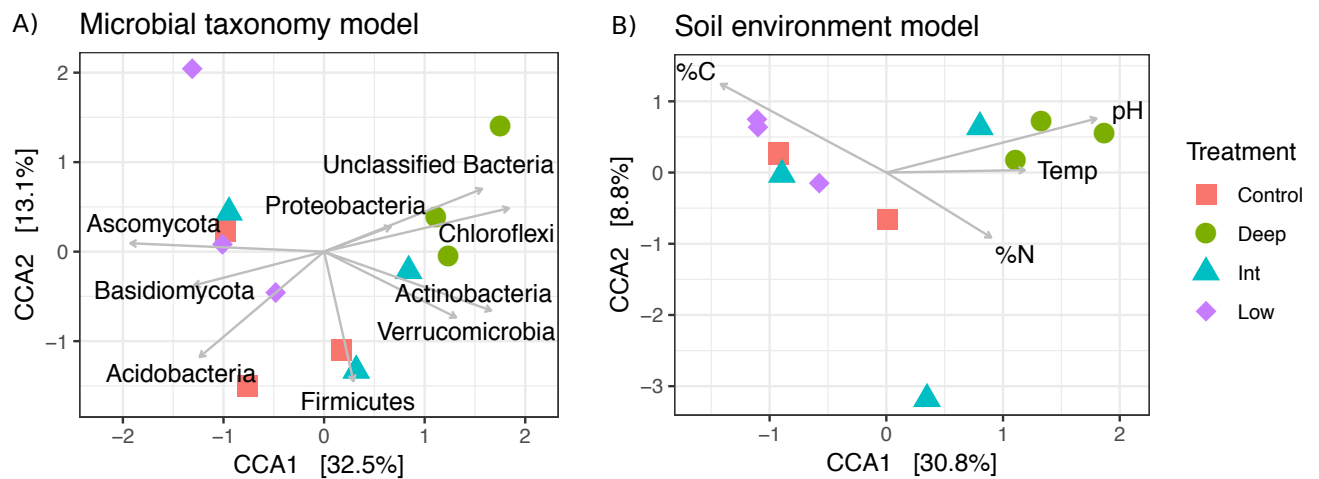


Figure 5.3. Constrained ordinations from canonical correspondence analysis (CCA) of overall microbial community genetic functional capacity. Each point represents the functional gene matrix from a single sample as assigned by SEED subsystems at the “function” level. Distances between sample points indicate differences in the overall functional capacity of the communities. Ordinations are constrained by microbial taxonomy (A) and soil environmental characteristics (B). Arrow length and direction indicate corollary power and influence on functional gene matrix structure.

Table 5.4. Statistics from constrained correspondence analysis (CCA), adonis (PERMANOVA), and Mantel tests examining the effects of the soil environment on overall microbial community functional capacity. Blank cells indicate that test assumptions did not pass. †=variables not included in the full model due to collinearity determined by variance inflation factors (VIF).

Soil Environment	Constrained Correspondence Analysis (CCA)							
			% variance explained		Adj R^2		p -value	
Full model ($n=4$)			51.2		0.232		0.003**	
Parsimonious model (pH+%C)			38.9		0.253		<0.001***	
	Adonis		Mantel		CCA			
<i>Individual Variables</i>	R^2	p -value	r -statistic	p -value	% variance explained	Adj R^2	p -value	
Temperature	-	-	-0.014	0.456	14.9	0.065	0.07	
pH	0.408	2e-4***	0.606	<0.001***	26.5	0.192	<0.001***	
%C	0.223	0.032*	0.184	0.146	19.5	0.115	0.013*	
%N	-	-	0.013	0.413	0.112	0.027	0.182	
C:N †	0.197	0.053	0.144	0.159	16.8	0.085	0.028*	
Snow accumulation treatment †	0.508	0.011*	-	-	40.1	0.178	0.014*	

5.3.4 Microbial functional gene abundance analysis

Our analysis of functional genes manually curated into relevant functional groups revealed a number of snow accumulation treatment effects (Figure 5.4). Within carbohydrate catabolic processes, there were decreased relative abundances of genes associated with hemicellulose ($H=6.28$, $p=0.099$, *posthoc* $p=0.140$) and starch degradation ($H=6.38$, $p=0.094$, *posthoc* $p=0.140$) in the Deep zone relative to the Control zone. Similar results were found for peptidoglycan/chitin degradation ($H=6.44$, $p=0.092$, *posthoc* $p=0.061$) in the Deep zone relative to the Low zone.

Likewise, within carbohydrate anabolic processes, there were decreased relative abundances of

genes associated with cellulose biosynthesis ($H=7.62$, $p=0.055$, *posthoc* $p=0.033$) and starch biosynthesis ($H=7.31$, $p=0.063$, *posthoc* $p=0.081$) in the Deep zone relative to the Low zone. Similarly, hemicellulose/pectin biosynthesis genes were more abundant in the Deep zone relative to the Control zone ($H=7.82$, $p=0.050$, *posthoc* $p=0.033$). Although not significant, the relative abundances of genes associated with methane metabolism did follow trends along the snow depth gradient where genes linked to methanogenesis increased with deeper snow ($H=5.87$, $p=0.118$) while genes linked to methanotrophy decreased as snow pack increased ($H=5.62$, $p=0.132$).

The relative abundances of genes involved in N and P cycling were also affected by the snow accumulation treatment (Figure 5.4). Specifically, the relative abundances of genes encoding enzymes for N-fixation and nitrate reduction were increased in the Deep zone relative to the Low zone ($H=6.28$, $p=0.099$, *posthoc* $p=0.140$ and $H=6.85$, $p=0.077$, *posthoc* $p=0.110$, respectively), while genes encoding carbonic anhydrases were increased in the Deep zone relative to the Control zone ($H=8.08$, $p=0.044$, *posthoc* $p=0.033$). Many P cycling genes showed an opposite response where the relative abundances of genes associated with inositol phosphate and triphosphoric monoester metabolisms were decreased in the Deep zone relative to the Low zone ($H=7.51$, $p=0.057$, *posthoc* $p=0.061$ and $H=8.13$, $p=0.043$, *posthoc* $p=0.061$, respectively). Genes associated with phosphodiester metabolism showed a similar pattern, although statistical power was not sufficient to show a difference ($H=5.97$, $p=0.113$). The relative abundances of genes involved in phosphomonoester metabolism, on the other hand, were greater in the Deep zone relative to the Control zone ($H=7.62$, $p=0.055$, *posthoc* $p=0.033$).

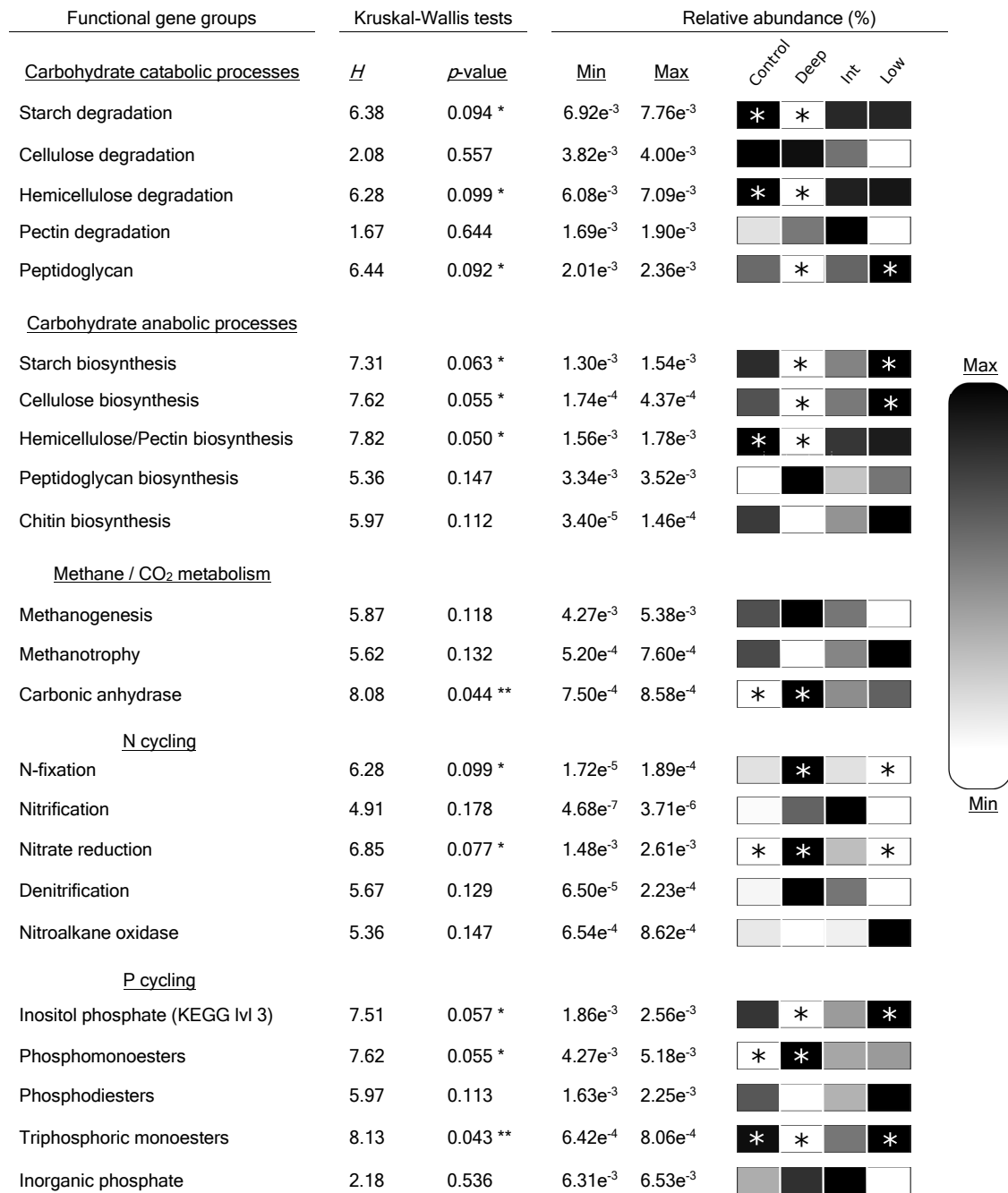


Figure 5.4. Heatmap and Kruskal-Wallis analysis of gene groups organized by association with various carbohydrate polymers found in organic matter, catabolic vs. anabolic processes, and methane/CO₂, N, and P metabolism. Columns in heatmap represent the four snow depth treatment zones. Black boxes indicate the maximum average relative abundance while white boxes indicate minimum average relative abundance (*n*=3). Maximum and minimum average values are shown in columns left of the heatmap. Asterisks (“*”) indicate Nemenyi posthoc differences with *p*<0.01.

Analysis of gene relative abundances organized by the SEED Subsystems functional gene classification system (Supplementary Table S5.2) revealed results similar to the analysis of our manually curated gene groups. Overall carbohydrate metabolism analyzed at level 1 was only marginally affected by the snow fence treatments ($H=6.08$, $p=0.108$), however posthoc tests showed decreased relative abundances of genes in the Deep zone relative to the Control zone (*posthoc* $p=0.081$). At finer resolution (level 2), central carbohydrate metabolism, di- and oligosaccharides, and fermentation functional gene groups all had decreased relative abundances in the Deep zone relative to the Control zone ($H=8.74$, $p=0.033$, *posthoc* $p=0.017$, $H=6.44$, $p=0.092$, *posthoc* $p=0.110$, and $H=8.23$, $p=0.041$, *posthoc* $p=0.033$, respectively), while the organic acids functional group had decreased relative abundances in the Deep zone relative to the Low zone ($H=7.51$, $p=0.057$, *posthoc* $p=0.046$).

The SEED Subsystems functional groups related to N metabolisms all had consistently higher relative abundances in the DEEP zone, including in overall N metabolism analyzed at level 1 relative to the Low zone ($H=6.90$, $p=0.075$, *posthoc* $p=0.081$), as well as in the level 2 functional groups ammonia assimilation, denitrification, and N-fixation ($H=6.69$, $p=0.082$, *posthoc* $p=0.081$, $H=6.28$, $p=0.099$, *posthoc* $p=0.081$, and $H=7.82$, $p=0.050$, *posthoc* $p=0.033$, respectively) relative to the Low zone. Likewise, relative gene abundances in dissimilatory nitrite reductase and nitrate and nitrite ammonification functional groups were higher in the Deep zone relative to the Low zone ($H=8.54$, $p=0.036$, *posthoc* $p=0.081$, and $H=7.82$, $p=0.050$, *posthoc* $p=0.046$, respectively). Analysis of the P metabolism SEED Subsystem level 1 functional group showed higher relative abundances of genes in the Deep zone relative to the Control zone ($H=6.38$, $p=0.094$, *posthoc* $p=0.081$), contradicting some of the results from the analysis of our manually curated classification. While only marginally significant, the relative gene abundances

related to potassium metabolism increased along the snow accumulation gradient with highest values in the Deep zone ($H=6.18$, $p=0.103$). The genes associated with sulfur metabolism (level 1) were lowest in the Intermediate zone compared to both Deep and Low zones ($H=6.90$, $p=0.075$). When separated into inorganic versus organic sulfur assimilation (SEED Subsystem level 2), relative abundances were higher in the Deep zone relative to the Intermediate zone for inorganic sulfur assimilation ($H=6.28$, $p=0.099$, *posthoc* $p=0.140$), but higher in the Low zone relative to the Intermediate zone for organic sulfur assimilation ($H=6.49$, $p=0.090$, *posthoc* $p=0.061$).

5.4 Discussion

This research provides an in-depth genetic analysis of how soil microorganisms in Arctic tundra soils respond to increases and decreases in snow accumulation and associated environmental effects, such as altered plant community and tissue chemistry, increased soil temperature and moisture, and decreased soil C concentration and soil acidity (Blanc-Betes et al. 2016, Ricketts et al. 2016). As snow accumulation increased as a result of our snow fence treatment, the bacterial to fungal ratios also increased, driven by the marked decrease in the relative abundance of fungal taxa in the Deep zone (Figure 5.1). These taxonomic responses contributed to overall microbial community structure differences, as well as bacterial and fungal community differences, but only past a snow-depth threshold in the Deep zone (Figure 5.2). Soil pH affected both bacterial and fungal communities equally, whereas soil temperature seemed to have more of an effect on the fungal community structure than that of bacteria (Table 5.2). Functionally, overall microbial genetic functional capacity was also found to be affected by the snow accumulation treatment, and driven by the Ascomycota and Chloroflexi phyla, as well as

soil pH and %C. (Figure 5.3, Table 5.3, and Table 5.4). The relative abundance of genes associated with carbohydrate metabolism (specifically related to starch metabolism, hemicellulose metabolism, and chitin degradation) decreased in the Deep zone relative to the Control and Low zones (Figure 5.4). Mineralization of N and P shifted from complex organic insoluble substrates at low snow to anaerobic N metabolism and to inorganic P and soluble organic P in the Deep zone (Figure 5.4). Results from this study further our understanding of soil microbial dynamics in response to predicted climate induced environmental changes in the Arctic and extrapolate biogeochemical functional effects of microbial community shifts likely to occur in a rapidly changing ecosystem.

5.4.1 *Microbial taxonomic responses*

In Arctic ecosystems, cryoturbation and long seasonal periods of sub-zero temperatures has resulted in largely unaggregated soils with very high particulate SOM and %C content (Table 5.1; Ping et al. 1998, 2015) and microbial C-substrate availability and decomposition are primarily limited by temperature. As both increased air temperatures and winter thermal insulation due to snowpack (*i.e.* changes in snow accumulation) warm Arctic tundra soils, C-substrate availability for microbial consumption also increases. Additionally, soil enzyme kinetics will be increased due to warmer temperatures (German et al. 2012). Overtime, this may result in increased SOM decomposition rates, releasing nutrients that facilitate the growth of plants and certain microbes that may have previously been limited by nutrient availability, thus inducing shifts in the soil microbial and plant communities (Epstein et al. 2004, Elmendorf et al. 2012, Pearson et al. 2013, Ricketts et al. 2016). Our long-term snow-fence experiment has reproduced these predicted community dynamics, and the soil microbial communities associated

with it. Besides the obvious overall community structural differences in both bacterial and fungal communities in the Deep zone (Figure 5.2), many microbial taxa from our study showed relative abundance differences between snow accumulation treatment zones that trended along with snow depth. For instance, we found increasing relative abundances of Actinobacteria and Chloroflexi associated with increasing snow depth along the snow accumulation gradient (Figure 5.1B), which support the results of our previous 16S rRNA analysis from these same samples (Ricketts et al. 2016). Interestingly, these patterns hold true even at the kingdom taxonomic level (Figure 5.1A), which can be observed using a shotgun metagenomic approach.

One of the advantages of using shotgun metagenomic sequencing in this study, is that it has allowed us to examine fungal community dynamics in relation to bacterial abundances. Our results showed decreasing relative abundance of fungi and increasing relative abundance of bacteria associated with snow depth, resulting in increasing bacterial to fungal ratios in soils covered by deeper snow. These results support previous research at this site where the abundances of ectomycorrhizal, lichenized, plant pathogenic, saprotrophic, and bryophyte-associated fungal functional groups were decreased as a result of increased snow depth (Semenova et al. 2016), and were also reflected at the phylum taxonomic level in our data, where nearly all fungal phyla, with the exception of low-abundance Chytridiomycota and Glomeromycota, showed decreasing relative abundances associated with increasing snow depth (Figure 5.1C). The decreased abundance of fungi in soils affected by deep snowpack may have functional ramifications, where the decomposition of lignified and recalcitrant compounds may be reduced as a result of fewer microorganisms that specialize in decomposition.

The snow accumulation treatment, which affects a number of environmental factors, was found to be a significant driving force in determining microbial community structure in both

bacterial and fungal communities (Table 5.2). The analyses of abiotic factors affected by snow treatments revealed soil pH, temperature, and to a lesser extent %C, to be the primary drivers of differences in soil microbial community structure in this ecosystem. Soil pH has been well documented as one of the main soil chemical variables affecting microbial community structure across many different ecosystems and environments (Lauber et al. 2009, Cho et al. 2016) and had was also found to affect bacterial and fungal communities in this study (Table 5.2). Soil temperature, however, affected fungal communities more than bacterial communities (Table 5.2), suggesting greater temperature sensitivity of fungi under snow treatment conditions. Other studies have shown temperature effects on species-specific fungal groups to primarily occur in moist acidic tundra as opposed to dry heath tundra ecosystems (Geml et al. 2015, 2016, Semenova et al. 2015). Therefore, it is important to further characterize taxonomic and functional fungal responses to changes in the environment at finer phylogenetic levels, and appropriately distinguish effects between ecosystem types to fully understand fungal dynamics in Arctic tundra ecosystems.

5.4.2 *Microbial genetic functional responses*

Logic might suggest that compositional differences in community structure equate to differences in the genetic functional capabilities of the community (Langille et al. 2013). While this assumption likely holds true at coarse taxonomic levels and within broad functional guilds, certain characteristics of microorganisms, such as functional redundancy, horizontal gene transfer, and variation in gene copy numbers per genome may complicate this interpretation. The proper differentiation of genetic functions among microbial communities requires the direct evaluation of genetic material using, for instance, shotgun metagenomic sequencing.

Our shotgun metagenome results indicate that increased winter precipitation in the Arctic tundra may reach a threshold thereby affecting the overall genetic functional capacity of the soil microbial community. Increased in snow accumulation decreased the potential for carbohydrate metabolism, increased the potential for anaerobic N metabolism and altered the sources of mineralizable P (Figure 5.4). Differences in functional capacity were tightly linked to the relative abundances of microbial taxa (Figure 5.3A and Table 5.3). In particular, Ascomycota, Chloroflexi, and unclassified fungi had the greatest influence over genetic functional metabolic capacity of the community, even though they were not among the most abundant phyla. These results suggest that these phyla may play a disproportionate quantitative role in microbial decomposition. At coarse taxonomic scales, it is difficult to attribute specific functions to these phyla (especially the unclassified fungi) but considering the degree of phylogenetic diversity within both Ascomycota and Chloroflexi, they likely perform a wide range of functions. Although these phyla are commonly found in tundra ecosystems, we found little research exploring their genetic functional capacities at finer taxonomic resolutions in tundra or other natural environments. We therefore suggest targeting these phyla for future research into microbial functional capacities in the Arctic.

Environmental factors also shape the composition of microbial communities, and constrain growth limitations and the biochemical efficiency of enzymes. Stark et al. (2014) showed that soil pH and nutrient availability in tundra soils have opposing effects on extracellular enzyme activity related to SOM decomposition. They found that while increasing nutrient availability resulted in increased extracellular enzyme activity, increasing soil pH decreased it. In a temperature and nutrient limited ecosystem such as the Arctic tundra, nutrient additions via fertilization will likely alleviate microbial limitations to produce expensive extracellular

enzymes. However, increased pH may result in greater solubility and degradability of certain forms of SOM in the soil matrix (Andersson et al. 2000, Kleber 2010). Additionally, warmer temperatures directly increase enzyme kinetics, and thus their metabolic efficiency (German et al. 2012, Ricketts et al. 2016). Thus, the combination of increasing soil temperatures and pH may result in decreasing microbial investment into enzyme production for SOM decomposition, as enzyme catalytic efficiency increases, and alternate C sources become more available. In this study, soil pH and %C were the main driving factors influencing microbial community genetic functional capacity (Figure 5.3B and Table 5.4). Our results show an inverse relationship between soil pH (Table 5.1) and relative abundance of genes associated with carbohydrate metabolism in the Deep zone (Figure 5.4 and Supplementary Table S5.2), supporting the idea of a reduced requirement for enzyme production in warmer soils with higher pH. This in combination with the decreased soil C:N in the Deep zone (Table 5.1) and the increased relative abundance of genes associated with N metabolism (Figure 5.4 and Supplementary Table S5.2) may suggest a C-substrate preference shift towards more readily soluble and simple organic C sources, which may be caused by alterations in the plant community.

At finer functional levels of carbohydrate metabolism, the gene relative abundances associated with starch, peptidoglycan/chitin, and hemicellulose catabolic processes, as well as those associated with starch, hemicellulose/pectin, and cellulose anabolic processes, were reduced in the Deep zone relative to the Control zone (Figure 5.4). Overall, this suggests either a decreased turnover of both starch and hemicellulose polymers under deeper snowpack or an increased efficiency of enzymes that catalyze these reactions, or a combination of the two. Likewise, the decreased relative abundance of chitin/peptidoglycan degrading enzymes could be reflective of the decreased relative abundance of fungi in the Deep zone, or the increased

efficiency of enzymes required for the turnover of bacterial biomass.

The results from the SEED subsystem classification system generally agreed with those of our manually curated classification. While the relative gene abundance of genes for beta-glucoside metabolism were not affected by snow depth treatments, the relative abundance of genes for di- and oligosaccharide metabolism were reduced in the Deep zone relative to the Control zone (Supplementary Table S5.2), perhaps due to increased metabolic efficiency with higher temperatures under deeper snowpack. The only functional genes within carbohydrate metabolism that had greater relative abundances in the Deep zone were those associated with the characteristically anaerobic functions of methanogenesis and cellulosome production (Supplementary Table S5.2). Cellulosomes are multi-enzyme complexes produced by anaerobic bacteria to facilitate the extracellular hydrolysis of cellulose (Schwarz 2001), while methanogenesis is a process primarily mediated by anaerobic Archaea, which were only found in very low abundance in our study (data not shown). However, Blanc-Betes et al. (2016) found substantial evidence of elevated CH₄ production and enhanced rates of methanogenesis in the Deep snow treatment zone, substantiating the functional genetic evidence from this study and suggesting that methanogens are likely present. Blanc-Betes et al. (2016) also documented increasing soil water content with snow accumulation and showed an associated reduction in %O₂ levels which contributed to CH₄ production. These results, along with indications of anaerobic N metabolisms, may indicate a shift toward more anaerobic conditions in the Deep zone. We did find that the genes involved in fermentation pathways were reduced under deeper snowpack, which is counterintuitive to an anaerobic environment, however this can be explained by an increase in catalytic efficiency as soil temperature and pH increase with added snow cover.

Both classification systems indicate increased relative abundances of genes associated with anaerobic N-fixation and N-reduction and ammonification with increased snow depth (Figure 5.4 and Supplementary Table S5.2). These results suggest an increased capacity to transform N compounds into biologically available forms such as nitrate and ammonium (Crawford 2002), and support previous research at this site using soil incubations which found higher N-mineralization rates in soils under deeper snow (Schimel et al. 2004). Additionally, plant tissues affected by long-term increases in snow depth and temperature were found to contain higher leaf N concentrations than those under ambient conditions (Welker et al. 2005, Leffler and Welker 2013). In a nitrogen-limited ecosystem such as the Arctic tundra, microbial N mineralization may be a key first step in initiating both above- and belowground community shifts, producing a positive feedback which ultimately establishes tighter ecological links between soil microorganisms and plants in areas that receive more snow accumulation.

Phosphorus is another limiting essential nutrient to microbial and plant growth. We found genes related to general P metabolic pathways identified by SEED subsystems classification had increased relative abundance in the Deep zone relative to the Control zone (Supplementary Table S5.2). However, examination of genes related to specific P compounds using our manually curated classification revealed that only genes associated with phosphomonoester metabolism were increased in the Deep zone relative to the Control zone, while those associated with inositol phosphate and triphosphoric monoester metabolism were decreased in the Deep zone relative to the Control and Low zones (Figure 5.4). These results may suggest a switch in microbial P substrate preference from insoluble organic P pools to soluble organic P pools (and possibly inorganic P pools) in the Deep snow zone compared to the Low and Control zones. This indicates that the relative abundances of genes associated with P metabolism may be driven by

the solubility of P substrates and soil pH, as opposed to O₂ availability which seem to be driving gene abundances for carbohydrate and N metabolisms. Inositol phosphates are insoluble organic P compounds that tend to accumulate in the environment due to strong sorption to clays and minerals in the soil matrix, whereas phosphomonoesters are soluble organic P compounds and are generally less energetically expensive to metabolize (Turner et al. 2005, George et al. 2018). Furthermore, soil pH is known to differentially affect the amount of specific forms of P in soils through variations in stabilization and phosphatase pH optimums (Richardson and Simpson 2011, Turner and Blackwell 2013). For example, the overall amount of organic P compounds in soils is inversely related to soil pH due to decreased phosphatase efficiency at lower pH. However, inositol phosphates are more stable in acidic conditions and thus tend to accumulate in acidic soils, requiring specific enzymes with lower pH optimums (phytases) relative to other phosphatases (Turner and Blackwell 2013). The difference in soil pH between our treatment zones (Table 5.1) may thus help to explain our genetic data, where higher soil pH in the Deep zone may result in less inositol phosphates, and greater turnover of soluble P compounds such as phosphomonoesters (Figure 5.4). Likewise, lower soil pH in the Low zone may facilitate the accumulation of inositol phosphates, and simultaneous loss of soluble P compounds, resulting in inositol phosphate as the sole source of P, thus requiring the increased production of phytases. To fully resolve the P dynamics of this system requires a more detailed analysis that focuses specifically on genes related to P cycling, and integrates measurements of the various forms of P in soils (Richardson and Simpson 2011).

5.5 Conclusions

The combination of our phylogenetic and functional results suggests that the decreased relative abundances of fungi (and perhaps Acidobacteria) under deeper snow pack may be driving decreasing genetic capacities for carbohydrate and inositol phosphate metabolism, while increasing relative abundances of bacteria (specifically Actinobacteria, Chloroflexi, and unclassified bacteria) may be driving increases in anaerobic N and phosphomonoester metabolism. In addition, our analyses found that altered soil chemical and physical properties in the Deep zone (*i.e.* higher pH, lower %C, warmer temperatures) contribute to shaping the genetic functional capacity of soil microbial communities, likely through their direct effects on enzyme efficiency and substrate solubility/availability. Our genetic data also suggests a greater prevalence of anaerobic processes such as methanogenesis, cellulose production, and anaerobic N pathways in the Deep zone, which could indicate that O₂ availability may also be a contributing factor in shaping microbial community structure. Overall, these results suggest predicted increased snowfall and soil temperatures in the Arctic tundra may 1) increase soil nutrient availability, potentially facilitating plant community shifts, and 2) decrease fungal abundance leading to reduced SOM decomposition potential and the re-accrual of soil carbon in this ecosystem over time. This research sheds new light into growing concerns that Arctic tundra ecosystem may become a large source of C emissions into the atmosphere and highlights the need for continued long-term *in situ* experimental research.

5.6 Acknowledgements

Funding for this project primarily came from the United States Department of Energy, Terrestrial Ecosystem Science Program to M. A. Gonzalez-Meler (DE-SC 0006607). Initiation and maintenance of the snow fence experiment was funded by the National Science Foundation Long Term Ecological Research Program beginning in 1994 (9412782, 0632184, 0612534, 0856728) to J. M. Welker. Michael Ricketts received additional support from the Elmer Hadley Graduate Research Award, the W.C. and May Preble Deiss Award for Graduate Research, and the Bodmer International Travel Award. Further acknowledgments can be found in chapter 4.

5.7 References

- Andersson, S., S. I. Nilsson, and P. Saetre. 2000. Leaching of dissolved organic carbon (DOC) and dissolved organic nitrogen (DON) in mor humus as affected by temperature and pH. *Soil biology & biochemistry* 32:1–10.
- Berendsen, R. L., C. M. J. Pieterse, and P. A. H. M. Bakker. 2012. The rhizosphere microbiome and plant health. *Trends in Plant Science* 17:478–486.
- Blanc-Betes, E., J. M. Welker, N. C. Sturchio, J. P. Chanton, and M. A. Gonzalez-Meler. 2016. Winter precipitation and snow accumulation drive the methane sink or source strength of Arctic tussock tundra. *Global Change Biology*:n/a-n/a.
- Bowman, S. M., and S. J. Free. 2006. The structure and synthesis of the fungal cell wall. *BioEssays* 28:799–808.
- Castro, H. F., A. T. Classen, E. E. Austin, R. J. Norby, and C. W. Schadt. 2010. Soil microbial community responses to multiple experimental climate change drivers. *Applied and Environmental Microbiology* 76:999–1007.
- Cho, S.-J., M.-H. Kim, and Y.-O. Lee. 2016. Effect of pH on soil bacterial diversity. *Journal of Ecology and Environment* 40:10.
- Crawford, N. 2002. The Molecular Genetics of Nitrate Assimilation in Fungi and Plants. *Annual Review of Genetics* 27:115–146.
- Elmendorf, S. C., G. H. R. Henry, R. D. Hollister, R. G. Björk, A. D. Bjorkman, T. V. Callaghan, L. S. Collier, E. J. Cooper, J. H. C. Cornelissen, T. A. Day, A. M. Fosaa, W. A. Gould, J. Grétarsdóttir, J. Harte, L. Hermanutz, D. S. Hik, A. Hofgaard, F. Jarrad, I. S. Jónsdóttir, F. Keuper, K. Klanderud, J. A. Klein, S. Koh, G. Kudo, S. I. Lang, V. Loewen, J. L. May, J. Mercado, A. Michelsen, U. Molau, I. H. Myers-Smith, S. F. Oberbauer, S. Pieper, E. Post, C. Rixen, C. H. Robinson, N. M. Schmidt, G. R. Shaver, A. Stenström, A. Tolvanen, Ø. Totland, T. Troxler, C. H. Wahren, P. J. Webber, J. M. Welker, and P. A. Wookey. 2012. Global assessment of experimental climate warming on tundra vegetation: Heterogeneity over space and time. *Ecology Letters* 15:164–175.
- Epstein, H., M. Calef, F. Cooperative, and S. Paul. 2004. Detecting changes in arctic tundra plant communities in response to warming over decadal time scales. *Global Change ...*:1325–1334.
- Geml, J., L. N. Morgado, T. A. Semenova, J. M. Welker, M. D. Walker, and E. Smets. 2015. Long-term warming alters richness and composition of taxonomic and functional groups of arctic fungi. *FEMS Microbiology Ecology* 91:1–13.

- Geml, J., T. A. Semenova, L. N. Morgado, and J. M. Welker. 2016. Changes in composition and abundance of functional groups of arctic fungi in response to long-term summer warming. *Biology letters* 12:1–6.
- George, T. S., C. D. Giles, D. Menezes-Blackburn, L. M. Condon, A. C. Gama-Rodrigues, D. Jaisi, F. Lang, A. L. Neal, M. I. Stutter, D. S. Almeida, R. Bol, K. G. Cabugao, L. Celi, J. B. Cotner, G. Feng, D. S. Goll, M. Hallama, J. Krueger, C. Plassard, A. Rosling, T. Darch, T. Fraser, R. Giesler, A. E. Richardson, F. Tamburini, C. A. Shand, D. G. Lumsdon, H. Zhang, M. S. A. Blackwell, C. Wearing, M. M. Mezeli, R. Almås, Y. Audette, I. Bertrand, E. Beyhaut, G. Boitt, N. Bradshaw, C. A. Brearley, T. W. Bruulsema, P. Ciais, V. Cozzolino, P. C. Duran, M. L. Mora, A. B. de Menezes, R. J. Dodd, K. Dunfield, C. Engl, J. J. Frazão, G. Garland, J. L. González Jiménez, J. Graca, S. J. Granger, A. F. Harrison, C. Heuck, E. Q. Hou, P. J. Johnes, K. Kaiser, H. A. Kjær, E. Klumpp, A. L. Lamb, K. A. Macintosh, E. B. Mackay, J. McGrath, C. McIntyre, T. McLaren, E. Mészáros, A. Missong, M. Mooshammer, C. P. Negrón, L. A. Nelson, V. Pfahler, P. Pobleto-Grant, M. Randall, A. Seguel, K. Seth, A. C. Smith, M. M. Smits, J. A. Sobarzo, M. Spohn, K. Tawarayaya, M. Tibbett, P. Voroney, H. Wallander, L. Wang, J. Wasaki, and P. M. Haygarth. 2018. Organic phosphorus in the terrestrial environment: a perspective on the state of the art and future priorities. *Plant and Soil* 427:191–208.
- Gerday, C., M. Aittaleb, M. Bentahir, J. Chessa, P. Claverie, T. Collins, S. D. Amico, J. Dumont, G. Garsoux, D. Georlette, A. Hoyoux, T. Lonhienne, M. Meuwis, and G. Feller. 2000. Cold-adapted enzymes: from fundamentals to biotechnology. *Trends in Biotechnology* 18:103–107.
- German, D. P., K. R. B. Marcelo, M. M. Stone, and S. D. Allison. 2012. The Michaelis-Menten kinetics of soil extracellular enzymes in response to temperature: a cross-latitudinal study. *Global Change Biology* 18:1468–1479.
- Harholt, J., A. Suttangkakul, and H. V. Scheller. 2010. Biosynthesis of pectin. *Plant physiology* 153:384–395.
- Jones, M. H., J. T. Fahnestock, D. A. Walker, M. D. Walker, and J. M. Welker. 1998. Carbon dioxide fluxes in moist and dry Arctic tundra during the snow-free season : Responses to increases in summer temperature and winter snow accumulation. *Arctic, Antarctic, and Alpine Research* 30:373–380.
- Kanehisa, M., and S. Goto. 2000. KEGG: kyoto encyclopedia of genes and genomes. *Nucleic acids research* 28:27–30.
- Kleber, M. 2010. What is recalcitrant soil organic matter? *Environmental Chemistry* 7:320.
- Kögel-Knabner, I. 2002. The macromolecular organic composition of plant and microbial residues as inputs to soil organic matter. *Soil biology & biochemistry* 34:139–162.

- Langille, M. G. I., J. Zaneveld, J. G. Caporaso, D. McDonald, D. Knights, J. A. Reyes, J. C. Clemente, D. E. Burkepille, R. L. Vega Thurber, R. Knight, R. G. Beiko, and C. Huttenhower. 2013. Predictive functional profiling of microbial communities using 16S rRNA marker gene sequences. *Nature biotechnology* 31:814–821.
- Lauber, C. L., M. Hamady, R. Knight, and N. Fierer. 2009. Pyrosequencing-based assessment of soil pH as a predictor of soil bacterial community structure at the continental scale. *Applied and environmental microbiology* 75:5111–5120.
- Leffler, A. J., and J. M. Welker. 2013. Long-term increases in snow pack elevate leaf N and photosynthesis in *Salix arctica* : responses to a snow fence experiment in the High Arctic of NW Greenland. *Environmental Research Letters* 8:025023.
- Lombard, V., H. Golaconda Ramulu, E. Drula, P. M. Coutinho, and B. Henrissat. 2014. The carbohydrate-active enzymes database (CAZy) in 2013. *Nucleic Acids Research* 42:490–495.
- Meyer, F., D. Paarmann, M. D’Souza, R. Olson, E. M. Glass, M. Kubal, T. Paczian, a Rodriguez, R. Stevens, A. Wilke, J. Wilkening, R. a Edwards, and M. D. Souza. 2008. The metagenomics RAST server - a public resource for the automatic phylogenetic and functional analysis of metagenomes. *BMC bioinformatics* 9:386.
- Mohnen, D. 2008. Pectin structure and biosynthesis. *Current Opinion in Plant Biology* 11:266–277.
- NC-IUBMB, and E. Webb, editors. 1992. *Enzyme Nomenclature 1992: Recommendations of the Nomenclature Committee of the International Union of Biochemistry and Molecular Biology and the Nomenclature and Classification of Enzymes*. 1st Editio. Academic Press.
- Overbeek, R., T. Begley, R. M. Butler, J. V Choudhuri, H.-Y. Chuang, M. Cohoon, V. de Crécy-Lagard, N. Diaz, T. Disz, R. Edwards, M. Fonstein, E. D. Frank, S. Gerdes, E. M. Glass, A. Goesmann, A. Hanson, D. Iwata-Reuyl, R. Jensen, N. Jamshidi, L. Krause, M. Kubal, N. Larsen, B. Linke, A. C. McHardy, F. Meyer, H. Neuweger, G. Olsen, R. Olson, A. Osterman, V. Portnoy, G. D. Pusch, D. a Rodionov, C. Rückert, J. Steiner, R. Stevens, I. Thiele, O. Vassieva, Y. Ye, O. Zagnitko, and V. Vonstein. 2005. The subsystems approach to genome annotation and its use in the project to annotate 1000 genomes. *Nucleic acids research* 33:5691–702.
- Overbeek, R., R. Olson, G. D. Pusch, G. J. Olsen, J. J. Davis, T. Disz, R. A. Edwards, S. Gerdes, B. Parrello, M. Shukla, V. Vonstein, A. R. Wattam, F. Xia, and R. Stevens. 2014. The SEED and the Rapid Annotation of microbial genomes using Subsystems Technology (RAST). *Nucleic Acids Research* 42:206–214.
- Paterson, E., T. Gebbing, C. Abel, A. Sim, and G. Telfer. 2007. Rhizodeposition shapes rhizosphere microbial community structure in organic soil. *The New phytologist* 173:600–

10.

- Paul, E. A. 2016. The nature and dynamics of soil organic matter: Plant inputs, microbial transformations, and organic matter stabilization. *Soil Biology and Biochemistry* 98:109–126.
- Pearson, R. G., S. J. Phillips, M. M. Lorant, P. S. A. Beck, T. Damoulas, S. J. Knight, and S. J. Goetz. 2013. Shifts in Arctic vegetation and associated feedbacks under climate change. *Nature Climate Change* 3:673–677.
- Ping, C. L., J. G. Bockheim, J. M. Kimble, G. J. Michaelson, and D. A. Walker. 1998. Characteristics of cryogenic soils along a latitudinal transect in arctic Alaska. *Journal of Geophysical Research* 103:28,917–28,928.
- Ping, C. L., J. D. Jastrow, M. T. Jorgenson, G. J. Michaelson, and Y. L. Shur. 2015. Permafrost soils and carbon cycling. *Soil* 1:147–171.
- Richardson, A. E., and R. J. Simpson. 2011. Soil Microorganisms Mediating Phosphorus Availability Update on Microbial Phosphorus. *Plant Physiology* 156:989–996.
- Ricketts, M. P., C. E. Flower, K. S. Knight, and M. A. Gonzalez-Meler. 2018. Evidence of ash tree (*Fraxinus* spp.) specific associations with soil bacterial community structure and functional capacity. *Forests* 9:1–16.
- Ricketts, M. P., R. S. Poretsky, J. M. Welker, and M. Gonzalez-Meler. 2016. Soil bacterial community and functional shifts in response to altered snowpack in moist acidic tundra of Northern Alaska. *Soil* 2:459–474.
- Schimel, J. P., C. Bilbrough, and J. M. Welker. 2004. Increased snow depth affects microbial activity and nitrogen mineralization in two Arctic tundra communities. *Soil Biology and Biochemistry* 36:217–227.
- Schwarz, W. H. 2001. The cellulosome and cellulose degradation by anaerobic bacteria. *Applied Microbiology and Biotechnology* 56:634–649.
- Semenova, T. A., L. N. Morgado, J. M. Welker, M. D. Walker, E. Smets, and J. Geml. 2015. Long-term experimental warming alters community composition of ascomycetes in Alaskan moist and dry arctic tundra. *Molecular Ecology* 24:424–437.
- Semenova, T. A., L. N. Morgado, J. M. Welker, M. D. Walker, E. Smets, and J. Geml. 2016. Compositional and functional shifts in arctic fungal communities in response to experimentally increased snow depth. *Soil Biology and Biochemistry* 100:201–209.
- Stark, S., M. K. Männistö, and A. Eskelinen. 2014. Nutrient availability and pH jointly constrain microbial extracellular enzyme activities in nutrient-poor tundra soils. *Plant and Soil*.

- Turner, B. L., and M. S. A. Blackwell. 2013. Isolating the influence of pH on the amounts and forms of soil organic phosphorus. *European Journal of Soil Science* 64:249–259.
- Turner, B. L., B. J. Cade-Menun, L. M. Condon, and S. Newman. 2005. Extraction of soil organic phosphorus. *Talanta* 66:294–306.
- Walker, M., D. Walker, J. Welker, A. Arft, T. Bardsley, P. Brooks, J. T. Fahnestock, M. Jones, M. Losleben, A. Parsons, T. Seastedt, and P. Turner. 1999. Long-term experimental manipulation of winter snow regime and summer temperature in arctic and alpine tundra. *Hydrological Processes* 13:2315–2330.
- Welker, J. M., J. T. Fahnestock, P. F. Sullivan, and R. a. Chimner. 2005. Leaf mineral nutrition of Arctic plants in response to warming and deeper snow in northern Alaska. *Oikos* 109:167–177.

6 Broader Impacts

The results presented here contribute to an ever-growing body of research aimed at understanding soil microbial communities, how they interact with their environment, and the potential impacts microbial responses to change might have on ecosystem dynamics. Exploring patterns, commonalities, and differences between multiple ecosystem types (*i.e.* temperate deciduous forest and Arctic tundra) and methods (*i.e.* 16S rRNA amplicon vs. shotgun sequencing and EA vs. FTIR) provides a more holistic view of soil microbial dynamics which can then inform and improve predictive models. In addition, the experimental manipulation of environmental factors, both *in vitro* and *in situ*, that are anticipated to change in future climate scenarios allows the prediction of potential successional trajectories of soil microbial communities and subsequent functional consequences over time. This research has applications in a wide range of industries, including agriculture (plant/microbe interactions and nutrient management), energy development (microbial metabolic manipulation), medicine (host microbiome research and drug discovery), and waste management (environmental remediation), indicating great potential for societal gain.

Moving forward, there are specific areas of genomic microbial ecology that I envision requiring further research including:

- 1) Linking microbial metagenomic data to ecosystem scale measurements. While challenging, this could be accomplished by the strategic collection of multiple data types from a natural ecosystem scale experiment, including the validation of gene abundance data (qPCR vs. shotgun sequencing), quantification of enzyme concentration/activity as well as biochemical reactants and products, and the collection of gas flux and thorough environmental data collected within gradients of spatial and temporal scales.

2) Integration of appropriate ecological contexts across multiple trophic levels of soil organisms (viruses, protozoa, nematodes, mites, collembola, *etc.*). There are surprisingly few soil metagenomic studies that consider organisms other than bacteria, archaea, or fungi in their analyses, despite the fact that ecological interactions such as competition, predation, mutualism, and commensalism exist. Integrating the collection of abundance data from a wider range of soil organisms, perhaps in concert with isotopic tracer experiments, may help to clarify soil community dynamics.

3) Identify specific factors or measurements that most accurately predict microbial community structure and develop predictive models using Bayesian statistics and machine learning. Although sequencing technologies continue to improve and become more affordable, they still require relatively expensive and labor-intensive methods that are not compatible with rapid measurements in the field. To overcome this limitation, much research has been done to determine soil factors that are most useful in predicting microbial community structure and function, often showing soil chemical factors such as pH, redox potential, and C and N concentrations to be the most influential drivers of community structure. Because FTIR spectroscopy can reveal detailed information about the chemical nature of a soil, with full spectral bands acting as a “fingerprints”, it promises to be a fast, accurate, and portable method for estimating microbial community structure and thus functional capacity. Using advanced Bayesian and machine learning statistical techniques, development of increasingly accurate FTIR predictive models has potential to be a very promising area of research.

7 APPENDICES

7.1 Supplementary materials – Chapter 2

Supplementary Table S2.1. Summary statistics of re-analyzed data using only sites that have ash canopy condition (AC) values less than or equal to 3, resulting in 2 sites (BHN and KRS), consisting of 6 ash plots (meanAC=2.42±0.30) and 4 non-ash plots. Adonis tests were used to analyze differences in overall bacterial community structure and overall soil chemical characteristics between categorical variables (a). Continuous variables were analyzed individually (b) for differences between ash and non-ash plots, and differences between sites using Mann-Whitney *U* tests, and for correlations between overall bacterial community structure and individual variables using Mantel tests. Text in bold and italics represents a significant result ($p < 0.05$).

(a)	Adonis test					
	Bacterial community		Soil environment			
	<i>R</i> ²	<i>p</i> -value	<i>R</i> ²	<i>p</i> -value		
Categorical variables						
Ash vs. Non-ash	<i>0.457</i>	<i>0.029</i>	0.139	0.222		
Forest site	0.045	0.660	0.232	0.055		
(b)	Mann-Whitney <i>U</i> test				Mantel test	
	(Ash vs. Non-ash)		(Forest site; n=2)		(Bacterial community)	
	<i>W</i>	<i>p</i> -value	<i>W</i>	<i>p</i> -value	<i>r</i> -statistic	<i>p</i> -value
Continuous variables						
Mean AC (ash only)	-	-	0	0.064	0.066	0.333
Mean Stems (#/ha)	19	0.158	5.5	0.167	0.112	0.197
Mean BA (m ² /ha)	1	0.694	18	0.310	-0.137	0.797
Ash (%)	-	-	10	0.666	<i>0.553</i>	<i>0.007</i>
Maple (%)	14	0.762	23	<i>0.032</i>	0.271	0.059
Oak (%)	4	0.088	20	0.119	0.140	0.165
Beech (%)	12	1.000	2	<i>0.036</i>	0.156	0.182
Hickory (%)	18	0.149	20	0.072	-0.213	0.957
α -diversity (tree)	20.5	0.087	19.5	0.173	-0.077	0.644
α -diversity (bacteria)	21	0.067	6	0.222	-0.120	0.744
Soil pH	20	0.114	7	0.310	<i>0.513</i>	<i>0.010</i>
%C	17.5	0.285	13.5	0.917	-0.204	0.937
%N	19	0.163	22.5	<i>0.046</i>	-0.221	0.958
C:N	11.5	1.000	6.5	0.249	-0.234	0.985

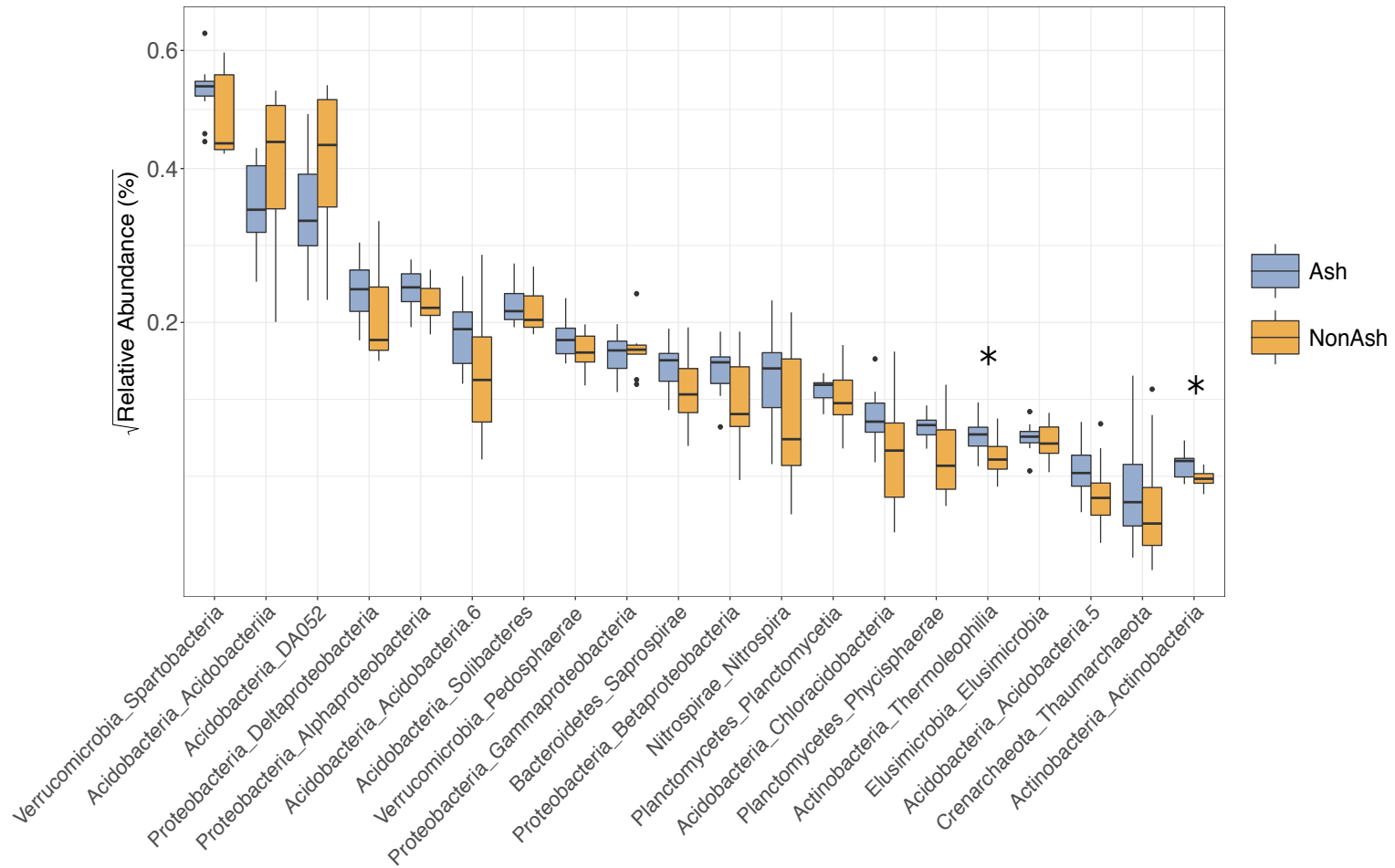
Ca	17	0.352	4	0.095	0.502	0.011
K	15	0.610	6	0.222	0.312	0.044
Mg	19	0.171	6	0.222	0.461	0.008
P	14	0.762	2	0.032	-0.009	0.482
Al	9	0.610	25	0.008	0.387	0.023
B	11.5	1.000	8.5	0.463	-0.001	0.473
Cu	4.5	0.134	12.5	1.000	0.306	0.045
Fe	2	0.038	15	0.691	0.606	0.005
Mn	14	0.762	13	1.000	-0.125	0.783
Na	12	1.000	8	0.421	-0.069	0.644
S	8	0.476	15	0.691	-0.048	0.592
Zn	7	0.352	2	0.032	0.165	0.149

Supplementary Table S2.2. Means and standard errors of all measured variables separated by forest site. Alpha diversity was calculated using the Shannon diversity index (H). Kruskal Wallis test significance ($p < 0.05$) is indicated by “*”. Nemenyi post hoc test significant differences ($p < 0.05$) are indicated by superscripts “a” and “b”.

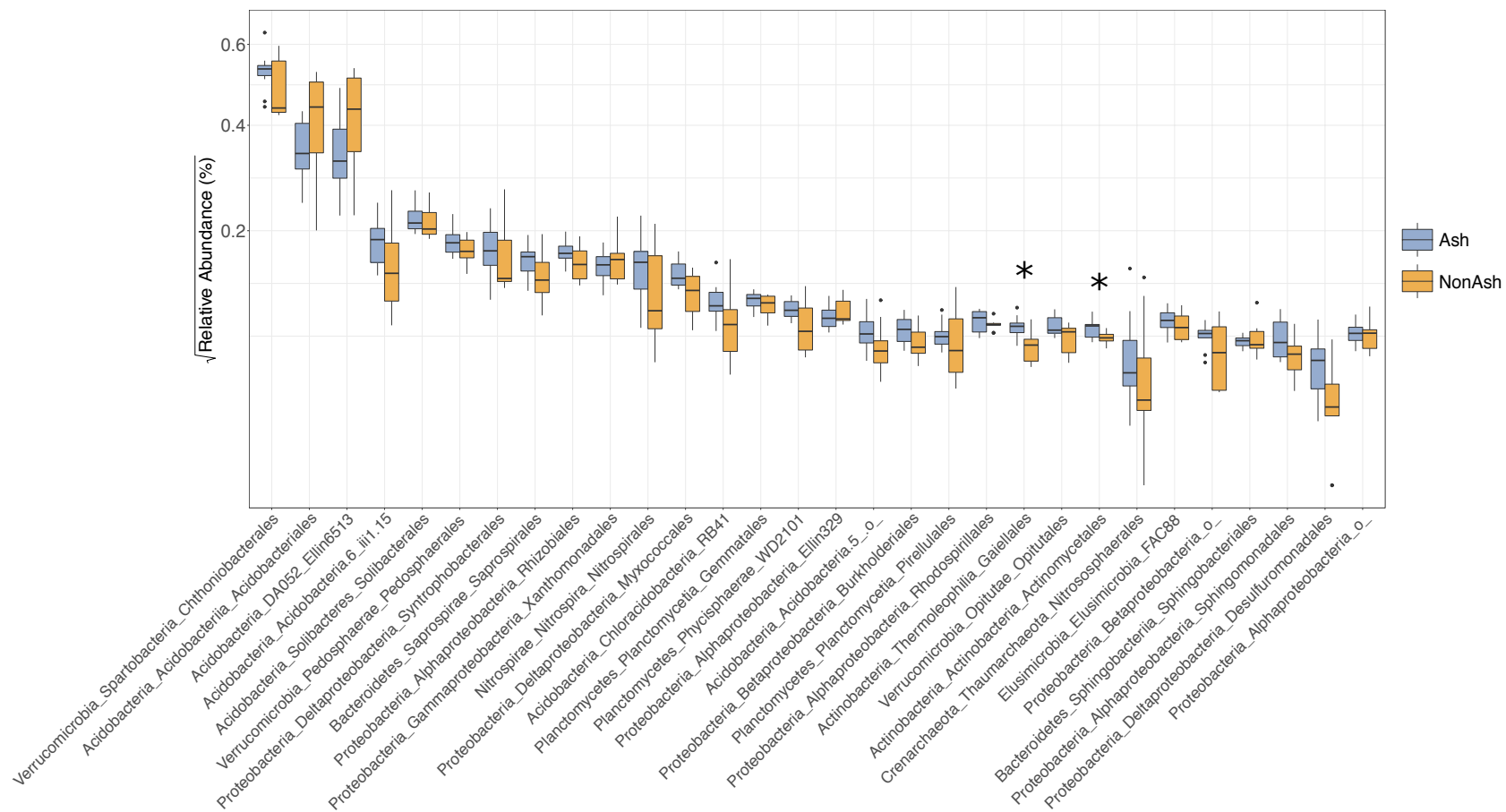
Variables	Forest Site			
	BHN (n=5)	KRS (n=5)	SYM (n=4)	STR (n=6)
AC (ash only)	1.83±0.33 ^a	3.00±0.00 ^{ab}	4.40±0.20 ^{ab}	4.83±0.17 ^b
Stems (#/ha) *	323.0±24.1 ^{ab}	385.0±48.5 ^{ab}	600.0±103.6 ^b	295.8±36.2 ^a
BA (m ² /ha)	37.72±2.57	34.75±2.99	25.98±2.97	33.93±5.05
α-diversity (tree)	1.164±0.155	1.065±0.070	1.415±0.124	1.281±0.162
α-diversity (bacteria)	8.221±0.095	8.432±0.090	8.619±0.072	8.523±0.284
pH	4.78±0.05	4.99±0.12	4.98±0.09	4.97±0.09
%C *	3.26±0.48 ^{ab}	2.91±0.15 ^{ab}	2.18±0.14 ^b	3.66±0.18 ^a
%N *	0.37±0.03 ^a	0.28±0.02 ^{ab}	0.21±0.01 ^b	0.31±0.01 ^{ab}
C:N *	8.80±0.80 ^a	10.29±0.33 ^{ab}	10.41±0.47 ^{ab}	11.78±0.31 ^b
Ca	554.0±117.6	1046.8±203.1	601.3±63.4	811.9±119.6
K	73.22±10.75	90.04±10.08	87.33±13.23	69.67±9.63
Mg	116.43±18.77	168.46±27.49	102.38±9.84	146.57±21.67
P *	1.14±0.09 ^{ab}	1.52±0.08 ^a	0.58±0.07 ^b	0.98±0.15 ^{ab}
Al *	188.64±10.27 ^a	104.65±22.37 ^b	124.89±15.31 ^{ab}	144.28±21.83 ^{ab}
B	0.11±0.01	0.14±0.02	0.09±0.01	0.13±0.02
Cu	0.21±0.03	0.20±0.02	0.19±0.03	0.26±0.06
Fe	23.90±3.60	20.24±6.78	16.87±4.36	21.56±5.21
Mn	61.25±16.67	54.36±11.36	34.72±5.23	41.16±6.68
Na	7.18±0.54	7.89±0.57	5.95±0.39	7.51±0.67
S	10.87±0.67	9.98±0.70	9.48±1.70	9.89±0.47
Zn *	1.84±0.27 ^{ab}	2.97±0.32 ^a	1.20±0.21 ^b	2.63±0.70 ^{ab}

Supplementary Table S2.3. Plot level characteristics of soil pH, tree community health (AC), total basal area (BA), percent dominance of tree genera by BA, and alpha-diversity as calculated by the Shannon diversity index.

Site / Plot	Soil pH	Mean AC	Total BA (m ² /ha)	Ash (%)	Maple (%)	Oak (%)	Beech (%)	Hickory (%)	α -diversity (H)
BHN1-Ash	4.86	2	44.67	44.3	16.3	11.0	24.4	3.9	1.287
BHN2-Ash	4.80	2.3	40.07	43.0	27.9	-	11.2	5.6	1.264
BHN3-Ash	4.73	1.2	36.36	60.7	21.5	6.6	0.9	1.0	1.475
BHN1-NonAsh	4.87	1	29.00	-	16.6	54.3	-	-	1.228
BHN2-NonAsh	4.63	1	38.53	-	49.0	51.0	-	-	0.566
KRS1-Ash	5.31	3	33.96	58.5	16.7	-	22.1	-	1.040
KRS2-Ash	5.14	3	42.96	59.1	5.2	-	35.7	-	1.160
KRS3-Ash	5.10	3	36.11	72.1	11.8	-	12.4	-	1.228
KRS1-NonAsh	4.65	1	24.42	-	3.8	-	91.6	-	1.082
KRS2-NonAsh	4.75	1	36.30	-	5.6	45.9	47.6	-	0.817
SYM1-Ash	5.23	5	31.29	40.5	11.2	25.2	-	-	1.477
SYM2-Ash	5.00	4.5	19.81	52.4	38.6	-	-	-	1.075
SYM1-NonAsh	4.78	5	30.82	3.9	22.6	73.6	-	-	1.437
SYM2-NonAsh	4.97	1	21.99	1.5	11.7	11.5	-	70.9	1.672
STR1-Ash	4.96	1	45.10	29.0	34.7	27.5	8.9	-	1.221
STR2-Ash	4.97	1	12.46	17.0	36.0	-	-	13.9	1.408
STR3-Ash	5.09	4.6	46.25	60.6	3.5	31.5	-	-	1.622
STR1-NonAsh	5.03	4.2	31.09	-	60.4	33.2	-	6.4	0.849
STR2-NonAsh	4.55	1	37.33	-	32.5	50.1	16.4	-	1.386
STR3-NonAsh	5.23	1	31.36	-	5.4	92.0	-	-	1.265

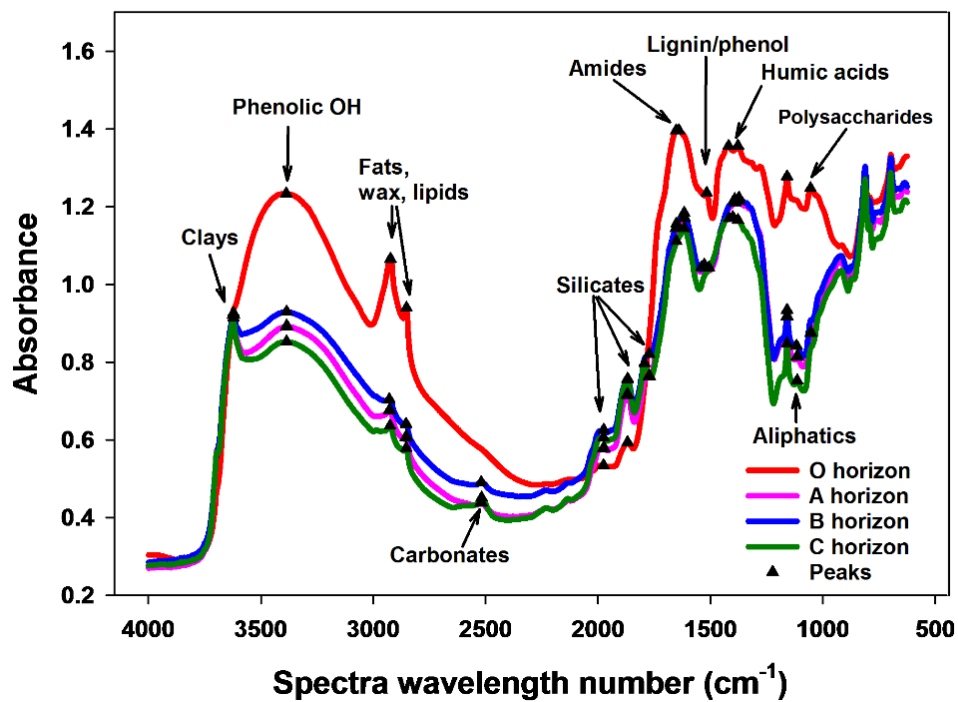


Supplementary Figure S2.1. Boxplot comparing the average Hellinger transformed abundances of the 20 most abundant bacterial/archaeal classes between ash (blue) and non-ash (orange) plots. Mann-Whitney U -test significance is denoted by asterisks, where $*=p<0.05$.



Supplementary Figure S2.2. Boxplot comparing the average Hellinger transformed abundances of the 30 most abundant bacterial/archaeal orders between ash (blue) and non-ash (orange) plots. Mann-Whitney U -test significance is denoted by asterisks, where $*=p<0.05$.

7.2 Supplementary materials – Chapter 3



Supplementary Figure S3.1. Example of Fourier transformed mid infrared (FTIR) spectra identifying peaks associated with soil chemical properties.

Supplementary Table S3.1. List of wavelength peak numbers associated with soil chemical properties. Adapted from Matamala et al. 2019. For complete list of references a-z, see Matamala et al. 2019.

Wavenumber (cm ⁻¹)	Functional group
3694	Clay minerals ^{a-c}
3622	Clay minerals ^{a-e}
3394	Phenolic OH, H- bonded water ^f
2984-2924	Aliphatic methyl & methylene groups ^{h-v}
2877-2852	Aliphatic methyl & methylene groups ^{h-v}
2516	Carbonates ^{h,m,q,x}
2237	CN iso-cyanate, nitrile and cyanamide groups ^w
2137	Carbohydrates ^p
1993	Silicates ^{a,z}
1870	Silicates ^{a,z}
1788	Silicates ^{a,z}
1656	C=O of amide ^{d,g,n,o,q}
1616	Aromatics ^y or amine ^d
1521	Lignin ^{g,k,q}
1423	Carboxylate/carboxylic structures ^g
1380	Phenolic, lignin ^g
1270	Phenolic OH ^f
1159	Polysaccharides ^k , nucleic acids, proteins ^{k,o}
1116	n/a [*]
1060	Carbohydrates ^{d,k,p}
1000	Clay minerals ^{q,u}
916	Kaolinite and smectite ^{b,c,d}
873	Carbonates ^q
848	Primary amine ^q
811	Quartz ^e

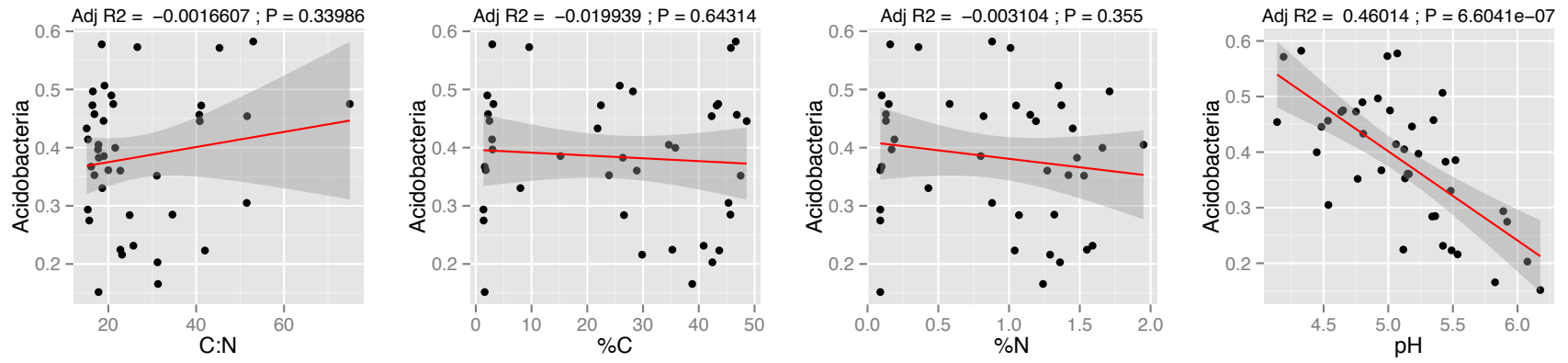
^aNguyen et al., 1991; ^bMadejova and Komadel, 2001; ^cNayak and Singh, 2007; ^dViscarra Rossel and Behrens, 2010; ^eChurchman et al., 2010; ^fVeum et al., 2014; ^gArtz et al., 2008; ^hSoriano-Disla et al., 2014; ⁱEllerbrock and Gerke, 2004; ^jHaberhauer and Gerzabek, 1999; ^kCalderon et al., 2013; ^lPedersen et al., 2011; ^mBernier et al., 2013; ⁿLeifield, 2006; ^oMovasaghi et al., 2008; ^pJanik et al., 2007; ^qSmidt and Meissl, 2007; ^rNiemeyer et al., 1992; ^sD'Acqui et al., 1999; ^tDu and Zhou, 2011; ^uMadejova, 2003; ^vCoates, 2000; ^wFrancioso et al., 2009, 2011; ^xParikh et al., 2014; ^yVerchot et al., 2011; ^zCalderon et al. 2011; ^{*}not identified in the literature.

7.3 Supplementary materials – Chapter 4

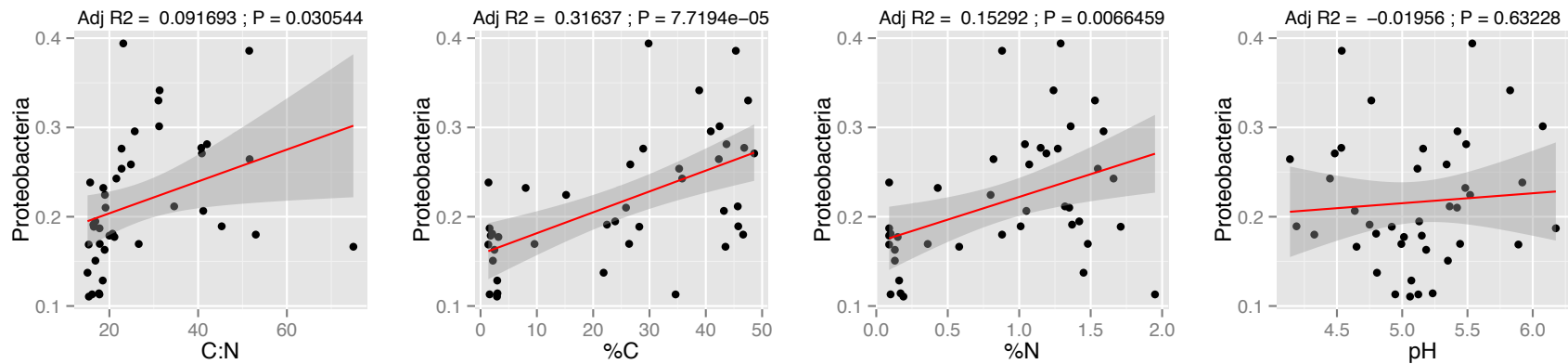
Supplementary Table S4.1. List of targeted KEGG ortholog enzymes used in the PICRUSt analyses. For more information see materials and methods in main text.

Functional role	Enzyme name	EC number	KEGG orthology number
PRESENT IN SAMPLES			
Arabinoside degradation	arabinogalactan endo-beta-1,4-galactanase	3.2.1.89	K01224
	arabinan endo-1,5-alpha-L-arabinanase	3.2.1.99	K06113
Cellulose degradation	cellulase	3.2.1.4	K01179
	beta-glucosidase	3.2.1.21	K01188, K05349, K05350
	cellulose 1,4-beta-cellobiosidase (CBH)	3.2.1.91	K01225
Chitin degradation	chitinase (NAG)	3.2.1.14	K01183
	bifunctional chitinase/lysozyme	3.2.1.14 & 3.2.1.17	K13381
Nitrogen mobilization	leucyl aminopeptidase (LAP)	3.4.11.1	K01255
	urease	3.5.1.5	K01427, K01428, K01429, K01430, K14048
Lignin degradation	tyrosinase (phenol oxidase)	1.14.18.1	K00505
Pectin degradation	polygalacturonase	3.2.1.15	K01184
	alpha-L-rhamnosidase	3.2.1.40	K05989
Phosphate mobilization	alkaline phosphatase (AP)	3.1.3.1	K01077, K01113
	acid phosphatase (AP)	3.1.3.2	K01078, K01093, K09474, K03788, K14379
Superoxides	superoxide dismutase	1.15.1.1	K00518, K04564, K04565
	superoxide reductase	1.15.1.2	K05919

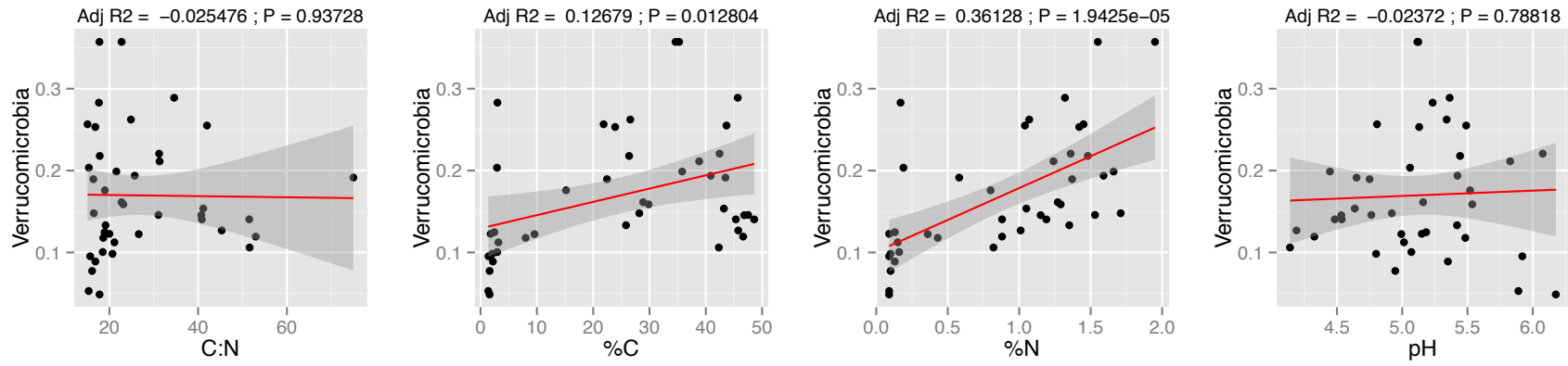
Xylan degradation	xylan 1,4-beta-xylosidase	3.2.1.37	K01198
NOT FOUND IN ANY SAMPLES			
	polyphenol oxidase	1.10.3.1	K00422
	peroxidase	1.11.1.7	K00430
	fructan beta-fructosidase	3.2.1.80	K03332
	laccase (oxidoreductase)	1.10.3.2	K05909
	eosinophil peroxidase	1.11.1.7	K10788
	cytosol aminopeptidase	3.4.11.1 & 3.4.11.5	K11142
	peroxiredoxin 6, 1-Cys peroxiredoxin	1.11.1.7, 1.11.1.15, & 3.1.1.-	K11188
	lactoperoxidase	1.11.1.7	K12550
	low molecular weight phosphotyrosine protein phosphatase	3.1.3.2 3.1.3.48	K14394
	lysophosphatidic acid phosphatase type 6	3.1.3.2	K14395
	acid phosphatase	3.1.3.2	K14410
	beta-D-xylosidase 4	3.2.1.37	K15920



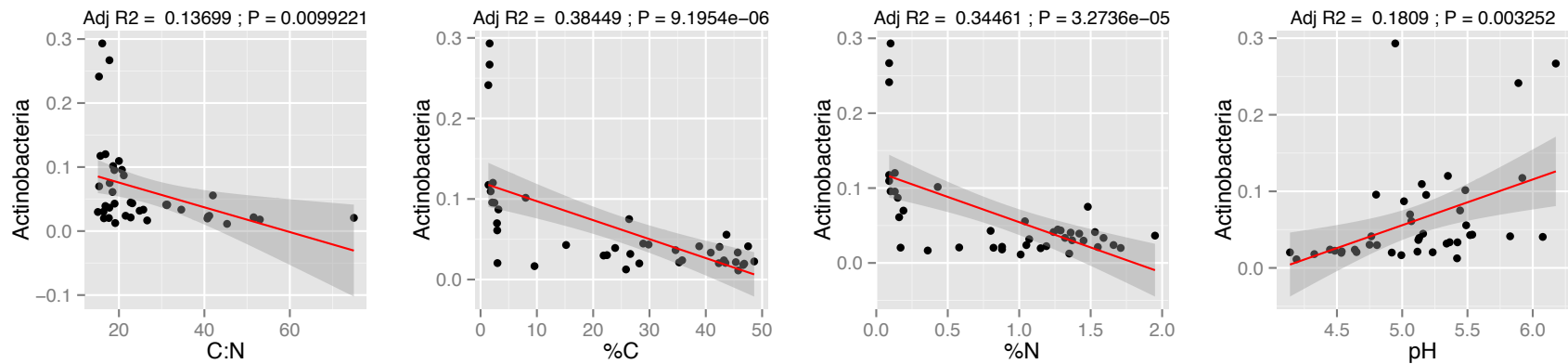
Supplementary Figure S4.1. Linear fit regression of Acidobacteria relative abundance with respect to soil C:N, %C, %N, and pH across all snow treatment sites and all soil depths ($n=41$). Shaded areas indicate 95% confidence intervals.



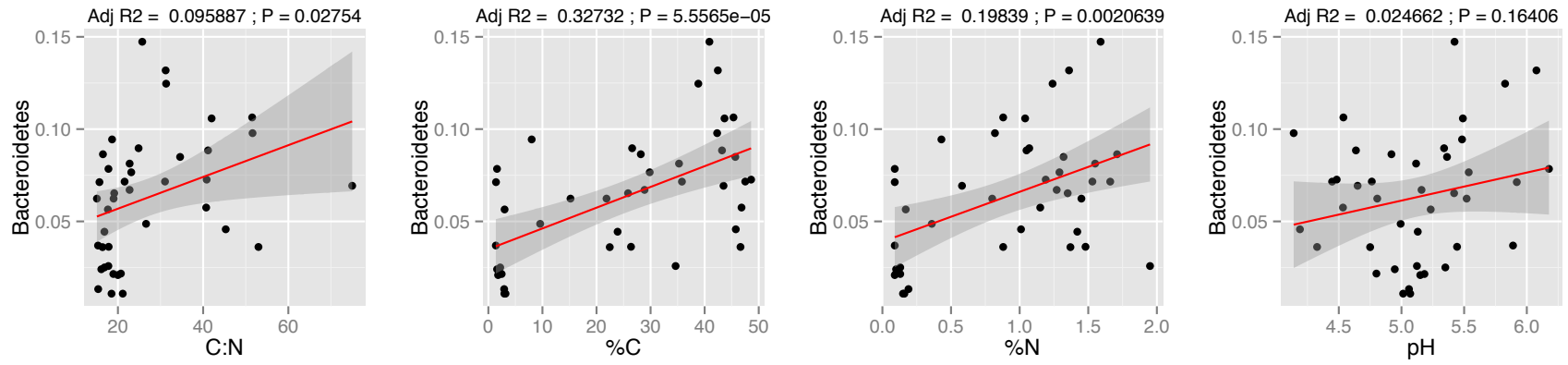
Supplementary Figure S4.2. Linear fit regression of Proteobacteria relative abundance with respect to soil C:N, %C, %N, and pH across all snow treatment sites and all soil depths ($n=41$). Shaded areas indicate 95% confidence intervals.



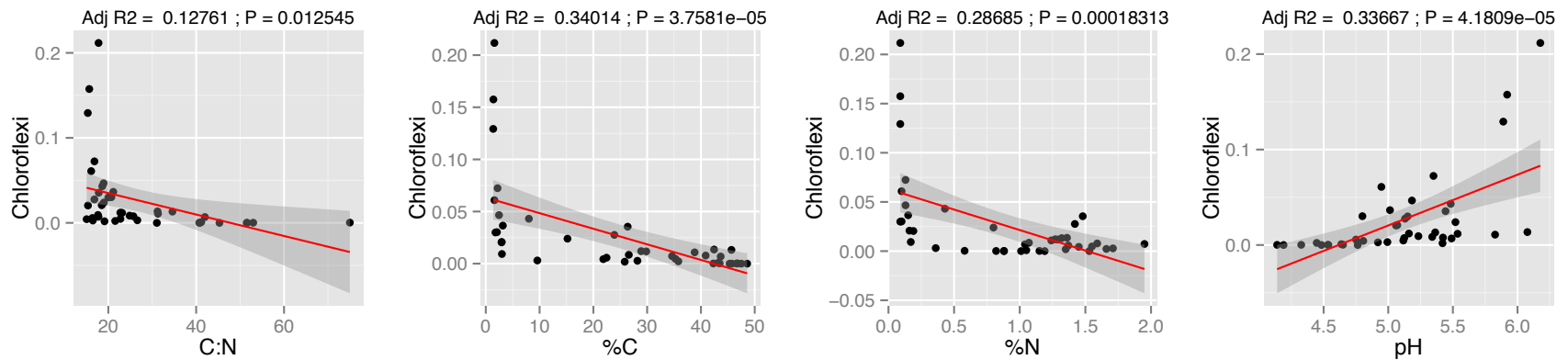
Supplementary Figure S4.3. Linear fit regression of Verrucomicrobia relative abundance with respect to soil C:N, %C, %N, and pH across all snow treatment sites and all soil depths ($n=41$). Shaded areas indicate 95% confidence intervals.



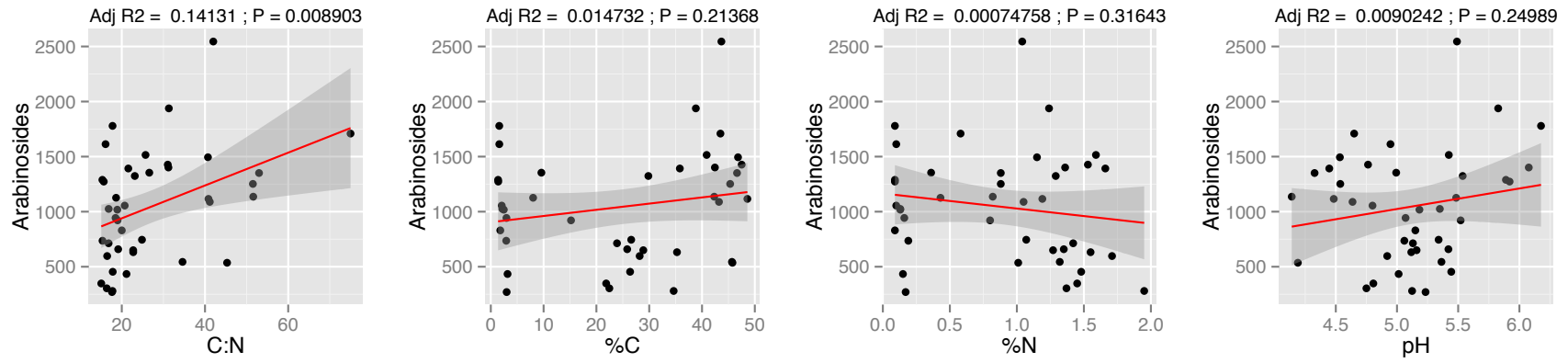
Supplementary Figure S4.4. Linear fit regression of Actinobacteria relative abundance with respect to soil C:N, %C, %N, and pH across all snow treatment sites and all soil depths ($n=41$). Shaded areas indicate 95% confidence intervals.



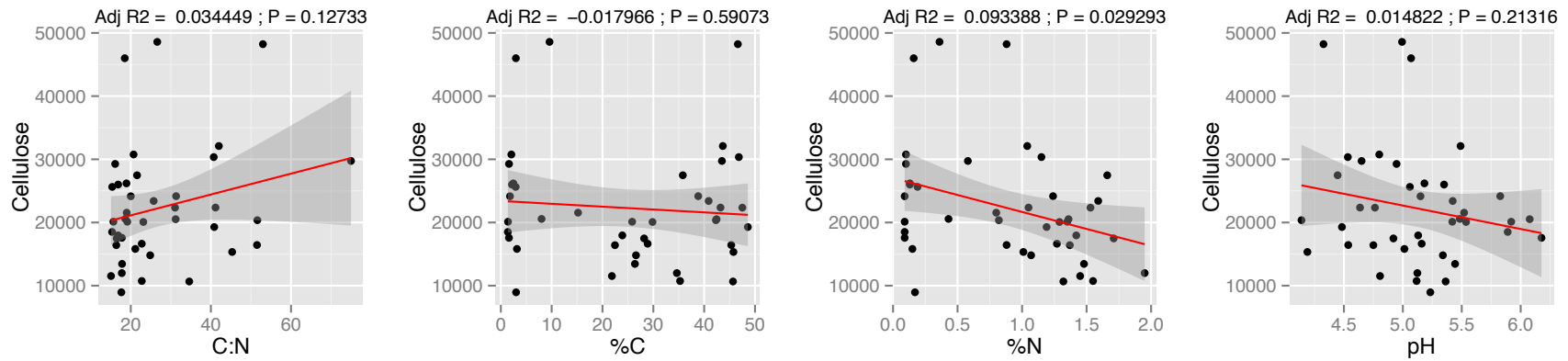
Supplementary Figure S4.5. Linear fit regression of Bacteroidetes relative abundance with respect to soil C:N, %C, %N, and pH across all snow treatment sites and all soil depths ($n=41$). Shaded areas indicate 95% confidence intervals.



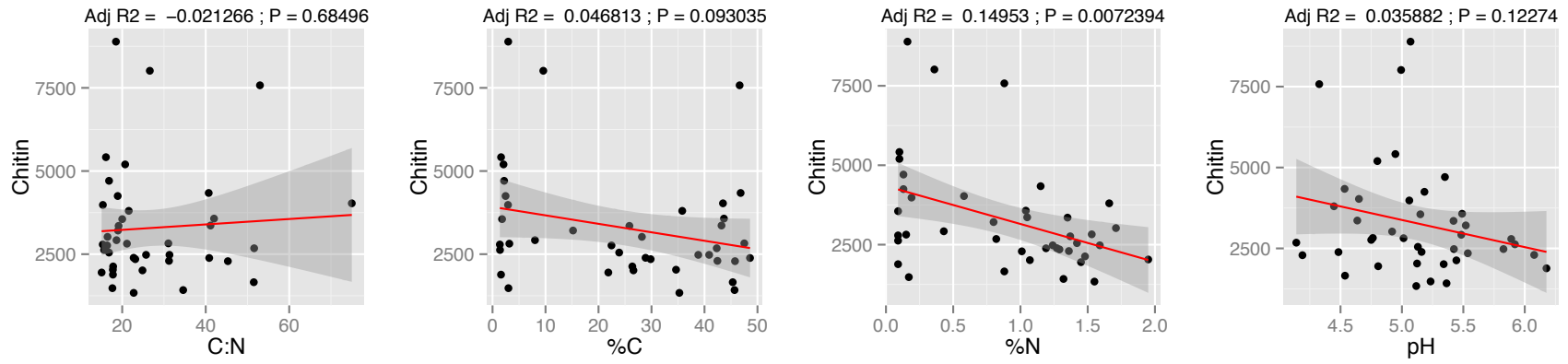
Supplementary Figure S4.6. Linear fit regression of Chloroflexi relative abundance with respect to soil C:N, %C, %N, and pH across all snow treatment sites and all soil depths ($n=41$). Shaded areas indicate 95% confidence intervals.



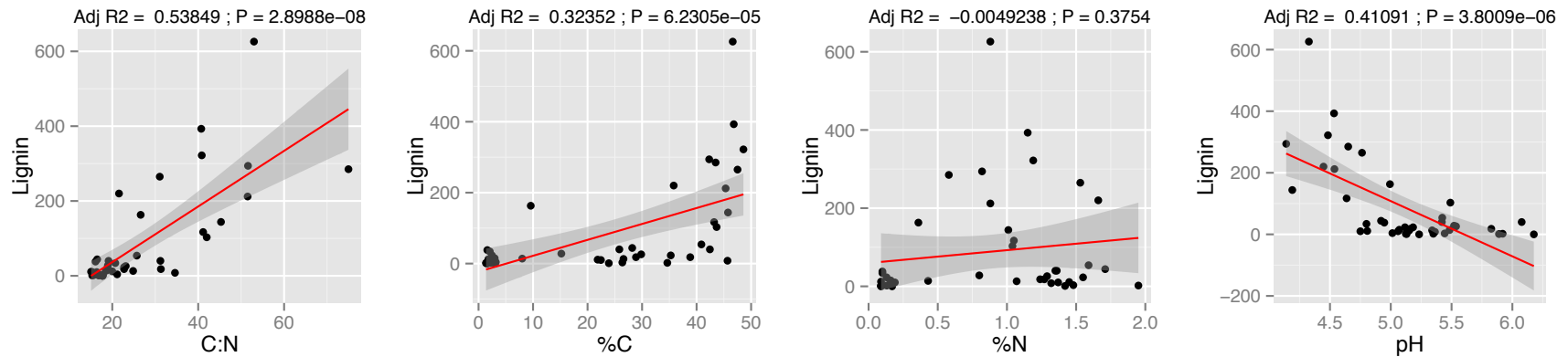
Supplementary Figure S4.7. Linear fit regression of estimated gene copy number of genes required for arabinoside degradation with respect to soil C:N, %C, %N, and pH across all snow treatment sites and all soil depths ($n=41$). Shaded areas indicate 95% confidence intervals.



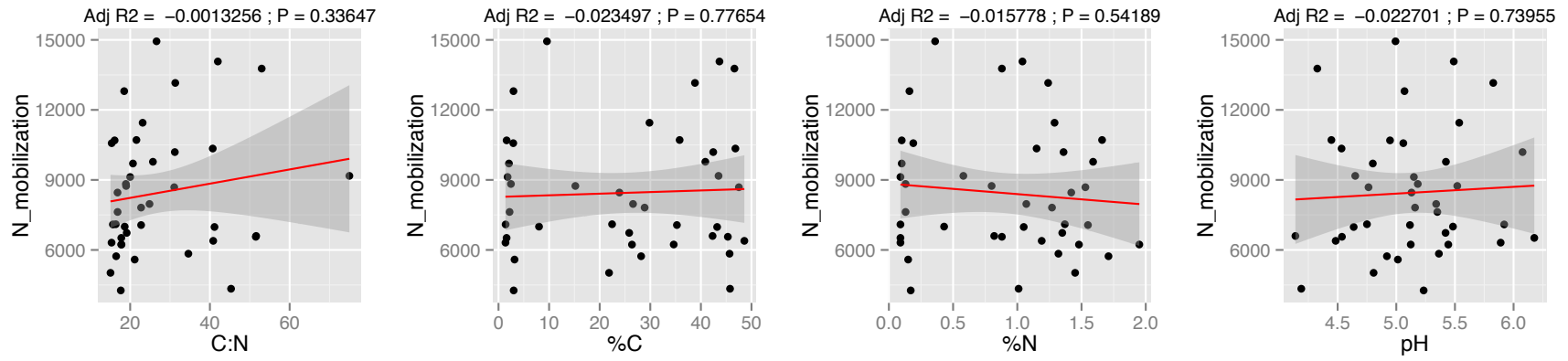
Supplementary Figure S4.8. Linear fit regression of estimated gene copy number of genes required for cellulose degradation with respect to soil C:N, %C, %N, and pH across all snow treatment sites and all soil depths ($n=41$). Shaded areas indicate 95% confidence intervals.



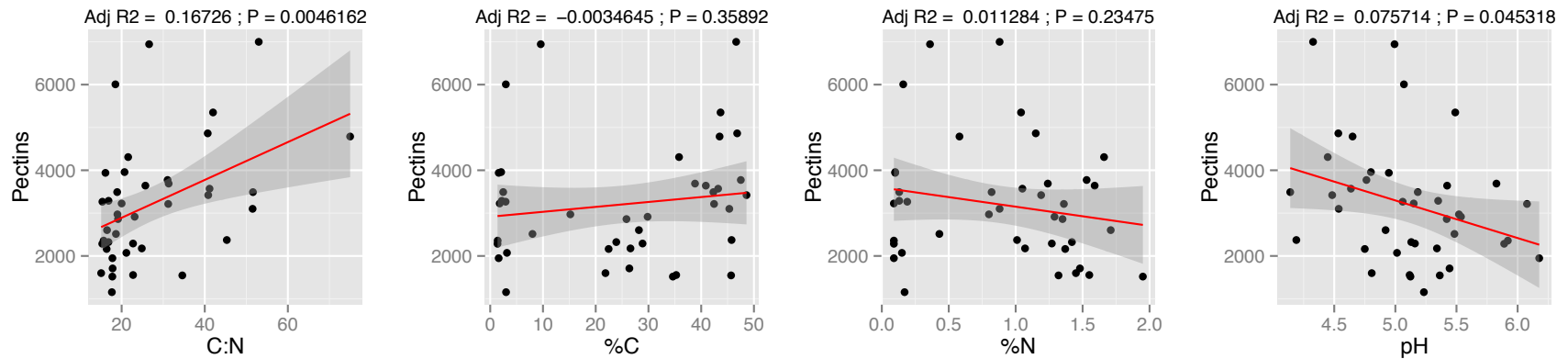
Supplementary Figure S4.9. Linear fit regression of estimated gene copy number of genes required for chitin degradation with respect to soil C:N, %C, %N, and pH across all snow treatment sites and all soil depths ($n=41$). Shaded areas indicate 95% confidence intervals.



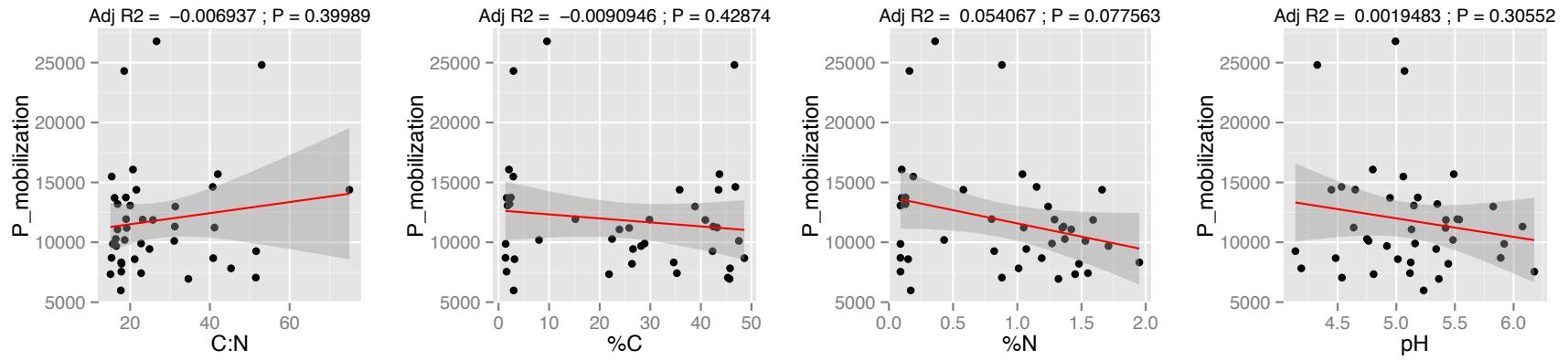
Supplementary Figure S4.10. Linear fit regression of estimated gene copy number of genes required for lignin degradation with respect to soil C:N, %C, %N, and pH across all snow treatment sites and all soil depths ($n=41$). Shaded areas indicate 95% confidence intervals.



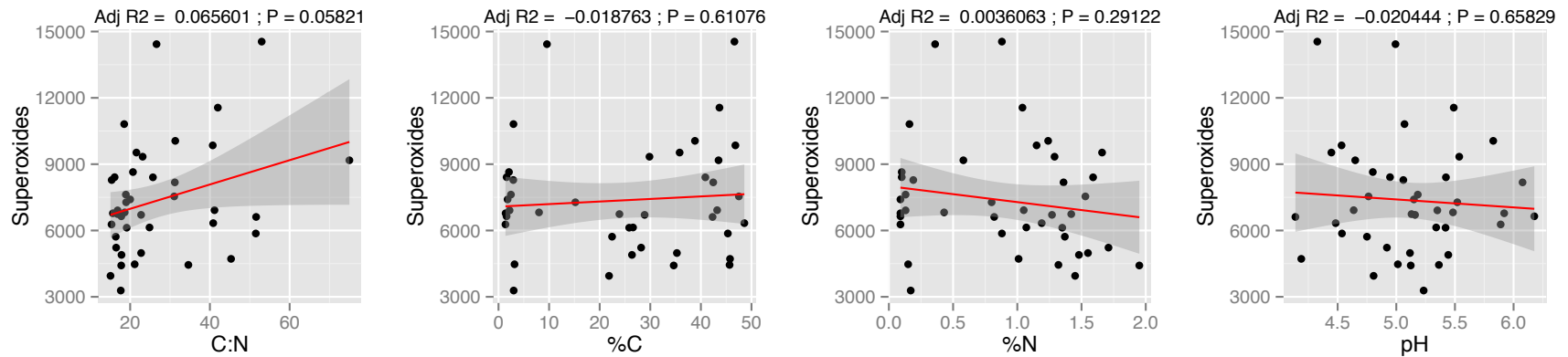
Supplementary Figure S4.11. Linear fit regression of estimated gene copy number of genes required for N mobilization with respect to soil C:N, %C, %N, and pH across all snow treatment sites and all soil depths ($n=41$). Shaded areas indicate 95% confidence intervals.



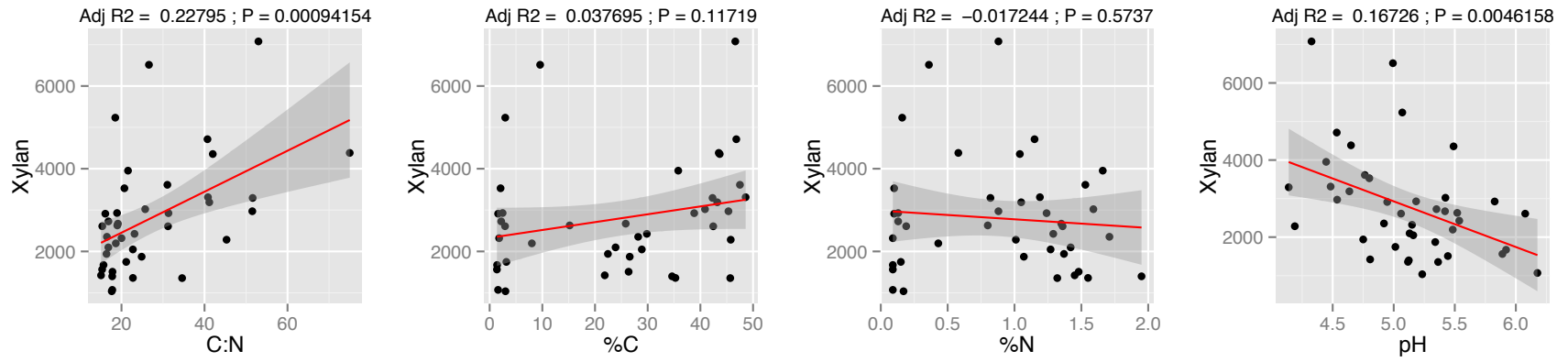
Supplementary Figure S4.12. Linear fit regression of estimated gene copy number of genes required for Pectin degradation with respect to soil C:N, %C, %N, and pH across all snow treatment sites and all soil depths ($n=41$). Shaded areas indicate 95% confidence intervals.



Supplementary Figure S4.13. Linear fit regression of estimated gene copy number of genes required for P mobilization with respect to soil C:N, %C, %N, and pH across all snow treatment sites and all soil depths ($n=41$). Shaded areas indicate 95% confidence intervals.



Supplementary Figure S4.14. Linear fit regression of estimated gene copy number of genes required for superoxide regulation with respect to soil C:N, %C, %N, and pH across all snow treatment sites and all soil depths ($n=41$). Shaded areas indicate 95% confidence intervals.



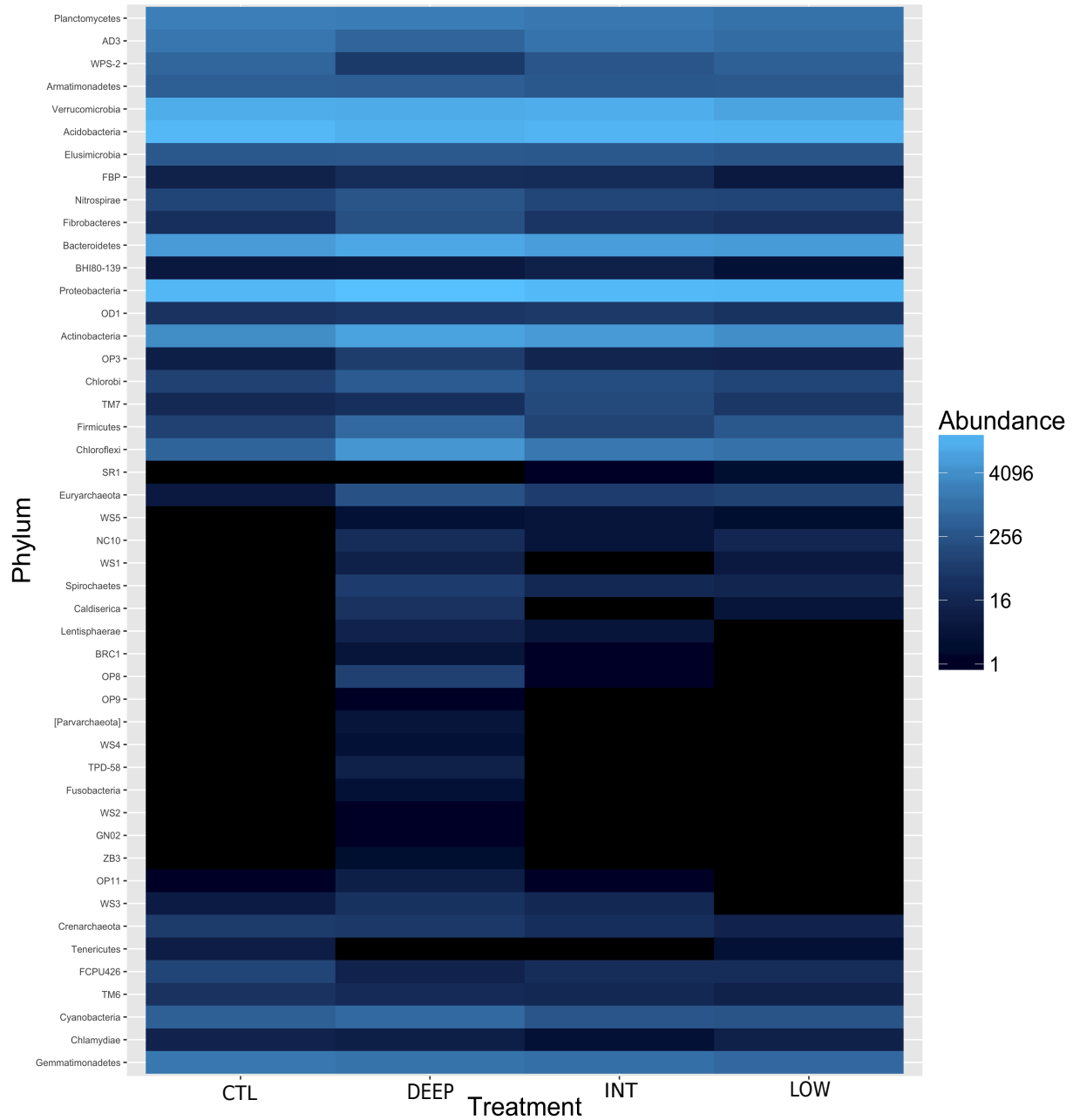
Supplementary Figure S4.15. Linear fit regression of estimated gene copy number of genes required for superoxide regulation with respect to soil C:N, %C, %N, and pH across all snow treatment sites and all soil depths ($n=41$). Shaded areas indicate 95% confidence intervals.

Supplementary Table S4.2. Effects of soil depth characteristics (Organic, Transition, Mineral) on soil chemistry, bacterial phylum relative abundance, and relative abundance of genes organized by functional groups, as determined by the Kruskal-Wallis test. Degrees of freedom=2 for all analyses. *= $p<0.05$, **= $p<0.01$, ***= $p<0.001$.

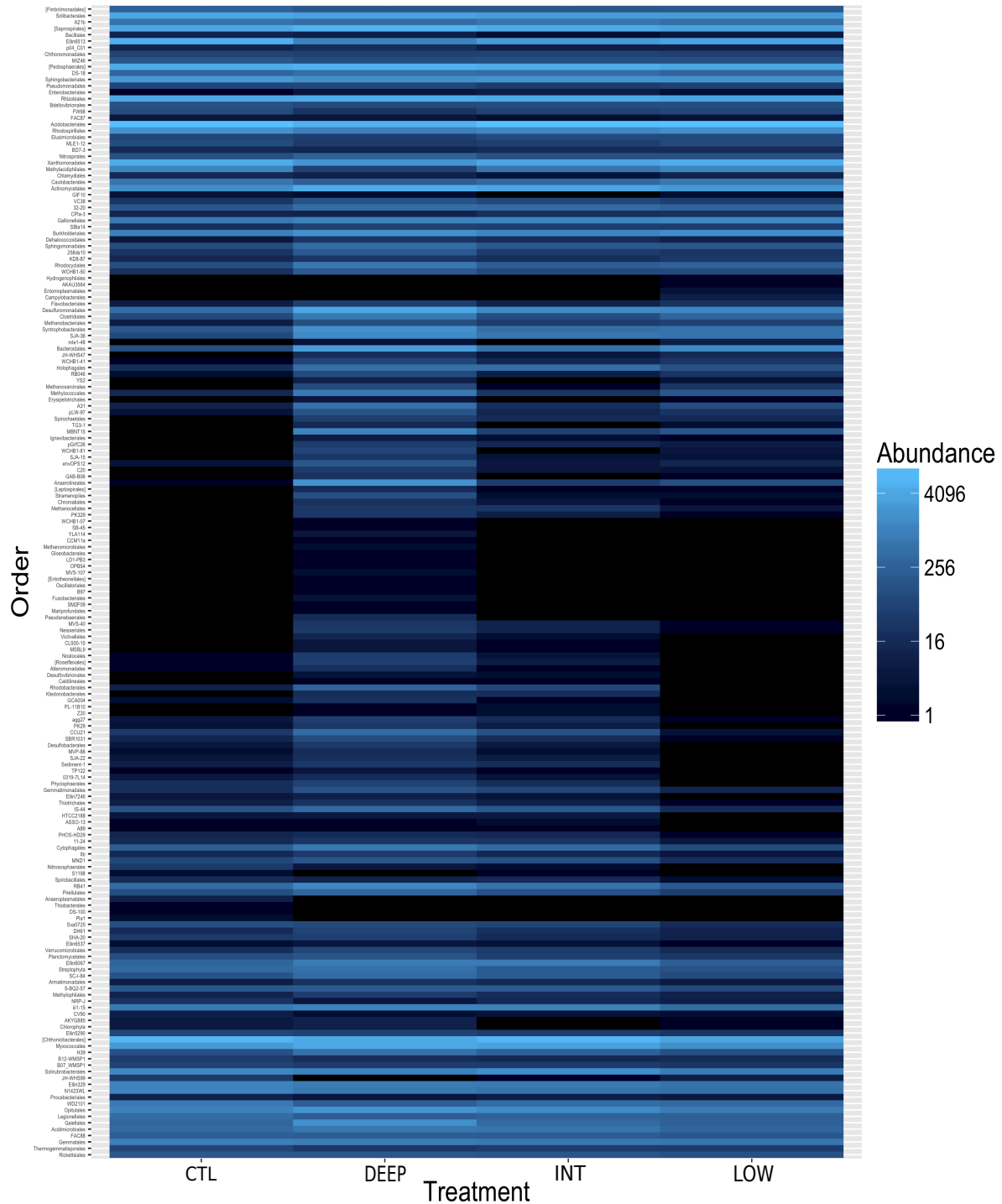
	<i>H</i> -statistic	<i>p</i> -value	Soil layer w/ highest value (Org vs. Min)
<u>Soil Chemistry</u>			
%C	32.32	9.57×10^{-8} ***	Organic
%N	26.53	1.74×10^{-6} ***	Organic
C:N	21.70	1.94×10^{-5} ***	Organic
pH	6.81	0.03 *	Mineral
<u>Bacterial phylum abundance</u>			
Acidobacteria	0.05	0.98	n/a
Proteobacteria	14.78	6.17×10^{-4} ***	Organic
Verrucomicrobia	14.93	5.73×10^{-4} ***	Organic
Actinobacteria	20.16	4.12×10^{-5} ***	Mineral
Bacteroidetes	13.08	1.45×10^{-3} **	Organic
Chloroflexi	24.80	4.13×10^{-6} ***	Mineral
<u>Enzyme gene abundance</u>			
Lignin	20.17	4.17×10^{-5} ***	Organic
Chitin	3.00	0.22	n/a
Cellulose	8.36	0.02 *	Organic
Pectin	17.25	1.80×10^{-4} ***	Organic
Xylan	15.79	3.72×10^{-4} ***	Organic
Arabinoside	13.62	1.10×10^{-3} **	Organic
N mobilization	11.67	2.92×10^{-3} **	Organic
P mobilization	3.30	0.19	n/a
Superoxide	29.61	3.72×10^{-7} ***	Organic

Supplementary Table S4.3. Statistical analyses of alpha diversity using non-parametric two-sample t-tests with 999 Monte Carlo permutations. Pairwise comparisons of Shannon diversity metrics from each sample were made between each soil layer (Organic, Transition, Mineral) and each snow accumulation treatment (Control, Deep, Intermediate, Low). $*=p<0.05$, $**=p<0.01$, $***=p<0.001$.

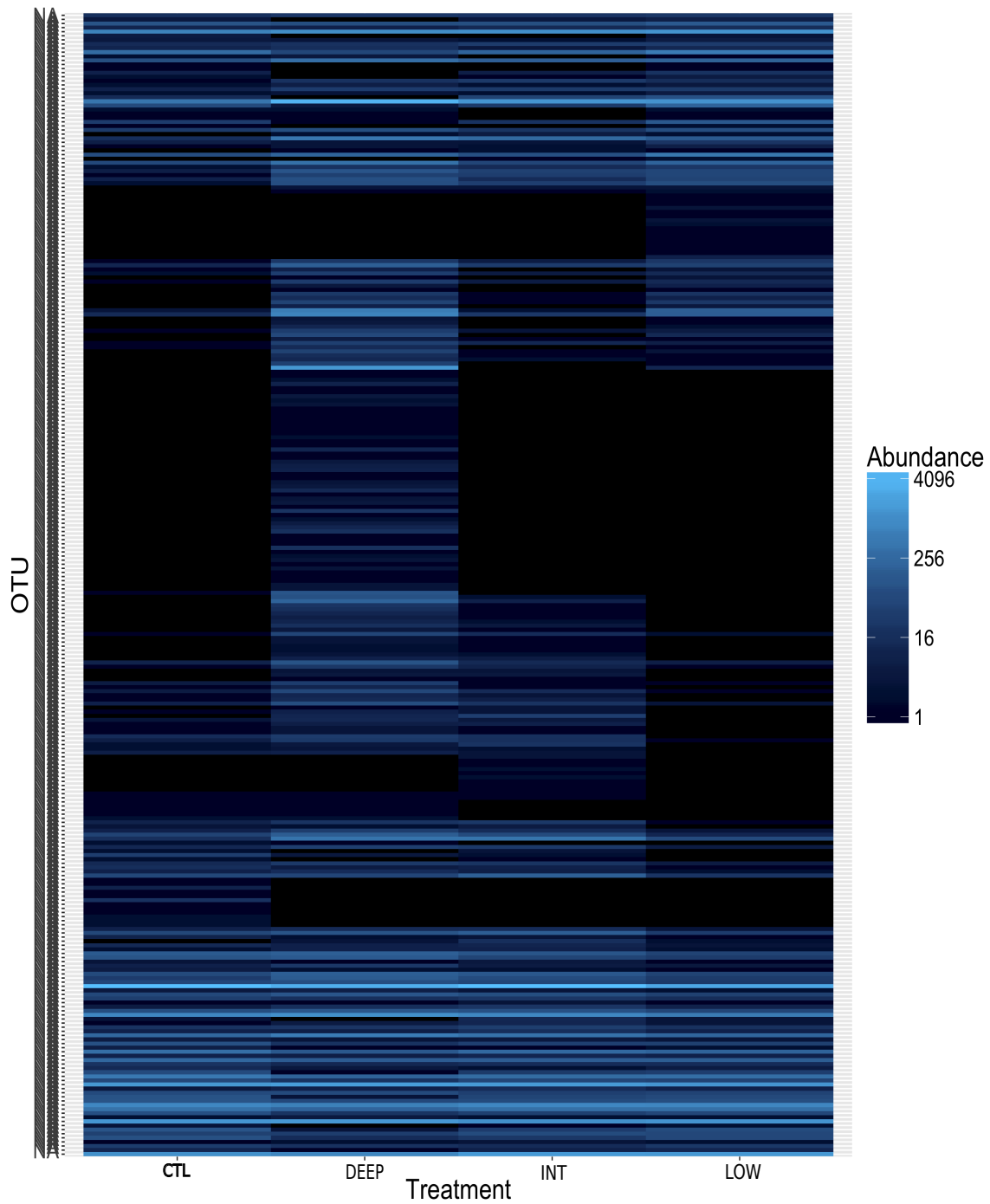
Two-sample t-tests		
Soil layers	<i>t</i> - statistic	<i>p</i> -value
Organic / Mineral	5.58	0.003 **
Trans / Organic	-0.26	1
Trans / Mineral	5.22	0.003**
Treatment		
Cont / Deep	0.30	1
Cont/ Int	-0.49	1
Cont / Low	1.70	0.6
Deep / Int	-4.0×10^{-4}	1
Deep / Low	-0.30	1
Int / Low	0.51	1



Supplementary Figure S4.16. Heatmap of raw gene abundance (# of OTU's) for all detected bacterial Phyla. Columns represent snow accumulation treatment groups, where the control = "CTL", 100% more snow accumulation = "DEEP", 50% more snow = "INT", and 25% less snow than control = "LOW".



Supplementary Figure S4.18. Heatmap of raw gene abundance (# of OTU's) for all detected bacterial Orders. Columns represent snow accumulation treatment groups, where the control =”CTL”, 100% more snow accumulation=”DEEP”, 50% more snow=”INT”, and 25% less snow than control=”LOW”.



Supplementary Figure S4.20. Heatmap of raw gene abundance (# of OTU's) for all detected bacterial OTU's. Columns represent snow accumulation treatment groups, where the control ="CTL", 100% more snow accumulation="DEEP", 50% more snow="INT", and 25% less snow than control="LOW".

7.4 Supplementary materials – Chapter 5

Supplementary Table S5.1. Manually curated list of functions, as assigned by the KEGG orthologous classification system, organized by the roles they perform in the metabolism of specific carbohydrate groups related to organic matter, methane/CO₂ metabolism, nitrogen metabolism, and phosphorus metabolism. Columns 1-4 represent the KEGG classification tiers. “EC#” represents the enzyme commission number, “CAZy” represents the classifications from the Carbohydrate Active Enzymes database, and “Role” represents the role these functions were assigned to. See Figure 5.4.

Carbohydrate catabolic processes						
<u>Level 1</u>	<u>Level 2</u>	<u>Level 3</u>	<u>Function</u>	<u>EC #</u>	<u>CAZy</u>	<u>Role</u>
Metabolism	Carbohydrate metabolism	00052 Galactose metabolism [PATH:ko00052]	E3.2.1.10; oligo-1,6-glucosidase [EC:3.2.1.10]	3.2.1.10	GH13, GH31	Starch degradation
Metabolism	Carbohydrate metabolism	00052 Galactose metabolism [PATH:ko00052]	MGAM; maltase-glucoamylase [EC:3.2.1.20 3.2.1.3]	3.2.1.20, 3.2.1.3	GH4, GH13, GH31, GH63, GH97, GH122, CBM34	Starch degradation
Metabolism	Carbohydrate metabolism	00500 Starch and sucrose metabolism [PATH:ko00500]	AGL; glycogen debranching enzyme [EC:2.4.1.25 3.2.1.33]	2.4.1.25, 3.2.1.33	CBM48, GH13	Starch degradation
Metabolism	Carbohydrate metabolism	00500 Starch and sucrose metabolism [PATH:ko00500]	E2.4.1.1, glgP, PYG; starch phosphorylase [EC:2.4.1.1]	2.4.1.1	GT35	Starch degradation
Metabolism	Carbohydrate metabolism	00500 Starch and sucrose metabolism [PATH:ko00500]	E2.4.1.20; cellobiose phosphorylase [EC:2.4.1.20]	2.4.1.20	GH94	Starch degradation
Metabolism	Carbohydrate metabolism	00500 Starch and sucrose metabolism [PATH:ko00500]	E2.4.1.4; amylosucrase [EC:2.4.1.4]	2.4.1.4	GH13	Starch degradation
Metabolism	Carbohydrate metabolism	00500 Starch and sucrose metabolism [PATH:ko00500]	E2.4.1.7; sucrose phosphorylase [EC:2.4.1.7]	2.4.1.7	GH13	Starch degradation
Metabolism	Carbohydrate metabolism	00500 Starch and sucrose metabolism [PATH:ko00500]	E2.4.1.8, mapA; maltose phosphorylase [EC:2.4.1.8]	2.4.1.8	GH65	Starch degradation
Metabolism	Carbohydrate metabolism	00500 Starch and sucrose metabolism [PATH:ko00500]	E3.2.1.1, amyA, malS; alpha-amylase [EC:3.2.1.1]	3.2.1.1	CBM20, CBM21,	Starch degradation

					CBM26, CBM41, GH13	
Metabolism	Carbohydrate metabolism	00500 Starch and sucrose metabolism [PATH:ko00500]	E3.2.1.1A; alpha-amylase [EC:3.2.1.1]	3.2.1.1	CBM20, CBM21, CBM26, CBM41, GH13	Starch degradation
Metabolism	Carbohydrate metabolism	00500 Starch and sucrose metabolism [PATH:ko00500]	E3.2.1.54; cyclomaltodextrinase [EC:3.2.1.54]	3.2.1.54	GH13, CBM34, CBM48	Starch degradation
Metabolism	Carbohydrate metabolism	00500 Starch and sucrose metabolism [PATH:ko00500]	glgB; 1,4-alpha-glucan branching enzyme [EC:2.4.1.18]	2.4.1.18	GH13, GH57, CBM48	Starch degradation
Metabolism	Carbohydrate metabolism	00500 Starch and sucrose metabolism [PATH:ko00500]	malQ; 4-alpha-glucanotransferase [EC:2.4.1.25]	2.4.1.25	GH77	Starch degradation
Metabolism	Carbohydrate metabolism	00500 Starch and sucrose metabolism [PATH:ko00500]	otsB; trehalose 6-phosphate phosphatase [EC:3.1.3.12]	3.1.3.12	GT20	Starch degradation
Metabolism	Carbohydrate metabolism	00500 Starch and sucrose metabolism [PATH:ko00500]	treC; trehalose-6-phosphate hydrolase [EC:3.2.1.93]	3.2.1.93	GH13	Starch degradation
Metabolism	Carbohydrate metabolism	00500 Starch and sucrose metabolism [PATH:ko00500]	treS; maltose alpha-D-glucosyltransferase/ alpha-amylase [EC:5.4.99.16 3.2.1.1]	5.4.99.16, 3.2.1.1	GH13	Starch degradation
Metabolism	Biosynthesis of other secondary metabolites	00940 Phenylpropanoid biosynthesis [PATH:ko00940]	bglB; beta-glucosidase [EC:3.2.1.21]	3.2.1.21	GH1, GH3, GH5 , GH9, GH30, GH116, CBM1	Cellulose degradation
Metabolism	Biosynthesis of other secondary metabolites	00940 Phenylpropanoid biosynthesis [PATH:ko00940]	bglX; beta-glucosidase [EC:3.2.1.21]	3.2.1.21	GH1, GH3, GH5 , GH9, GH30, GH116, CBM1	Cellulose degradation
Metabolism	Biosynthesis of other secondary metabolites	00940 Phenylpropanoid biosynthesis [PATH:ko00940]	E3.2.1.21; beta-glucosidase [EC:3.2.1.21]	3.2.1.21	GH1, GH3, GH5 , GH9, GH30, GH116,	Cellulose degradation

					CBM1	
Metabolism	Carbohydrate metabolism	00500 Starch and sucrose metabolism [PATH:ko00500]	E3.2.1.4; endoglucanase [EC:3.2.1.4]	3.2.1.4	GH5 , GH6, GH7, GH8, GH9, GH10, GH12, GH26, GH44, GH45, GH48, GH51, GH74, GH124, CBM1, CBM2, CBM3, CBM4, CBM5, CBM46, CBM49, CBM63, CBM72, CBM76, CBM81, +many more	Cellulose degradation
Metabolism	Carbohydrate metabolism	00500 Starch and sucrose metabolism [PATH:ko00500]	E3.2.1.91; cellulose 1,4-beta-cellobiosidase [EC:3.2.1.91]	3.2.1.91	GH5 , GH6, GH9, CBM1, CBM2, CBM3, CBM4	Cellulose degradation
Cellular Processes	Transport and catabolism	04142 Lysosome [PATH:ko04142]	E3.2.1.25, MANBA, manB; beta-mannosidase [EC:3.2.1.25]	3.2.1.25	GH1, GH2, GH5 ,	Hemicellulose degradation
Cellular Processes	Transport and catabolism	04142 Lysosome [PATH:ko04142]	E3.2.1.31, GUSB, uidA; beta-glucuronidase [EC:3.2.1.31]	3.2.1.31	GH1, GH2 , GH30, GH79, GH137, CBM57	Hemicellulose degradation
Cellular Processes	Transport and catabolism	04142 Lysosome [PATH:ko04142]	GAA; lysosomal alpha-glucosidase [EC:3.2.1.20]	3.2.1.20	GH4, GH13, GH31, GH63, GH97, GH122, CBM34	Hemicellulose degradation
Cellular	Transport and	04142 Lysosome	GLA; alpha-galactosidase	3.2.1.22	GH4, GH27,	Hemicellulose

Processes	catabolism	[PATH:ko04142]	[EC:3.2.1.22]		GH31, GH36, GH57, GH97, GH110, CBM35, CBM13	degradation
Cellular Processes	Transport and catabolism	04142 Lysosome [PATH:ko04142]	MAN2B1, LAMAN; lysosomal alpha-mannosidase [EC:3.2.1.24]	3.2.1.24	GH31, GH38, GH92	Hemicellulose degradation
Environmental Information Processing	Signal transduction	02020 Two-component system [PATH:ko02020]	sacB; levansucrase [EC:2.4.1.10]	2.4.1.10	GH68	Hemicellulose degradation
Genetic Information Processing	Folding, sorting and degradation	04141 Protein processing in endoplasmic reticulum [PATH:ko04141]	GANAB; alpha 1,3-glucosidase [EC:3.2.1.84]	3.2.1.84	GH31	Hemicellulose degradation
Genetic Information Processing	Folding, sorting and degradation	04141 Protein processing in endoplasmic reticulum [PATH:ko04141]	GCS1; mannosyl-oligosaccharide glucosidase [EC:3.2.1.106]	3.2.1.106	GH63	Hemicellulose degradation
Genetic Information Processing	Folding, sorting and degradation	04141 Protein processing in endoplasmic reticulum [PATH:ko04141]	MAN1; mannosyl-oligosaccharide alpha-1,2-mannosidase [EC:3.2.1.113]	3.2.1.113	GH38, GH47, GH92, CBM32	Hemicellulose degradation
Metabolism	Carbohydrate metabolism	00040 Pentose and glucuronate interconversions [PATH:ko00040]	E3.2.1.67; galacturan 1,4-alpha-galacturonidase [EC:3.2.1.67]	3.2.1.67	GH4, GH28	Hemicellulose degradation
Metabolism	Carbohydrate metabolism	00051 Fructose and mannose metabolism [PATH:ko00051]	algL; poly(beta-D-mannuronate) lyase [EC:4.2.2.3]	4.2.2.3	PL5, PL6, PL7, PL14, PL15, PL17, CBM32	Hemicellulose degradation
Metabolism	Carbohydrate metabolism	00051 Fructose and mannose metabolism [PATH:ko00051]	E2.4.1.-; [EC:2.4.1.-]	2.4.1.-	Many GH and GT	Hemicellulose degradation
Metabolism	Carbohydrate metabolism	00051 Fructose and mannose metabolism [PATH:ko00051]	E3.1.3.-; [EC:3.1.3.-]	3.1.3.-	GT20, CBM21	Hemicellulose degradation
Metabolism	Carbohydrate metabolism	00051 Fructose and mannose metabolism [PATH:ko00051]	E3.2.1.80; fructan beta-fructosidase [EC:3.2.1.80]	3.2.1.80	GH32, CBM38, CBM66	Hemicellulose degradation
Metabolism	Carbohydrate metabolism	00052 Galactose metabolism [PATH:ko00052]	E1.1.3.9; galactose oxidase [EC:1.1.3.9]	1.1.3.9	AA5	Hemicellulose degradation
Metabolism	Carbohydrate metabolism	00052 Galactose metabolism [PATH:ko00052]	E3.2.1.20, malZ; alpha-glucosidase [EC:3.2.1.20]	3.2.1.20	GH4, GH13, GH31, GH63,	Hemicellulose degradation

					GH97, GH122, CBM34	
Metabolism	Carbohydrate metabolism	00052 Galactose metabolism [PATH:ko00052]	E3.2.1.22B, galA, rafA; alpha-galactosidase [EC:3.2.1.22]	3.2.1.22	GH4, GH27, GH31, GH36, GH57, GH97, GH110, CBM35, CBM13	Hemicellulose degradation
Metabolism	Carbohydrate metabolism	00052 Galactose metabolism [PATH:ko00052]	E3.2.1.26, sacA; beta-fructofuranosidase [EC:3.2.1.26]	3.2.1.26	GH32, GH100, CBM38	Hemicellulose degradation
Metabolism	Carbohydrate metabolism	00052 Galactose metabolism [PATH:ko00052]	melA; alpha-galactosidase [EC:3.2.1.22]	3.2.1.22	GH4, GH27, GH31, GH36, GH57, GH97, GH110, CBM35, CBM13	Hemicellulose degradation
Metabolism	Carbohydrate metabolism	00500 Starch and sucrose metabolism [PATH:ko00500]	E3.2.1.28, treA, treF; alpha,alpha-trehalase [EC:3.2.1.28]	3.2.1.28	GH15, GH37, GH65	Hemicellulose degradation
Metabolism	Carbohydrate metabolism	00500 Starch and sucrose metabolism [PATH:ko00500]	E3.2.1.3; glucoamylase [EC:3.2.1.3]	3.2.1.3	GH15, GH97, CBM20, CBM21	Hemicellulose degradation
Metabolism	Carbohydrate metabolism	00500 Starch and sucrose metabolism [PATH:ko00500]	E3.2.1.39; glucan endo-1,3-beta-D-glucosidase [EC:3.2.1.39]	3.2.1.39	GH16, GH17, GH55, GH64, GH81, GH128, GH152, CBM6, CBM13, CBM18, CBM32, CBM43, CBM52, CBM56	Hemicellulose degradation
Metabolism	Carbohydrate metabolism	00500 Starch and sucrose metabolism [PATH:ko00500]	E3.2.1.58; glucan 1,3-beta-glucosidase [EC:3.2.1.58]	3.2.1.58	GH3, GH5 , GH17, GH55	Hemicellulose degradation

Metabolism	Carbohydrate metabolism	00500 Starch and sucrose metabolism [PATH:ko00500]	xynB; xylan 1,4-beta-xylosidase [EC:3.2.1.37]	3.2.1.37	GH1, GH3, GH30, GH39, GH43 , GH50, GH51, GH52, GH54, GH116, GH120, CBM42	Hemicellulose degradation
Metabolism	Carbohydrate metabolism	00520 Amino sugar and nucleotide sugar metabolism [PATH:ko00520]	E3.2.1.55, abfA; alpha-N-arabinofuranosidase [EC:3.2.1.55]	3.2.1.55	GH2, GH3, GH10, GH43, GH51 , GH54, GH62, GH155, CBM1, CBM6, CBM13, CBM32, CBM35, CBM42, CBM75	Hemicellulose degradation
Metabolism	Glycan biosynthesis and metabolism	00510 N-Glycan biosynthesis [PATH:ko00510]	MAN2; alpha-mannosidase II [EC:3.2.1.114]	3.2.1.114	GH38, GH92	Hemicellulose degradation
Metabolism	Glycan biosynthesis and metabolism	00511 Other glycan degradation [PATH:ko00511]	E3.2.1.24; alpha-mannosidase [EC:3.2.1.24]	3.2.1.24	GH31, GH38, GH92	Hemicellulose degradation
Metabolism	Glycan biosynthesis and metabolism	00511 Other glycan degradation [PATH:ko00511]	FUCA; alpha-L-fucosidase [EC:3.2.1.51]	3.2.1.51	GH29, GH141	Hemicellulose degradation
Cellular Processes	Transport and catabolism	04142 Lysosome [PATH:ko04142]	GLB1, ELNR1; beta-galactosidase [EC:3.2.1.23]	3.2.1.23	GH1, GH2, GH 35, GH42, GH59, GH147, CBM71	Pectin degradation
Metabolism	Carbohydrate metabolism	00010 Glycolysis / Gluconeogenesis [PATH:ko00010]	E3.2.1.86A, celF; 6-phospho-beta-glucosidase [EC:3.2.1.86]	3.2.1.86	GH1, GH4	Pectin degradation
Metabolism	Carbohydrate	00010 Glycolysis /	E3.2.1.86B, bglA; 6-phospho-	3.2.1.86	GH1, GH4	Pectin degradation

	metabolism	Gluconeogenesis [PATH:ko00010]	beta-glucosidase [EC:3.2.1.86]			
Metabolism	Carbohydrate metabolism	00040 Pentose and glucuronate interconversions [PATH:ko00040]	E3.1.1.11; pectinesterase [EC:3.1.1.11]	3.1.1.11	CE8	Pectin degradation
Metabolism	Carbohydrate metabolism	00040 Pentose and glucuronate interconversions [PATH:ko00040]	E3.2.1.15; polygalacturonase [EC:3.2.1.15]	3.2.1.15	GH28	Pectin degradation
Metabolism	Carbohydrate metabolism	00040 Pentose and glucuronate interconversions [PATH:ko00040]	E4.2.2.2, pel; pectate lyase [EC:4.2.2.2]	4.2.2.2	PL1, PL2, PL3, PL9, PL10, CBM2, CBM13, CBM35, CBM66	Pectin degradation
Metabolism	Carbohydrate metabolism	00040 Pentose and glucuronate interconversions [PATH:ko00040]	E4.2.2.6; oligogalacturonide lyase [EC:4.2.2.6]	4.2.2.6	PL22	Pectin degradation
Metabolism	Carbohydrate metabolism	00052 Galactose metabolism [PATH:ko00052]	bgaB, lacA; beta-galactosidase [EC:3.2.1.23]	3.2.1.23	GH2, GH 35, GH42	Pectin degradation
Metabolism	Carbohydrate metabolism	00052 Galactose metabolism [PATH:ko00052]	E3.2.1.85, lacG; 6-phospho-beta-galactosidase [EC:3.2.1.85]	3.2.1.85	GH1	Pectin degradation
Metabolism	Carbohydrate metabolism	00052 Galactose metabolism [PATH:ko00052]	ebgA; evolved beta-galactosidase subunit alpha [EC:3.2.1.23]	3.2.1.23	GH2	Pectin degradation
Metabolism	Carbohydrate metabolism	00052 Galactose metabolism [PATH:ko00052]	lacZ; beta-galactosidase [EC:3.2.1.23]	3.2.1.23	GH2, GH42	Pectin degradation
Metabolism	Carbohydrate metabolism	00052 Galactose metabolism [PATH:ko00052]	LCT; lactase-phlorizin hydrolase [EC:3.2.1.108 3.2.1.62]	3.2.1.108 3.2.1.62	GH1	Pectin degradation
Cellular Processes	Transport and catabolism	04142 Lysosome [PATH:ko04142]	E3.2.1.45, GBA, srfJ; glucosylceramidase [EC:3.2.1.45]	3.2.1.45	GH3, GH5 , GH30, GH116	Peptidoglycan / Chitin degradation
Cellular Processes	Transport and catabolism	04142 Lysosome [PATH:ko04142]	GALC; galactosylceramidase [EC:3.2.1.46]	3.2.1.46	GH59	Peptidoglycan / Chitin degradation
Cellular Processes	Transport and catabolism	04142 Lysosome [PATH:ko04142]	HEXA_B; hexosaminidase [EC:3.2.1.52]	3.2.1.52	GH3, GH18, GH20 , GH84, CBM32	Peptidoglycan / Chitin degradation

Cellular Processes	Transport and catabolism	04142 Lysosome [PATH:ko04142]	NAGA; alpha-N-acetylgalactosaminidase [EC:3.2.1.49]	3.2.1.49	GH27, GH36, GH109, GH129, CBM13	Peptidoglycan / Chitin degradation
Cellular Processes	Transport and catabolism	04142 Lysosome [PATH:ko04142]	NAGLU; alpha-N-acetylglucosaminidase [EC:3.2.1.50]	3.2.1.50	GH89, CBM32	Peptidoglycan / Chitin degradation
Metabolism	Carbohydrate metabolism	00520 Amino sugar and nucleotide sugar metabolism [PATH:ko00520]	csn; chitosanase [EC:3.2.1.132]	3.2.1.132	GH8, GH46	Peptidoglycan / Chitin degradation
Metabolism	Carbohydrate metabolism	00520 Amino sugar and nucleotide sugar metabolism [PATH:ko00520]	E3.2.1.52, nagZ; beta-N-acetylhexosaminidase [EC:3.2.1.52]	3.2.1.52	GH3, GH18, GH20 , GH84, CBM32	Peptidoglycan / Chitin degradation
Metabolism	Carbohydrate metabolism	00520 Amino sugar and nucleotide sugar metabolism [PATH:ko00520]	E3.5.1.25, nagA, AMDHD2; N-acetylglucosamine-6-phosphate deacetylase [EC:3.5.1.25]	3.5.1.25	CE9	Peptidoglycan / Chitin degradation
Metabolism	Carbohydrate metabolism	00520 Amino sugar and nucleotide sugar metabolism [PATH:ko00520]	E3.5.1.41; chitin deacetylase [EC:3.5.1.41]	3.5.1.41	CE4	Peptidoglycan / Chitin degradation
Metabolism	Glycan biosynthesis and metabolism	00540 Lipopolysaccharide biosynthesis [PATH:ko00540]	lpxC; UDP-3-O-[3-hydroxymyristoyl] N-acetylglucosamine deacetylase [EC:3.5.1.108]	3.5.1.108	CE11	Peptidoglycan / Chitin degradation
Metabolism	Glycan biosynthesis and metabolism	00563 Glycosylphosphatidylinositol (GPI)-anchor biosynthesis [PATH:ko00563]	PIGL; N-acetylglucosaminylphosphatidylinositol deacetylase [EC:3.5.1.89]	3.5.1.89	CE14	Peptidoglycan / Chitin degradation

Carbohydrate anabolic processes

<u>Level 1</u>	<u>Level 2</u>	<u>Level 3</u>	<u>Function</u>	<u>EC #</u>	<u>CAZy</u>	<u>Role</u>
Environmental Information Processing	Signal transduction	04151 PI3K-Akt signaling pathway [PATH:ko04151]	GYS; glycogen(starch) synthase [EC:2.4.1.11]	2.4.1.11	GT3	Starch biosynthesis
Metabolism	Carbohydrate metabolism	00500 Starch and sucrose metabolism [PATH:ko00500]	E2.4.1.21, glgA; starch synthase [EC:2.4.1.21]	2.4.1.21	GT4	Starch biosynthesis

Metabolism	Carbohydrate metabolism	00500 Starch and sucrose metabolism [PATH:ko00500]	otsA; trehalose 6-phosphate synthase [EC:2.4.1.15]	2.4.1.15	GT20	Starch biosynthesis
Metabolism	Carbohydrate metabolism	00500 Starch and sucrose metabolism [PATH:ko00500]	bcsA; cellulose synthase (UDP-forming) [EC:2.4.1.12]	2.4.1.12	GT2	Cellulose biosynthesis
Genetic Information Processing	Folding, sorting and degradation	04141 Protein processing in endoplasmic reticulum [PATH:ko04141]	HUGT; UDP-glucose:glycoprotein glucosyltransferase [EC:2.4.1.-]	2.4.1.-	GT24	Hemicellulose biosynthesis
Metabolism	Carbohydrate metabolism	00051 Fructose and mannose metabolism [PATH:ko00051]	E2.4.1.217; mannosyl-3-phosphoglycerate synthase [EC:2.4.1.217]	2.4.1.217	GT55, GT78, GT81	Hemicellulose biosynthesis
Metabolism	Carbohydrate metabolism	00500 Starch and sucrose metabolism [PATH:ko00500]	E2.4.1.13; sucrose synthase [EC:2.4.1.13]	2.4.1.13	GT4	Hemicellulose biosynthesis
Metabolism	Carbohydrate metabolism	00500 Starch and sucrose metabolism [PATH:ko00500]	E2.4.1.14; sucrose-phosphate synthase [EC:2.4.1.14]	2.4.1.14	GT4	Hemicellulose biosynthesis
Metabolism	Carbohydrate metabolism	00500 Starch and sucrose metabolism [PATH:ko00500]	E2.4.1.34; 1,3-beta-glucan synthase [EC:2.4.1.34]	2.4.1.34	GT48	Hemicellulose biosynthesis
Metabolism	Glycan biosynthesis and metabolism	00510 N-Glycan biosynthesis [PATH:ko00510]	ALG1; beta-1,4-mannosyltransferase [EC:2.4.1.142]	2.4.1.142	GT33	Hemicellulose biosynthesis
Metabolism	Glycan biosynthesis and metabolism	00510 N-Glycan biosynthesis [PATH:ko00510]	ALG10; alpha-1,2-glucosyltransferase [EC:2.4.1.256]	2.4.1.256	GT59	Hemicellulose biosynthesis
Metabolism	Glycan biosynthesis and metabolism	00510 N-Glycan biosynthesis [PATH:ko00510]	ALG11; alpha-1,2-mannosyltransferase [EC:2.4.1.-]	2.4.1.-	GT83	Hemicellulose biosynthesis
Metabolism	Glycan biosynthesis and metabolism	00510 N-Glycan biosynthesis [PATH:ko00510]	ALG12; alpha-1,6-mannosyltransferase [EC:2.4.1.260]	2.4.1.260	GT22	Hemicellulose biosynthesis
Metabolism	Glycan biosynthesis and metabolism	00510 N-Glycan biosynthesis [PATH:ko00510]	ALG2; alpha-1,3/alpha-1,6-mannosyltransferase [EC:2.4.1.132 2.4.1.257]	2.4.1.132 2.4.1.257	GT4	Hemicellulose biosynthesis
Metabolism	Glycan biosynthesis and metabolism	00510 N-Glycan biosynthesis [PATH:ko00510]	ALG3; alpha-1,3-mannosyltransferase [EC:2.4.1.258]	2.4.1.258	GT58	Hemicellulose biosynthesis
Metabolism	Glycan biosynthesis and metabolism	00510 N-Glycan biosynthesis [PATH:ko00510]	ALG5; dolichyl-phosphate beta-glucosyltransferase [EC:2.4.1.117]	2.4.1.117	GT2	Hemicellulose biosynthesis
Metabolism	Glycan	00510 N-Glycan biosynthesis	ALG6; alpha-1,3-	2.4.1.267	GT57	Hemicellulose

	biosynthesis and metabolism	[PATH:ko00510]	glucosyltransferase [EC:2.4.1.267]			biosynthesis
Metabolism	Glycan biosynthesis and metabolism	00510 N-Glycan biosynthesis [PATH:ko00510]	ALG8; alpha-1,3-glucosyltransferase [EC:2.4.1.265]	2.4.1.265	GT57	Hemicellulose biosynthesis
Metabolism	Glycan biosynthesis and metabolism	00510 N-Glycan biosynthesis [PATH:ko00510]	ALG9; alpha-1,2-mannosyltransferase [EC:2.4.1.259 2.4.1.261]	2.4.1.259, 2.4.1.261	GT22	Hemicellulose biosynthesis
Metabolism	Glycan biosynthesis and metabolism	00510 N-Glycan biosynthesis [PATH:ko00510]	DPM1; dolichol-phosphate mannosyltransferase [EC:2.4.1.83]	2.4.1.83	GT2	Hemicellulose biosynthesis
Metabolism	Glycan biosynthesis and metabolism	00513 Various types of N-glycan biosynthesis [PATH:ko00513]	MNN2; alpha 1,2-mannosyltransferase [EC:2.4.1.-]	2.4.1.-	GT71	Hemicellulose biosynthesis
Metabolism	Glycan biosynthesis and metabolism	00513 Various types of N-glycan biosynthesis [PATH:ko00513]	MNN9; mannan polymerase complexes MNN9 subunit [EC:2.4.1.-]	2.4.1.-	GT62	Hemicellulose biosynthesis
Metabolism	Glycan biosynthesis and metabolism	00513 Various types of N-glycan biosynthesis [PATH:ko00513]	OCH1; alpha 1,6-mannosyltransferase [EC:2.4.1.232]	2.4.1.232	GT32	Hemicellulose biosynthesis
Metabolism	Glycan biosynthesis and metabolism	00514 Other types of O-glycan biosynthesis [PATH:ko00514]	POFUT; peptide-O-fucosyltransferase [EC:2.4.1.221]	2.4.1.221	GT65	Hemicellulose biosynthesis
Metabolism	Glycan biosynthesis and metabolism	00514 Other types of O-glycan biosynthesis [PATH:ko00514]	POMT; dolichyl-phosphate-mannose-protein mannosyltransferase [EC:2.4.1.109]	2.4.1.109	GT39	Hemicellulose biosynthesis
Metabolism	Glycan biosynthesis and metabolism	00540 Lipopolysaccharide biosynthesis [PATH:ko00540]	lpxB; lipid-A-disaccharide synthase [EC:2.4.1.182]	2.4.1.182	GT19	Hemicellulose biosynthesis
Metabolism	Glycan biosynthesis and metabolism	00540 Lipopolysaccharide biosynthesis [PATH:ko00540]	waaG, rfaG; UDP-glucose:(heptosyl)LPS alpha-1,3-glucosyltransferase [EC:2.4.1.-]	2.4.1.-	GT4	Hemicellulose biosynthesis
Metabolism	Glycan biosynthesis and metabolism	00563 Glycosylphosphatidylinositol (GPI)-anchor biosynthesis [PATH:ko00563]	PIGB; phosphatidylinositol glycan, class B [EC:2.4.1.-]	2.4.1.-	GT22	Hemicellulose biosynthesis

Metabolism	Glycan biosynthesis and metabolism	00563 Glycosylphosphatidylinositol (GPI)-anchor biosynthesis [PATH:ko00563]	PIGM; phosphatidylinositol glycan, class M [EC:2.4.1.-]	2.4.1.-	GT35	Hemicellulose biosynthesis
Metabolism	Glycan biosynthesis and metabolism	00563 Glycosylphosphatidylinositol (GPI)-anchor biosynthesis [PATH:ko00563]	PIGZ, SMP3; phosphatidylinositol glycan, class Z [EC:2.4.1.-]	2.4.1.-	GT22	Hemicellulose biosynthesis
Metabolism	Lipid metabolism	00561 Glycerolipid metabolism [PATH:ko00561]	DGAT1; diacylglycerol O-acyltransferase 1 [EC:2.3.1.20 2.3.1.75 2.3.1.76]	2.3.1.20, 2.3.1.75, 2.3.1.76	CE1	Hemicellulose biosynthesis
Metabolism	Lipid metabolism	00561 Glycerolipid metabolism [PATH:ko00561]	E2.3.1.20; diacylglycerol O-acyltransferase [EC:2.3.1.20]	2.3.1.20	CE1	Hemicellulose biosynthesis
Metabolism	Lipid metabolism	00561 Glycerolipid metabolism [PATH:ko00561]	E2.4.1.46; 1,2-diacylglycerol 3-beta-galactosyltransferase [EC:2.4.1.46]	2.4.1.46	GT28	Hemicellulose biosynthesis
Metabolism	Lipid metabolism	00561 Glycerolipid metabolism [PATH:ko00561]	ugtP; 1,2-diacylglycerol 3-glucosyltransferase [EC:2.4.1.157]	2.4.1.157	GT28	Hemicellulose biosynthesis
Cellular Processes	Cell growth and death	04112 Cell cycle - Caulobacter [PATH:ko04112]	murG; UDP-N-acetylglucosamine--N-acetylmuramyl-(pentapeptide) pyrophosphoryl-undecaprenol N-acetylglucosamine transferase [EC:2.4.1.227]	2.4.1.227	GT28	Peptidoglycan biosynthesis
Metabolism	Biosynthesis of other secondary metabolites	00311 Penicillin and cephalosporin biosynthesis [PATH:ko00311]	E3.1.1.41; cephalosporin-C deacetylase [EC:3.1.1.41]	3.1.1.41	CE7	Peptidoglycan biosynthesis
Metabolism	Glycan biosynthesis and metabolism	00550 Peptidoglycan biosynthesis [PATH:ko00550]	E2.4.1.129; peptidoglycan glycosyltransferase [EC:2.4.1.129]	2.4.1.129	GT51	Peptidoglycan biosynthesis
Metabolism	Glycan biosynthesis and metabolism	00550 Peptidoglycan biosynthesis [PATH:ko00550]	ftsI; cell division protein FtsI (penicillin-binding protein 3) [EC:2.4.1.129]	2.4.1.129	GT51	Peptidoglycan biosynthesis
Metabolism	Glycan biosynthesis and metabolism	00550 Peptidoglycan biosynthesis [PATH:ko00550]	mrcA; penicillin-binding protein 1A [EC:2.4.1.- 3.4.-.-]	2.4.1.-, 3.4.-.-	GT51	Peptidoglycan biosynthesis
Metabolism	Glycan	00550 Peptidoglycan	mrcB; penicillin-binding	2.4.1.129,	GT51	Peptidoglycan

	biosynthesis and metabolism	biosynthesis [PATH:ko00550]	protein 1B [EC:2.4.1.129 3.4.-.- 3.4.-.-]			biosynthesis
Metabolism	Glycan biosynthesis and metabolism	00550 Peptidoglycan biosynthesis [PATH:ko00550]	mtgA; monofunctional biosynthetic peptidoglycan transglycosylase [EC:2.4.1.-]	2.4.1.-	GT51	Peptidoglycan biosynthesis
Metabolism	Glycan biosynthesis and metabolism	00550 Peptidoglycan biosynthesis [PATH:ko00550]	pbp2A; penicillin-binding protein 2A [EC:2.4.1.129 2.3.2.-]	2.4.1.129, 2.3.2.-	GT51	Peptidoglycan biosynthesis
Metabolism	Carbohydrate metabolism	00520 Amino sugar and nucleotide sugar metabolism [PATH:ko00520]	CHS1; chitin synthase [EC:2.4.1.16]	2.4.1.16	GT2	Chitin biosynthesis
Metabolism	Glycan biosynthesis and metabolism	00510 N-Glycan biosynthesis [PATH:ko00510]	MGAT1; alpha-1,3-mannosyl-glycoprotein beta-1,2-N-acetylglucosaminyltransferase [EC:2.4.1.101]	2.4.1.101	GT13	Chitin biosynthesis
Metabolism	Glycan biosynthesis and metabolism	00510 N-Glycan biosynthesis [PATH:ko00510]	MGAT3; beta-1,4-mannosyl-glycoprotein beta-1,4-N-acetylglucosaminyltransferase [EC:2.4.1.144]	2.4.1.144	GT17	Chitin biosynthesis
Metabolism	Glycan biosynthesis and metabolism	00512 Mucin type O-glycan biosynthesis [PATH:ko00512]	C1GALT1; glycoprotein-N-acetylgalactosamine 3-beta-galactosyltransferase [EC:2.4.1.122]	2.4.1.122	GT31	Chitin biosynthesis
Metabolism	Glycan biosynthesis and metabolism	00534 Glycosaminoglycan biosynthesis - heparan sulfate / heparin [PATH:ko00534]	EXTL3; alpha-1,4-N-acetylglucosaminyltransferase EXTL3 [EC:2.4.1.223 2.4.1.224]	2.4.1.223, 2.4.1.224	GT47, GT64	Chitin biosynthesis

Methane / CO2 metabolism

Level 1	Level 2	Level 3	Function	EC #	CAZy	Role
Metabolism	Energy metabolism	00680 Methane metabolism [PATH:ko00680]	cdhE; acetyl-CoA decarboxylase/synthase complex subunit gamma [EC:2.1.1.245]	2.1.1.245		Methanogenesis
Metabolism	Energy metabolism	00680 Methane metabolism [PATH:ko00680]	CODH-ACSA; carbon monoxide dehydrogenase / acetyl-CoA synthase subunit	1.2.7.4, 1.2.99.2, 2.3.1.169		Methanogenesis

			alpha [EC:1.2.7.4 1.2.99.2 2.3.1.169]		
Metabolism	Energy metabolism	00680 Methane metabolism [PATH:ko00680]	E1.2.99.2C, cooS; carbon-monoxide dehydrogenase catalytic subunit [EC:1.2.99.2]	1.2.99.2	Methanogenesis
Metabolism	Energy metabolism	00680 Methane metabolism [PATH:ko00680]	E1.2.99.2L, cutL, coxL; carbon-monoxide dehydrogenase large subunit [EC:1.2.99.2]	1.2.99.2	Methanogenesis
Metabolism	Energy metabolism	00680 Methane metabolism [PATH:ko00680]	E1.2.99.2M, cutM, coxM; carbon-monoxide dehydrogenase medium subunit [EC:1.2.99.2]	1.2.99.2	Methanogenesis
Metabolism	Energy metabolism	00680 Methane metabolism [PATH:ko00680]	E1.2.99.2S, coxS; carbon-monoxide dehydrogenase small subunit [EC:1.2.99.2]	1.2.99.2	Methanogenesis
Metabolism	Energy metabolism	00680 Methane metabolism [PATH:ko00680]	E1.2.99.5A, fwdA, fmdA; formylmethanofuran dehydrogenase subunit A [EC:1.2.99.5]	1.2.99.5	Methanogenesis
Metabolism	Energy metabolism	00680 Methane metabolism [PATH:ko00680]	E1.2.99.5B, fwdB, fmdB; formylmethanofuran dehydrogenase subunit B [EC:1.2.99.5]	1.2.99.5	Methanogenesis
Metabolism	Energy metabolism	00680 Methane metabolism [PATH:ko00680]	E1.2.99.5C, fwdC, fmdC; formylmethanofuran dehydrogenase subunit C [EC:1.2.99.5]	1.2.99.5	Methanogenesis
Metabolism	Energy metabolism	00680 Methane metabolism [PATH:ko00680]	E1.2.99.5E, fmdE; formylmethanofuran dehydrogenase subunit E [EC:1.2.99.5]	1.2.99.5	Methanogenesis
Metabolism	Energy metabolism	00680 Methane metabolism [PATH:ko00680]	E1.5.1.20, metF; methylenetetrahydrofolate reductase (NADPH) [EC:1.5.1.20]	1.5.1.20	Methanogenesis
Metabolism	Energy metabolism	00680 Methane metabolism [PATH:ko00680]	E1.5.8.2; trimethylamine dehydrogenase [EC:1.5.8.2]	1.5.8.2	Methanogenesis

Metabolism	Energy metabolism	00680 Methane metabolism [PATH:ko00680]	E2.3.1.101, ftr; formylmethanofuran--tetrahydromethanopterin N-formyltransferase [EC:2.3.1.101]	2.3.1.101	Methanogenesis
Metabolism	Energy metabolism	00680 Methane metabolism [PATH:ko00680]	E3.1.3.71, comB; 2-phosphosulfolactate phosphatase [EC:3.1.3.71]	3.1.3.71	Methanogenesis
Metabolism	Energy metabolism	00680 Methane metabolism [PATH:ko00680]	E4.4.1.19, comA; phosphosulfolactate synthase [EC:4.4.1.19]	4.4.1.19	Methanogenesis
Metabolism	Energy metabolism	00680 Methane metabolism [PATH:ko00680]	ehbQ; energy-converting hydrogenase B subunit Q		Methanogenesis
Metabolism	Energy metabolism	00680 Methane metabolism [PATH:ko00680]	frhB; coenzyme F420 hydrogenase beta subunit [EC:1.12.98.1]	1.12.98.1	Methanogenesis
Metabolism	Energy metabolism	00680 Methane metabolism [PATH:ko00680]	hdrA; heterodisulfide reductase subunit A [EC:1.8.98.1]	1.8.98.1	Methanogenesis
Metabolism	Energy metabolism	00680 Methane metabolism [PATH:ko00680]	hdrB; heterodisulfide reductase subunit B [EC:1.8.98.1]	1.8.98.1	Methanogenesis
Metabolism	Energy metabolism	00680 Methane metabolism [PATH:ko00680]	K06034, comD; sulfopyruvate decarboxylase subunit alpha [EC:4.1.1.79]	4.1.1.79	Methanogenesis
Metabolism	Energy metabolism	00680 Methane metabolism [PATH:ko00680]	K13039, comE; sulfopyruvate decarboxylase subunit beta [EC:4.1.1.79]	4.1.1.79	Methanogenesis
Metabolism	Energy metabolism	00680 Methane metabolism [PATH:ko00680]	mer; coenzyme F420-dependent N5,N10-methenyltetrahydromethanopterin reductase [EC:1.5.99.11]	1.5.99.11	Methanogenesis
Metabolism	Energy metabolism	00680 Methane metabolism [PATH:ko00680]	mtdB; methylene-tetrahydromethanopterin dehydrogenase [EC:1.5.1.-]	1.5.1.-	Methanogenesis
Metabolism	Energy metabolism	00680 Methane metabolism [PATH:ko00680]	mttB; trimethylamine---corrinoide protein Co-methyltransferase [EC:2.1.1.250]	2.1.1.250	Methanogenesis
Metabolism	Energy	00680 Methane metabolism	mttC; trimethylamine corrinoide protein		Methanogenesis

	metabolism	[PATH:ko00680]			
Metabolism	Energy metabolism	00680 Methane metabolism [PATH:ko00680]	mvhA, vhuA, vhcA; F420-non-reducing hydrogenase subunit A [EC:1.12.99.-]	1.12.99.-	Methanogenesis
Metabolism	Energy metabolism	00680 Methane metabolism [PATH:ko00680]	nhaA; Na+:H+ antiporter, NhaA family		Methanogenesis
Metabolism	Energy metabolism	00680 Methane metabolism [PATH:ko00680]	nhaB; Na+:H+ antiporter, NhaB family		Methanogenesis
Metabolism	Energy metabolism	00680 Methane metabolism [PATH:ko00680]	nhaC; Na+:H+ antiporter, NhaC family		Methanogenesis
Metabolism	Energy metabolism	00680 Methane metabolism [PATH:ko00680]	E1.14.13.8; dimethylaniline monooxygenase (N-oxide forming) [EC:1.14.13.8]	1.14.13.8	Methanogenesis
Metabolism	Energy metabolism	00680 Methane metabolism [PATH:ko00680]	mch; methenyltetrahydromethanopterin cyclohydrolase [EC:3.5.4.27]	3.5.4.27	Methanogenesis
Metabolism	Energy metabolism	00680 Methane metabolism [PATH:ko00680]	E2.7.1.29, DAK1, DAK2; dihydroxyacetone kinase [EC:2.7.1.29]	2.7.1.29	Methanotrophy
Metabolism	Energy metabolism	00680 Methane metabolism [PATH:ko00680]	fae; formaldehyde-activating enzyme [EC:4.3.-.-]	4.3.-.-	Methanotrophy
Metabolism	Energy metabolism	00680 Methane metabolism [PATH:ko00680]	fdhA; glutathione-independent formaldehyde dehydrogenase [EC:1.2.1.46]	1.2.1.46	Methanotrophy
Metabolism	Energy metabolism	00680 Methane metabolism [PATH:ko00680]	frmB, ESD, fghA; S-formylglutathione hydrolase [EC:3.1.2.12]	3.1.2.12	Methanotrophy
Metabolism	Energy metabolism	00680 Methane metabolism [PATH:ko00680]	qhpA; quinohemoprotein amine dehydrogenase [EC:1.4.9.1]	1.4.9.1	Methanotrophy
Metabolism	Energy metabolism	00680 Methane metabolism [PATH:ko00680]	E1.12.1.2; hydrogen dehydrogenase [EC:1.12.1.2]	1.12.1.2	Methanotrophy
Metabolism	Energy metabolism	00680 Methane metabolism [PATH:ko00680]	E1.12.7.2S; ferredoxin hydrogenase small subunit [EC:1.12.7.2]	1.12.7.2	Methanotrophy
Metabolism	Energy metabolism	00680 Methane metabolism [PATH:ko00680]	gfa; S-(hydroxymethyl)glutathione synthase [EC:4.4.1.22]	4.4.1.22	Methanotrophy

Metabolism	Energy metabolism	00910 Nitrogen metabolism [PATH:ko00910]	cah; carbonic anhydrase [EC:4.2.1.1]	4.2.1.1	Carbonic anhydrase
Metabolism	Energy metabolism	00910 Nitrogen metabolism [PATH:ko00910]	cynT, can; carbonic anhydrase [EC:4.2.1.1]	4.2.1.1	Carbonic anhydrase
Metabolism	Energy metabolism	00910 Nitrogen metabolism [PATH:ko00910]	E4.2.1.1; carbonic anhydrase [EC:4.2.1.1]	4.2.1.1	Carbonic anhydrase

Nitrogen cycling

Level 1	Level 2	Level 3	Function		EC #
Metabolism	Energy metabolism	00910 Nitrogen metabolism [PATH:ko00910]	nifB; nitrogen fixation protein NifB		N-fixation
Metabolism	Energy metabolism	00910 Nitrogen metabolism [PATH:ko00910]	nifD; nitrogenase molybdenum-iron protein alpha chain [EC:1.18.6.1]	1.18.6.1	N-fixation
Metabolism	Energy metabolism	00910 Nitrogen metabolism [PATH:ko00910]	nifH; nitrogenase iron protein NifH [EC:1.18.6.1]	1.18.6.1	N-fixation
Metabolism	Energy metabolism	00910 Nitrogen metabolism [PATH:ko00910]	nifK; nitrogenase molybdenum-iron protein beta chain [EC:1.18.6.1]	1.18.6.1	N-fixation
Metabolism	Energy metabolism	00910 Nitrogen metabolism [PATH:ko00910]	nifN; nitrogenase molybdenum-iron protein NifN		N-fixation
Metabolism	Energy metabolism	00910 Nitrogen metabolism [PATH:ko00910]	nifT; nitrogen fixation protein NifT		N-fixation
Metabolism	Energy metabolism	00910 Nitrogen metabolism [PATH:ko00910]	nifV; homocitrate synthase NifV		N-fixation
Metabolism	Energy metabolism	00910 Nitrogen metabolism [PATH:ko00910]	nifW; nitrogen fixation protein NifW		N-fixation
Metabolism	Energy metabolism	00910 Nitrogen metabolism [PATH:ko00910]	nifW; nitrogenase-stabilizing/protective protein		N-fixation
Metabolism	Energy metabolism	00910 Nitrogen metabolism [PATH:ko00910]	amoB; ammonia monooxygenase subunit B		Nitrification
Metabolism	Energy metabolism	00910 Nitrogen metabolism [PATH:ko00910]	amoC; ammonia monooxygenase subunit C		Nitrification
Metabolism	Energy metabolism	00910 Nitrogen metabolism [PATH:ko00910]	hao; hydroxylamine oxidase [EC:1.7.3.4]	1.7.3.4	Nitrification
Metabolism	Energy metabolism	00910 Nitrogen metabolism [PATH:ko00910]	E1.7.1.1; nitrate reductase (NADH) [EC:1.7.1.1]	1.7.1.1	Nitrate reduction

Metabolism	Energy metabolism	00910 Nitrogen metabolism [PATH:ko00910]	E1.7.2.1; nitrite reductase (NO-forming) [EC:1.7.2.1]	1.7.2.1	Nitrate reduction
Metabolism	Energy metabolism	00910 Nitrogen metabolism [PATH:ko00910]	E1.7.99.1, hcp; hydroxylamine reductase [EC:1.7.99.1]	1.7.99.1	Nitrate reduction
Metabolism	Energy metabolism	00910 Nitrogen metabolism [PATH:ko00910]	E1.7.99.4C; nitrate reductase catalytic subunit [EC:1.7.99.4]	1.7.99.4	Nitrate reduction
Metabolism	Energy metabolism	00910 Nitrogen metabolism [PATH:ko00910]	napA; periplasmic nitrate reductase NapA [EC:1.7.99.4]	1.7.99.4	Nitrate reduction
Metabolism	Energy metabolism	00910 Nitrogen metabolism [PATH:ko00910]	napB; cytochrome c-type protein NapB		Nitrate reduction
Metabolism	Energy metabolism	00910 Nitrogen metabolism [PATH:ko00910]	napC; cytochrome c-type protein NapC		Nitrate reduction
Metabolism	Energy metabolism	00910 Nitrogen metabolism [PATH:ko00910]	napE; periplasmic nitrate reductase NapE		Nitrate reduction
Metabolism	Energy metabolism	00910 Nitrogen metabolism [PATH:ko00910]	napG; ferredoxin-type protein NapG		Nitrate reduction
Metabolism	Energy metabolism	00910 Nitrogen metabolism [PATH:ko00910]	narB; ferredoxin-nitrate reductase [EC:1.7.7.2]	1.7.7.2	Nitrate reduction
Metabolism	Energy metabolism	00910 Nitrogen metabolism [PATH:ko00910]	NIAD; nitrate reductase (NADPH) [EC:1.7.1.3]	1.7.1.3	Nitrate reduction
Metabolism	Energy metabolism	00910 Nitrogen metabolism [PATH:ko00910]	nirA; ferredoxin-nitrite reductase [EC:1.7.7.1]	1.7.7.1	Nitrate reduction
Metabolism	Energy metabolism	00910 Nitrogen metabolism [PATH:ko00910]	nirB; nitrite reductase (NAD(P)H) large subunit [EC:1.7.1.4]	1.7.1.4	Nitrate reduction
Metabolism	Energy metabolism	00910 Nitrogen metabolism [PATH:ko00910]	nirD; nitrite reductase (NAD(P)H) small subunit [EC:1.7.1.4]	1.7.1.4	Nitrate reduction
Metabolism	Energy metabolism	00910 Nitrogen metabolism [PATH:ko00910]	nrfC; protein NrfC		Nitrate reduction
Metabolism	Energy Metabolism	00910 Nitrogen metabolism [PATH:ko00910]	nrfD; formate-dependent nitrate reductase complex, transmembrane protein		Nitrate reduction
Metabolism	Energy metabolism	00910 Nitrogen metabolism [PATH:ko00910]	norB; nitric oxide reductase subunit B [EC:1.7.2.5]	1.7.2.5	Denitrification
Metabolism	Energy metabolism	00910 Nitrogen metabolism [PATH:ko00910]	norC; nitric oxide reductase subunit C		Denitrification
Metabolism	Energy metabolism	00910 Nitrogen metabolism [PATH:ko00910]	norC; nitric-oxide reductase, cytochrome c-containing	1.7.99.7	Denitrification

			subunit II [EC:1.7.99.7]		
Metabolism	Energy metabolism	00910 Nitrogen metabolism [PATH:ko00910]	norF; nitric-oxide reductase NorF protein [EC:1.7.99.7]	1.7.99.7	Denitrification
Metabolism	Energy metabolism	00910 Nitrogen metabolism [PATH:ko00910]	nosZ; nitrous-oxide reductase [EC:1.7.2.4]	1.7.2.4	Denitrification
Metabolism	Energy metabolism	00910 Nitrogen metabolism [PATH:ko00910]	E1.13.12.16; nitronate monooxygenase [EC:1.13.12.16]	1.13.12.16	Nitroalkane oxidase

Phosphorus cycling

<u>Level 1</u>	<u>Level 2</u>	<u>Level 3</u>	<u>Function</u>	<u>EC #</u>	<u>CAZy</u>
Metabolism	Carbohydrate metabolism	00562 Inositol phosphate metabolism [PATH:ko00562]	appA; 4-phytase / acid phosphatase [EC:3.1.3.26, 3.1.3.2]	3.1.3.26, 3.1.3.2	Inositol phosphate
Metabolism	Carbohydrate metabolism	00562 Inositol phosphate metabolism [PATH:ko00562]	E3.1.3.8; 3-phytase [EC:3.1.3.8]	3.1.3.8	Inositol phosphate
Metabolism	Carbohydrate metabolism	00562 Inositol phosphate metabolism [PATH:ko00562]	E4.6.1.13, plc; 1-phosphatidylinositol phosphodiesterase [EC:4.6.1.13]	4.6.1.13	Inositol phosphate
Metabolism	Carbohydrate metabolism	00562 Inositol phosphate metabolism [PATH:ko00562]	iolB; 5-deoxy-glucuronate isomerase [EC:5.3.1.-]	5.3.1.-	Inositol phosphate
Metabolism	Carbohydrate metabolism	00562 Inositol phosphate metabolism [PATH:ko00562]	iolC; 5-dehydro-2-deoxygluconokinase [EC:2.7.1.92]	2.7.1.92	Inositol phosphate
Metabolism	Carbohydrate metabolism	00562 Inositol phosphate metabolism [PATH:ko00562]	iolD; 3D-(3,5/4)-trihydroxycyclohexane-1,2-dione hydrolase [EC:3.7.1.-]	3.7.1.-	Inositol phosphate
Metabolism	Carbohydrate metabolism	00562 Inositol phosphate metabolism [PATH:ko00562]	iolE; inosose dehydratase [EC:4.2.1.44]	4.2.1.44	Inositol phosphate
Metabolism	Carbohydrate metabolism	00562 Inositol phosphate metabolism [PATH:ko00562]	iolJ; 6-phospho-5-dehydro-2-deoxy-D-gluconate aldolase [EC:4.1.2.29]	4.1.2.29	Inositol phosphate
Metabolism	Carbohydrate metabolism	00562 Inositol phosphate metabolism [PATH:ko00562]	MINPP1; multiple inositol-polyphosphate phosphatase [EC:3.1.3.62]	3.1.3.62	Inositol phosphate

Metabolism	Carbohydrate metabolism	00562 Inositol phosphate metabolism [PATH:ko00562]	plcC; phospholipase C [EC:3.1.4.3]	3.1.4.3	Inositol phosphate
Cellular Processes	Cell communication	04510 Focal adhesion [PATH:ko04510]	PPP1C; protein phosphatase 1, catalytic subunit [EC:3.1.3.16]	3.1.3.16	Phosphomonoesters
Cellular Processes	Cell communication	04510 Focal adhesion [PATH:ko04510]	PTEN; phosphatidylinositol-3,4,5-trisphosphate 3-phosphatase and dual-specificity protein phosphatase PTEN [EC:3.1.3.16 3.1.3.48 3.1.3.67]	3.1.3.16, 3.1.3.48, 3.1.3.67	Phosphomonoesters
Cellular Processes	Cell communication	04530 Tight junction [PATH:ko04530]	PPP2C; protein phosphatase 2 (formerly 2A), catalytic subunit [EC:3.1.3.16]	3.1.3.16	Phosphomonoesters
Cellular Processes	Cell growth and death	04110 Cell cycle [PATH:ko04110]	CDC14; cell division cycle 14 [EC:3.1.3.48]	3.1.3.48	Phosphomonoesters
Cellular Processes	Cell growth and death	04111 Cell cycle - yeast [PATH:ko04111]	MIH1; M-phase inducer tyrosine phosphatase [EC:3.1.3.48]	3.1.3.48	Phosphomonoesters
Cellular Processes	Cell growth and death	04114 Oocyte meiosis [PATH:ko04114]	PPP3C, CNA; protein phosphatase 3, catalytic subunit [EC:3.1.3.16]	3.1.3.16	Phosphomonoesters
Environmental Information Processing	Membrane transport	03070 Bacterial secretion system [PATH:ko03070]	stp1, pppA; serine/threonine protein phosphatase Stp1 [EC:3.1.3.16]	3.1.3.16	Phosphomonoesters
Environmental Information Processing	Signal transduction	02020 Two-component system [PATH:ko02020]	E3.1.3.1, phoA, phoB; alkaline phosphatase [EC:3.1.3.1]	3.1.3.1	Phosphomonoesters
Environmental Information Processing	Signal transduction	02020 Two-component system [PATH:ko02020]	phoD; alkaline phosphatase D [EC:3.1.3.1]	3.1.3.1	Phosphomonoesters
Environmental Information Processing	Signal transduction	02020 Two-component system [PATH:ko02020]	phoN; acid phosphatase (class A) [EC:3.1.3.2]	3.1.3.2	Phosphomonoesters
Environmental Information Processing	Signal transduction	04010 MAPK signaling pathway [PATH:ko04010]	DUSP, MKP; dual specificity phosphatase [EC:3.1.3.16 3.1.3.48]	3.1.3.16, 3.1.3.48	Phosphomonoesters
Environmental Information	Signal transduction	04010 MAPK signaling pathway [PATH:ko04010]	PPP5C, PP5; protein phosphatase 5 [EC:3.1.3.16]	3.1.3.16	Phosphomonoesters

Processing					
Environmental Information Processing	Signal transduction	04011 MAPK signaling pathway - yeast [PATH:ko04011]	MSG5; tyrosine-protein phosphatase [EC:3.1.3.48]	3.1.3.48	Phosphomonoesters
Environmental Information Processing	Signal transduction	04013 MAPK signaling pathway - fly [PATH:ko04013]	PTPN11; tyrosine-protein phosphatase non-receptor type 11 [EC:3.1.3.48]	3.1.3.48	Phosphomonoesters
Environmental Information Processing	Signal transduction	04070 Phosphatidylinositol signaling system [PATH:ko04070]	E3.1.3.25, IMPA, suhB; myo-inositol-1(or 4)-monophosphatase [EC:3.1.3.25]	3.1.3.25	Phosphomonoesters
Environmental Information Processing	Signal transduction	04070 Phosphatidylinositol signaling system [PATH:ko04070]	E3.1.3.36; phosphatidylinositol-bisphosphatase [EC:3.1.3.36]	3.1.3.36	Phosphomonoesters
Environmental Information Processing	Signal transduction	04070 Phosphatidylinositol signaling system [PATH:ko04070]	INPP1; inositol polyphosphate 1-phosphatase [EC:3.1.3.57]	3.1.3.57	Phosphomonoesters
Environmental Information Processing	Signal transduction	04070 Phosphatidylinositol signaling system [PATH:ko04070]	VTC4; inositol-phosphate phosphatase / L-galactose 1-phosphate phosphatase [EC:3.1.3.25 3.1.3.-]	3.1.3.25, 3.1.3.-	Phosphomonoesters
Human Diseases	Infectious diseases	05152 Tuberculosis [PATH:ko05152]	E3.1.3.2; acid phosphatase [EC:3.1.3.2]	3.1.3.2	Phosphomonoesters
Metabolism	Amino acid metabolism	00260 Glycine, serine and threonine metabolism [PATH:ko00260]	serB, PSPH; phosphoserine phosphatase [EC:3.1.3.3]	3.1.3.3	Phosphomonoesters
Metabolism	Amino acid metabolism	00260 Glycine, serine and threonine metabolism [PATH:ko00260]	thrH; phosphoserine / homoserine phosphotransferase [EC:3.1.3.3 2.7.1.39]	3.1.3.3, 2.7.1.39	Phosphomonoesters
Metabolism	Amino acid metabolism	00270 Cysteine and methionine metabolism [PATH:ko00270]	mtnC, ENOPH1; enolase-phosphatase E1 [EC:3.1.3.77]	3.1.3.77	Phosphomonoesters
Metabolism	Amino acid metabolism	00270 Cysteine and methionine metabolism [PATH:ko00270]	mtnX; 2-hydroxy-3-keto-5-methylthiopentenyl-1-phosphate phosphatase [EC:3.1.3.87]	3.1.3.87	Phosphomonoesters
Metabolism	Amino acid metabolism	00340 Histidine metabolism [PATH:ko00340]	E3.1.3.15B; histidinol-phosphatase (PHP family)	3.1.3.15	Phosphomonoesters

			[EC:3.1.3.15]		
Metabolism	Biosynthesis of other secondary metabolites	00521 Streptomycin biosynthesis [PATH:ko00521]	strK; streptomycin-6-phosphatase [EC:3.1.3.39]	3.1.3.39	Phosphomonoesters
Metabolism	Carbohydrate metabolism	00010 Glycolysis / Gluconeogenesis [PATH:ko00010]	FBP, fbp; fructose-1,6-bisphosphatase I [EC:3.1.3.11]	3.1.3.11	Phosphomonoesters
Metabolism	Carbohydrate metabolism	00010 Glycolysis / Gluconeogenesis [PATH:ko00010]	fbp3; fructose-1,6-bisphosphatase III [EC:3.1.3.11]	3.1.3.11	Phosphomonoesters
Metabolism	Carbohydrate metabolism	00010 Glycolysis / Gluconeogenesis [PATH:ko00010]	glpX-SEBP; fructose-1,6-bisphosphatase II / sedoheptulose-1,7-bisphosphatase [EC:3.1.3.11 3.1.3.37]	3.1.3.11, 3.1.3.37	Phosphomonoesters
Metabolism	Carbohydrate metabolism	00010 Glycolysis / Gluconeogenesis [PATH:ko00010]	glpX; fructose-1,6-bisphosphatase II [EC:3.1.3.11]	3.1.3.11	Phosphomonoesters
Metabolism	Carbohydrate metabolism	00500 Starch and sucrose metabolism [PATH:ko00500]	otsB; trehalose 6-phosphate phosphatase [EC:3.1.3.12]	3.1.3.12	Phosphomonoesters
Metabolism	Carbohydrate metabolism	00562 Inositol phosphate metabolism [PATH:ko00562]	appA; 4-phytase / acid phosphatase [EC:3.1.3.26 3.1.3.2]	3.1.3.26, 3.1.3.2	Phosphomonoesters
Metabolism	Carbohydrate metabolism	00562 Inositol phosphate metabolism [PATH:ko00562]	E3.1.3.8; 3-phytase [EC:3.1.3.8]	3.1.3.8	Phosphomonoesters
Metabolism	Carbohydrate metabolism	00562 Inositol phosphate metabolism [PATH:ko00562]	MINPP1; multiple inositol-polyphosphate phosphatase [EC:3.1.3.62]	3.1.3.62	Phosphomonoesters
Metabolism	Carbohydrate metabolism	00630 Glyoxylate and dicarboxylate metabolism [PATH:ko00630]	E3.1.3.18, gph; phosphoglycolate phosphatase [EC:3.1.3.18]	3.1.3.18	Phosphomonoesters
Metabolism	Energy metabolism	00680 Methane metabolism [PATH:ko00680]	E3.1.3.71, comB; 2-phosphosulfolactate phosphatase [EC:3.1.3.71]	3.1.3.71	Phosphomonoesters
Metabolism	Energy metabolism	00920 Sulfur metabolism [PATH:ko00920]	E3.1.3.7, cysQ, MET22, BPNT1; 3'(2'), 5'-bisphosphate nucleotidase [EC:3.1.3.7]	3.1.3.7	Phosphomonoesters

Metabolism	Glycan biosynthesis and metabolism	00540 Lipopolysaccharide biosynthesis [PATH:ko00540]	gmhB; D-glycero-D-manno-heptose 1,7-bisphosphate phosphatase [EC:3.1.3.82 3.1.3.83]	3.1.3.82, 3.1.3.83	Phosphomonoesters
Metabolism	Glycan biosynthesis and metabolism	00540 Lipopolysaccharide biosynthesis [PATH:ko00540]	kdsC; 3-deoxy-D-manno-octulosonate 8-phosphate phosphatase (KDO 8-P phosphatase) [EC:3.1.3.45]	3.1.3.45	Phosphomonoesters
Metabolism	Lipid metabolism	00561 Glycerolipid metabolism [PATH:ko00561]	GPP1; glycerol 3-phosphatase 1 [EC:3.1.3.21]	3.1.3.21	Phosphomonoesters
Metabolism	Lipid metabolism	00564 Glycerophospholipid metabolism [PATH:ko00564]	pgpA; phosphatidylglycerophosphatase A [EC:3.1.3.27]	3.1.3.27	Phosphomonoesters
Metabolism	Lipid metabolism	00564 Glycerophospholipid metabolism [PATH:ko00564]	pgpB; phosphatidylglycerophosphatase B [EC:3.1.3.27]	3.1.3.27	Phosphomonoesters
Metabolism	Metabolism of cofactors and vitamins	00740 Riboflavin metabolism [PATH:ko00740]	ACP1; low molecular weight phosphotyrosine protein phosphatase [EC:3.1.3.2 3.1.3.48]	3.1.3.2, 3.1.3.48	Phosphomonoesters
Metabolism	Metabolism of cofactors and vitamins	00760 Nicotinate and nicotinamide metabolism [PATH:ko00760]	E3.1.3.5; 5'-nucleotidase [EC:3.1.3.5]	3.1.3.5	Phosphomonoesters
Metabolism	Metabolism of cofactors and vitamins	00760 Nicotinate and nicotinamide metabolism [PATH:ko00760]	surE; 5'-nucleotidase [EC:3.1.3.5]	3.1.3.5	Phosphomonoesters
Metabolism	Metabolism of cofactors and vitamins	00760 Nicotinate and nicotinamide metabolism [PATH:ko00760]	ushA; 5'-nucleotidase / UDP-sugar diphosphatase [EC:3.1.3.5 3.6.1.45]	3.1.3.5, 3.6.1.45	Phosphomonoesters
Metabolism	Metabolism of cofactors and vitamins	00760 Nicotinate and nicotinamide metabolism [PATH:ko00760]	yfbR; 5'-nucleotidase [EC:3.1.3.5]	3.1.3.5	Phosphomonoesters
Metabolism	Nucleotide metabolism	00230 Purine metabolism [PATH:ko00230]	E3.1.3.6; 3'-nucleotidase [EC:3.1.3.6]	3.1.3.6	Phosphomonoesters
Metabolism	Xenobiotics biodegradation and metabolism	00627 Aminobenzoate degradation [PATH:ko00627]	E3.1.3.41; 4-nitrophenyl phosphatase [EC:3.1.3.41]	3.1.3.41	Phosphomonoesters
Cellular	Cell	04540 Gap junction	PLCB; phosphatidylinositol	3.1.4.11	Phosphodiester

Processes	communication	[PATH:ko04540]	phospholipase C, beta [EC:3.1.4.11]		
Cellular Processes	Cell growth and death	04112 Cell cycle - Caulobacter [PATH:ko04112]	pdeA; c-di-GMP-specific phosphodiesterase [EC:3.1.4.52]	3.1.4.52	Phosphodiesterases
Cellular Processes	Transport and catabolism	04142 Lysosome [PATH:ko04142]	SMPD1, ASM; sphingomyelin phosphodiesterase [EC:3.1.4.12]	3.1.4.12	Phosphodiesterases
Cellular Processes	Transport and catabolism	04144 Endocytosis [PATH:ko04144]	PLD; phospholipase D [EC:3.1.4.4]	3.1.4.4	Phosphodiesterases
Environmental Information Processing	Signal transduction	04012 ErbB signaling pathway [PATH:ko04012]	PLCG1; phosphatidylinositol phospholipase C, gamma-1 [EC:3.1.4.11]	3.1.4.11	Phosphodiesterases
Environmental Information Processing	Signal transduction	04020 Calcium signaling pathway [PATH:ko04020]	PDE1; calcium/calmodulin-dependent 3',5'-cyclic nucleotide phosphodiesterase [EC:3.1.4.17]	3.1.4.17	Phosphodiesterases
Environmental Information Processing	Signal transduction	04020 Calcium signaling pathway [PATH:ko04020]	PLCD; phosphatidylinositol phospholipase C, delta [EC:3.1.4.11]	3.1.4.11	Phosphodiesterases
Environmental Information Processing	Signal transduction	04020 Calcium signaling pathway [PATH:ko04020]	PLCE; phosphatidylinositol phospholipase C, epsilon [EC:3.1.4.11]	3.1.4.11	Phosphodiesterases
Human Diseases	Substance dependence	05032 Morphine addiction [PATH:ko05032]	PDE; 3',5'-cyclic-nucleotide phosphodiesterase [EC:3.1.4.17]	3.1.4.17	Phosphodiesterases
Human Diseases	Substance dependence	05032 Morphine addiction [PATH:ko05032]	PDE11; dual 3',5'-cyclic-AMP and -GMP phosphodiesterase 11 [EC:3.1.4.17 3.1.4.35]	3.1.4.17, 3.1.4.35	Phosphodiesterases
Metabolism	Carbohydrate metabolism	00500 Starch and sucrose metabolism [PATH:ko00500]	ENPP1_3; ectonucleotide pyrophosphatase/phosphodiesterase family member 1/3 [EC:3.1.4.1 3.6.1.9]	3.1.4.1, 3.6.1.9	Phosphodiesterases
Metabolism	Carbohydrate metabolism	00562 Inositol phosphate metabolism [PATH:ko00562]	E4.6.1.13, plc; 1-phosphatidylinositol phosphodiesterase [EC:4.6.1.13]	4.6.1.13	Phosphodiesterases
Metabolism	Carbohydrate	00562 Inositol phosphate	plcC; phospholipase C	3.1.4.3	Phosphodiesterases

	metabolism	metabolism [PATH:ko00562]	[EC:3.1.4.3]		
Metabolism	Glycan biosynthesis and metabolism	00563 Glycosylphosphatidylinositol (GPI)-anchor biosynthesis [PATH:ko00563]	E3.1.4.50; glycosylphosphatidylinositol phospholipase D [EC:3.1.4.50]	3.1.4.50	Phosphodiesterases
Metabolism	Lipid metabolism	00564 Glycerophospholipid metabolism [PATH:ko00564]	E3.1.4.46, glpQ, ugpQ; glycerophosphoryl diester phosphodiesterase [EC:3.1.4.46]	3.1.4.46	Phosphodiesterases
Metabolism	Nucleotide metabolism	00230 Purine metabolism [PATH:ko00230]	cpdB; 2',3'-cyclic-nucleotide 2'-phosphodiesterase [EC:3.1.4.16]	3.1.4.16	Phosphodiesterases
Metabolism	Nucleotide metabolism	00230 Purine metabolism [PATH:ko00230]	PDE5; cGMP-specific 3',5'-cyclic phosphodiesterase [EC:3.1.4.35]	3.1.4.35	Phosphodiesterases
Metabolism	Nucleotide metabolism	00230 Purine metabolism [PATH:ko00230]	PDE6N; cGMP-specific 3',5'-cyclic phosphodiesterase, invertebrate [EC:3.1.4.35]	3.1.4.35	Phosphodiesterases
Metabolism	Nucleotide metabolism	00230 Purine metabolism [PATH:ko00230]	PDEB2, PDE2B; cAMP-specific phosphodiesterase [EC:3.1.4.53]	3.1.4.53	Phosphodiesterases
Metabolism	Nucleotide metabolism	00230 Purine metabolism [PATH:ko00230]	dgt; dGTPase [EC:3.1.5.1]	3.1.5.1	Triphosphoric monoester hydrolase
Cellular Processes	Transport and catabolism	04146 Peroxisome [PATH:ko04146]	E3.6.1.22, NUDT12, nudC; NAD ⁺ diphosphatase [EC:3.6.1.22]	3.6.1.22	Inorganic phosphate
Genetic Information Processing	Folding, sorting and degradation	03018 RNA degradation [PATH:ko03018]	nudH; putative (di)nucleoside polyphosphate hydrolase [EC:3.6.1.-]	3.6.1.-	Inorganic phosphate
Metabolism	Amino acid metabolism	00340 Histidine metabolism [PATH:ko00340]	HIS4; phosphoribosyl-ATP pyrophosphohydrolase / phosphoribosyl-AMP cyclohydrolase / histidinol dehydrogenase [EC:3.6.1.31 3.5.4.19 1.1.1.23]	3.6.1.31, 3.5.4.19, 1.1.1.23	Inorganic phosphate
Metabolism	Amino acid metabolism	00340 Histidine metabolism [PATH:ko00340]	hisE; phosphoribosyl-ATP pyrophosphohydrolase [EC:3.6.1.31]	3.6.1.31	Inorganic phosphate

Metabolism	Amino acid metabolism	00340 Histidine metabolism [PATH:ko00340]	hisIE; phosphoribosyl-ATP pyrophosphohydrolase / phosphoribosyl-AMP cyclohydrolase [EC:3.6.1.31 3.5.4.19]	3.6.1.31, 3.5.4.19	Inorganic phosphate
Metabolism	Carbohydrate metabolism	00620 Pyruvate metabolism [PATH:ko00620]	acyP; acylphosphatase [EC:3.6.1.7]	3.6.1.7	Inorganic phosphate
Metabolism	Energy metabolism	00190 Oxidative phosphorylation [PATH:ko00190]	LHPP; phospholysine phosphohistidine inorganic pyrophosphate phosphatase [EC:3.6.1.1 3.1.3.-]	3.6.1.1, 3.1.3.-	Inorganic phosphate
Metabolism	Energy metabolism	00190 Oxidative phosphorylation [PATH:ko00190]	ppa; inorganic pyrophosphatase [EC:3.6.1.1]	3.6.1.1	Inorganic phosphate
Metabolism	Energy metabolism	00190 Oxidative phosphorylation [PATH:ko00190]	ppaX; pyrophosphatase PpaX [EC:3.6.1.1]	3.6.1.1	Inorganic phosphate
Metabolism	Glycan biosynthesis and metabolism	00510 N-Glycan biosynthesis [PATH:ko00510]	E3.6.1.43; dolichyldiphosphatase [EC:3.6.1.43]	3.6.1.43	Inorganic phosphate
Metabolism	Glycan biosynthesis and metabolism	00540 Lipopolysaccharide biosynthesis [PATH:ko00540]	lpxH; UDP-2,3-diacylglucosamine hydrolase [EC:3.6.1.54]	3.6.1.54	Inorganic phosphate
Metabolism	Glycan biosynthesis and metabolism	00550 Peptidoglycan biosynthesis [PATH:ko00550]	E3.6.1.27, bacA; undecaprenyl-diphosphatase [EC:3.6.1.27]	3.6.1.27	Inorganic phosphate
Metabolism	Lipid metabolism	00564 Glycerophospholipid metabolism [PATH:ko00564]	cdh; CDP-diacylglycerol pyrophosphatase [EC:3.6.1.26]	3.6.1.26	Inorganic phosphate
Metabolism	Nucleotide metabolism	00230 Purine metabolism [PATH:ko00230]	apaH; bis(5'-nucleosyl)-tetrphosphatase (symmetrical) [EC:3.6.1.41]	3.6.1.41	Inorganic phosphate
Metabolism	Nucleotide metabolism	00230 Purine metabolism [PATH:ko00230]	E3.6.1.17; bis(5'-nucleosidyl)-tetrphosphatase [EC:3.6.1.17]	3.6.1.17	Inorganic phosphate
Metabolism	Nucleotide metabolism	00230 Purine metabolism [PATH:ko00230]	E3.6.1.3; adenosinetriphosphatase [EC:3.6.1.3]	3.6.1.3	Inorganic phosphate
Metabolism	Nucleotide metabolism	00230 Purine metabolism [PATH:ko00230]	ITPA; inosine triphosphate pyrophosphatase [EC:3.6.1.19]	3.6.1.19	Inorganic phosphate

Metabolism	Nucleotide metabolism	00230 Purine metabolism [PATH:ko00230]	nudE; ADP-ribose diphosphatase [EC:3.6.1.-]	3.6.1.-	Inorganic phosphate
Metabolism	Nucleotide metabolism	00230 Purine metabolism [PATH:ko00230]	nudF; ADP-ribose pyrophosphatase [EC:3.6.1.13]	3.6.1.13	Inorganic phosphate
Metabolism	Nucleotide metabolism	00230 Purine metabolism [PATH:ko00230]	ppx-gppA; exopolyphosphatase / guanosine-5'-triphosphate,3'-diphosphate pyrophosphatase [EC:3.6.1.11 3.6.1.40]	3.6.1.11, 3.6.1.40	Inorganic phosphate
Metabolism	Nucleotide metabolism	00230 Purine metabolism [PATH:ko00230]	PPX1; exopolyphosphatase [EC:3.6.1.11]	3.6.1.11	Inorganic phosphate
Metabolism	Nucleotide metabolism	00230 Purine metabolism [PATH:ko00230]	rdgB; dITP/XTP pyrophosphatase [EC:3.6.1.19]	3.6.1.19	Inorganic phosphate
Metabolism	Nucleotide metabolism	00240 Pyrimidine metabolism [PATH:ko00240]	E3.6.1.23, dut; dUTP pyrophosphatase [EC:3.6.1.23]	3.6.1.23	Inorganic phosphate

Supplementary Table S5.2. Kruskal-Wallis and posthoc Nemenyi test results comparing the relative abundances of functional genes between snow fence treatment zones (Ctl, Deep, Int, Low). Genes are grouped into functional categories based on the SEED Subsystems classification system. Posthoc Nemenyi test results are only shown for functional groups with Kruskal-Wallis p -values < 0.15 and are displayed as the treatment zone with the highest abundance, followed by the treatment zone with the lowest abundance, followed by the p -value (e.g. “highest-lowest=0.10”).

SEED Subsystem functional classification of gene groups			Kruskal-Wallis	Posthoc Nemenyi
<u>Lvl 1</u>	<u>Lvl 2</u>	<u>Lvl 3</u>	<u>H</u>	<u>p-value</u>
<u>Amino Acids and Derivatives</u>			6.23	0.101
	Arginine, urea cycle, polyamines	Urea decomposition	6.28	0.099*
<u>Carbohydrates</u>			6.08	0.108
	Aminosugars	Chitin and N-acetylglucosamine utilization	3.00	0.392
	Central carbohydrate metabolism		8.74	0.033**
	Di- and oligosaccharides		6.44	0.092*
		Beta-Glucoside Metabolism	1.46	0.691
	Fermentation		8.23	0.041**
	Monosaccharides		2.28	0.516
	One-carbon Metabolism	Methanogenesis	9.46	0.024**

	Serine-glyoxylate cycle	4.18	0.243	<i>n/a</i>
Organic acids		7.51	0.057*	Low-Deep=0.046
Polysaccharides	Cellulosome	7.51	0.057*	Deep-Ctl=0.061
	Glycogen metabolism	3.41	0.333	<i>n/a</i>
Sugar alcohols		3.15	0.369	<i>n/a</i>
<u>Cell Wall and Capsule</u>		6.44	0.092*	Int-Deep=0.061
	Capsular and extracellular polysaccharides	8.74	0.033**	Int-Low=0.046
	Gram-Negative cell wall components	5.26	0.154	<i>n/a</i>
	Gram-Positive cell wall components	6.18	0.103	Ctl-Deep=0.110
NULL	Murein Hydrolases	4.38	0.223	<i>n/a</i>
NULL	Peptidoglycan Biosynthesis	4.85	0.183	<i>n/a</i>
<u>Fatty Acids, Lipids, and Isoprenoids</u>		5.62	0.132	Low-Deep/Ctl=0.170
	Fatty acids	5.46	0.141	Low-Deep=0.220
	Isoprenoids	5.15	0.161	<i>n/a</i>
	Phospholipids	3.62	0.306	<i>n/a</i>
	Triacylglycerols	6.38	0.094*	Low-Ctl=0.110
<u>Membrane Transport</u>		6.28	0.99	<i>n/a</i>

ABC transporters		6.85	0.077*	Deep-Low=0.061
Protein and nucleoprotein secretion system, Type IV		6.90	0.075*	Low-Deep=0.140
Protein secretion system, Type I		9.15	0.027**	Deep-Ctl=0.017
Protein secretion system, Type II		0.95	0.814	<i>n/a</i>
Protein secretion system, Type III		6.23	0.101	Deep-Ctl/Int/Low= 0.170
Protein secretion system, Type V		2.90	0.408	<i>n/a</i>
Protein secretion system, Type VI		0.74	0.863	<i>n/a</i>
Protein secretion system, Type VII (Chaperone/Usher pathway, CU)		5.36	0.1473	Low-Deep=0.110
Protein secretion system, Type VIII (Extracellular nucleation/precipitation pathway, ENP)		5.36	0.1473	Deep-Ctl=0.140
Protein translocation across cytoplasmic membrane		0.28	0.963	<i>n/a</i>
<u>Metabolism of Aromatic Compounds</u>		0.74	0.863	<i>n/a</i>
<u>Motility and Chemotaxis</u>		5.15	0.161	<i>n/a</i>
<u>Nitrogen Metabolism</u>		6.90	0.075*	Deep-Low=0.081
NULL	Ammonia assimilation	6.69	0.082*	Deep-Low=0.081
NULL	Denitrification	6.28	0.099*	Deep-Low=0.081

NULL	Dissimilatory nitrite reductase	8.54	0.036**	Deep-Ctl=0.081
NULL	Nitrate and nitrite ammonification	7.82	0.050**	Deep-Ctl=0.046
NULL	Nitrogen fixation	7.82	0.050**	Deep-Low=0.033
<u>Phosphorus Metabolism</u>		6.38	0.094*	Deep-Ctl=0.081
<u>Potassium metabolism</u>		6.18	0.103	Deep-Low/Ctl=0.14
<u>Protein Metabolism</u>		1.51	0.679	<i>n/a</i>
	Protein biosynthesis	1.77	0.622	<i>n/a</i>
	Protein degradation	2.28	0.516	<i>n/a</i>
<u>Respiration</u>		4.79	0.187	<i>n/a</i>
	Electron accepting reactions	4.64	0.200	<i>n/a</i>
	Electron donating reactions	5.21	0.157	<i>n/a</i>
<u>Stress Response</u>		4.44	0.218	<i>n/a</i>
	Cold shock	6.69	0.082*	Low-Deep=0.081
	Oxidative stress	4.13	0.248	<i>n/a</i>
<u>Sulfur Metabolism</u>		6.90	0.075	Deep-Int=0.140
	Inorganic sulfur assimilation	6.28	0.099*	Deep-Int=0.140
	Organic sulfur assimilation	6.49	0.090*	Low-Int=0.061

8 Vita

Michael P. Ricketts

Education

Graduate

2011-present University of Illinois at Chicago - Chicago, IL
Ph.D. candidate in Department of Biological Sciences – Ecology and Evolution
Advisor - Dr. Miquel Gonzalez-Meler
Expected completion date – 4/10/2019

2010-2011 University of Illinois at Champaign/Urbana - Urbana, IL
Natural Resources and Environmental Science online courses

Undergraduate

1994-1998 University of Illinois at Champaign/Urbana - Urbana, IL
B.S. in Cell and Structural Biology

Experience

2011-present **Teaching Assistant** – University of Illinois at Chicago – Chicago, IL
Department of Biological Sciences
BIOS 331 – General Ecology Laboratory
BIOS 350 – Microbiology Lecture
BIOS 351 – Microbiology Laboratory
BIOS 240 - Homeostasis
BIOS 100 - Cells and Organisms
BIOS 101 - Populations and Communities

2016-2017 **Adjunct Instructor** – Loyola University Chicago – Chicago, IL
Institute of Environmental Sustainability
ENVS 238 – Foundations of Environmental Science Lab

2008–2011 **Medical Technician** - University of Chicago Medical Center - Chicago, IL
Microbiology Laboratory – Inoculate, plate, and culture specimens for antibiotic sensitivities, slide preparation and staining.
Laboratory Service Center - Specimen preparation and processing for in-house and referral testing. Problem solving and customer service.

1998-2008 **Founder / Musician** - Planes Mistaken For Stars, Inc. - Denver, CO
Co-owner and financier- Responsible for financial records, accounting, merchandising,

and booking national /international travel arrangements and logistics.

Accomplishments – Four full-length LP records, two EP records, three 7” records (including artwork), two music videos, and numerous tours in U.S. (50+), Europe (5), and Japan (1).

- 2002 **Laboratory Assistant** – Labcorp, Inc. - Englewood, CO
Microbiology Laboratory - Inoculate, plate, and culture specimens for antibiotic sensitivities, slide preparation and staining.
Accessioning Department - Organize incoming medical samples into laboratory database.
- 1999-2001 **Laboratory Technician** – On Assignment, Inc. - Lab Support - Denver, CO
Commercial Testing & Engineering, Inc. - Test mineral purity using spectrophotometry, pH testing, and titrations.
Cobe Cardiovascular, Inc. - Perform quality control for lung/heart machine products measuring blood gas exchange and blood chemistry.
Colorado Med Tech, Inc. - Perform quality control for blood chemistry machine testing for the presence of HIV/HCV using volumes/dilutions, gravimetric precision, and spectrophotometer.

Awards & Honors

- 2017 Graduate Student Research Award - \$200
2016 Elmer Hadley Graduate Research Award - \$2,000
2016 Undergraduate Biological Colloquium Award for Best Teaching Assistant
2013 W.C. and May Preble Deiss Award for Graduate Research - \$4,000
2013 Graduate Student Teaching Award - \$200
2013 Bodmer International Travel Award - \$1,400
2013 Elmer Hadley Graduate Research Award - \$2,000
2012 Graduate Student Teaching Award - \$250

Service

- 2018 Reviewer for PeerJ journal - DOI - 10.7287/peerj.6147v0.1/reviews/1
2017-2018 UIC LASURI Award Project Supervisor – Theresa Ewa
2016-2017 UIC Undergraduate Honors College Capstone Project Supervisor – James Chang
2016-2017 Biology Graduate Student Association, Ecology and Evolution liaison
2016-2017 Graduate Policy Committee, Ecology and Evolution student representative
2016 Reviewer for the European Journal of Soil Science
2015 SES Biological Sciences Colloquium organizer
2012 Undergraduate Elmer Hadley research award committee
2011-2012 Plants of Concern Research Project volunteer - Chicago Botanic Garden
2009-2012 Forest Preserve District of Cook County / Chicago Wilderness volunteer

Publications

Ricketts, M.P., Flower, C. E., Knight, K. S. and Gonzalez-Meler, M.A. 2018. Evidence of ash tree (*Fraxinus* spp.) specific associations with soil bacterial community structure and functional capacity, *Forests*, 9(4), 1–16, doi:10.3390/f9040187.

Ricketts, M.P., Poretsky, R.S., Welker, J.M., and Gonzalez-Meler, M.A. 2016. Soil bacterial community and functional shifts in response to altered snowpack in moist acidic tundra of Northern Alaska, *SOIL*, 2, 459-474, doi:10.5194/soil-2015-89.

In preparation

Ricketts, M.P., Koval, J.C., Antonopoulos, D.A., Jastrow, J.D., Calderón, F.J., Liang, C., Fan, Z., Michaelson, G.J., Ping, C.L., Gonzalez-Meler, M.A., Matamala, R., Carbon mineralization susceptibility in Arctic tundra soils: How organic matter chemistry and temperature relate to bacterial community structure and soil respiration. **In preparation for submission to *Soil Biology and Biochemistry* 5/19.**

DeFranco, K., **Ricketts, M.P.**, Welker, J.M., Gonzalez-Meler, M.A., and Sturchio, N.C. Deeper Arctic snow drives increased active-layer organic carbon accrual rate in moist acidic tussock tundra: ²¹⁰Pb evidence. **In preparation for submission to *Nature Geosciences* 5/19.**

Ricketts, M.P., Greene, S.J., Matamala, R., Welker, J.M., and Gonzalez-Meler, M.A. Shotgun metagenomic analysis of microbial soil organic matter decomposition and nutrient cycling in an Arctic snowfence experiment. **In preparation for submission to *ISME* 7/19.**

Dias de Oliveira, E.A., Manchon, F.T., **Ricketts, M.P.**, Martinez, C.A., and Gonzalez-Meler, M.A. Soil respiration in a C4-dominated grassland is controlled by vegetation biomass under warming. **In preparation for submission 5/19.**

Oral Presentations

Ricketts, M.P., Matamala, R., Welker, J.M., Poretsky, R.S., Green, S., and Gonzalez-Meler, M.A. Arctic soil carbon mineralization potential mediated by microbial genetic responses to warming. Soil Science Society of America International Soils meeting. San Diego, CA, January 6-9, 2019.

Ricketts, M.P., Matamala, R., Welker, J.M., Poretsky, R.S., Green, S., and Gonzalez-Meler, M.A. Challenges in microbial community analysis specific to Arctic soils. Microbiome Soil Sensors Workshop. La Jolla, CA, August 21-22, 2018. **(Invited)**

Ricketts, M.P., Flower, C.E., Poretsky, R.S., Welker, J.M., Green S., and Gonzalez-Meler, M.A. Ecological drivers of soil bacterial community structure in the Arctic... and Ohio. 8th Argonne National Laboratory Soil Metagenomics Meeting. Lemont, IL, November 1-3, 2017.

Ricketts, M.P. 2017. Arctic soil microbial community functional shifts in response to increased snow accumulation. University of Illinois at Chicago Hadley Presentations. Chicago, IL, April 4, 2017.

Ricketts M.P. 2014. Soil bacterial community shifts in response to climate change in moist acidic tundra of Northern Alaska. University of Illinois at Chicago Hadley Presentations. Chicago, IL, January 24, 2014.

Poster Presentations

Ewa, T., **Ricketts, M.P.**, Gonzalez-Meler, M.A. 2018. Gene abundance and carbon cycling in microbial communities. University of Illinois at Chicago Student Research Forum. Chicago, IL, April 11, 2018.

Ricketts, M.P., Flower, C.E., Gonzalez-Meler, M.A. 2017. Evidence of ash tree (*Fraxinus* spp.) associations with soil bacterial community structure and function. 8th Argonne National Laboratory Soil Metagenomics Meeting. Lemont, IL November 1-3, 2017.

Ricketts, M.P., Flower, C.E., Gonzalez-Meler, M.A. 2017. Evidence of ash tree (*Fraxinus* spp.) associations with soil bacterial community structure and function. ESA Annual Meeting 2017. Portland, OR, August 6-11, 2017.

Flower, C.E., **Ricketts, M.P.**, Knight, K.S., Long, R., Gonzalez-Meler, M.A. 2017. Emerald ash borer induced ash decline and its effects on belowground nutrient and microbial community dynamics. Workshop on the Science and Management of Ash Forests after Emerald Ash Borer. Duluth, MN, July 25-27, 2017.

Chang, J., **Ricketts, M.P.**, Welker, J.M., Gonzalez-Meler, M.A. 2017. The effects of climate change on carbon storage in soils of Alaskan tundra. University of Illinois at Chicago Student Research Forum. Chicago, IL, April 3, 2017.

Ricketts, M.P., Poretsky, R.S., Welker, J.M., Gonzalez-Meler, M.A. 2015. Arctic bacterial functional shifts associated with SOM decomposition in response to increased winter snow accumulation. U.S. Department of Energy Environmental System Science (ESS) Principal Investigator Meeting. Potomac, MD, April 28-29, 2015.

Ricketts, M.P., Poretsky, R.S., Welker, J.M., Gonzalez-Meler, M.A. 2014. Bacterial shifts in response to soil thermal insulation in moist acidic tundra of Northern Alaska: A functional analysis of 16S data using PICRUSt. Complex Soil Systems Conference. Berkeley, CA, September 3–5, 2014.

Ricketts, M.P., Poretsky, R.S., Gonzalez-Meler, M.A. 2013. Soil bacterial community shifts in response to soil thermal insulation and vegetation change in moist acidic tundra of Northern Alaska. AGU Fall Meeting. San Francisco, CA, December 9-13, 2013.

Ricketts, M.P., Poretsky, R.S., Gonzalez-Meler, M.A. 2013. Soil bacterial community shifts in response to soil thermal insulation and vegetation change in moist acidic tundra of Northern Alaska. 5th Annual Argonne Soil Metagenomics Meeting. Bloomingdale, IL, October 2-4, 2013.

Media

UIC Access to Excellence video: Prepared in honor of Dr. Arnold Bodmer
<https://www.youtube.com/watch?v=sbdDYKySvzk> - at 5:24

UIC Campus Insights video
<https://www.youtube.com/watch?v=kqvQh4zqjkA&index=1&list=PLmq5H6mJIf-JhHDP4FrOsQndCu8hIQJQk> - at 2:40

Affiliations

American Geophysical Union, American Society of Agronomy, Crop Science Society of America, Ecological Society of America, Honor Society of Phi Kappa Phi, Soil Ecology Society, Soil Science Society of America